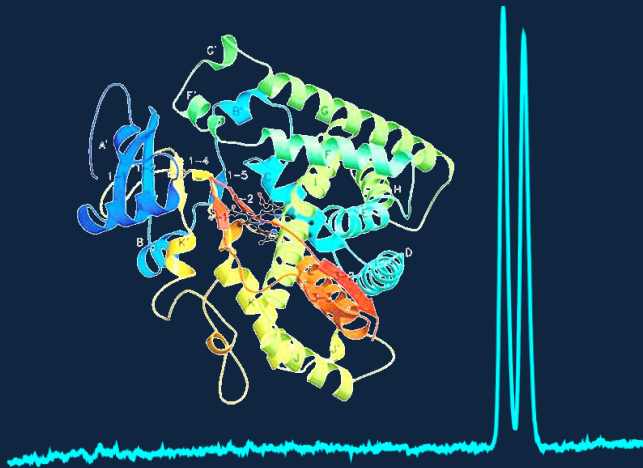




UNIVERSITAT DE VALÈNCIA
Departamento de Química Analítica
Doctorado en Química

Development and application of (bio)analytical methodologies in capillary electrophoresis. Enantioselectivity considerations



PhD Thesis
Lucía Asensi Bernardi

Supervised by:

Prof. Dr. Yolanda Martín Biosca
Prof. Dr. Salvador Sagrado Vives
Prof. Dr. María José Medina Hernández

Valencia, January 2014

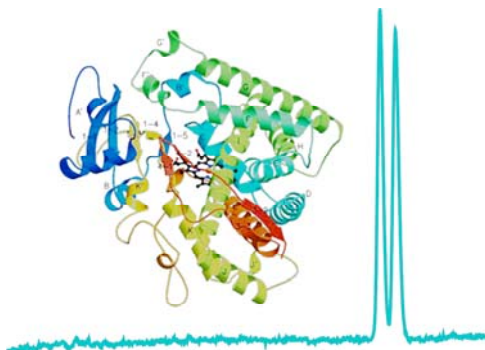


VNIVERSITAT Đ VALÈNCIA

Departamento de Química Analítica

Doctorado en Química

**Development and application of
(bio)analytical methodologies in capillary
electrophoresis. Enantioselectivity
considerations**



**PhD Thesis
Lucía Asensi Bernardi**

Supervised by:

Prof. Dr. Yolanda Martín Biosca

Prof. Dr. Salvador Sagrado Vives

Prof. Dr. María José Medina Hernández

Valencia, January 2014



VNIVERSITAT D VALÈNCIA

D^a YOLANDA MARTÍN BIOSCA, Profesora Titular de Universidad, D. SALVADOR SAGRADO VIVES, Catedrático de Universidad, y D^a MARÍA JOSÉ MEDINA HERNÁNDEZ, Catedrática de Universidad del Departamento de Química Analítica de la Universitat de València,

CERTIFICAN:

Que la presente Memoria titulada *"Development and application of (bio)analytical methodologies in capillary electrophoresis. Enantioselectivity considerations"*, realizada en el Departamento de Química Analítica de la Universitat de València, constituye la Tesis Doctoral de D^a LUCÍA ASENSI BERNARDI.

Asimismo, certifican haber dirigido y supervisado los distintos aspectos del presente trabajo así como su redacción.

Y para que conste a los efectos oportunos, firman la presente en Valencia, a 19 de noviembre de 2013.

D^a Yolanda Martín Biosca

D. Salvador Sagrado Vives

D^a María José Medina Hernández

PUBLICATIONS

The results of this PhD Thesis are summarized in the research papers listed below. Their corresponding impact factors from the Journal of Citation Reports (JCR) are also shown.

- I. Characterizing the interaction between enantiomers of eight psychoactive drugs and highly sulfated β -cyclodextrin by counter-current capillary electrophoresis
L. Asensi-Bernardi, L. Escuder-Gilabert, Y. Martín-Biosca, S. Sagrado and M.J. Medina-Hernández
Biomedical Chromatography 2014, 28, 120-126
Impact factor (JCR 2012): 1.945

- II. Modeling the chiral resolution ability of highly sulfated β -cyclodextrin for basic compounds in electrokinetic chromatography
L. Asensi-Bernardi, L. Escuder-Gilabert, Y. Martín-Biosca, M.J. Medina-Hernández and S. Sagrado
Journal of Chromatography A 2013, 1308, 152-160
Impact factor (JCR 2012): 4.612

- III. Determination of fluoxetine enantiomers in pharmaceutical formulations by electrokinetic chromatography-counter current technique
L. Asensi-Bernardi, Y. Martín-Biosca, E. Fornet-Herrero, S. Sagrado and M.J. Medina-Hernández
Biomedical Chromatography 2013, 27, 377-381
Impact factor (JCR 2012): 1.945

- IV. Chiral separations by non-aqueous capillary electrophoresis in DMSO-based background electrolytes
L. Asensi-Bernardi, A. Van Schepdael
Talanta 2014, 118, 328-332.
Impact factor (JCR 2012): 3.498

- V. Evaluation of enantioselective binding of fluoxetine to human serum albumin by ultrafiltration and CE – Experimental design and quality considerations
L. Asensi-Bernardi, Y. Martín-Biosca, R.M. Villanueva-Camañas, M.J. Medina-Hernández and S. Sagrado
Electrophoresis 2010, 31, 3268-3280
Impact factor (JCR 2012): 3.261
- VI. On the zopiclone enantioselective binding to human albumin and plasma proteins. An electrokinetic chromatography approach
L. Asensi-Bernardi, Y. Martín-Biosca, M.J. Medina-Hernández and S. Sagrado
Journal of Chromatography A 2011, 1218, 3111-3117
Impact factor (JCR 2012): 4.612
- VII. Electrokinetic chromatographic estimation of the enantioselective binding of nomifensine to human serum albumin and total plasma proteins
L. Asensi-Bernardi, Y. Martín-Biosca, S. Sagrado and M.J. Medina-Hernández
Biomedical Chromatography 2012, 26, 1357-1363
Impact factor (JCR 2012): 1.945
- VIII. Screening of acetylcholinesterase inhibitors by CE after enzymatic reaction at capillary inlet
Y. Martín-Biosca, L. Asensi-Bernardi, R.M. Villanueva-Camañas, S. Sagrado and M.J. Medina-Hernández
Journal of Separation Science 2009, 32, 1748-1756
Impact factor (JCR 2012): 2.591
- IX. In-line capillary electrophoretic evaluation of the enantioselective metabolism of verapamil by cytochrome P3A4
L. Asensi-Bernardi, Y. Martín-Biosca, L. Escuder-Gilabert, S. Sagrado and M.J. Medina-Hernández
Journal of Chromatography A 2013, 1298, 139-145
Impact factor (JCR 2012): 4.612

- X. Fast evaluation of enantioselective drug metabolism by electrophoretically mediated microanalysis: application to fluoxetine metabolism by CYP2D6
L. Asensi-Bernardi, Y. Martín-Biosca, L. Escuder-Gilabert, S. Sagrado and M.J. Medina-Hernández
Electrophoresis 2013, 34, 3214-3220
Impact factor (JCR 2012): 3.261

The results of this Thesis are part of the following research projects:

- Project SAF2005-01435 "Desarrollo de microsistemas de separación de alto rendimiento para la evaluación de las interacciones no específicas xenobiótico-biomembrana y específicas xenobiótico quiral-proteína plasmática" (Spanish Ministry of Science and Technology)
- Project SAF2008-00859 "Desarrollo de microtecnologías de alto rendimiento para el estudio de interacciones xenobiótico-biomacromolécula. Enantioselectividad de procesos de distribución y metabolismo de xenobióticos quirales" (Spanish Ministry of Science and Innovation)
- Project UV-INV-AE112-6629 "Desarrollo de microtecnologías de alto rendimiento y sensibilidad para la evaluación del metabolismo de xenobióticos. Enantioselectividad metabólica de xenobióticos quirales" (University of Valencia)

This PhD Thesis has been carried out thanks to two pre-doctoral scholarships:

- ACIF/2011/114 (Generalitat Valenciana)
- FPU2010-1984 (Spanish Ministry of Education)

To my parents

To Josep

*Quan surts per fer el viatge cap a Ítaca,
has de pregar que el camí sigui llarg,
ple d'aventures, ple de coneixences.
Has de pregar que el camí sigui llarg,
que siguin moltes les matinades
que entraràs en un port que els teus ulls ignoraven,
i vagis a ciutats per aprendre dels que saben.
Tingues sempre al cor la idea d'Ítaca.
Has d'arribar-hi, és el teu destí,
però no forçis gens la travessia.
És preferible que duri molts anys,
que siguis vell quan fondegis l'illa,
ric de tot el que hauràs guanyat fent el camí,
sense esperar que et doni més riqueses.
Ítaca t'ha donat el bell viatge,
sense ella no hauries sortit.
I si la trobes pobra, no és que Ítaca
t'hagi enganyat. Savi, com bé t'has fet,
sabràs el que volen dir les Ítaques.*

Lluís Llach, Ítaca

ACKNOWLEDGEMENTS

During the development of my Thesis, one of the most frequent feelings I had was the gratitude to some people that made it possible. Now I have the opportunity to express this feeling and acknowledge all these people in a few words.

First of all, I want to acknowledge my professors, Yolanda Martín, Salvador Sagrado and María José Medina, not only for their supervision but also for their friendship during the more than six years I have spent in their laboratory. Thanks for trusting in me since the first day, for giving me the opportunity of working in my Thesis and for joining me in several important moments of my academic and professional development.

Thanks to Yolanda for being much more than a supervisor and for teaching me not only capillary electrophoresis but also being a better person. I want to acknowledge you all the moments we spent together in the lab and outside it, I have had a lot of fun with you and you have been always willing to help me with whatever I needed. Thanks also to Emilio, Ana and Joan for being like a family for me and for sharing with me a bit of your lives.

Thanks to Salva and María José for completing the team and being part of this project. Thanks also to them for supporting me every time and giving me advice when I needed.

Special thanks to my parents, Pepe and Helena, for being the best parents in the world. Thanks for encouraging me always to study and improve myself and for supporting me in my decisions during all my life. Thanks for trusting in me, being proud of me and taking care of me always. Thanks for your unconditional love that I will keep always with me.

Many thanks to Josep for his unconditional love and for being a key part of my life. Thanks for understanding me always and for sharing and discussing with me all the work I did in my Thesis. I think you have learnt so much about CE during this time. Thanks also for encouraging me to continue with it when things were difficult, and for sharing with me all the good and bad things of our daily life and all the goals we

have. Thanks for making future plans with me, for taking care of me and for making me laugh and enjoy every day.

Thanks to the other members of my research group, Laura and Rosa, for sharing with me all this time in the lab. Thanks to all people that have worked in the lab for different periods during my stay there, because they gave me the opportunity of sharing very good moments, teaching some things and also learning from them. Special thanks to María Amparo, José María and Sagrario for making my starting in the lab easier and pleasant, and to Eder, Cris, Casandra and Laura for sharing the year of my Master Thesis and making the lab a very funny place to work. Thanks to Maria for reading pieces of this Thesis and giving me valuable feedback. Thanks to the other PhD students of the Department of Analytical Chemistry for their friendship.

Thanks to Professor Ann Van Schepdael for giving me the opportunity of working a few months in the Laboratory for Pharmaceutical Analysis in Leuven and learning about non-aqueous CE. Thanks also to the other people in the lab for making pleasant my stay there. Special thanks to Irene for bringing a bit of Spain to Belgium and sharing with me all our experiences there. Special thanks also to Bart for being a good friend and helping me so much during my stay; thanks also for "opening my eyes" and for our interesting discussions about research and life. Thanks to Kris for his technical support, to Jochen for his help and to Lan for her invaluable and kindly help during my first week there. Thanks to Huiying, Ye, HIMAL, Marwa and Eva for making me feel a good researcher and a useful person. Thanks to Marta, Martina and Judith for these pleasant moments in GroepT.

Thanks also to my family and my friends that always trusted in me and supported me during not only this period, but my whole life. Thanks for being there when I needed you and for teaching me important things every day. Special thanks to María for being much more than a friend and because I am sure that I can always ask you for everything I could need. Special thanks also to Empar and Lolo for their good advice in several aspects of my life. Thanks also to my Scout group and to my athletics team and friends for sharing with me interesting activities in my free time; I

think this is extremely important for keeping your mind fresh and being able to work properly during the week.

Finally, I would like to acknowledge the Generalitat Valenciana and the Spanish Ministry of Education for the pre-doctoral scholarships that gave me the financial support for my Thesis.

I would also like to tell that without the support and care of all the people I mentioned in these pages, and for sure much others that do not appear here, probably I would not be writing the acknowledgements of a PhD Thesis now, so many thanks to everyone for making it possible.

CONTENTS

ABBREVIATIONS AND VARIABLES	xxi
ABSTRACT	xxix
RESUMEN	xli
I. INTRODUCTION	3
I.1. Chirality and its importance in pharmaceutical sciences	3
I.1.1. Enantioselectivity in pharmacokinetic processes	4
I.1.1.1. Absorption	4
I.1.1.2. Distribution and protein binding	5
I.1.1.3. Metabolism	8
I.1.1.4. Renal clearance	13
I.1.2. Enantioselectivity in pharmacodynamic properties	13
I.2. Chiral analysis	14
I.3. Capillary electrophoresis for chiral analysis and enzymatic studies	16
I.3.1. Principles of separation in CE	18
I.3.2. Chiral analysis in CE	19
I.3.2.1. Chiral selectors in CE	20
I.3.2.2. Modes of CE employed for chiral analysis	22
I.3.2.3. Selector-selectand binding studies	24
I.3.3. Enzymatic reactions in CE: electrophoretically mediated microanalysis	27
I.4. <i>In vitro</i> evaluation of pharmacokinetic and pharmacodynamic properties	30
I.4.1. Protein binding	31
I.4.2. Drug metabolism	38
I.4.3. Enzyme inhibition	44
I.5. Drugs and pesticides in study	47
II. OBJECTIVES	57
III. METHODOLOGY	61
III.1. Instrumentation	61
III.2. Chemicals and reagents	62
III.3. Experimental procedures	67
III.3.1. Capillaries conditioning	67

III.3.2. Procedure for the chiral separation of xenobiotics	67
III.3.3. Procedure for protein binding studies	68
III.3.4. Procedure for electrophoretically mediated microanalysis	69
III.4. Software and calculations	71
IV. RESULTS AND DISCUSSION	75
IV.1. Chiral separations of xenobiotics by capillary electrophoresis	75
IV.1.1. Characterizing the interaction between enantiomers of eight psychoactive drugs and highly sulfated- β -cyclodextrin by counter-current capillary electrophoresis (Paper I)	81
IV.1.2. Modeling the chiral resolution ability of highly sulfated β -cyclodextrin in electrokinetic chromatography (Paper II)	88
IV.1.3. Determination of fluoxetine enantiomers in pharmaceutical formulations by electrokinetic chromatography-counter current technique (Paper III)	96
IV.1.4. Chiral separations by non-aqueous capillary electrophoresis in DMSO-based background electrolytes (Paper IV)	100
IV.2. Study of enantioselective binding of drugs to plasma proteins	104
IV.2.1. Evaluation of enantioselective binding of fluoxetine to human serum albumin by ultrafiltration and CE – Experimental design and quality considerations (Paper V)	105
IV.2.2. On the zopiclone enantioselective binding to human albumin and plasma proteins. An electrokinetic chromatography approach (Paper VI)	113
IV.2.3. Electrokinetic chromatographic estimation of the enantioselective binding of nomifensine to human serum albumin and total plasma proteins (Paper VII)	117
IV.3. Study of enzymatic reactions by capillary electrophoresis	120
IV.3.1. Screening of acetylcholinesterase inhibitors by CE after enzymatic reaction at capillary inlet (Paper VIII)	121
IV.3.2. In-line capillary electrophoretic evaluation of the enantioselective metabolism of verapamil by cytochrome P3A4 (Paper IX)	127
IV.3.3. Fast evaluation of enantioselective drug metabolism by electrophoretically mediated microanalysis: application to fluoxetine metabolism by cytochrome P2D6 (Paper X)	134
V. CONCLUSIONS	141
VI. REFERENCES	147
VII. PUBLICATIONS	167



Abbreviations and variables

ABBREVIATIONS AND VARIABLES

ACE: affinity capillary electrophoresis

Acetyl CoA: acetyl coenzyme A

ACh: acetylcholine

AChE: acetylcholinesterase

AGP: α_1 -acid glycoprotein

APIs: active pharmaceutical ingredients

AThCh: acetylthiocholine

α : modifying factor (enzyme inhibition)

α_e : electrophoretic enantioselectivity

α_t : thermodynamic enantioselectivity

b : bound concentration of drug after equilibrium

b: regression coefficients

b_0 : intercept

b_1 : slope

BGE: background electrolyte

BSA: bovine serum albumin

BUP: bupropion

CD: cyclodextrin

CE: capillary electrophoresis

CFT: complete filling technique

Cl_i : intrinsic clearance

CM- β -CD: carboxymethyl- β -cyclodextrin

CM- γ -CD: carboxymethyl- γ -cyclodextrin

CSP: chiral stationary phase

C_{ss} : steady-state concentration

C_i : concentration of drug in the protein reservoir (in equilibrium dialysis)

C_u : concentration of drug in the buffer reservoir (in equilibrium dialysis)

CYP: cytochrome P450

CYP2D6: cytochrome P450, isoform 2D6

CYP3A4: cytochrome P450, isoform 3A4

CZE: capillary zone electrophoresis
 a' : free concentration of drug after equilibrium
 D : total drug (or enantiomer) concentration
DATs: dopamine transporters
 DE : dreading energy
DIM: dimethindene
DMSO: dimethyl sulfoxide
DNA: deoxyribonucleic acid
DPLS1: discriminant-partial least squares analysis
DSC: differential scanning calorimetry
ED: equilibrium dialysis
EKC: electrokinetic chromatography
EMMA: electrophoretically mediated microanalysis
ENAC: Spanish accreditation entity
EOF: electroosmotic flow
 ES : enantioselectivity degree
EV: explained variance
 EV_{CV} : explained variance in cross-validation
 ϵ : dielectric constant
 f : dilution factor
FA: frontal analysis
FDA: Food and Drug Administration
FLX: fluoxetine
FMOs: flavin-containing monooxygenases
G6P: glucose-6-phosphate
G6PDH: glucose-6-phosphate dehydrogenase
GABA: γ -aminobutyric acid
GC: gas chromatography
 HBA : hydrogen bond acceptors
 HBD : hydrogen bond donors
HLMs: human liver microsomes
HPAC: high-performance affinity chromatography

HPLC: high-performance liquid chromatography
HSA: human serum albumin
HS- β -CD: highly sulfated β -cyclodextrin
HTS: high-throughput screening
I.S.: internal standard
IC₅₀: half maximal inhibitory concentration (inhibitory potency)
ICH: International Conference on Harmonization
ITC: isothermal titration calorimetry
IUPAC: International Union of Pure and Applied Chemistry
 K : affinity constant (binding constant)
 K_i : inhibition constant
 k_i : number of latent variables (or principal components)
 K_m : Michaelis-Menten constant
 K^q : binding constant of the q th CD isomer in the mixture (multi-CD systems)
 l : effective capillary length
 L : total capillary length
LC: liquid chromatography
lgD: *lgP* estimated at pH 7.4
lgP: logarithm of octanol-water partition coefficient
LV: latent variable
 m : number of classes of active sites in the protein molecule
MA: maximal projection area
MADe: median absolute deviation
MEKC: micellar electrokinetic chromatography
MES: 2-(N-morpholino)ethanesulfonic acid
MM: molecular mass
MR: molar refractivity
MS: mass spectrometry
MSA: molecular surface area
MV: molecular volume
MW: molecular weight
 μ : electrophoretic mobility

μ^0 : electrophoretic mobility of the free enantiomer

μ^{CD} : electrophoretic mobility of the enantiomer-CD complex

μ^{EOF} : electrophoretic mobility of the electroosmotic flow

μ^q : individual mobility of the enantiomer- q th CD complex (multi-CD systems)

n : apparent binding stoichiometry

n : number of replicates/samples

η : viscosity

NACE: non-aqueous capillary electrophoresis

NADP⁺: nicotinamide adenine dinucleotide phosphate (oxidized form)

NADPH: nicotinamide adenine dinucleotide phosphate (reduced form)

NFLX: norfluoxetine

NMF: nomifensine

NOR: norverapamil

OEC: orbital electronegativity of the chiral carbon atom

ORP: orphenadrine

OVM: ovomucoid protein

P : total protein concentration

PAMPA: parallel artificial membrane permeability assay

PB%: percentage of protein binding

PB: protein binding

PCA: principal component analysis

PCs: principal components

PD: Parkinson's disease

PET: positron emission tomography

PFT: partial filling technique

pK_a : minus logarithm of acidity constant

pK_{auto} : autoprotolysis constant

PLS: partial least squares

POL: polarizability

poly-LL-SUCLV: poly(sodium N-undecenoxy carbonyl-LL-leucyl-valinate)

poly-L-SUCL: poly(sodium N-undecenoxy carbonyl-L-leucinate)

Pp: predictive power

PRO: promethazine
PSA: polar surface area
QSPR: quantitative structure-property relationship
r: fraction of bound xenobiotic *per* molecule of protein
 R^2 : determination coefficient
RB: rotatable bonds
RPS: rapid polarity switching
Rs: resolution
RSD: relative standard deviation
SD: standard deviation
SEC: size-exclusion chromatography
SPL: selector plug length
SPR: surface plasmon resonance
T: temperature
 t_0 : migration time of the EOF
TCh: thiocholine
TDLFP: transverse diffusion of the laminar flow profiles
TER: terfenadine
 t_r : migration time of a peak
TLC: thin-layer chromatography
TM- β -CD: heptakis-(2,3,6-O-methyl)- β -cyclodextrin
Tris: Tris-(hydroxymethyl)-aminomethane
 t_s : confidence interval at the 95% probability level
UF: ultrafiltration
UGT: uridine 5'-diphospho-glucuronosyltransferase
UV: ultraviolet
V: separation voltage
 V_0 : initial velocity (enzymatic reaction)
VER: verapamil
VLX: viloxazine
 V_{max} : maximum reaction velocity
W: Van der Waals volume

w_i : width at 50% peak height

X: data matrix

χ^q : molar fraction of the q th CD isomer in the mixture (multi-CD systems)

y: response variable



Abstract

ABSTRACT

The development of new drugs is a long, complex and expensive process that involves the evaluation of pharmacokinetic and pharmacodynamic properties of the new molecule in different stages. In the early stages of drug development, *in vitro* methods for the high-throughput screening of new molecules' properties are commonly used, with the aim of having preliminary data about the potential pharmacological activity of a molecule and also its pharmacokinetics. When chiral molecules are employed, both pharmacokinetic and pharmacodynamic properties can show a certain degree of enantioselectivity due to the interaction with optically active biomacromolecules (Brocks, 2006), so the methods applied in these preclinical early stages must allow evaluating these properties in an enantioselective way. This need comes from the growing interest of the pharmaceutical industry in the development of single-enantiomer formulations, and also from the regulations concerning racemic drugs, which indicate that enantioselective analysis should be performed also over racemates (Food and Drug Administration, 1992; European Medicines Agency, 1993).

Capillary electrophoresis (CE) is a convenient analytical technique to be applied for these preclinical studies. It provides advantageous possibilities for the chiral analysis of small molecules and also for the in-line evaluation of some pharmacokinetic and pharmacodynamic processes, such as the binding of drugs to plasma proteins or their behavior in different enzymatic reactions. Its main features, which are extremely interesting for these applications, are speediness of analysis, low consumption of chemicals and reagents, ease of automation, high peak efficiencies and low environmental impact (Lin *et al.*, 2003).

The main purpose of this Thesis is the development and application of capillary electrophoretic methodologies for the *in vitro* enantioselective evaluation of pharmacological properties of drugs, in order to provide to the pharmaceutical industry fast and reliable alternatives for the preclinical stages of drug development. It is divided into three main parts: development of methods and theoretical studies for chiral separations of xenobiotics by CE (Papers I-IV), evaluation of the

enantioselective binding of drugs to plasma proteins (Papers V-VII) and study of enzymatic reactions by electrophoretically mediated microanalysis, EMMA (Papers VIII-X).

A powerful chiral selector, the highly sulfated β -cyclodextrin (HS- β -CD), has been widely used along this Thesis to perform enantioseparations. So, the first and second studies of this Thesis are theoretical; about its enantioselectivity. In Paper I, apparent binding constants between HS- β -CD and enantiomers of eight psychoactive drugs were estimated by electrokinetic chromatography-complete filling technique (EKC-CFT). The experimental mobility data of both enantiomers were fitted *vs.* the cyclodextrin concentration using a non-linear model that allows the estimation of apparent binding constants and overall limit mobilities. From these estimations, it was possible to calculate the thermodynamic (α_t) and electrophoretic (α_e) enantioselectivities of the separation process. The results show that this cyclodextrin strongly binds to the enantiomers of these basic drugs, with high enantioselectivity in most of the cases. The binding constants of HS- β -CD to the studied drugs are equal or higher than those found in the literature for other compounds (Vaccher *et al.*, 2005, Lipka *et al.*, 2007).

Both thermodynamic (due to the difference between the apparent binding constants of the enantiomers) and electrophoretic (related to the difference between the overall complex enantiomer-CD mobilities) enantioselectivities were found to be responsible for the enantioseparation with the HS- β -CD, with a major contribution of α_t . However, in one of the cases, where no thermodynamic enantioselectivity was found, only the electrophoretic one was enough to achieve complete separation of the enantiomers. The use of complete filling technique for the evaluation of binding constants, which is discussed in this Thesis, is presented as an alternative to conventional electrokinetic chromatography with a saving on chiral selector of around 99%.

The second Paper included in this Thesis is a quantitative structure-property relationship study that models the enantioselectivity of the HS- β -CD for basic compounds in EKC, by relating the resolution obtained for forty xenobiotics (drugs and pesticides) with some of their structural properties. This is an attempt to provide

researchers in the field of enantioseparations an alternative to the usually employed trial-and-error procedures for the development of chiral methods. A discriminant-partial least squares analysis over a single response variable (DPLS1) has been performed using a categorical resolution (R_s) value as \mathbf{y} -vector and the structural properties of the xenobiotics as \mathbf{X} -matrix. Only four structural variables were selected as significant in the final model: logarithm of octanol-water partition coefficient estimated at pH 7.4 (lgD), polar surface area (PSA), number of hydrogen bond donors (HBD) and acceptors (HBA). From the de-scaled coefficients of the model, an explicit equation that relates the categorical R_s with these four variables was obtained: $R_s = 2.354 + 0.095lgD - 0.008PSA - 0.159HBD - 0.137HBA$. This model shows an explained variance of 72.4%.

For those xenobiotics whose predicted R_s is not so high (i.e., expected chiral separation only under concrete experimental conditions) a multivariate optimization of the most influential experimental conditions affecting enantioseparation (cyclodextrin concentration, pH of the background electrolyte (BGE) and capillary temperature) has been proposed, *via* a Box-Behnken experimental design and a posterior adjust of the experimental results to a PLS2 model, which allows estimating the migration time and the R_s for each set of experimental conditions.

Paper III is an application of the enantioseparation of the antidepressant fluoxetine with HS- β -CD to the chiral analysis of three pharmaceutical formulations. The separation conditions were adjusted in order to avoid a matrix interference and a suitable EKC-CFT method has been obtained, which allows the quantification of both fluoxetine enantiomers in less than 2 min with a R_s of 2.4. A partial validation of the chiral analytical method was performed following the guidance of the International Conference on Harmonization (ICH) and the US Pharmacopeia in terms of identity, linearity, precision and accuracy. Good analytical features were obtained: determination coefficients (R^2) of 0.996 for the calibration curves of both enantiomers, relative standard deviations (RSD) less than 20%, obtained under intermediate precision conditions, and recoveries of 92 ± 13 and 105 ± 6 % for the first and second eluted enantiomers, respectively. For all samples, the content of racemic fluoxetine was within specifications of the US Pharmacopeia ($20 \text{ mg} \pm 15\%$),

and stereoisomer ratios were around 1. So, the suitability of HS- β -CD for the enantioseparation of basic drugs has been proved here, not only with theoretical studies but also with an application to chiral pharmaceutical analysis.

An approach of non-aqueous capillary electrophoresis (NACE) to the chiral separation of drugs, developed during a research stay in the Katholieke Universiteit of Leuven, is described in Paper IV. It responded to the interest on developing analysis methods based on non-aqueous systems that could be able to determine new active pharmaceutical ingredients (APIs) which are non-soluble in aqueous or methanolic mediums. Many drugs in the pipeline suggested by combinatorial chemistry show low aqueous solubility due to high molecular weight. If a badly soluble lead molecule has very good potency and low toxicity, the drug might go into further development anyway, and in these cases chiral methods for their analytical control may be developed. In this work, the use of dimethyl sulfoxide (DMSO) is proposed as an alternative to the most commonly used BGEs of alcoholic nature, due to its lower volatility and hazardousness, and better solvent properties for drugs with low polarity. However, it may be taken into account that the enantioseparation is disfavored in the DMSO medium because the intermolecular forces responsible for the enantiorecognition are weaker in organic media (Chankvetadze and Blaschke, 2001).

The enantioseparation of three drugs, verapamil, pindolol and fenfluramine, has been performed with this NACE methodology, using univariate optimization in order to select the best separation conditions. Finally, DMSO-based BGEs containing a variable amount of methanol (0-30%), 0.5-1 M HAc, 125 mM NH₄Ac and 40 mM carboxymethyl- γ -cyclodextrin were selected, with a capillary temperature of 15 °C and a separation voltage of 30 kV. Using these conditions, *Rs* values of 1.5, 2.0 and 1.2 were obtained for verapamil, pindolol and fenfluramine, respectively. The electric current was stable during all the separations performed, despite the fact that one of the most common drawbacks of NACE is current breakdowns.

Papers V-VII of this Thesis deal with the enantioselective evaluation of an important pharmacokinetic property at the level of drugs distribution, the protein binding. The amount of drug that binds to plasma proteins, as well as the strength of this binding,

influences considerably the availability of the drug for reaching target organs and also for being eliminated. As plasma proteins are optically active molecules, chiral drugs can show different binding properties between enantiomers. Therefore, the development of fast and reliable procedures for the *in vitro* evaluation of enantioselective drug-protein binding is interesting for the pharmaceutical industry research. The most abundant protein in human plasma is albumin (HSA), and it presents a high degree of enantioselectivity in its binding with drugs.

In this Thesis, the evaluation of enantioselective binding of drugs to HSA and total plasma proteins has been performed by ultrafiltration followed by chiral analysis by EKC. In ultrafiltration, a pre-equilibrated drug-protein mixture is filtered through a membrane that retains the protein and only allows the pass of the unbound drug fraction. This unbound fraction is then analyzed, here using chiral EKC.

Paper V points out some weak aspects of the experimental methodologies and mathematical models previously published for the study of protein binding (Katrachali *et al.*, 2010; Fielding *et al.*, 2005), and proposes a novel strategy for a reliable binding evaluation. An extended discussion concerning the different mathematical approaches to protein binding is performed, using the enantioselective binding of the antidepressant fluoxetine to HSA as an example. The analysis of fluoxetine enantiomers has been performed here using HS- β -CD as chiral selector in CFT, in a 30 mM phosphate buffer of pH 7.0. The separation temperature and voltage have been fixed at 30 °C and 15 kV.

The proposed strategy implies working close to physiological conditions, thus keeping always the ratio between the drug concentration (D) and the protein concentration (P) lower than 0.5, and P near the physiological level (around 475 μ M). In this situation, a simple binding model that assumes that only one kind of binding site is occupied in the protein molecule and the stoichiometry of the binding is 1:1 can be used, always confirming these assumptions *via* other equations. Also, data were inspected in order to detect and eliminate outliers that could affect the reliability of the estimations. Enantiomer-protein binding constants (K_I) have been estimated for fluoxetine, as well as the enantioselectivity, defined as the ratio between binding constants.

Finally, the percentage of protein binding (*PB%*), which is an interesting parameter from a pharmacokinetic point of view, has been also estimated for both fluoxetine enantiomers, being 95.2 and 90.0% for the first and second eluted enantiomers, respectively. The correspondent enantioselectivity is around 2, in favor of the first eluted enantiomer.

Still in the field of enantioselective drug-protein interactions, Papers VI and VII study the enantioselective binding of the hypnotic zopiclone and the antidepressant nomifensine to HSA and total plasma proteins, also by ultrafiltration and chiral EKC using the partial (PFT) or complete filling techniques. In Paper VI, the enantioseparation of zopiclone with carboxymethyl- β -cyclodextrin (CM- β -CD) is adjusted for the analysis of the unbound fractions after ultrafiltration. A solution containing 30 mM CM- β -CD in 50 mM Tris buffer at pH 6.0 has been used as chiral selector in PFT, injecting it at 0.5 psi during 99 s prior to samples injection. The chiral separation has been performed at 25 °C by applying 15 kV. The mathematical approaches and experimental designs developed in Paper V have been also applied here to calculate the binding constants, enantioselectivity and protein binding. The *PB%* values to HSA were found to be 47 and 36% for S- and R-zopiclone, respectively, and to total plasma proteins 45 and 49%, respectively. These values were in agreement with those reported in the literature for racemic zopiclone, around 45% (Gaillet *et al.*, 1983; Spanish Drug Agency, 2011).

The enantioselective binding of nomifensine to HSA and total plasma proteins is evaluated in Paper VII, in this case using 30 mM heptakis-(2,3,6-O-methyl)- β -cyclodextrin as chiral selector in CFT for the enantioseparation of the unbound fraction, with the same BGE and voltage as in Paper VI but with a capillary temperature of 50 °C. The experimental design of calibration curves and samples was repeated in two independent sessions in order to check the inter-day precision of the procedure. As no significant differences were found between the data of both working sessions, all data were used together for estimations. The *PB%* to HSA was estimated at 40 and 63% for the first and second eluted enantiomers respectively. For the binding to total plasma proteins, the estimated values were 63 and 64% respectively. By comparing these values, it can be concluded that the second eluted

enantiomer of nomifensine binds mainly to HSA while the first enantiomer binds also to other plasma proteins.

The experimental design and mathematical approaches proposed in this Thesis for a reliable estimation of enantioselective protein binding with ultrafiltration and chiral EKC have demonstrated to be a robust tool which allows obtaining good *in vitro* estimates in near-physiological conditions, thus providing valuable data from a pharmacokinetic point of view. Enantioselective protein binding data for fluoxetine, zopiclone and nomifensine have been estimated here, thus completing the information available in the literature about these drugs.

The third part of this Thesis is related to the development of in-capillary enzymatic reactions by electrophoretically mediated microanalysis (EMMA). In EMMA the reagents are sequentially introduced in an electrophoretic capillary and left to mix and react for a fixed time. The separation of substrates, enzymes and products is then performed by electrophoresis. The main advantage of EMMA is that the reaction takes place in a nanoliter scale, so the consumption of reagents is extremely low. Furthermore, it is fully automated since the reaction and the separation take part in a unique step inside the capillary, which is another important advantage for screening procedures.

In Paper VIII an EMMA screening methodology for the evaluation of acetylcholinesterase (AChE) inhibitors has been developed and applied to the study of five drugs with known inhibitory activity. Tacrine has been used as model compound in order to optimize the method conditions. The progress of the enzymatic reaction of the hydrolysis of acetylthiocholine in presence of AChE and the inhibitors has been determined by measuring the peak area of the reaction product thiocholine. A "sandwich" injection has been performed by injecting the substrate plug between two enzyme plugs. The plugs' mixing has been performed by simple diffusion, with an incubation time of 2 min. The BGE for the reaction and separation was 30 mM borate-phosphate buffer at pH 8.0, the capillary temperature has been set at 37 °C and the separation voltage at 15 kV. Due to the dilution of solutes in the EMMA methodology, a correction may be performed in calculations to achieve accurate results. Here, a dilution factor is estimated by comparing the calculated

inhibitory potency of tacrine with that reported with the reference method (Andrisano *et al.*, 2001), and applied then to all calculations.

The proposed screening methodology has proved to be useful for the estimation of inhibitory constants, inhibitory potency, a qualitative approach to the inhibition mechanism and the percentage of inhibition of tacrine, edrophonium, neostigmine, pyridostigmine and eserine. The screening results show that according to their percentage of inhibition under fixed conditions, the order of inhibitor potency for these compounds is tacrine > edrophonium > neostigmine > eserine > pyridostigmine. This screening procedure, with an analysis time shorter than 5 min, can be employed for the evaluation of new potential AChE inhibitors.

Continuing with the use of EMMA methodologies for the evaluation of drug-enzyme interactions, Papers IX and X are studies of enantioselective metabolism by different isoforms of the cytochrome P450. In these studies, the capillary acts simultaneously as reactor and chiral separation system, thus providing enantioselective information with a fast, fully automated assay. The chiral separation is performed in both cases using HS- β -CD and the partial filling technique.

Paper IX deals with the enantioselective metabolism of the Ca⁺²-channel blocker verapamil by CYP3A4, the most important isoform of cytochrome P450 in humans. Different possibilities for the EMMA assay have been considered and variables have been optimized prior to calculation of the Michaelis-Menten parameters for the enantioselective metabolism kinetics. The selected experimental conditions for the EMMA assay included a "sandwich" injection of the substrate plug between two enzyme plugs, and two plugs of incubation buffer before and after the "sandwich" in order to give to the enzyme its adequate reaction medium. The mixing of plugs has been performed by simple diffusion during an incubation time of 5 min. After that, the separation of all the reaction mixture, including the enantiomers of verapamil and its major metabolite norverapamil, has been performed in the same capillary with the following conditions: 50 mM phosphate at pH 8.8 as BGE, 2.5% HS- β -CD injected at 10 psi/2 min, 25°C and 20 kV with a little pressure of 0.2 psi in order to shorten the migration times. The result is a fully automated methodology that allows

the enantioselective evaluation of verapamil metabolism by CYP3A4 in less than 35 min including capillary preconditioning, injection, incubation and separation.

Michaelis-Menten parameters (K_m and V_{max}) have been calculated for the overall enantioselective metabolism of verapamil by CYP3A4. K_m values have been estimated as 51 ± 9 and 47 ± 9 μM for S- and R-verapamil, respectively, while V_{max} estimates were 22 ± 2 and 21 ± 2 $\text{pmol}\cdot\text{min}^{-1}\cdot(\text{pmol CYP})^{-1}$ for S- and R-verapamil, respectively. Intrinsic clearances, defined as the amount of plasma from which a xenobiotic is removed in a certain time, and estimated in vitro as V_{max}/K_m (Kroemer *et al.*, 1992), have been also calculated for both enantiomers.

The enantioselective metabolism of fluoxetine by other CYP450 isoform, CYP2D6, is estimated in Paper X following the same methodology as in the previous work. The EMMA conditions from Paper IX were directly applied, while the separation conditions were adjusted in order to separate the enantiomers of fluoxetine and its major metabolite norfluoxetine. The influence of the most important variable on the enantioseparation, the concentration of HS- β -CD, was studied and a final concentration of 1.25% was selected for the separation of the reaction mixture. The other separation conditions were kept as in Paper IX. Kinetic parameters have been estimated by non-linear fitting of experimental data to the Michaelis-Menten equation. K_m values were found to be 30 ± 3 μM for S-fluoxetine and 39 ± 5 μM for R-fluoxetine. V_{max} estimates were 28.6 ± 1.2 and 34 ± 2 $\text{pmol}\cdot\text{min}^{-1}\cdot(\text{pmol CYP})^{-1}$ for S- and R-fluoxetine, respectively. The kinetic assay was repeated using a single enantiomer (R-fluoxetine) instead of the racemic mixture. Similar results were obtained indicating that the use of the racemate is a good option for obtaining enantioselective estimations.

The usefulness of EMMA as screening methodology for the *in vitro* evaluation, enantioselective or not, of drug-enzyme interactions has been proved in this Thesis. The developed methods allow to estimate kinetic and inhibition parameters in fast assays with low consumption of reagents and samples. The coupling of EMMA with the enantioseparation of substrates and products in a unique step carried out in the CE system provides valuable enantioselective information about the pharmacokinetic or pharmacodynamic processes evaluated.

All the methods proposed and applied in this Thesis (chiral separations, prediction models, enantioselective protein binding evaluation and drug-enzyme interaction) can be applied in the pharmaceutical industry to obtain useful *in vitro* information in the preclinical phases of drug development and for the enantioselective quality control of raw materials, synthesis intermediates and final products.



Resumen

RESUMEN

El desarrollo de nuevos fármacos es un proceso largo, complejo y costoso que incluye la evaluación en diferentes etapas de propiedades farmacocinéticas y farmacodinámicas de la nueva molécula. En las primeras etapas del desarrollo de un fármaco es habitual el uso de métodos *in vitro* para el cribado de alto rendimiento de las propiedades de nuevas moléculas, con el objetivo de obtener datos preliminares sobre la potencial actividad farmacológica de una molécula y sobre su farmacocinética. Cuando se emplean moléculas quirales, tanto sus propiedades farmacocinéticas como las farmacodinámicas pueden presentar un cierto grado de enantioselectividad debido a la interacción con biomacromoléculas ópticamente activas (Brocks, 2006), por lo que los métodos aplicados en estas primeras etapas preclínicas deben permitir la evaluación de estas propiedades de una manera enantioselectiva. Esta necesidad proviene del creciente interés de la industria farmacéutica en el desarrollo de formulaciones enantioméricamente puras, y también de las normativas en torno a medicamentos racémicos, que indican que el control de calidad realizado sobre estos fármacos también debe ser enantioselectivo (Food and Drug Administration, 1992; European Medicines Agency, 1993).

La electroforesis capilar (CE, del inglés *capillary electrophoresis*) es una técnica analítica conveniente para abordar estos estudios preclínicos. Proporciona ventajosas posibilidades para el análisis quiral de moléculas pequeñas y para la evaluación en línea de numerosos procesos farmacocinéticos y farmacodinámicos, como la unión de fármacos a las proteínas plasmáticas o su comportamiento en diferentes reacciones enzimáticas. Sus principales características, extremadamente interesantes para estas aplicaciones, son rapidez de análisis, bajo consumo de reactivos y muestras, facilidad de automatización, elevadas eficacias de pico y bajo impacto medioambiental (Lin y col., 2003).

El principal objetivo de esta Tesis es el desarrollo y aplicación de metodologías electroforéticas para la evaluación enantioselectiva *in vitro* de propiedades farmacológicas de medicamentos, con el fin de proporcionar a la industria farmacéutica alternativas rápidas y fiables en las fases preclínicas del desarrollo de

nuevos fármacos. Esta Tesis se divide en tres bloques principales: desarrollo de métodos y estudios teóricos para la separación quiral de xenobióticos mediante electroforesis capilar (Artículos I-IV), evaluación de la unión enantioselectiva de fármacos a las proteínas plasmáticas (Artículos V-VII) y estudio de reacciones enzimáticas empleando microanálisis mediante electroforesis (EMMA, del inglés *electrophoretically mediated microanalysis*) (Artículos VIII-X).

Los dos primeros trabajos incluidos en esta Tesis son estudios teóricos sobre la capacidad de enantioconocimiento de la β -ciclodextrina altamente sulfatada (HS- β -CD, del inglés *highly sulfated β -cyclodextrin*), potente selector quiral que se ha utilizado en una gran parte de las separaciones quirales desarrolladas en esta Tesis. En el Artículo I se han estimado constantes de unión aparentes entre la HS- β -CD y los enantiómeros de ocho fármacos psicoactivos empleando cromatografía electrocinética y la técnica del llenado completo del capilar (EKC-CFT, del inglés *electrokinetic chromatography-complete filling technique*). Los datos experimentales de movilidad electroforética de ambos enantiómeros se representaron frente a la concentración de ciclodextrina empleando un modelo de ajuste no lineal que permite la estimación de constantes de unión aparentes y movilidades límite. A partir de estas estimaciones se calcularon las enantioselectividades termodinámica (α_t) y electroforética (α_e) del proceso de separación. Los resultados mostraron que esta ciclodextrina se une fuertemente a los enantiómeros de los ocho fármacos básicos seleccionados, con elevada enantioselectividad en la mayoría de los casos. Las constantes aparentes de unión de la HS- β -CD a los fármacos estudiados son iguales o mayores que las descritas en la bibliografía para otros compuestos (Vaccher y col., 2005, Lipka y col., 2007).

Ambas enantioselectividades, termodinámica (relacionada con las diferencias entre las constantes de unión aparentes de ambos enantiómeros) y electroforética (debida a las diferentes movilidades de los complejos enantiómero-ciclodextrina), resultaron ser responsables de la separación quiral con HS- β -CD, aunque con una mayor contribución de α_t . Sin embargo, en uno de los casos en el que no se vio enantioselectividad termodinámica, los enantiómeros se resolvieron completamente debido únicamente a la enantioselectividad electroforética. Por otro lado, el uso de la

técnica del llenado completo del capilar para la evaluación de constantes de unión se presenta en esta Tesis como una alternativa a la cromatografía electrocinética convencional con un ahorro en selector quiral en torno al 99%.

El segundo Artículo incluido en esta Tesis es un estudio de relación cuantitativa estructura-actividad que modela la capacidad de enantioconocimiento de la HS- β -CD para compuestos básicos en EKC, relacionando la resolución obtenida para cuarenta xenobióticos (fármacos y plaguicidas) con algunas de sus propiedades estructurales. Este trabajo proporciona a los investigadores en el campo de las separaciones quirales una alternativa a los procedimientos habituales de ensayo y error para el desarrollo de métodos enantioselectivos. Se llevó a cabo una regresión de mínimos cuadrados parciales discriminante sobre una variable respuesta (DPLS1, del inglés *discriminant-partial least squares*) empleando como vector \mathbf{y} un valor categórico de resolución (R_s) y como matriz \mathbf{X} las propiedades estructurales de los xenobióticos. Únicamente se seleccionaron cuatro variables estructurales como significativas en el modelo final: logaritmo del coeficiente de partición octanol-agua estimado a pH 7,4 (lgD), área superficial polar (PSA), número de dadores (HBD) y aceptores (HBA) de enlaces de hidrógeno. A partir de los coeficientes no escalados del modelo, se obtuvo una ecuación explícita que relaciona el valor categórico de R_s con las cuatro variables estructurales seleccionadas: $R_s = 2,354 + 0,095lgD - 0,008PSA - 0,159HBD - 0,137HBA$. El modelo seleccionado presentó una varianza explicada del 72,4%.

Para aquellos xenobióticos cuya R_s predicha no es muy elevada, que puede interpretarse como posible separación quiral pero sólo en determinadas condiciones experimentales, se propuso una optimización multivariante de las tres condiciones experimentales más influyentes en la enantioseparación (concentración de ciclodextrina, pH del tampón de separación (BGE, del inglés *background electrolyte*) y temperatura del capilar), a través de un diseño experimental Box-Behnken y un ajuste posterior de los resultados experimentales a un modelo PLS2, que permite la estimación del tiempo de migración y la resolución para cada conjunto de condiciones experimentales.

El Artículo III es una aplicación de la enantioseparación del antidepresivo fluoxetina con HS- β -CD al análisis quiral de tres formulaciones farmacéuticas. Las condiciones de separación se optimizaron para evitar una interferencia de la matriz y se obtuvo un método de separación adecuado mediante EKC-CFT que permite la cuantificación de ambos enantiómeros de fluoxetina en menos de 2 minutos con un valor de R_s de 2,4. Se llevó a cabo una validación parcial del método quiral siguiendo las indicaciones de la International Conference on Harmonization (ICH) y de la US Pharmacopeia sobre identidad, linealidad, precisión y exactitud. Se obtuvieron buenas características analíticas: coeficientes de determinación (R^2) de 0,996 para las curvas de calibrado de ambos enantiómeros, desviaciones estándar relativas (RSD, del inglés *relative standard deviation*) inferiores al 20%, obtenidas en condiciones de precisión intermedia, y recuperaciones de 92 ± 13 y 105 ± 6 % para el primer y segundo enantiómero eluidos, respectivamente. Para todas las muestras se obtuvo un contenido en fluoxetina racémica dentro de las especificaciones de la US Pharmacopeia ($20 \text{ mg} \pm 15\%$), con relaciones estereoisoméricas en torno a 1. Así pues, en esta Tesis se ha demostrado la idoneidad de la HS- β -CD para la enantioseparación de fármacos básicos, no sólo con estudios teóricos sino también con una aplicación al análisis quiral de productos farmacéuticos.

En el Artículo IV se describe una aplicación de la electroforesis capilar no acuosa (NACE, del inglés *non-aqueous capillary electrophoresis*) a la separación quiral de fármacos, llevada a cabo durante una estancia de investigación en la Katholieke Universiteit of Leuven. Este trabajo responde al interés en desarrollar metodologías basadas en sistemas no acuosos que sean capaces de disolver y analizar nuevos principios activos que sean insolubles en medios acuosos o metanólicos. Muchos fármacos en desarrollo sugeridos por aplicación de la química combinatoria presentan baja solubilidad en agua debida a un elevado peso molecular. Si una molécula objetivo poco soluble en medios acuosos presenta buena potencia y baja toxicidad, puede resultar de interés continuar en fase de desarrollo a pesar de esta baja solubilidad y en estos casos se requieren métodos de análisis quiral para su control analítico. En este trabajo se propuso el uso de dimetilsulfóxido (DMSO) como alternativa a los BGEs de naturaleza alcohólica más comúnmente empleados, debido a su baja volatilidad y toxicidad y mejores propiedades disolventes para moléculas

poco polares. Sin embargo, debe tenerse en cuenta que la enantioseparación en DMSO se encuentra desfavorecida debido a que las fuerzas intermoleculares responsables del enantioconocimiento son más débiles en medios orgánicos (Chankvetadze y Blaschke, 2001).

Se llevó a cabo la separación quiral de tres fármacos, verapamilo, pindolol y fenfluramina, mediante NACE y empleando una optimización univariante para la selección de las mejores condiciones experimentales. Finalmente, se seleccionaron BGEs basados en DMSO y que contenían proporciones variables de metanol (0-30%), HAc 0,5-1 M, NH₄Ac 125 mM y carboximetil- γ -ciclodextrina 40 mM, con una temperatura de separación de 15 °C y un potencial aplicado de 30 kV. Empleando estas condiciones se obtuvieron valores de *Rs* de 1,5; 2,0 y 1,2 para verapamilo, pindolol y fenfluramina, respectivamente. La corriente fue estable durante todas las separaciones llevadas a cabo, a pesar de que uno de los principales problemas de NACE son los frecuentes cortes de corriente.

Los Artículos V-VII de esta Tesis se refieren a la evaluación enantioselectiva de una importante propiedad farmacocinética al nivel de la distribución de fármacos, la unión a proteínas plasmáticas. La cantidad de un fármaco que se une a las proteínas plasmáticas, así como la fuerza de esta unión, influyen considerablemente en la disponibilidad de los fármacos para alcanzar órganos diana y también para su eliminación. Dado que las proteínas plasmáticas son moléculas ópticamente activas, los fármacos quirales pueden presentar diferencias en las propiedades de unión de sus enantiómeros a éstas. Así pues, el desarrollo de metodologías rápidas y fiables para la evaluación *in vitro* de la unión enantioselectiva de fármacos a las proteínas plasmáticas resulta de gran interés para la investigación en la industria farmacéutica. La proteína más abundante en el plasma humano es la albúmina (HSA, del inglés *human serum albumin*), que presenta un elevado grado de enantioselectividad en su unión a fármacos.

En esta Tesis se ha evaluado la unión enantioselectiva de fármacos a HSA y al total de las proteínas plasmáticas mediante ultrafiltración seguida de análisis quiral mediante EKC. En la ultrafiltración se filtra una mezcla pre-equilibrada de fármaco y proteína a través de una membrana que retiene la proteína y sólo permite el paso de

la fracción libre de fármaco. Esta fracción libre se analiza posteriormente, en este caso empleando EKC quiral.

El Artículo V destaca algunos aspectos débiles de las metodologías experimentales y modelos matemáticos previamente publicados para el estudio de la unión a proteínas plasmáticas (Katrachalli y col., 2010; Fielding y col., 2005), y propone una estrategia novedosa para una evaluación fiable de la unión a proteínas. Se lleva a cabo una amplia discusión acerca de los diferentes modelos matemáticos de unión a proteínas, empleando como ejemplo la unión enantioselectiva del antidepresivo fluoxetina a HSA. El análisis enantioselectivo de fluoxetina se realizó empleando HS- β -CD como selector quiral en el modo de llenado completo del capilar, en un tampón fosfato 30 mM de pH 7,0. La temperatura y el potencial de separación se fijaron a 30 °C y 15 kV respectivamente.

La estrategia propuesta implica trabajar en condiciones cercanas a las fisiológicas, por tanto, manteniendo el cociente entre la concentración de fármaco (D) y la de proteína (P) por debajo de 0,5; y P cerca del nivel fisiológico (en torno a 475 μ M). En estas condiciones, se puede emplear un modelo simple de unión que considera que sólo se ocupa un tipo de sitio de unión en la molécula de proteína y que la estequiometría de dicha unión es 1:1, siempre y cuando estas consideraciones se confirmen a través de otras ecuaciones. Además, los datos fueron evaluados con el fin de detectar y eliminar valores anómalos que pudieran afectar a la fiabilidad de las estimaciones. Se estimaron para ambos enantiómeros de fluoxetina constantes de unión enantiómero-proteína (K_1), así como la enantioselectividad en el proceso de unión, definida como el cociente entre ambas constantes.

Finalmente, se estimó para ambos enantiómeros el porcentaje de unión a proteína ($PB\%$, del inglés *protein binding*), que es un parámetro interesante desde un punto de vista farmacocinético. Se obtuvieron porcentajes de 95,2 y 90,0% para el primero y segundo enantiómero eluidos, respectivamente. Se obtuvo una enantioselectividad en torno a 2 en favor del primer enantiómero eluido.

Todavía en el campo de las interacciones enantioselectivas fármaco-proteína, los Artículos VI y VII estudian la unión enantioselectiva del hipnótico zopiclona y del antidepresivo nomifensina a HSA y al total de las proteínas plasmáticas, de nuevo

mediante ultrafiltración y EKC quiral. En el Artículo VI, la enantioseparación de zopiclona con carboximetil- β -ciclodextrina (CM- β -CD) se ajustó para el análisis de la fracción de fármaco libre post-ultrafiltración. Se empleó como selector quiral una disolución de CM- β -CD 30 mM en tampón Tris 50 mM de pH 6,0, que se inyectó en el modo de llenado parcial del capilar aplicando una presión de 0,5 psi durante 99 s antes de la inyección de muestra. La separación quiral se llevó a cabo a 25 °C aplicando un potencial de 15 kV. Los modelos matemáticos y diseños experimentales desarrollados en el Artículo V se aplicaron aquí para el cálculo de las constantes de unión, enantioselectividad y porcentaje de unión a las proteínas plasmáticas. Los valores de *PB%* a HSA fueron 47 y 36% para S- y R-zopiclona, respectivamente, mientras que los valores de *PB%* al total de las proteínas plasmáticas fueron 45 y 49%, respectivamente. Estos valores concuerdan con el *PB%* descrito en la bibliografía para zopiclona racémica, en torno al 45% (Gaillot y col., 1983; Agencia Española del Medicamento, 2011).

La unión enantioselectiva de nomifensina a HSA y al total de las proteínas plasmáticas se evaluó en el Artículo VII, en este caso usando heptakis-(2,3,6-O-metil)- β -ciclodextrina 30 mM como selector quiral en el modo de llenado completo del capilar, con el mismo BGE y potencial de separación del Artículo VI pero con una temperatura del capilar de 50 °C. El diseño experimental para la obtención de curvas de calibrado y análisis de muestras se repitió en dos sesiones independientes con el fin de evaluar la precisión inter-día del procedimiento. Como no se encontraron diferencias significativas entre los datos de ambas sesiones de trabajo, todos los datos se emplearon en conjunto para realizar las estimaciones. El *PB%* a HSA estimado fue de 40 y 63% para el primer y segundo enantiómero eluidos, respectivamente. Para la unión al total de proteínas plasmáticas, los valores estimados fueron de 63 y 64% respectivamente. Comparando estos valores, puede concluirse que el segundo enantiómero eluido de la nomifensina se une principalmente a la HSA, mientras que el primero se une también a otras proteínas plasmáticas.

El diseño experimental y los modelos matemáticos propuestos en esta Tesis para una estimación fiable de la unión enantioselectiva de fármacos a las proteínas

plasmáticas mediante ultrafiltración y EKC han demostrado ser una herramienta robusta que permite la obtención de buenas estimaciones *in vitro* en condiciones cercanas a las fisiológicas, proporcionando por lo tanto datos valiosos desde un punto de vista farmacocinético. En esta Tesis se han estimado datos de unión enantioselectiva de fluoxetina, zopiclona y nomifensina a las proteínas plasmáticas, completando la información disponible en la bibliografía sobre estos fármacos.

La tercera parte de esta Tesis se dedica al desarrollo de reacciones enzimáticas en el interior del capilar empleando la metodología EMMA. En EMMA los reactivos se introducen secuencialmente en el capilar electroforético y se dejan mezclar y reaccionar durante un tiempo determinado. Después se lleva a cabo la separación de sustratos, enzimas y productos mediante electroforesis. La principal ventaja de la metodología EMMA es que la reacción tiene lugar a escala de nanolitros, por lo que el consumo de reactivos y muestras es extremadamente bajo. Además, es una metodología completamente automatizada, ya que la reacción y la separación tienen lugar en una única etapa en el interior del capilar, lo que constituye otra importante ventaja para su empleo en procedimientos de cribado.

En el Artículo VIII se desarrolla una metodología de cribado mediante EMMA para la evaluación de inhibidores de la acetilcolinesterasa (AChE), y se aplica al estudio de cinco fármacos de actividad inhibidora conocida. Para la optimización de condiciones del método se empleó tacrina como fármaco modelo. El avance de la reacción enzimática de hidrólisis de acetiltiocolina en presencia de AChE y de los diferentes inhibidores se determinó midiendo el área de pico del producto de reacción tiocolina. Se llevó a cabo una inyección en "sándwich", introduciendo una zona de sustrato entre dos zonas de enzima. El mezclado de las zonas se llevó a cabo mediante difusión simple, con un tiempo de incubación de 2 minutos. El tampón empleado para la reacción y la separación fue borato-fosfato 30 mM a pH 8,0; la temperatura del capilar se fijó a 37 °C y el potencial de separación a 15 kV. Debido a la dilución de los solutos en la metodología EMMA, se realizó una corrección en los cálculos para obtener una buena exactitud en los resultados. Se estimó un factor de dilución comparando la potencia inhibitoria de la tacrina calculada en este trabajo con la

descrita en la bibliografía empleando el método de referencia (Andrisano y col., 2001). Dicho factor se aplicó posteriormente a todos los cálculos realizados.

La metodología de cribado propuesta ha demostrado ser de utilidad para la estimación de constantes de inhibición, potencia inhibitoria, una aproximación cualitativa al mecanismo de inhibición y el porcentaje de inhibición de tacrina, edrophonium, neostigmina, piridostigmina y eserina. Los resultados del cribado muestran que, de acuerdo con su porcentaje de inhibición en condiciones prefijadas, el orden de potencia inhibitoria para estos compuestos es tacrina > edrophonium > neostigmina > eserina > piridostigmina. Esta metodología de cribado, con un tiempo de análisis inferior a 5 minutos, puede ser empleada para la evaluación de nuevas moléculas que sean inhibidores potenciales de la AChE.

Continuando con el uso de la metodología EMMA para la evaluación de interacciones fármaco-enzima, los Artículos IX y X son estudios de metabolismo enantioselectivo empleando diferentes isoformas del citocromo P450. En estos estudios, el capilar actúa simultáneamente como reactor y como sistema de separación quiral, de modo que proporciona información enantioselectiva a través de un ensayo rápido y completamente automatizado. La separación quiral se lleva a cabo en ambos casos usando HS- β -CD y la técnica del llenado parcial del capilar.

El Artículo IX hace referencia al metabolismo enantioselectivo de verapamilo, bloqueante de canales de Ca^{+2} , mediante CYP3A4, la isoforma más importante del citocromo P450 en humanos. En este artículo se consideraron diferentes posibilidades para el ensayo mediante EMMA y se optimizaron variables experimentales previamente al cálculo de los parámetros cinéticos de Michaelis-Menten para el metabolismo enantioselectivo del verapamilo. Las condiciones experimentales seleccionadas incluyeron una inyección tipo "sándwich" de la zona de sustrato entre dos zonas de enzima, y la inyección de dos zonas de tampón de incubación antes y después del "sándwich" con el fin de proporcionar a la enzima su medio de reacción adecuado. El mezclado de las zonas se llevó a cabo mediante difusión simple durante un tiempo de incubación de 5 min. A continuación se llevó a cabo la separación de toda la mezcla de reacción incluyendo los enantiómeros del verapamilo y su metabolito principal norverapamilo en el mismo capilar, empleando

las siguientes condiciones experimentales: fosfato 50 mM de pH 8,8 como BGE, HS- β -CD al 2,5% inyectada a 10 psi/2 min, 25 °C y separación a 20 kV con una pequeña presión de 0,2 psi con el fin de acortar los tiempos de migración. El resultado es una metodología completamente automatizada que permite la evaluación enantioselectiva del metabolismo de verapamilo por el CYP3A4 en menos de 35 minutos, incluyendo el acondicionamiento previo del capilar, inyección, incubación y separación.

A partir de la ecuación de Michaelis-Menten se calcularon parámetros cinéticos (K_m y V_{max}) para el metabolismo global de verapamilo por el CYP3A4. Los valores de K_m estimados fueron de 51 ± 9 y 47 ± 9 μM para S- y R-verapamilo, respectivamente, mientras que los valores de V_{max} obtenidos fueron 22 ± 2 y 21 ± 2 $\text{pmol}\cdot\text{min}^{-1}\cdot(\text{pmol CYP})^{-1}$ para S- y R-verapamilo, respectivamente. También se calcularon para cada enantiómero valores de aclaramiento intrínseco, definido como la cantidad de plasma de la cual el fármaco es eliminado por unidad de tiempo, y estimado *in vitro* como el cociente entre V_{max} y K_m (Kroemer y col., 1992).

El metabolismo enantioselectivo de fluoxetina mediante otra isoforma del CYP450, CYP2D6, se evaluó en el Artículo X siguiendo la misma metodología que en el trabajo anterior. Las condiciones del ensayo EMMA empleadas en el Artículo IX se aplicaron directamente, mientras que las condiciones de separación se ajustaron con el fin de separar los enantiómeros de fluoxetina y su metabolito principal norfluoxetina. Se estudió la influencia de la variable experimental más importante en la enantioseparación, la concentración de HS- β -CD, y se seleccionó una concentración final de 1,25% para la separación de la mezcla de reacción. Las otras condiciones de separación fueron las empleadas en el Artículo IX. Se estimaron parámetros cinéticos mediante un ajuste no lineal de los datos experimentales a la ecuación de Michaelis-Menten. Los valores de K_m obtenidos fueron de 30 ± 3 μM para S-fluoxetina y 39 ± 5 μM para R-fluoxetina, mientras que las V_{max} estimadas fueron de $28,6 \pm 1,2$ y 34 ± 2 $\text{pmol}\cdot\text{min}^{-1}\cdot(\text{pmol CYP})^{-1}$ para S- y R-fluoxetina, respectivamente. El ensayo cinético fue repetido empleando un único enantiómero (R-fluoxetina) en lugar de la mezcla racémica. Se obtuvieron resultados similares, lo que indica que el uso del racemato es una buena opción para la obtención de estimaciones enantioselectivas.

En esta Tesis se ha demostrado la utilidad de EMMA como metodología de cribado para la evaluación *in vitro*, enantioselectiva o no, de interacciones fármaco-enzima. Los métodos desarrollados permiten la estimación de parámetros cinéticos y de inhibición mediante ensayos rápidos con un bajo consumo de reactivos y muestras. El acoplamiento de la metodología EMMA con la enantioseparación de sustratos y productos en una única etapa llevada a cabo en el equipo de electroforesis capilar proporciona valiosa información enantioselectiva sobre los procesos farmacocinéticos o farmacodinámicos evaluados.

Todos los métodos propuestos y aplicados en esta Tesis (separaciones quirales, modelos de predicción, evaluación enantioselectiva de la unión a proteínas e interacciones fármaco-enzima) son de aplicación en la industria farmacéutica para la obtención de información útil *in vitro* en las fases preclínicas del desarrollo de medicamentos, y para el control de calidad enantioselectivo de materias primas, intermedios de síntesis y productos finales.



I. INTRODUCTION

I. INTRODUCTION

I.1. Chirality and its importance in pharmaceutical sciences

Chirality is a structural characteristic of a molecule whereby it is able to exist in two asymmetric forms, which are non-superimposable. These two asymmetric forms are known as enantiomers (Figure I.1), and are non-distinguishable by a physicochemical point of view due to their identical properties like melting point, lipophilicity or acidity constant.

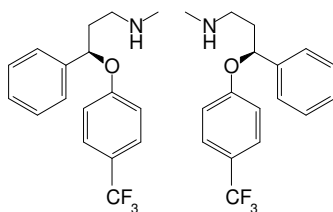


Figure I.1: The two enantiomers of a chiral drug (fluoxetine).

However, the body can readily distinguish between such molecules. Because the two enantiomers are non-superimposable they have different abilities to bind to receptors or enzymes and this confers stereoselectivity to all the processes in which a specific site interaction with biomolecules is involved (Evans, 2004).

An important percentage of commercially available drugs and molecules that are in the stage of drug development have a chiral center and could be employed as racemates or as pure enantiomers. When a racemic drug enters the human body, there are some pharmacokinetic and pharmacodynamic processes that may exhibit a certain degree of enantioselectivity, so it could result in different pharmaceutical activity of the enantiomers (Brocks, 2006). Due to that, the Food and Drug Administration (FDA) (USA) and the European Medicines Agency have developed regulations and guidance for the development of chiral drugs and investigation of chiral active substances (Food and Drug Administration, 1992; European Medicines Agency, 1993).

The FDA considers that the development of racemates as new drugs may continue to be appropriate despite the advances carried out in asymmetric synthesis, which

make possible the synthesis of pure enantiomers for some pharmaceuticals. However, some considerations should be taken into account in product development (Food and Drug Administration, 1992):

- Appropriate manufacturing and control procedures should be used to assure stereoisomeric composition of a product, with respect to identity, strength, quality and purity.
- Pharmacokinetic evaluations that do not use a chiral assay will be misleading if the disposition of enantiomers is different. Therefore, techniques that quantify individual stereoisomers in pharmacokinetical samples should be available early.

The FDA also indicates that the main pharmacological activities of the isomers should be compared in *in vitro* systems, in animals and/or in humans. The European Medicines Agency emphasizes that when new active substances appear promising, both enantiomers should be studied separately (European Medicines Agency, 1993) in terms of pharmacokinetic and pharmacological properties. This is applicable both to racemates and single enantiomer formulations.

Due to all these reasons, there is a special interest in analytical methods able to determine the stereoisomer ratios in synthetic products, pharmaceutical formulations and biological samples (Scriba, 2011), and also in methodologies for the *in vitro* evaluation of enantioselective pharmacokinetic and pharmacological properties.

I.1.1. Enantioselectivity in pharmacokinetic processes

The term pharmacokinetics involves all the processes that take part since a drug enters the human body and until the moment it is eliminated by different pathways. Pharmacokinetic processes are drug absorption, distribution, metabolism and excretion, and all of them can be affected by enantioselectivity. The main prerequisite of a biological process for being enantioselective is stereospecific recognition of the substrate by a biomolecule responsible for the process (Brocks, 2006). So, markedly enantioselective are processes that involve interaction with

specific sites of biomolecules, like active transport, protein binding or enzymatic reactions such as metabolism.

I.1.1.1. Absorption

The absorption of a drug is the process that takes place from the administration of the drug until it reaches the circulatory system. The complexity of the absorption process depends on the administration route, which is the way the drug is administered to the patient. It can be intravenous, parenteral extravascular (where the drug is injected but not directly to a vein, like the intramuscular injections), oral, nasal, sublingual, ophthalmic... and each one has an absorption process dependent on the tissues and epitheliums the drug may pass.

Intravenous administration has no absorption since the drug is directly introduced in the circulatory system. In other parenteral routes the drug has to reach the blood by passing through the vascular endothelium. Most of the existent administration routes imply the pass of the drug through epithelial cells, like the intestinal, gastric or nasal epithelium (Doménech Berrozpe *et al.*, 1998). Oral administration is by far the most common route and most of the drugs orally taken have their absorption window in the intestine. So, the mechanisms responsible for intestinal absorption are the most frequently studied.

The main process responsible for the intestinal absorption of the majority of drugs is passive diffusion through the intestine membrane, which is due purely to the lipophilicity and degree of ionization of the drugs. Since there will be no difference in these parameters between two enantiomers, there will be no difference in the extent or rate of absorption and passive diffusion can be considered achiral (Evans, 2004).

When active transport with carrier proteins is responsible for the intestinal absorption, however, differences in absorption between enantiomers can be found. There have been reported preferential absorptions for the L-isomer of dopamine (Lee and Williams, 1990), R-methotrexate (Hendel and Brodthages, 1984), D-eflornithine (Jansson *et al.*, 2008) and R-fexofenadine (Togami *et al.*, 2012) after oral administration. In the case of D-eflornithine, the preferential absorption is for

the less potent enantiomer, which may be the cause of the failure of this drug in oral treatments (Jansson *et al.*, 2008).

I.1.1.2. Distribution and protein binding

The distribution of a drug involves its penetration, movement and storage in different tissue compartments. The distribution properties of a drug are of vital importance, since they determine if the drug can reach the active site and be effective. As distribution requires interaction with biomolecules, there is some potential for enantioselectivity in its processes. One important process at the distribution level is the protein binding (PB). Drugs usually do not travel through the circulatory system themselves, but they bind to different plasmatic proteins. This can affect their disposition for other processes such as first-pass metabolism, metabolic and renal clearance, and distribution to other compartments. Acting as drug carriers, plasma proteins facilitate their transport throughout the body but also can limit their availability for reaching target organs, since only the free fraction of the drug can leave plasma and penetrate membranes.

When proteins and chiral drugs interact in an enantioselective way, two diastereomeric adducts are formed with potential differences in the protein binding that may result in different pharmacokinetic profiles for the individual enantiomers (Chuang and Otagiri, 2006). For drugs that are highly protein bound, small changes in protein binding result in large changes in the free active fraction and thus the therapeutic benefit of such compounds can be markedly affected by stereoselective protein binding. Enantioselective binding of drugs to human serum albumin (HSA) and other plasma proteins has been extensively described in the literature (Martínez-Gómez *et al.*, 2007a; Brocks, 2006). Stereoselectivity in protein binding has been described in the literature for verapamil (Mehvar *et al.*, 2002), warfarin (Yacobi *et al.*, 1977), propranolol (Mehvar and Brocks, 2001) and some antihistamines (Martínez-Gómez *et al.*, 2007b) among much other drugs.

Human serum albumin

HSA is the most abundant protein in human plasma (60 per cent of the total plasma proteins, (Evans, 2004)) and it presents a high degree of enantioselective interaction with drugs (Ascoli *et al.*, 2006). Its interaction with xenobiotics is mainly due to hydrogen bonds and Van der Waals intermolecular forces, which can be markedly different between enantiomers due to the spatial position of the interacting groups in the molecules. HSA is a single peptide chain of 585 amino acid residues. Its 3D structure, shown in Figure I.2, consists of a monomeric globular protein made out of three domains, I, II and III, with a similar helical pattern (He and Carter, 1992; Carter and Ho, 1994; Sugio *et al.*, 1999).

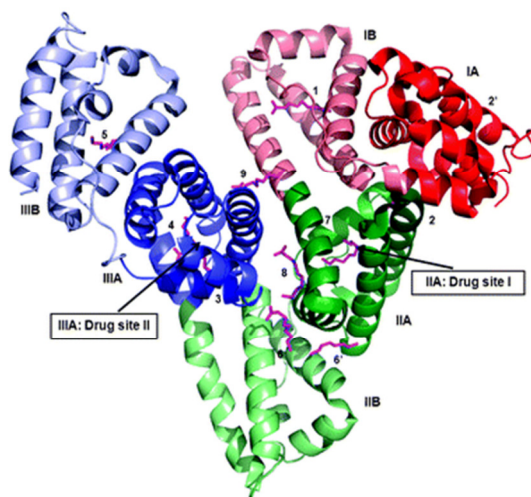


Figure I.2: Structure of HSA with its two main binding sites for drugs.

Two primary areas of “high affinity” drug binding sites have been defined on albumin. These have been denominated the warfarin site (site I) and the benzodiazepine site (site II) (Ascoli *et al.*, 2006; Kwong, 1985; Kurz, 1986). Site I is the highest-affinity binding site for, among others, anticoagulants and non-steroidal anti-inflammatory drugs. Site II is also a specific site for profens, an important family of drugs used worldwide as anti-inflammatories.

Despite the fact that sites I and II seem to be responsible for most of the drug-HSA interactions, crystallographic (Hage and Sengupta, 1998; Hage and Sengupta, 1999) and chromatographic studies (Sengupta and Hage, 1999; Hage and Sengupta, 1999) confirm the existence of other less important binding sites in the HSA molecule, like digitoxin site (site III) or the bilirubin and tamoxifen sites, which are still not well identified in the HSA molecule.

α_1 -acid glycoprotein and other plasma proteins

The second plasma protein in abundance is α_1 -acid glycoprotein (AGP). This is a monomer of 181 amino acids and is characterized by its high carbohydrate content. Binding of drugs to AGP involves hydrophobic rather than electrostatic forces, and not only basic but also acidic and neutral drugs bind to AGP. The contribution of AGP to the total plasma protein binding of drugs is much lower than HSA's, due to its lower concentration in plasma. The binding of drugs to AGP can be also enantioselective.

Also lipoproteins can show a certain ability to bind hydrophobic drugs, which are thought to be partitioning into the lipid core of the protein instead of associating with a specific site, so no enantioselectivity may be expected for this interaction (Evans, 2004).

I.1.1.3. Metabolism

The main objective of the organism when exposed to some xenobiotics (including drugs) is to remove them from the body as soon as possible. The efficient removal of drugs from the organism involves not only their renal excretion but also some structural changes in the molecule that are called metabolism. Metabolic reactions usually make xenobiotics more polar and easier to be excreted and can be classified into two groups attending to the nature of the molecule modification.

Phase I includes some reactions that generally lead to the introduction or uncovering of key functional groups (e.g. OH, COOH, NH₂, SH, etc.) increasing the molecule polarity, which may facilitate removal from the body. The main enzymatic system

responsible for phase I reactions is the cytochrome P450 (CYP), despite other enzymes can be also involved. In phase II metabolism there is a conjugation between the xenobiotic and some endogenous molecule or group. It increases the molecule size favoring its excretion and usually its inactivation. Not all compounds suffer phase I and II processes. For some ones this is the case, but others are directly eliminated after a phase I metabolic reaction or are directly conjugated by a phase II one. Table I.1 summarizes the different reactions involved in phases I and II metabolism (Gordon Gibson and Skett, 2001; Doménech Berrozpe *et al.*, 1998).

Table I.1: Phase I and II metabolic reactions.

Phase I	Phase II
Oxydation	Glucuronidation/glucosidation
Reduction	Sulfation
Hydrolysis	Methylation
Hydration	Acetylation
Dethioacetylation	Amino acid conjugation
Isomerisation	Glutathione conjugation
	Fatty acid conjugation
	Condensation

Cytochrome P450

The cytochrome P450s (CYPs) are a superfamily of haemthiolate containing enzymes which play a major role in the metabolism of many drugs and other xenobiotics such as organic solvents, pesticides, hydrocarbons and carcinogenic substances. The name P450 is due to their light absorption at 450 nm when combined with carbon monoxide (Doménech Berrozpe *et al.*, 1998). Their structure, with the haem group in the center of the molecule, is shown in Figure I.3 (Williams *et al.*, 2003).

It has been estimated that more than 90 per cent of drug oxidations in humans are mediated by CYPs (Lewis, 2003). In addition to their role in drug metabolism, CYPs

have important endogenous functions such as the synthesis and regulation of steroid hormones, eicosanoids and bile acids. Because of this, CYPs are almost ubiquitous in the human body, although the major site of drug metabolism is the liver (Evans, 2004).

57 human CYPs have been identified (Lewis, 2004), and are classified with a systematic nomenclature that is based on the amino acid sequence on each isoform, which does not provide information on the function of the enzymes. The group of isoforms majorly involved in human drug metabolism is currently limited to only six: CYP1A2, 2C9, 2C19, 2D6, 3A4 and 3A5 (Evans, 2004). CYP3A4 is the most abundant isoform in the human liver and is responsible of almost half of P450-mediated oxidations of drugs available on the pharmaceutical market as well as a high number of clinically significant drug-drug interactions.

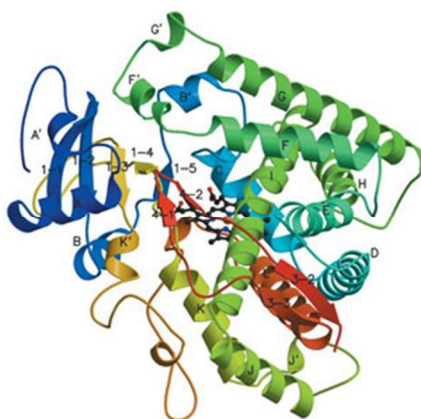


Figure I.3: Structure of cytochrome P450 (isoform 2C9).

The catalytic cycle of CYP, schematized in Figure I.4 (Kirsty *et al.*, 2006), includes the following steps (Ortiz de Montellano, 2005):

- i. Binding of substrate (RH) to the enzyme, sometimes accompanied by a spin-state change of the iron, to afford an enzyme-substrate adduct.

- ii. Reduction of the ferric CYP by an associated reductase with an NADPH-derived electron to the ferrous CYP.
- iii. Binding of molecular oxygen to the ferrous heme to produce a ferric CYP-dioxygen complex.
- iv. Second one-electron reduction.
- v. Protonation to arrive at the Fe(III) hydroperoxy complex.
- vi. Protonation and heterolytic cleavage of the O-O bond with concurrent production of a water molecule to form a reactive iron-oxo intermediate.
- vii. Oxygen-atom transfer from this iron-oxo complex to the bound substrate to form the oxygenated product complex.
- viii. Product dissociation.

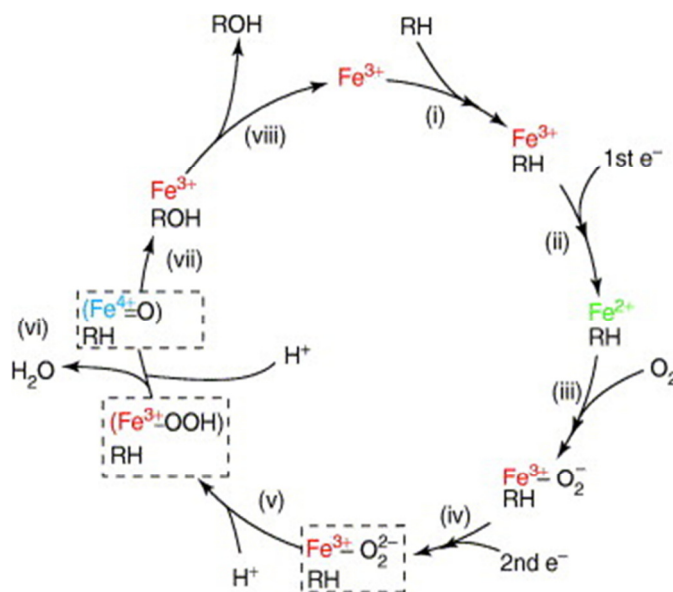
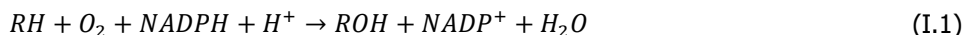


Figure I.4: The catalytic cycle of cytochrome P450.

In this catalytic cycle, the reductase redox partner of CYP (P450 reductase) supplies sequentially reducing equivalents employing reduced nicotinamide adenine

dinucleotide phosphate (NADPH) as a cofactor. Protons employed in protonation steps are taken from the reaction medium. The general equation for a P450-mediated mono-oxygenation, that summarizes this cycle, is generally reported as follows:



where *RH* is the substrate, *ROH* the oxidized product, and *NADPH/NADP⁺* the reduced/oxidized forms of nicotinamide adenine dinucleotide phosphate.

Although CYPs have broad substrate specificity, they show significant stereoselectivity of metabolism towards chiral substrates. A good example illustrating this enantioselectivity is the case of the anticoagulant warfarin, for which the clearance (amount of plasma from which a drug is removed in a certain time) of the R-enantiomer is 42 per cent greater than that of the S-enantiomer (Toon *et al.*, 1987). This should be due to the fact that CYP3A4 metabolizes R-warfarin and CYP2C9, whose amount in human liver is lower than that of the 3A4 isoform, metabolizes the S-enantiomer (Rettie *et al.*, 1988). There have been also reported enantioselective hepatic clearances for the β -blocker propranolol (Walle *et al.*, 1988), the calcium channel antagonist verapamil (Eichelbaum *et al.*, 1984; Thöm *et al.*, 2012) and the antiarrhythmic propafenone (Afshar and Thormann, 2006). Some proton pump inhibitors (omeprazole, lansoprazole, pantoprazole or tenatoprazole) are also enantioselectively metabolized by different isoforms of CYP (Zhou *et al.*, 2008).

Unless the main enzymatic system responsible for drug metabolism is the CYP, there are some other enzymes involved in phases I and II metabolism, and their reactions can also exhibit enantioselectivity. There have been reported enantioselective N-oxygenations for chlorpheniramine and verapamil catalyzed by flavin-containing monooxygenases (FMOs), which are also important phase I metabolic enzymes (Cashman *et al.*, 1992; Cashman, 1989). Metabolic pathways for different amphetamines have found to be also enantioselective, since different elimination has been reported for their enantiomers *in vivo*. Metabolism of these compounds involves different enzymes, starting with CYP, and continuing with different pathways including another phase I reaction with catechol-*O*-methyl transferase and

some phase II conjugations by sulfotransferases and glucuronyltransferases. All of them have found to exhibit a certain degree of enantioselectivity (Schwaninger *et al.*, 2012).

I.1.1.4. Renal clearance

Renal clearance is the amount of plasma from which a drug is removed by a renal pathway in a certain time. Enantioselectivity in renal clearance of drugs will only be found if they are actively secreted by tubular transporters, which may have different affinity for the enantiomers. This is the case of disopyramide (Lima *et al.*, 1985) and terbutaline (Borgstrom *et al.*, 1989). Also enantioselective renal clearance has been reported for the antihelmintic albendazole (Lanchote *et al.*, 2004). Nevertheless, the majority of drugs are filtered in the glomerulus and not actively secreted, so there will be no difference in the elimination of enantiomers (Evans, 2004).

I.1.2. Enantioselectivity in pharmacodynamic properties

Pharmacodynamics is the brand of pharmaceutical sciences that studies all the effects that a drug has over the organism. As the pharmacological activity of a drug involves in most of the cases its specific interaction with biomolecules (receptors, carriers, enzymes...), it becomes obvious that many differences in the pharmacodynamic properties of chiral drugs will be found. The case of thalidomide is a well-known example of the different pharmacological activity of two enantiomers. Thalidomide was employed in the 50s for the treatment of nausea in pregnant woman. In 1961 it was withdrawn from the pharmaceutical market because of its teratogenic effects (Kumar *et al.*, 2012), and it was discovered that despite the R-enantiomer had the desirable pharmacological activity, the S- one was highly teratogenic in humans (Caillet *et al.*, 2012).

The different behavior of thalidomide enantiomers reflects the importance of chirality in drug development. There are many other cases in which both enantiomers of a chiral drug act in a different way when introduced into the human body. Sometimes one of the enantiomers is active while the other has no pharmacological activity

(only the S-enantiomer of the hypnotic drug zopiclone is active (Monti and Pandi-Perumal, 2007), and the S-enantiomers of profens are responsible for the cyclooxygenase inhibitory activity (Klegerisa *et al.*, 2004)). In other cases one of them exhibits stronger activity (the S-enantiomer of the antidepressant citalopram is approximately 150 times more potent as a reuptake inhibitor than R-citalopram *in vitro* (Leonard and Taylor, 2010)). They can also have different pharmacological effects (dextromethorphan is widely employed as an antitussive agent and levomethorphan is a narcotic (Kikura-Hanajiri *et al.*, 2011)). Finally, one enantiomer can be active and the other responsible for the side effects of the drug, like the case of thalidomide.

Nowadays, there is an increasingly interest in the introduction of pure enantiomers in the pharmaceutical market. Apparently new drugs such as dextroketo profen (analgesic), eszopiclone (hypnotic), esomeprazole (proton pump inhibitor) or escitalopram (antidepressant) are only the active enantiomers of the racemic keto profen, zopiclone, omeprazole and citalopram, also commercialized. A great effort is being done in the study of enantioselective pharmacological as well as pharmacokinetic properties, in order to obtain drugs with higher potency, better safety profiles and fewer side effects.

I.2. Chiral analysis

The importance of chirality in pharmaceutical sciences has been widely discussed during this Introduction. As a consequence, different methods for the chiral analysis of drugs have been developed employing diverse methodologies.

Chiral separations can be carried out employing direct or indirect methodologies. The indirect way implies derivatization of enantiomers with an enantiomerically pure reagent, and the formation of diastereoisomers that can be separated with classical separation techniques. The direct approach consists on the formation of transitory complexes between the enantiomers and a chiral molecule (called chiral selector) in a separation system. Chiral recognition in direct methods can be due to electrostatic forces, hydrogen bonds, Van der Waals forces, hydrophobic interactions or inclusion phenomena. The direct way is easier, faster and cheaper than the indirect

one, so nowadays is the preferred for carrying out chiral separations, especially in analytical scale (Martínez Gómez, 2007c).

The most usually employed analytical techniques for performing direct separations are thin-layer chromatography (TLC), high-performance liquid chromatography (HPLC), gas chromatography (GC) and capillary electrophoresis (CE). The first direct enantioseparation was carried out by GC with a chiral stationary phase (CSP) in 1966 (Gil-Av *et al.*, 1966). The enantiomers of an amino acid were separated there. Since then, applications have been developed with a broad variety of performances: inclusion of the chiral selector in the stationary phase or in the mobile phase, development of chiral columns for HPLC and GC, development and research on new families of chiral selectors and, more recently, synthesis of monolithic chiral stationary phases and the introduction of nanomaterials in different separation techniques.

Nowadays most of the applications are carried out by HPLC and CE. Nevertheless, a recent review remarks the importance of TLC also in this field, due to its simplicity, flexibility and low cost. Chiral TLC is performed using chiral stationary phases, both commercial and home-made. The most frequently used CSPs are home-made of cellulose derivatives: microcrystalline cellulose triacetate and cellulose tribenzoate (Del Bubba *et al.*, 2013). Their main disadvantage is their lack of reproducibility.

In HPLC, the chiral selector can be in the stationary phase (CSP) or added to the mobile phase. Numerous chiral molecules are employed as CSPs: polysaccharide derivatives (cellulose, amylose), which are the most commonly employed, synthetic polymers, proteins (HSA, AGP), cyclodextrins and crown ethers among others (Lämmerhofer, 2010). A recent trend is the use of monolithic chiral columns for micro- and nano-LC (Healey and Ghanem, 2013), which can be home-made with the same chiral selectors available in commercial CSPs (cyclodextrins, polysaccharides, proteins...). Less employed is the addition of chiral selectors to the mobile phase, due to the high consumption of chiral selector. For this methodology, the use of nano-LC is a good alternative since the working flow rate is of a few hundred nanoliters per minute (Rocco *et al.*, 2013). These new possibilities have improved the performance of HPLC as an analytical technique for chiral analysis.

However, chiral CE is considered superior to chiral HPLC by many authors, because chiral HPLC is suffering from low peak capacity (broad peaks), problems with system stability (often normal phase HPLC), pressure sensitivity of columns (often cellulose-based chiral columns) and long separation times (Ahuja and Jimidar, 2008). CE is nowadays the technique of choice for analytical-scale enantioseparations, due to its numerous advantages as separation technique and the broad variety of chiral selectors available for performing separations in many different CE modes. The next section of this Introduction deals with the separation features of CE and its applications in chiral analysis.

Another recent trend in enantioseparations which merits special mention is the use of nanomaterials in different separation techniques. This use has several advantages such as the easy modification of the nanomaterials with chiral selectors, to be used as chiral stationary or pseudo-stationary phases; the increment on column capacity, separation selectivity, stability and efficiency for chiral chromatographic separations, and the unique surface properties of nanomaterials that allow the development of simple, rapid and sensitive sensors for chiral recognition (Chang *et al.*, 2012). Mesoporous silica nanomaterials have been successfully employed for chiral separations in HPLC (Guo *et al.*, 2010) and CE (Dong *et al.*, 2008); gold nanoparticles modified with β -cyclodextrin and bovine serum albumin in CE (Li *et al.*, 2011; Li *et al.*, 2009); and carbon nanotubes with different surface modifications in TLC (Yu *et al.*, 2011), GC (Zhao *et al.*, 2011) and CE (Moliner-Martínez *et al.*, 2007).

1.3. Capillary electrophoresis for chiral analysis and enzymatic studies

Capillary electrophoresis is a powerful separation technique whose basic separation principle is the different mobility of ions when affected by an electric field. Since the first application of an open-tubular glass capillary as electrophoretic separation system, which was carried out by Jorgenson and Lukacs in 1981 (Jorgenson and Lukacs, 1981), several improvements in the CE instrumentation have been done and applications of CE in different fields like analysis of clinical, pharmaceutical or environmental samples, separation of enantiomers, in-capillary reactions, separations of peptides, proteins and DNA and much others have been developed.

The main advantages of CE, which make it a technique of choice for several applications, are its short analysis time, low consumption of samples and reagents, high separation efficiency, versatility of conditions and performances that can be employed, easy conditioning of the column, compatibility with different detection systems and ease of automation (Lin *et al.*, 2003; Zhu *et al.*, 1999). Its main bottlenecks, when compared with liquid and gas chromatography, are less sensitivity (due to the small detection window) and less reproducibility (due to the injection procedure). However, different strategies have been developed to get over these disadvantages and nowadays CE can be successfully employed for many applications.

The CE instrumentation is relatively simple: it consists on a fused silica capillary whose extremes dip into two vials full of an electrolyte solution. Also two electrodes dip into these two vials and are connected to a high power source that applies the electric voltage to the system. The instrument is completed with a detection system and a computer for data acquisition. Figure I.5 shows a scheme of the CE instrument.

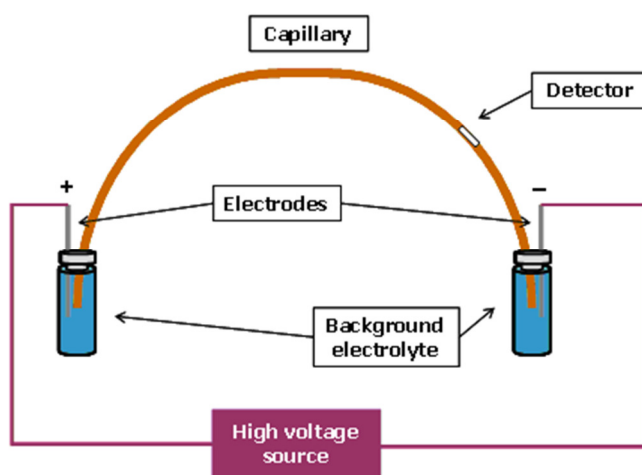


Figure I.5: Scheme of a CE system.

For samples injection, one of the electrolyte vials is replaced by the sample vial and some pressure or voltage is applied to it. The injection is called hydrodynamic when carried out by pressure, or electrokinetic when done by voltage. The actual CE systems allow injecting by both sides of the capillary, changing the polarity of the separation and separating simultaneously by voltage and pressure. They also allow the control of the capillary temperature (which is an important variable for separations) and sometimes also the sample storage temperature. All these characteristics increase notably the possibilities for development of new applications.

1.3.1. Principles of separation in CE

There are several modalities of CE with different separation mechanisms. In the simplest way, capillary zone electrophoresis (CZE), the separation of molecules is mainly due to two phenomena that contribute to their mobility through the capillary. The first phenomenon is the self-mobility of ions when introduced in an electric field, whereby positive molecules will migrate to the cathode, negatives to the anode and neutral ones will not migrate. The migration velocity is a function of the molecule charge/mass ratio. The second phenomenon is called electroosmotic flow (EOF), and will be briefly explained below.

Electroosmosis is a basic phenomenon in all electrophoretic separation processes. It can be described as the relative movement of a liquid to a fixed charged surface caused by an electric field. It takes place when a voltage is applied to a liquid system that is in close contact with a charged surface, as is the case of CE in a fused silica capillary (Kuhn and Hoffstetter-Kuhn, 1993). The capillary wall in a fused silica capillary is covered by silanol (Si-OH) groups, which are deprotonated when the pH of the background electrolyte (BGE) is above 4.0. Higher pH values lead to a more negative capillary wall.

The magnitude and the direction of the EOF depend on the composition of the capillary and the nature of the solution within the tube. Empirically it was discovered that the phase with the higher dielectric constant is positively polarized versus the other. Due to its extremely high dielectric constant, water is usually positively polarized in comparison to the fused silica surface, and a thin double layer appears

in the capillary wall. If an electric field is applied across the fused silica capillary, the mobile ions of the solution migrate with their hydrate water towards the cathode resulting in a flow of the whole solution (Kuhn and Hoffstetter-Kuhn, 1993).

At working pHs above 4.0, as a consequence of the combination of the EOF and their self electrophoretic mobility, all molecules migrate to the detector being the typical elution order the following: positively charged molecules (from smaller to bigger), neutral, and negatively charged ones (from bigger to smaller). This migration order is schematically represented in Figure I.6.

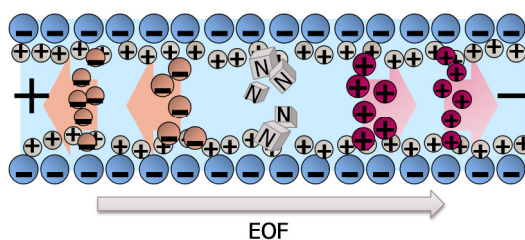


Figure I.6: Migration order in capillary electrophoresis.

I.3.2. Chiral analysis in CE

Chiral separations by CE are due to a chromatographic principle, not an electrophoretic one. As described in section I.3.1, two phenomena are responsible for the mobility in a CE system (the electrophoretic mobility of molecules, due to their charge/mass ratio, and the electroosmotic flow), and none of them are enantioselective. Thereby, the enantioseparation takes place due to the different non-covalent molecular interaction of the enantiomers with a chiral selector, whose electrophoretic mobility is different to that of the enantiomers (Chankvetadze and Blaschke, 2001). All the enantioseparations in CE may be unified under the term capillary electrokinetic chromatography (EKC), introduced by Terabe and coworkers in 1985 (Terabe *et al.*, 1985), where a pseudo-stationary phase takes part in the separation of compounds. In chiral EKC the host-guest complexation between the selector (pseudo-stationary phase) and the enantiomers is responsible for the

enantiodifferentiation and the electrophoresis and electroosmosis permit differential migrations of the host-guest complexes.

I.3.2.1. Chiral selectors in CE

Different chiral selectors have been employed in EKC for carrying out enantioseparations, including natural, semisynthetic and synthetic ones. Some of the most commonly used chiral selectors are the following:

- **Proteins:** HSA, bovine serum albumin (BSA), AGP and ovomucoid protein (OVM) have been widely employed with this purpose. Proteins show a broad range of enantioselectivity due to multiple possibilities of intermolecular interactions with the chiral compounds (Martínez-Gómez *et al.*, 2007d). Their main drawback, which can be overcome with an adequate capillary cleaning, is the variability of the results due to unspecific adsorption of proteins to the capillary wall.
- **Cyclodextrins (CDs):** polysaccharides with cyclic structure, formed by 6 (α -CD), 7 (β -CD) and 8 (γ -CD) glucose units (Figure I.7). Together with these three native CDs, there are actually several derivatized ones in which the $-\text{OH}$ residues have been substituted by different functional groups in order to increase the interaction with chiral molecules.

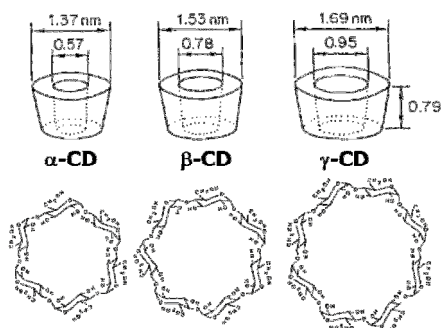


Figure I.7: Structure and dimensions of the three native CDs.

- **Micellar polymers:** polymers recently synthesized whose micelles are formed by covalent bounds, so there is not a micellar critic concentration. This kind of selectors, like poly(sodium N-undecenoxy carbonyl-L-leucinate) (poly-L-SUCL) or poly(sodium N-undecenoxy carbonyl-LL-leucyl-valinate) (poly-LL-SUCLV), have been employed for the enantioseparation in CE-MS (Sánchez-Hernández *et al.*, 2008; Kahle and Foley, 2007).
- **Crown ethers:** synthetic chiral selectors that are employed for the enantioseparation of analytes with a primary amine group, like amino acids. The enantio recognition mechanism is the formation of hydrogen bounds between the O atom of the ether and the H atom of the amine group (Schmid and Gübitz, 2004).
- **Glycopeptides:** natural antibiotics like vancomycin, ristocetin A and teicoplanin. Widely employed due to their high enantioselectivity and the broad range of compounds they can resolve (Kahle and Foley, 2007; Ward and Farris, 2001).
- **Metallic complexes with chiral ligands:** chelates of metallic ions such as Cu(II), Zn(II), Ni(II) and two chiral ligands, usually amino acids, have been employed to enantioseparate analytes like amino acids or amino alcohols by an ligand exchange mechanism (Schmid and Gübitz, 1996).
- **Chiral surfactants:** bile salts like sodium cholate, deoxycholate or deoxytaurocholate have been employed for the separation of binaphthyl derivatives, diltiazem analogues and local anesthetics (Nishi *et al.*, 1990; Amini *et al.*, 1996). Other synthetic chiral surfactants with a chiral amino acid or carbohydrate and an alkyl hydrophobic chain have been also employed as chiral selectors (Martínez Gómez, 2007c).
- **Others:** alkaloids, maltodextrins, macrocyclic antibiotics, different polysaccharides, bacteria...

The most employed selectors for chiral separation in EKC are cyclodextrins (Rudaz *et al.*, 2004; Sánchez-Hernández *et al.*, 2008). CDs form inclusion complexes with numerous compounds and their nature, hydrophilic in the outside and hydrophobic

in the inside, allows high water solubility and capacity of interaction with very different compounds (Cserhádi, 2008). Other important advantage of CDs is their UV transparency. Due to the broad range of neutral, anionic and cationic derivatized CDs available in the commercial market, and the possibility of employing dual systems with mixtures of CDs, there is a broad enantioselectivity capacity with these selectors (Matthijs *et al.*, 2004). Charged CD derivatives at very low concentration may allow the separation of oppositely charged chiral molecules due to the counter-current mobility of the chiral selector and the selectand in the capillary, which maximizes the interaction between the chiral molecule and the cyclodextrin (Chankvetadze *et al.*, 1994). Several chiral molecules including drugs, plaguicides, amino acids and other compounds of interest have been separated in the literature employing cyclodextrins. Enantioseparations employing different cyclodextrin derivatives can be found in several review papers (Jáč and Scriba, 2013; Scriba, 2008; Gübitz and Schmid, 2008; Cucinotta *et al.*, 2010).

I.3.2.2. Modes of CE employed for chiral analysis

The most traditional way to perform an enantioseparation in EKC is to fill the capillary and both the inlet and outlet vials with a background electrolyte containing a chiral selector, and let the analyte interact with the chiral selector during its migration to the detector. This usually provides good separations, but is sometimes unaffordable when expensive chiral selectors are employed. Some other alternative modes and their main advantages are briefly discussed below (Chankvetadze and Blaschke, 2001).

- **Partial- (PFT) and complete (CFT) filling techniques:** The partial filling technique has been proposed by Valtcheva and coworkers in 1993 (Valtcheva *et al.*, 1993). It involves the filling of a separation capillary only in part with a solution containing a chiral selector, while the rest of the capillary and the two separation vials contain a background electrolyte free of it. When the voltage is applied, the racemic drug migrates through the chiral selector plug and the separation is performed (Figure I.8). Its main advantages are the extremely low consumption of chiral selector (only

nanoliters of the solution in each run), the possibility of coupling the CE with MS detection (since the chiral selector does not arrive to the MS), and the possibility of employing chiral selectors with UV absorption (not the case of cyclodextrins). However, there is less analyte-selector interaction than in the conventional mode and the selector plug length (SPL) is a new variable that has to be adjusted carefully to perform the separation.

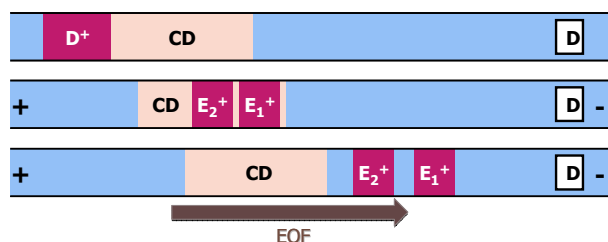


Figure I.8: Schematic representation of the enantioseparation by PFT.

Complete filling technique is a variation of that in which the capillary is completely filled with the chiral selector but the separation vials also remain free of it. It shares the advantage of low consumption of chiral selector. If the chiral selector possesses self electrophoretic mobility in the opposite direction to the chiral analyte, it is called counter-current technique (Chankvetadze and Blaschke, 2001).

- **Mobility counterbalanced mode:** In this mode the separation is enhanced by applying a pressure or vacuum that makes the bulk flow to move in the opposite direction to the analyte electrophoretic mobility. The opposite forces can strongly increase the separation factor (Chankvetadze *et al.*, 1999).
- **Carrier-mode separations:** In the carrier mode a chiral selector is not only the responsible for the separation but also for the transport of the analytes to the detector. Its most important advantage is that the analyte only migrates to the detector when it is associated with the chiral selector.

Charged chiral selectors, which possess their self electrophoretic mobility, may be used as carriers in CE (Terabe, 1989).

- **Enantioseparation in nonaqueous CE (NACE):** The use of organic solvents instead of water to make nonaqueous buffers for CE offers certain advantages, like better solubility and stability of some analytes and chiral selectors, less current and Joule heating, or easier coupling to MS detection. However, the interaction between the enantiomers and the chiral selector could be decreased comparing with aqueous buffers, because the intermolecular forces responsible for the complexation are disfavored in organic solvents (Chankvetadze and Blaschke, 2001). Therefore, the use of NACE becomes interesting principally with analytes or selectors that are non-soluble in an aqueous medium.
- **Micellar electrokinetic chromatography (MEKC):** MEKC, proposed by Terabe and coworkers in 1984 (Terabe *et al.*, 1984), consists on the use of micelles as pseudostationary phase in the background electrolyte to achieve separations based on the different partition coefficient of the analytes in the aqueous and micellar media (Dey *et al.*, 2004). When the micelles are formed by chiral surfactants, they can be employed to perform enantioseparations. Chiral surfactants employed in MEKC are digitonin, saponin, bile salts and others natural or synthetic. There is another option to perform chiral separations by MEKC: the combination of a chiral selector and a non-chiral surfactant in a background electrolyte. In this case, the micelles are added to improve the solubility of the analyte and/or the selectivity of the separation.

I.3.2.3. Selector-selectand binding studies

The chromatographic principles of enantioseparations include non-covalent interactions between the chiral selector and the selectand. When cyclodextrins are employed as chiral selectors, the phenomenon responsible for the enantioseparation is the formation of transitory complexes between the enantiomers and the cyclodextrin, usually with the introduction of the enantiomers in the hydrophobic

cavity of the CD. A thermodynamic equilibrium is established therefore between the free enantiomers and the complexed forms.

The determination of the constants that characterize the interactions of enantiomers with chiral selectors is helpful in chiral separations research, in order to control the complexation equilibrium, and better understand the separation mechanism and molecular interactions. The knowledge about the molecular mechanisms responsible for the chiral separation could be useful for predicting how different chiral selectors will behave in the separation of compounds of interest. Nowadays chiral separations are usually performed by carrying out some trial-and-error tests, but some time, effort and money can be saved if the knowledge about separation mechanisms and molecular interactions allows predicting the selector-selectand interaction.

In EKC with CDs as chiral selectors, the enantiomers form diastereomeric complexes with the CD whose electrophoretic mobilities (μ) are different than those of the free enantiomers. The observed electrophoretic mobility for a single enantiomer can be expressed with the following equation:

$$\mu_{obs} = \frac{[E - CD]}{[E] + [E - CD]} \cdot \mu^{CD} + \frac{[E]}{[E] + [E - CD]} \cdot \mu^0 + \mu_{EOF} \quad (I.2)$$

where $[E]$ and $[E-CD]$ are respectively the free and complexed enantiomer concentrations, μ^{CD} is the mobility of the E-CD complex, μ^0 is the mobility of the free enantiomer and μ_{EOF} is the mobility of the electroosmotic flow.

Assuming a 1:1 stoichiometry, which is the most common situation when the CD concentration is much larger than that of the enantiomer, the equilibrium constant for the enantiomer-CD complexation can be expressed by this equation:

$$K_E = \frac{[E - CD]}{[E][CD]} \quad (I.3)$$

where $[CD]$ is the cyclodextrin concentration. Combining I.2 and I.3:

$$\mu_{obs} = \frac{K_E[CD]}{1 + K_E[CD]} \cdot \mu^{CD} + \frac{1}{1 + K_E[CD]} \cdot \mu^0 + \mu_{EOF} \quad (I.4)$$

and rearranging terms, an equation that relates the effective mobility with the CD concentration is obtained:

$$\mu_i = \frac{\mu^0 + \mu^{CD} K_E [CD]}{1 + K_E [CD]} \quad (\text{I.5})$$

From this expression, the difference between the effective mobilities of two enantiomers can be calculated as:

$$\Delta\mu = \mu_1 - \mu_2 = \frac{\mu^0 + \mu_1^{CD} K_1 [CD]}{1 + K_1 [CD]} - \frac{\mu^0 + \mu_2^{CD} K_2 [CD]}{1 + K_2 [CD]} \quad (\text{I.6})$$

where μ_1 and μ_2 are the effective mobilities of the first and second eluted enantiomers, respectively. K_1 and K_2 are the binding constants between the enantiomers and the chiral selector, μ^0 is the mobility of the free analyte, and μ_1^{CD} and μ_2^{CD} are the mobilities of the complexes E1-CD and E2-CD, respectively. To achieve a chiral separation, the difference between the mobilities of both enantiomers has to be nonzero ($\Delta\mu \neq 0$) (Chankvetadze, 2007). According to Eq. I.6, this situation can be found with two different mechanisms:

- The residence time in the free and complexed forms is different for both enantiomers. This residence time is defined by the binding constants, so in this case $K_1 \neq K_2$ (thermodynamic enantioselectivity).
- Both enantiomers remain the same time in the free and complexed forms, so $K_1 = K_2 = K$. In this situation, the mobilities of the enantiomer-CD complexes may be different, so $\mu_1^{CD} \neq \mu_2^{CD}$ (electrophoretic enantioselectivity).

Among these two phenomena, the most commonly responsible for chiral separation in EKC is the first one, in which the binding constants are different, or a combination of both (Chankvetadze, 2007).

Binding studies have been carried out between compounds of pharmaceutical and environmental interest and different chiral selectors like AGP (Amini *et al.*, 1997), chiral antibiotics like vancomycin, teicoplanin and ristocetin (Machour *et al.*, 2005), or several cyclodextrins. Among others, there have been calculated binding constants of β -CD to naphthalene sulphonate derivatives (Hsiao *et al.*, 2006) and aromatase inhibitors (Foulon *et al.*, 2004), methyl- β -CD to orciprenaline (Amini *et al.*, 1999a) and local anesthetics (Amini and Paulsen-Sörman, 1997), hydroxypropyl- β -CD to fenoxycids (Martín-Biosca *et al.*, 2001) and aromatase inhibitors (Foulon *et*

al., 2004), sulfated- β -CD to modafinil (Al Azzam *et al.*, 2010), carboxymethyl- β -CD to alkylnaphthalene derivatives (Wu and Ding, 2005) and highly sulfated γ -CD to tramadol (Rudaz *et al.*, 2004).

I.3.3. Enzymatic reactions in CE: Electrophoretically mediated microanalysis

Enzymes are biologic catalysts, responsible for all the biochemical reactions that take place in live organisms. In enzymatic reactions a substrate (endogenous molecule, drug or other xenobiotic) is transformed to one or more products *via* the formation of an enzyme-substrate complex. As other chemical catalysts, the enzymes are not consumed in the reaction development. Several enzymes are extremely interesting from a pharmaceutical and clinical point of view, since enzymatic disorders are a common cause of diseases and consequently they are target of numerous drugs. New target enzymes and their substrates, inhibitors and cofactors are object of extensive research every year.

For enzymatic studies, CE has been classically employed only as separation system after off-line reactions. However, the use of CE not only for the separation but also for performing the reaction inside the capillary allows to decrease notably the volume of reagents employed (from microliters to only few nanoliters in each assay), which is interesting in the study of enzymatic reactions since enzymes and substrates use to be expensive, and to increase the automation of the process since the injection, mixing, reaction, separation and detection can be done in a unique step (Hai *et al.*, 2012). This in-capillary reaction procedure is known as electrophoretically mediated microanalysis (EMMA).

In the EMMA procedure an enzyme solution is injected into the capillary and it is allowed to mix with the substrate solution and react before the separation. The most frequent mechanism for mixing the reagents is to apply an electric field to make the substrate and enzyme zones interpenetrate due to their differences in electrophoretic mobility. This is known as EMMA plug-plug mode (Figure I.9a). One of the problems of this methodology is the high variability in peak areas of reagents and reaction products due to slight variations in the in-capillary contact period of the

enzyme and substrate plugs, which affect the extent of the reaction (Van Dyck *et al.*, 2003).

As an alternative to the classical plug-plug mode, the at-inlet EMMA procedure has been proposed. In this modality, the mixing of the enzyme and substrate plugs takes place by simple diffusion and they react for a given time in the inlet part of the capillary (Figure I.9b). This is especially interesting for enzymes that lose activity when exposed to an electric field. Classically, it has been described that longitudinal diffusion is responsible for the mixing of plugs in at-inlet EMMA. However, this is a slow process and can be not efficient if more than two plugs are involved in the reaction.

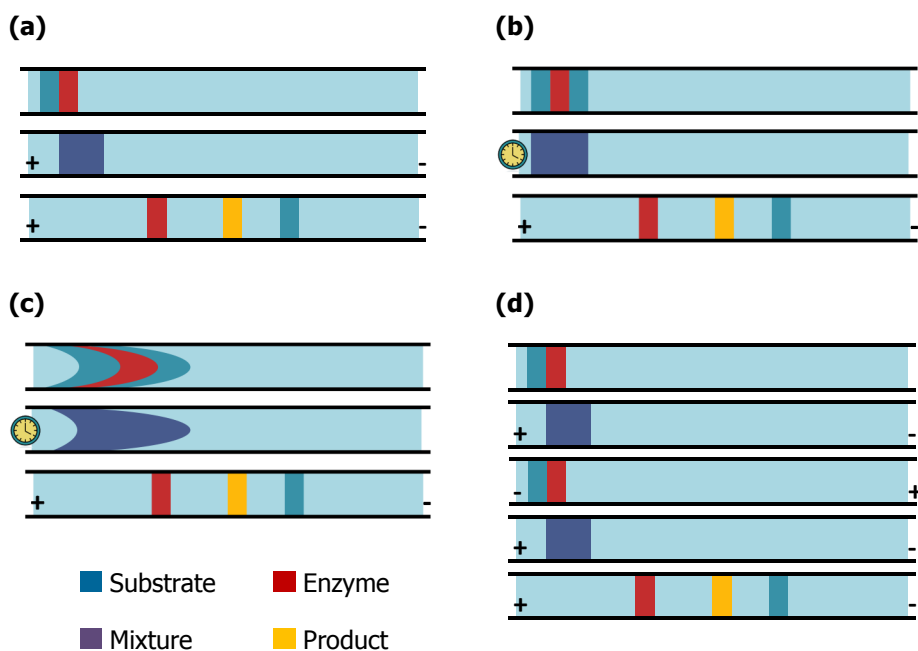


Figure I.9: Scheme of the plugs injection and mixing in the different EMMA modes: (a) plug-plug, (b) at inlet, (c) TDLFP and (d) RPS.

Recently, Okhonin and coworkers have described an alternative mode of mixing, which is called transverse diffusion of laminar flow profiles (TDLFP) (Okhonin *et al.*,

2005). In this mode, the plugs are introduced consecutively in the capillary by pressure and, due to the laminar nature of flow inside the capillary, the nondiffused plugs have parabolic profiles with predominantly longitudinal interfaces between them, and transverse diffusion is responsible for the mixing (Figure I.9c). They also developed mathematical models to estimate the mixing process and to show the concentration profile of each reagent in the capillary.

In practice, when the plugs in at-inlet EMMA are small (standard injection plugs of 0.5 μ l during 3 or 5 s), there is no difference between the experimental injection sequences shown in literature for at-inlet EMMA and TDLFP, so it follows that in at-inlet EMMA also transverse diffusion (which is more efficient than the longitudinal one due to the higher contact surface between plugs) can be responsible for the mixing.

Other alternative to the classical plug-plug mode, which is called rapid polarity switching (RPS) (Figure I.9d), consists in applying a series of positive and negative potentials to the capillary to have some shaking effect that increases the plugs mixing (Sanders *et al.*, 2005). A classification of the different modalities of EMMA, attending to their mixing procedure, is shown in Figure I.10.

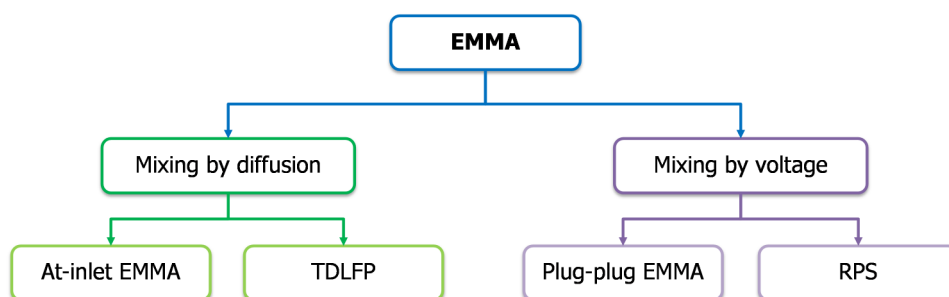


Figure I.10: Classification of EMMA modes.

In all the EMMA modes, usually the background electrolyte is not the same as the incubation medium in which substrates, enzymes and cofactors are dissolved, and its pH or components can affect the enzymatic activity. In order to preserve the correct

enzymatic activity and provide an adequate medium for the reaction turnover, two plugs of incubation buffer can be injected before and after the reaction plugs. This practice has been called "partial filling technique" in the literature (Hai *et al.*, 2012), but may not be confused with the partial filling of a chiral selector described in section I.3.2.2.

EMMA in its different modalities has been employed for some enzymatic reactions to study enzyme kinetics, inhibition of enzymes, and to determine substrates and enzymes in different biological samples (Hai *et al.*, 2012). The evaluation of the enzymatic activities of alkaline phosphatase (Sun *et al.*, 2006) and yeast alcohol dehydrogenase (Urban *et al.*, 2007) has been reported by EMMA. Also metabolic reactions, such as the kinetics of cytochrome P450 with testosterone and nifedipine as substrates (Zhang *et al.*, 2008), or the chiral metabolism of cimetidine by flavin-containing monooxygenases (Hai *et al.*, 2009), can be found in the literature. Due to its intrinsic characteristics such as fast analysis, low consumption of enzymes and reagents, and ease of automation, EMMA has been also employed for screening procedures, in order to evaluate inhibitors of hexokinase (Wang and Kang, 2009) or acetylcholinesterase (AChE) (Tang *et al.*, 2007). Also other chemical reactions (not only enzymatic) can be carried out using this methodology. More applications of EMMA can be found in two recent review papers concerning this topic (Fan and Scriba, 2010; Hai *et al.*, 2012).

I.4. *In vitro* evaluation of pharmacokinetic and pharmacodynamic properties

Preliminary studies in the discovery and development process of new drugs include the *in vitro* evaluation of the biological activity of candidate compounds. Efficacy, potency and toxicity, as well as pharmacokinetic profiles, have to be evaluated in *in vitro* models before reaching the more expensive and time-consuming *in vivo* studies. Figure I.11 shows a diagram of the drug discovery process where is seen that *in vitro* screening procedures and methodologies for pharmacokinetics evaluation play an important role (Evans, 2004). Proteins and enzymes, cell cultures, tissues and whole organs can be employed with this purpose.

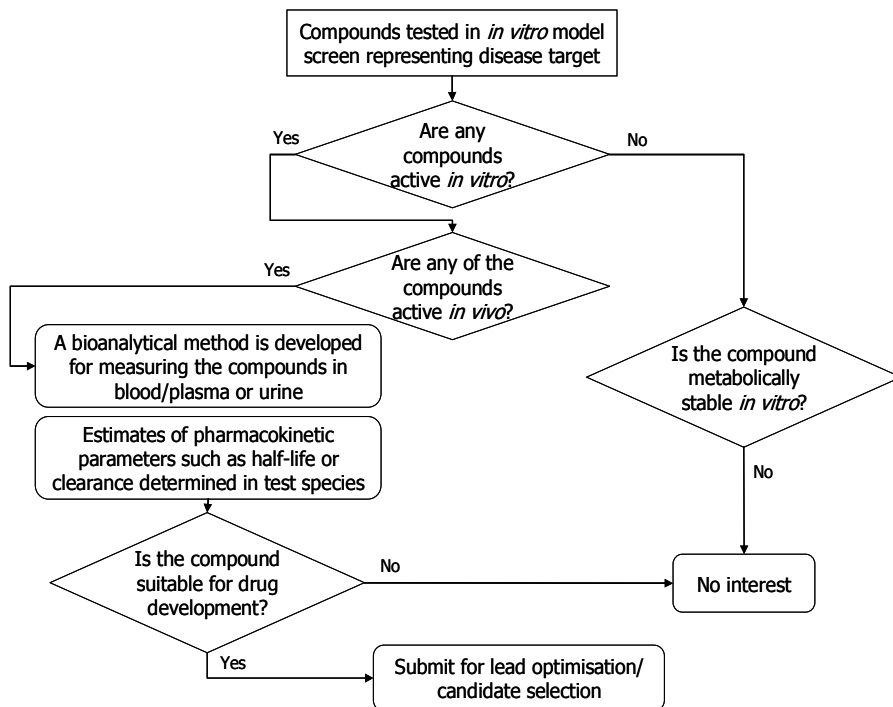


Figure I.11: Process diagram representing some steps of drug discovery.

I.4.1. Protein binding

The *in vitro* measurement of drug binding to plasma proteins is used to calculate pharmacokinetic parameters and make predictions on the pharmacokinetic behavior of the drug. It is therefore highly important to estimate the binding ability to plasma proteins in the early stages of drug discovery. Different approaches have been proposed for the evaluation of protein binding of drugs, and they can be classified into two main categories: separative and non-separative methods (Figure I.12) (Vuignier *et al.*, 2010). The first group involves the separation of the free ligand from the bound species and the determination of the drug in one fraction or both of them. As the determination usually implies the use of analytical techniques, it can be performed in an enantioselective way by using chiral separation systems (chromatographic or electrophoretic). The second group is based on the detection of a change in some physicochemical properties of the drug or the protein due to the

binding. Among all of them, equilibrium dialysis (ED) is by far the more widely used method to study ligand-protein interactions (Evans, 2004), and it has been presented as the reference method for PB measurements.

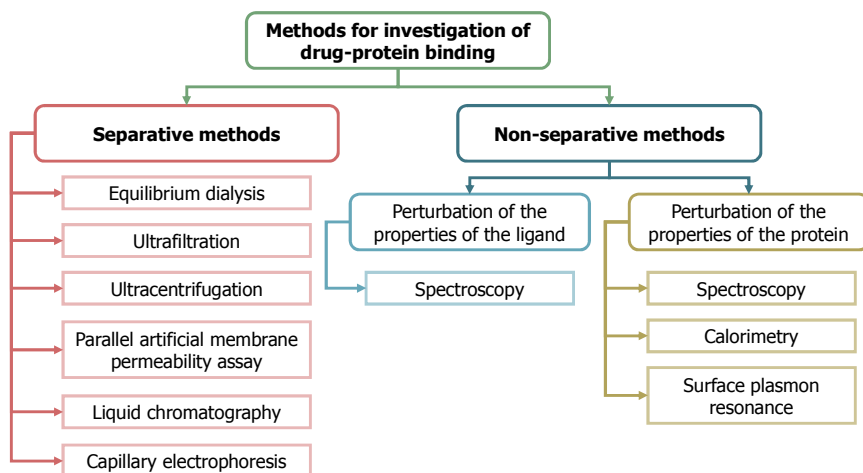


Figure I.12: Classification of methodologies applied to drug-protein binding studies.

Separative methods

Equilibrium dialysis is based on establishment of an equilibrium state between a protein compartment and buffer compartment which are separated by a membrane that has a known molecular weight cut-off and is permeable only for a low-molecular weight ligand (Oravcová *et al.*, 1996). In this methodology, after the equilibrium has been reached the concentration of the free ligand is equal on both sides of the membrane. The drug concentration is measured then in the fluids from both compartments, and the percent of binding can be expressed as (Evans, 2004):

$$\%bound = \frac{C_t - C_u}{C_t} \cdot 100 \quad (I.7)$$

where C_t and C_u are, respectively, the concentrations of drug in the protein and buffer reservoirs.

Despite the fact that ED has been considered the reference method for PB estimations, it suffers from many drawbacks (Vuignier *et al.*, 2010). The equilibration times are too long (12-48 h) and preliminary studies have to be carried out to make sure the time is enough for reaching equilibrium. Another problem is the volume shift associated with the oncotic pressure due to the presence of proteins, which can be up to 30%. Also nonspecific adsorption of drugs to the cell walls and dialysis membrane can happen.

Ultrafiltration (UF) is an alternative to ED where the drug-protein mixture is filtered through a membrane under the application of a negative pressure by centrifugation. This methodology is faster and cheaper than ED and it is broadly employed due to the availability of some commercial filtration devices. However, nonspecific retention of the drug to the filtration membrane is also a problem for UF. The percentage of binding follows the same expression than for ED (Eq. I.7), but in this case C_t is the total concentration of drug before the experiment and C_u is the concentration of drug in the ultrafiltrate (unbound fraction).

With **ultracentrifugation**, the drug-protein mixture is placed in a high speed centrifugal field, until all the protein and drug-protein complex sediment to the bottom of the tube and the free drug remains in the supernatant. The percentage of binding can be calculated in the same way as in UF. Its main advantage is that the drawbacks due to membranes are eliminated, but the equipment needed is more expensive than those for ED and UF, and there is also some error due to the partial sedimentation of the free drug, which is larger for drugs with higher molecular weights. Due to these disadvantages, ultracentrifugation is less extended than the other separative methods.

Parallel artificial membrane permeability assay (PAMPA) is a recently described methodology based on a 96-well filter plate coated with an artificial membrane made of phospholipids or organic solvents that separates two compartments, one with the drug and the protein and other with only fresh buffer. PAMPA is similar to ED but has some advantages in comparison with it: as the estimation of binding constants is based on a kinetic approach, it is not necessary to reach equilibrium, so it is faster; the nonspecific binding of the drug to the

membranes can be self-corrected by calculations, and as the membrane is not water permeable, there is no volume shift. The 96-well format employed makes automation of the procedure easy (Lázaro *et al.*, 2008).

In all these approaches, after the separation of fractions it becomes necessary a second step with an analytical method that allows the quantification of either the free or the bound fraction. This is usually carried out by LC or CE, and also chiral methods can be employed to estimate the enantioselectivity in the protein binding. However, LC and CE can be also employed themselves for drug-protein binding estimations.

There are two **LC** possibilities for assessing drug-protein interactions: size-exclusion chromatography (SEC), where the protein and drug-protein complex elute first due to their larger size and the free drug (smaller) elutes later, and high-performance affinity chromatography (HPAC), where the protein is immobilized on the stationary phase and the retention time of the drug can be employed for the estimation of protein binding (Vuignier *et al.*, 2010). SEC is rarely used nowadays due to some drawbacks such as low column efficiency and short column lifetimes. HPAC has more advantages, since only a small amount of protein is needed and can be reused for some experiments, enantioselective information can be achieved if the column separates the enantiomers, and automation is easy. Protein immobilization is the most critical aspect that has to be taken into account in this methodology.

CE can be also employed for the estimation of PB. Several approaches have been described, in which the protein, the drug or their mixture can be injected or included in the background electrolyte. Among all of them, the two most employed are frontal analysis (FA) and affinity capillary electrophoresis (ACE) (Vuignier *et al.*, 2010).

In FA, the protein and the drug are mixed in the sample vial and a large amount of sample is injected in the capillary (10-20% of the effective capillary length). The injection of large volumes gives rise to the appearance of plateaus instead of peaks. The height of the free drug plateau is proportional to the free drug concentration in the sample.

In ACE, the capillary is filled with buffer containing the protein in different concentrations and the free drug is injected as small plug. The migration time of the

drug depends on the protein concentration and the affinity constant can be calculated from the change in the electrophoretic mobility of the drug upon complexation. More information about separative and chromatographic techniques for protein binding evaluation can be found in a review paper concerning this topic (Escuder-Gilabert *et al.*, 2009).

Non-separative methods

Spectroscopic methods used in PB studies (UV-visible, fluorescence, infrared, nuclear magnetic resonance, optical rotatory dispersion and circular dichroism) are based on changes in the electronic and spectroscopic energy levels of the ligand or the protein due to the complexation process. These methods can be performed in solution, so they give true equilibrium measurements (Vuignier *et al.*, 2010). They can provide structural information about the protein, the drug and the complexation process and currently they are being used in combination with computational methods (molecular docking) to obtain a clear image of the drug-protein interaction.

Two **calorimetric techniques** have been employed to study protein binding, isothermal titration calorimetry (ITC) and differential scanning calorimetry (DSC). In ITC, successive additions of drug to a protein solution are done and the heat release in the complexation process is measured. In DSC, a drug-protein mixture is heated and the measurement is based on the stabilization of the native form of the protein due to the complexation with the drug. The drug-protein complex is more stable and requires more heating than the free protein to be denatured. Both techniques are slow and require a large amount of material to do accurate measurements, so their main interest is that they provide thermodynamic information about the binding process (Vuignier *et al.*, 2010).

Surface plasmon resonance (SPR) has been also employed to evaluate protein binding. It involves immobilizing the protein on a metal surface and monitoring its interaction with the drug that flows over the surface by the measurement of changes in the refractive index in the immediate vicinity of the surface layer due to the binding process. The changes in the angle of the reflected light are proportional to the mass in the surface. This is schematically shown in Figure I.13 (Cooper, 2002).

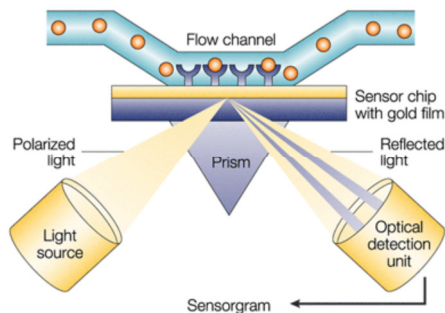


Figure I.13: Scheme of a surface plasmon resonance instrument.

SPR can provide kinetic information about the binding process and is able to characterize binding reactions in real time. Other advantage is the small amount of materials used (usually chip devices).

Mathematical models in protein binding

The reversible binding interaction between a drug and a protein has been usually described by the following model:

$$r = \frac{b}{P} = \frac{D - d}{P} = \sum_{i=1}^m n_i \frac{K_i d}{1 + K_i d} \quad (\text{I.8})$$

where r is the fraction of bound xenobiotic *per* molecule of protein, b is the bound concentration of drug after equilibrium, P is the total protein concentration, D is the total drug concentration, d is the free concentration of drug after equilibrium, m is the number of classes of independent active sites in the protein, n is the number of binding sites of one class *per* protein molecule (apparent stoichiometry), and K is the binding constant of the drug-protein interaction. For example, for the molecule of albumin, whose structure has been described in section I.1.1.2, m represents the different sites described in the molecule (site I, II, III...).

From this general model, where K_i and n_i have to be estimated for the m classes of binding sites, making the estimations difficult to perform, some simplifications have been derived assuming different situations.

– $m = 2$ (two main classes of binding sites):

$$r = n_1 \frac{K_1 d}{1 + K_1 d} + n_2 \frac{K_2 d}{1 + K_2 d} \quad (\text{I.9})$$

The main disadvantage of this equation is that different combinations of n_1 , K_1 , n_2 and K_2 estimates are feasible, so the validity of the calculated values may be checked.

– $m = 1$ (only one main class of binding sites):

$$r = n_1 \frac{K_1 d}{1 + K_1 d} \quad (\text{I.10})$$

This equation can suffer from the same problem as the $m = 2$ model, since more than one single set of suitable n_1 and K_1 values can be found (Šoltés and Mach, 2002).

From this model, several linear equations have been derived (Table I.2). However, linear plots can provide mathematically inconsistent results, since r and d appear both as independent and dependent variables. These mathematical models lack of robustness, so little differences in the experimental data will provide big changes in the estimations.

Table I.2: Linear models for protein binding estimations.

Model	Equation	
Klotz	$\frac{1}{r} = \frac{1}{n_1} + \frac{1}{n_1 K_1} \cdot \frac{1}{d}$	(I.11)
Scatchard	$\frac{r}{d} = n_1 K_1 - K_1 r$	(I.12)
y-reciprocal	$\frac{d}{r} = \frac{1}{n_1 K_1} + \frac{1}{n_1} d$	(I.13)

All these mathematical approaches can be employed also in the case of single enantiomers to obtain enantioselective estimations of n_1 and K_1 .

I.4.2. Drug metabolism

The use of *in vitro* techniques to study drug metabolism provides relevant information about the metabolites likely to be formed *in vivo* and about potential clinical interactions by induction or inhibition of metabolic enzymes. It also provides pharmacokinetic data useful in the first stages of drug development. As the liver is the major site for biotransformation, usually *in vitro* systems are focused on the liver and the enzymes it contains, so there can be different preparations which vary in their levels of cellular integrity, from single enzymes to whole liver perfusion (Evans, 2004). Figure I.14 shows the different possibilities for performing metabolic studies, including two *in vivo* approaches that will not be discussed here. They are compared in terms of complexity, easiness of application, ethics and similarity to the *in vivo* true situation (Brandon *et al.*, 2003). *In vitro* studies focus on both metabolism phases I and II, especially on CYP metabolic reactions. These are the most common phase I ones and also the most frequently affected by drug-drug interactions. Nevertheless, other enzymatic systems are also studied and, of course, the more complex the *in vitro* model is, the more global information about the metabolic process can be found, but at the same time the less information about each individual enzyme behavior is provided.

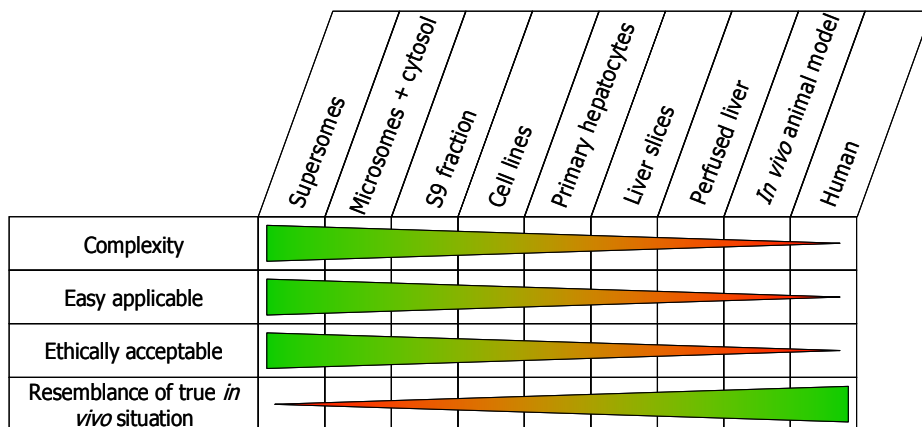


Figure I.14: *In vitro* and *in vivo* metabolism models used in drug development.

The most complex *in vitro* system employed for the evaluation of drug metabolism is the **perfused liver**. An isolated perfused liver is considered to be the best representation of the *in vivo* situation. However, it has never been used with human liver and only a few times with animal livers. In this system, the animal is killed and its liver is preserved in a thermostated bath, and usually perfused with Krebs-Henseleit buffer (a mixture of glucose, albumin, sodium chloride and other components of the human serum). Different procedures have been extensively described for carrying out these studies (Brauer *et al.*, 1959; Mischinger *et al.*, 1992).

Despite its important advantages such as the possibility of collecting bile for analysis, the presence of all cell types that can be found in a real liver (not only hepatocytes), and the three-dimensional architecture of the model, its drawbacks made this system less attractive as *in vitro* model. In this model, the liver is available for only few hours and it is a delicate system, difficult to handle. The impossibility of using human livers is also an important drawback for the purpose of the evaluation of drug metabolism, because animal livers not always reproduce reliably the human metabolism. In practice, this model is especially useful when there is interest in the collection and analysis of the bile secretion (Brandon *et al.*, 2003).

Liver slices, which are precision-cut with special devices, share the advantages of the perfused liver in terms of the presence of all types of cells and the three-dimensional architecture of the liver. This allows an assessment of the influence of cell diversity and cell-cell interaction on drug metabolism, and the maintenance of drug transport pathways (Hariparsad *et al.*, 2006). It has also another advantage that is the less amount of animal liver needed for each study. Its inconvenients are also similar to the perfused liver, since it is an expensive methodology difficult to handle with, and the availability of the slices without losing their enzymatic activity is just of few days. Another important drawback is the inadequate penetration of the medium into the inner part of the slice.

Primary hepatocytes are a popular *in vitro* system for drug biotransformation research due to their strong resemblance of *in vivo* human liver. They can be obtained from human (usually after partial resection) or animal livers, and then

immediately employed or cryopreserved for their further use. Cryopreservation is interesting especially for human hepatocytes since the availability of human livers is limited and this technique allows to have them commercially available (Hengstler *et al.*, 2000), with their phase I and II enzymatic activity preserved. This is an important advantage of hepatocytes over the liver slices and perfused liver. Disadvantages of this *in vitro* system are the absence of other cell types present *in vivo*, and the interindividual variation between pools of different liver cells. This can be overcome by using mixtures of hepatocytes from multiple donors, which provide an average of the enzyme content. Primary hepatocytes of different animal species can be also employed to choose the best animal *in vivo* model with the most resemblance with the human metabolic pathway (Brandon *et al.*, 2003).

Different **cell lines** have been developed and are commercially available for *in vitro* metabolic studies. Liver cell lines are isolated from hepatic tumors, such as hepatoma or hepatocellular carcinoma, and can be more easily cultured than the primary hepatocytes. However, liver cell lines are unpopular in drug biotransformation research due to their lack of phase I and II enzymes expression (Brandon *et al.*, 2003). The most frequently cell line used is Hep G2, obtained from an hepatocellular carcinoma. This shows a certain activity of different CYP isoforms that can be increased by induction.

Transgenic cell lines are an alternative to liver cell lines that increases the enzyme content of the cells to make them useful for biotransformation studies. Cells are transfected with one or more isoforms of CYP and uridine 5'-diphosphoglucuronosyltransferase (UGT), which allow studying the influence of different isoforms in the whole metabolic process (Gasser *et al.*, 1999). They can be also employed to generate metabolites for structure elucidation or pharmacological characterization.

On the other hand, at a subcellular level different fractions can be obtained from a liver homogenate by centrifugation. These fractions can be used separately to perform *in vitro* biotransformation studies. Figure I.15 shows a scheme of the different subcellular fractions that can be obtained from the liver tissue and a simple overview of the separation procedure (BD Gentest Tissue Fractions Brochure, 2010).

The most complex subcellular *in vitro* system available is **liver S9 fraction**. The S9 fraction is defined by the International Union of Pure and Applied Chemistry (IUPAC) as the supernatant fraction obtained from an organ (usually liver) homogenate by centrifuging at 9000 *g* for 20 min in a suitable medium; this fraction contains cytosol and microsomes (Duffus *et al.*, 2007). The microsomes are vesicles of the hepatocyte endoplasmic reticulum that contain CYP, FMO and UGT enzymes. In the cytosolic fraction, several soluble phase II enzymes are present, like N-acetyl transferase, glutathione S-transferase and sulfotransferase. In the S9 fraction all these enzymatic systems are present, so it offers a more complete representation of the metabolic profile than the use of microsomes or cytosol separately. All the cofactors needed for the enzymatic reactions may be added to this system: NADPH or a NADPH regenerating system for CYPs, and many other cofactors such as acetyl coenzyme A (acetyl CoA) or glutathione for phase II enzymes (Brandon *et al.*, 2003).

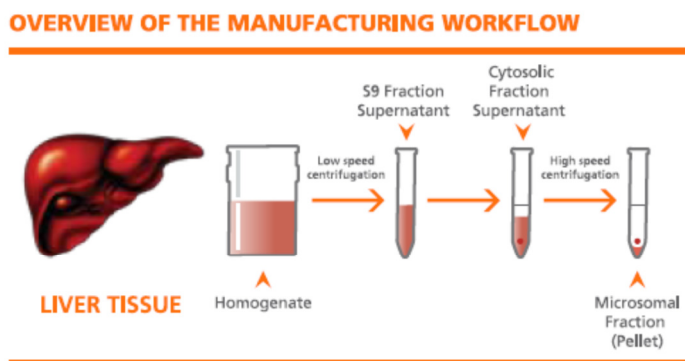


Figure I.15: Overview of the procedure for obtaining liver subcellular fractions.

Human liver microsomes (HLMs) are the most popular *in vitro* model employed for biotransformation studies. They are obtained also by differential centrifugation of the liver homogenate, and, as described before, contain CYP, FMO and UGT enzymes. They are well-characterized by the suppliers and easily employable. Interindividual variation of the enzyme content and activity can be avoided employing pooled microsomes that represent an average enzyme activity that can be considered representative. The companies that commercialize the HLMs have pools

with different characteristics of gender or enzyme polymorphism that allow providing averaged data but also study interindividual differences. They have large pools with small variability to allow carrying out long studies without significant differences (BD Gentest Tissue Fractions Brochure, 2010). As described for primary hepatocytes, microsomes of different animal species can be employed to choose the best *in vivo* animal model for resembling human metabolism.

Liver cytosol fractions can be also employed individually to study phase II metabolic reactions. The use of these fractions individually instead of the S9 fraction allows to better understand each reaction separately, and makes easier the identification of metabolites that can be in a very low concentration in the S9 fraction, since the enzyme content is higher in the HLMs and cytosol than in the S9 fraction. Both for HLMs and liver cytosol fractions, the adequate cofactors for each enzymatic reaction may be added to the biotransformation medium.

The last and simplest *in vitro* model for the study of drug metabolism is **supersomes**. Supersomes are vesicles of the hepatocyte endoplasmic reticulum of transfected insect cells. Insect cells lack endogenous CYP and UGT activity, so the expression of the human CYP and UGT enzymes is baculovirus mediated. At present, all common human CYPs, co-expressed with NADPH-cytochrome P450 reductase and cytochrome b₅ are offered in supersomes. Also UGTs are commercially available.

Supersomes are a valuable supplement to HLM (Huang *et al.*, 2000), and can be used in the same way. Their main advantage is that no human liver is necessary for their production. They can be used not only for biotransformation studies but also to evaluate drug-drug interactions and to study the influence of CYP polymorphisms on drug biotransformation pattern (Brandon *et al.*, 2003).

Subcellular fractions such as HLMs or supersomes can be employed for performing *in vitro* assays in solution, usually followed by the determination of substrates or products by analytical procedures, which can be also enantioselective if information about single enantiomers is required. Recently they have been also used by several authors in EMMA procedures, in which the reaction and the detection are performed in the same electrophoretic capillary (see section I.3.3).

Mathematical models in drug metabolism

Metabolic reactions are enzymatic ones, so they follow the mathematical approaches employed in enzymatic studies. The first equilibrium models were proposed by Henri in 1903 and by Michaelis and Menten in 1913. Later, Briggs and Haldane introduced in 1925 the steady state assumption which is a more realistic approach of the conditions employed in experimental studies (Copeland, 2005).

The enzymatic reactions in which one substrate forms one product can be described with the following general model:



where E is the enzyme, S the substrate, ES the enzyme-substrate complex and P the product. Each reaction has its own kinetic constant (k_1 and k_{-1} for the formation and dissociation of the ES complex, and k_2 for the formation of product), so the velocities of formation and dissociation of the ES complex can be defined as follows:

$$\text{Formation: } V_f = k_1[E][S] \quad (\text{I.15})$$

$$\text{Dissociation: } V_d = k_{-1}[ES] + k_2[ES] \quad (\text{I.16})$$

Steady state conditions assume that the concentration of the ES complex is held constant by a balance between the rates of its formation and dissociation. This is experimentally achieved by having a large molar excess of substrate over enzyme concentration. The formation and dissociation velocities (Eqs. I.15 and I.16) are thus equal, and after some mathematical treatment of these expressions and variables transformation an equation that relates the initial velocity (V_0) to the substrate concentration is derived (Nelson and Cox, 2006). This is commonly known as Michaelis-Menten equation:

$$V_0 = \frac{V_{max}[S]}{K_m + [S]} \quad (\text{I.17})$$

The terms V_{max} and K_m are the kinetic parameters of the enzymatic reaction. V_{max} represents the maximum reaction velocity (at infinite substrate concentration) and K_m which is a mathematical combination of k_1 , k_{-1} and k_2 , represents the concentration of substrate at which the velocity is half the V_{max} .

Experimental data have to be adjusted to Michaelis-Menten equation by non-linear fitting. There is also a linear model derived from it, which is known as Lineweaver-Burk plot (Eq. I.18). It suffers from the same drawbacks previously discussed for linear models in protein binding, so, if non-linear fitting is possible, linear plots should be avoided.

$$\frac{1}{V_0} = \frac{K_m}{V_{max}[S]} + \frac{1}{V_{max}} \quad (\text{I.18})$$

Metabolic enzymes are usually compared in terms of their K_m for different substrates transformation, which is a measurement of the enzyme-substrate affinity.

I.4.3. Enzyme inhibition

Enzymes are target of approximately 50% of the commercialized drugs. Most of the essential biochemical processes are catalyzed by enzymes, so they can be responsible for disease states. Enzymes are susceptible to be inhibited by small molecules and they are commonly the target of new drug discovery efforts. So, methods for the *in vitro* evaluation of enzyme inhibition are also important for the preclinical phases of drug development. High-throughput screening (HTS) is nowadays the most common method for identifying promising compounds, and is frequently applied to evaluate the potential inhibition of target enzymes by large libraries of molecules. The most common approach is to measure the reduction on the enzyme activity in presence of the candidate compound.

Several HTS strategies have been described recently, such as fluorescence or radiometric techniques, assays with surface plasmon resonance, or separation techniques such as LC or CE (Shanmuganathan and Britz-McKibbin, 2013), using similar approaches than those described for the evaluation of protein binding (see section I.4.1). Both LC and CE techniques can be employed for the detection of substrates, products and/or inhibitors after off-line incubation of the enzyme with a model substrate and its candidate inhibitors, and also by on-line methodologies. Immobilized enzyme-reactor columns and capillaries have been developed, such as a monolithic capillary column with AChE for inhibitors screening by nano-LC (Forsberg

et al., 2011), or a tyrosinase microreactor in CE (Jiang *et al.*, 2013). In CE, the use of EMMA for the screening of enzyme inhibition is also a common approach, employed for several enzymes such as transferases, hydrolases, oxidoreductases or isomerases (Shanmuganathan and Britz-McKibbin, 2013).

Finally, also computational methodologies have been developed for HTS of potential inhibitors, despite these techniques provide only initial information about their potential as drug candidates and may be always followed by experimental procedures. An artificial neuronal network has been developed for the screening of cyclooxygenase inhibitors (Gálvez-Llompert *et al.*, 2013) and molecular docking has been employed for evaluating monoaminoxxygenase-B inhibitors (Yelekçi *et al.*, 2013), among others.

Mathematical models in enzyme inhibition

The inhibition process is a reversible equilibrium where the inhibitor can bind to the free enzyme, the enzyme-substrate complex or both (Figure I.16).

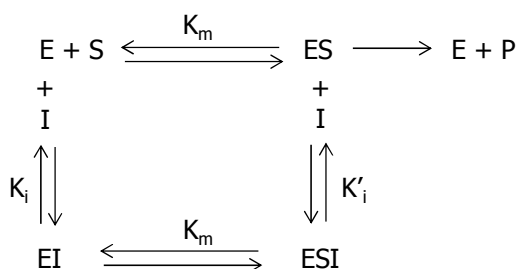


Figure I.16: Equilibrium scheme of the reversible enzyme inhibition.

A general mathematical approach has been developed with some simplifications that can be applied depending on the type of inhibition studied. The general model is a modification of the Michaelis-Menten equation:

$$V_0 = \frac{V_{max}[S]}{\alpha K_m + \alpha'[S]} \quad (\text{I.19})$$

where α and α' are the modifying factors defined by the inhibitor concentration, $[I]$, and its two dissociation constants, K_i (for the binding to the free enzyme) and K'_i (for the binding to the enzyme-substrate complex):

$$\alpha = 1 + \frac{[I]}{K_i} \quad (I.20)$$

$$\alpha' = 1 + \frac{[I]}{K'_i} \quad (I.21)$$

The general equation (Eq. I.19) is applied to the inhibitors that bind both to the enzyme and the enzyme-substrate complex, which are known as **non-competitive inhibitors**.

Competitive inhibitors can only bind to the free form of the enzyme, so they “compete” with the substrate for the free enzyme. In this situation, K'_i becomes infinite and $\alpha' = 1$, so the general model can be rewritten as follows:

$$V_0 = \frac{V_{max}[S]}{\alpha K_m + [S]} \quad (I.22)$$

It may be taken into account that the competitive inhibition does not imply that the substrate and the inhibitor bind to the same site of the enzyme. The inhibitor can bind to other site and modify the configuration of the active site impeding the binding of the substrate (Copeland, 2005).

The third situation that can be found is that the inhibitor can only bind to the ES complex. This is called **uncompetitive inhibition**, and, in this case, the term α becomes 1 and the model is simplified as follows:

$$V_0 = \frac{V_{max}[S]}{K_m + \alpha'[S]} \quad (I.23)$$

Inhibition constants can be calculated by using the described models. Another interesting parameter in enzyme inhibition is the IC_{50} , defined as the concentration of inhibitor that inhibits 50% of the enzyme activity. The percentage of inhibition can be calculated as follows:

$$\%inhibition = 100 - \left(\frac{[P]_i}{[P]_0} \cdot 100 \right) \quad (I.24)$$

where $[P]_i$ and $[P]_0$ are, respectively, the product concentrations in presence and absence of the inhibitor. By plotting the percentage of inhibition versus the logarithm of the inhibitor concentration, a sigmoid curve is obtained, where the inflexion point is the value of the IC_{50} .

I.5. Drugs and pesticides in study

All xenobiotics (drugs and pesticides) employed in this Thesis are summarized in Tables I.3 and I.4. Their chemical structures, minus logarithm of acidity constant (pK_a) and molecular weight (MW) values are also shown in these tables. For chiral compounds, the asymmetric carbon is marked with a (*).

Table I.3: Drugs in study in this Thesis.

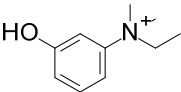
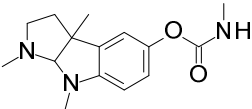
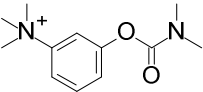
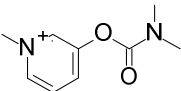
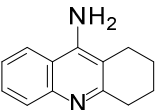
Drug	Structure	pK_a	MW ($g \cdot mol^{-1}$)
AChE inhibitors			
Edrophonium		8.59	166.2
Eserine		6.59	275.3
Neostigmine		-	223.3
Pyridostigmine		-	181.2
Tacrine		8.95	198.3

Table I.3: (Continued)

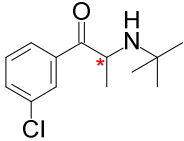
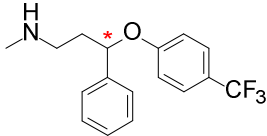
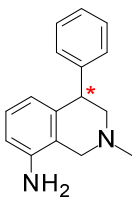
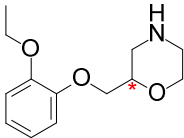
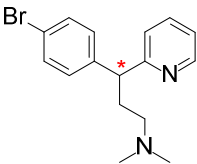
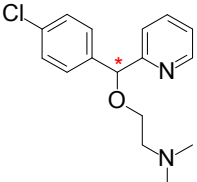
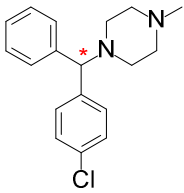
Drug	Structure	pK _a	MW (g·mol ⁻¹)
Antidepressants			
Bupropion		8.22	239.7
Fluoxetine		9.80	309.3
Nomifensine		8.88	238.3
Viloxazine		8.19	237.3
Antihistamines			
Brompheniramine		9.48	319.2
Carbinoxamine		8.87	290.1
Chlorcyclizine		8.00	300.8

Table I.3: (Continued)

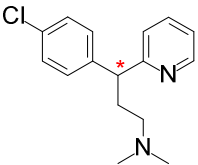
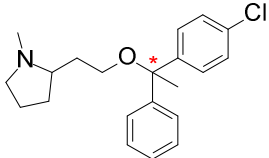
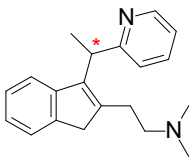
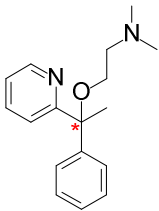
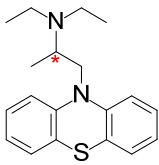
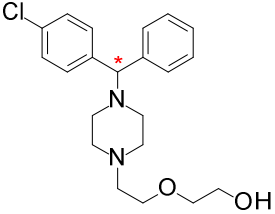
Drug	Structure	pK _a	MW (g·mol ⁻¹)
Antihistamines			
Chlorpheniramine		9.47	274.8
Clemastine		9.55	343.9
Dimethindene		9.70	292.4
Doxylamine		8.87	270.2
Ethopropazine		9.60	312.4
Hydroxyzine		7.82	374.0

Table I.3: (Continued)

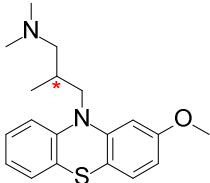
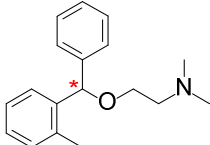
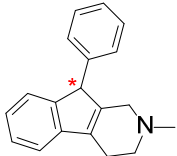
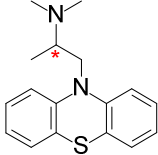
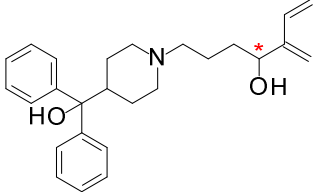
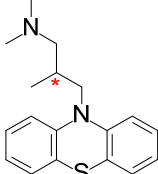
Drug	Structure	pK _a	MW (g·mol ⁻¹)
Antihistamines			
Methotrimeprazine		9.42	328.5
Orphenadrine		8.87	269.0
Phenindamine		9.00	261.3
Promethazine		9.05	284.4
Terfenadine		9.02	471.7
Trimeprazine		9.42	298.4

Table I.3: (Continued)

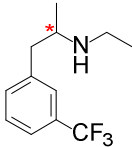
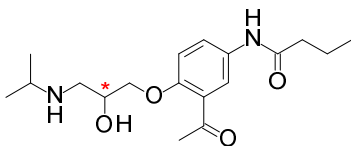
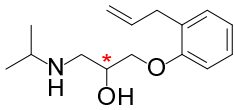
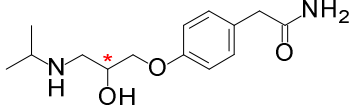
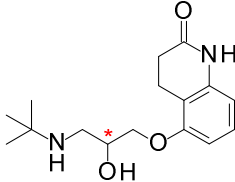
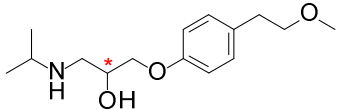
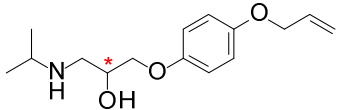
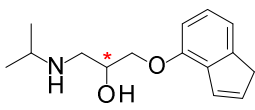
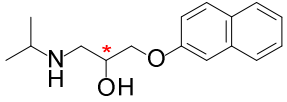
Drug	Structure	pK _a	MW (g·mol ⁻¹)
Anti-obesity			
Fenfluramine		10.22	231.3
β-blockers			
Acebutolol		9.57	336.4
Alprenolol		9.65	
Atenolol		9.67	266.3
Carteolol		9.76	292.4
Metoprolol		9.67	267.4
Oxprenolol		9.5	265.3
Pindolol		9.67	247.3
Propranolol		9.45	259.3

Table I.3: (Continued)

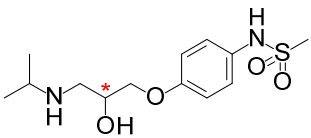
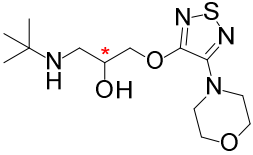
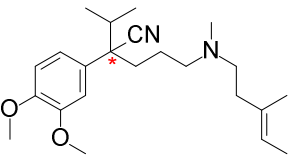
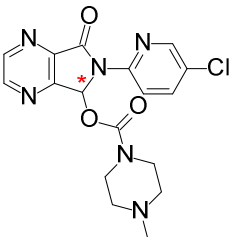
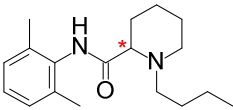
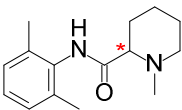
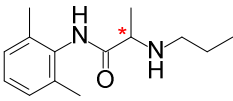
Drug	Structure	pK _a	MW (g·mol ⁻¹)
β-blockers			
Sotalol		9.43	272.4
Timolol		9.76	316.4
Ca⁺²-channel blockers			
Verapamil		9.68	454.6
Hypnotics			
Zopiclone		6.89	388.8
Local anesthetics			
Bupivacaine		8.10	288.4
Mepivacaine		7.70	246.3
Prilocaine		7.89	220.0

Table I.3: (Continued)

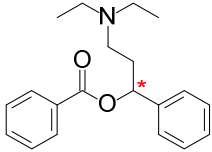
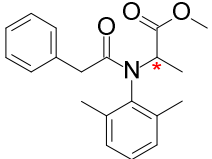
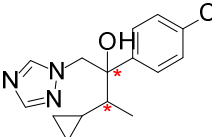
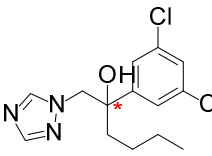
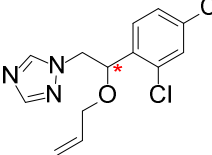
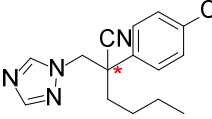
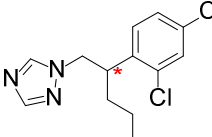
Drug	Structure	pK _a	MW (g·mol ⁻¹)
Local anesthetics			
Propanocaine		7.53	311.0

Table I.4: Pesticides in study in this Thesis.

Pesticide	Structure	pK _a	MW (g·mol ⁻¹)
Benalaxyl		-	325.0
Cyproconazole		2.26	291.8
Hexaconazole		2.26	314.2
Imazalil		6.77	296.0
Myclobutanil		2.27	288.1
Penconazole		2.28	284.2



II. OBJECTIVES

II. OBJECTIVES

This Thesis is part of a research line developed by our research group in the last years, consisting on the development of high-throughput methodologies for the chromatographic and electrophoretic evaluation of specific and non-specific interactions between xenobiotics and biomacromolecules, and in some cases the enantioselectivity shown by these interactions. The purpose of this research line is to provide to the pharmaceutical and chemical industry fast and reliable *in vitro* methodologies to evaluate the xenobiotic-biomacromolecule interaction, which can be interesting for the preclinical phases of drug development and for the development of new xenobiotics such as pesticides. The use of *in vitro* methodologies that minimize the use of animals in laboratory experimentation is an actual trend due to all the regulations trying to replace *in vivo* experiments by *in vitro* ones which provide information of the same quality, and reserve *in vivo* trials for the last steps of drug development in which they are necessary.

The main aim of this Thesis is the development of high-throughput electrophoretic systems that could be employed as screening methodologies for the characterization of the interaction of drugs with different biomacromolecules involved in pharmacokinetic and pharmacological processes, and for the study of pharmacological differences between the enantiomers of chiral drugs. This general purpose can be divided into three more specific objectives:

1. Development of enantioselective methods for the chiral separation of drugs by electrokinetic chromatography

This objective comprises the development of chiral methods for enantioseparation of drugs by the CE modality of electrokinetic chromatography. With this purpose, different neutral and anionic cyclodextrins will be employed as chiral selectors using the complete and partial filling techniques. Selector-selectand binding studies will be carried out to better understand the complexation mechanism responsible for the chiral separations. The developed methods will be applied to the determination of

drug enantiomers in pharmaceuticals. A non-aqueous CE system will be also proposed as an alternative for performing enantioseparations.

2. Development of high-throughput electrophoretic systems for the *in vitro* evaluation of the interaction between drugs and different biomacromolecules

This objective includes the development and improvement of methodologies for the evaluation of the interaction between drugs and plasma proteins (HSA and total plasma proteins), the inhibitory activity of some acetylcholinesterase inhibitors, and the interaction between drugs and metabolic enzymes (cytochrome P450), with the goal of achieving fast, reliable and reproducible methods that could be applied in drug development processes. The evaluation of the drug-protein interaction will be performed by ultrafiltration followed by chiral EKC. For the different enzymatic reactions evaluated, the EMMA methodology, which allows the reaction, separation and detection of the components inside the capillary, is proposed.

3. Development of high-throughput electrophoretic systems for the *in vitro* evaluation of the enantioselectivity of drugs in some distribution and metabolism processes

Due to the little amount of information available about stereoselectivity in the interaction of chiral drugs with biomacromolecules and its important impact over their pharmacodynamics, pharmacokinetics and toxicity, this objective involves the development of electrophoretic methodologies that allow the evaluation of the differential behavior of drug enantiomers in their interaction with plasmatic proteins and metabolic enzymes. With this purpose, the chiral methods developed in the first objective will be joined with some of the methodologies developed in the second one.



III. METHODOLOGY

III. METHODOLOGY

III.1. Instrumentation

Three different CE systems have been employed in the development of this Thesis: two P/ACE MDQ Capillary Electrophoresis systems from Beckman Coulter (Fullerton, CA, USA), both equipped with diode array detectors, and 32Karat software version 8.0, and a HP^{3D} CE system (Hewlett-Packard, Waldbronn, Germany), also equipped with a diode array detector, and HP^{3D} Chemstation software.

Fused-silica capillaries of 50 and 75 μm inner diameter (i.d.) and 363 μm outer diameter (o.d.) have been employed, with effective lengths varying from 21 and 50 cm, depending on the application. The capillaries were from Beckman Coulter (Fullerton, CA, USA) or from Agilent Technologies (Waldbronn, Germany).

The selection of the detection wavelength for each compound was based on reported data or previous work of our research group. When no reported data were available, the UV spectra were recorded in a first experience in order to choose the adequate detection wavelength.

All the electrophoretic solutions and samples were filtered through 0.45 μm pore size nylon membranes (Micron Separation, Westboro, MA, USA) and degassed in an ultrasonic bath (JP Selecta, Barcelona, Spain) prior to use. The pH of the buffer solutions was adjusted with a Crison Micro pH 2000 pH-meter (Instrumentos Crison, Barcelona, Spain). All solutions were prepared with Ultra Clear TWF UV deionized water (SG Water, Barsbüttel, Germany).

In protein binding studies, ultrafiltration was carried out through Microcon YM-10 cellulose filters, with a molecular weight cut-off of 10 kDa (Millipore Corporation, Bedford, MA, USA). The filtering devices had a volume capacity of 0.5 mL. A centrifuge Heraeus Biofuge Strate (Heraeus, Madrid, Spain) with capacity for 24 samples and temperature control was employed for the ultrafiltration. Samples were incubated in a Selecta thermostated bath (JP Selecta, Barcelona, Spain).

III.2. Chemicals and reagents

The reagents employed in this Thesis are summarized in Table III.1, with their commercial suppliers and the section(s) of this Thesis where they have been employed. All the reagents are of analytical grade.

Table III.1: Summary of all reagents and chemicals employed in this Thesis.

Chemical / reagent	Supplier	Section(s)
Drugs and metabolites		
Acebutolol hydrochloride	Italfarmaco*	IV.1.2.
Alprenolol hydrochloride	Sigma	IV.3.1.
Atenolol	Zeneca Farma*	IV.1.2.
Brompheniramine maleate	Sigma	IV.1.2.
Bupropion hydrochloride	Sigma	IV.1.1. IV.1.2.
Carbinoxamine maleate	Sigma	IV.1.2.
Carteolol hydrochloride	Miquel-Otsuka*	IV.1.2.
Celiprolol hydrochloride	Rhone-Poulenc*	IV.1.2.
Chlorcyclizine hydrochloride	Sigma	IV.1.2.
Chlorpheniramine maleate	Sigma	IV.1.2.
Clemastine fumarate	Sigma	IV.1.2.
Dimethindene maleate	Novartis*	IV.1.1. IV.1.2.
Doxylamine succinate	Sigma	IV.1.2.
Edrophonium chloride	Sigma	IV.3.1.
Eserine	Sigma	IV.3.1.
Ethopropazine hydrochloride	Sigma	IV.1.2.
Fluoxetine hydrochloride	Alter*	IV.1.1. IV.1.2. IV.1.3. IV.2.1. IV.3.3.
Fenfluramine hydrochloride	VUB*	IV.1.4.

Table III.1: (Continued)

Chemical / reagent	Supplier	Section(s)
Drugs and metabolites		
Hydroxyzine hydrochloride	Sigma	IV.1.2.
Labetalol hydrochloride	Sigma	IV.1.2.
Metoprolol tartrate	Ciba Geigy*	IV.1.2.
Methotrimeprazine maleate	Sigma	IV.1.2.
Nadolol	Squibb*	IV.1.2.
Neostigmine bromide	Sigma	IV.3.1.
Nomifensine maleate	Sigma	IV.1.1. IV.1.2. IV.2.3.
Norfluoxetine hydrochloride	Sigma	IV.3.3.
Norverapamil hydrochloride	Sigma	IV.3.2.
Orphenadrine hydrochloride	Sigma	IV.1.1. IV.1.2.
Oxprenolol hydrochloride	Ciba Geigy*	IV.1.2.
Phenindamine tartrate	Sigma	IV.1.2.
Pindolol	Sigma	IV.1.2. IV.1.4.
Promethazine hydrochloride	Guinama	IV.1.1. IV.1.2.
Propranolol chlorhydrate	ICI Farma*	IV.1.2.
Pyridostigmine bromide	Sigma	IV.3.1.
R-fluoxetine hydrochloride	Sigma	IV.3.3.
R-verapamil hydrochloride	Sigma	IV.3.2.
Sotalol hydrochloride	Sigma	IV.1.2.
Tacrine	Sigma	IV.3.1.
Terfenadine	Sigma	IV.1.1. IV.1.2.
Timolol maleate	Merck*	IV.1.2.
Trimeprazine hemi(+)-tartrate	Sigma	IV.1.2.

Table III.1: (Continued)

Chemical / reagent	Supplier	Section(s)
Drugs and metabolites		
Verapamil hydrochloride	Sigma	IV.1.2. IV.1.4. IV.3.2.
Viloxazine	Astra Zeneca*	IV.1.1. IV.1.2.
Zopiclone	Aventis Pharma*	IV.2.2.
Pesticides		
Benalaxyl	Dr. Ehrenstofer	IV.1.2.
Cyproconazole	Dr. Ehrenstofer	IV.1.2.
Hexaconazole	Dr. Ehrenstofer	IV.1.2.
Imazalil	Dr. Ehrenstofer	IV.1.2.
Myclobutanil	Dr. Ehrenstofer	IV.1.2.
Penconazole	Dr. Ehrenstofer	IV.1.2.
Proteins, enzymes and cofactors		
AChE from <i>Electrophorus electricus</i> (EC.3.1.1.7.)	Sigma	IV.3.1.
Acetolthiocholine chloride (AThCh)	Acros Organics	IV.3.1.
Human CYP2D6*1 + P450 Reductase SUPERSOMES™	BD Gentest	IV.3.3.
Human CYP3A4 + P450 Reductase + Cytochrome b ₅ SUPERSOMES™	BD Gentest	IV.3.2.
Human serum albumin Fraction V	Sigma	IV.2.1. IV.2.2. IV.2.3.
Lyophilized human sera	Sigma	IV.2.2. IV.2.3.
NADPH	Sigma	IV.3.2.
NADPH Regenerating System Solution A (Content: 26 mM NADP ⁺ , 66 mM Glucose-6- phosphate (G6P) and 66 mM MgCl ₂ in H ₂ O)	BD Gentest	IV.3.2. IV.3.3.
NADPH Regenerating System Solution B (Content: 40 U/mL Glucose-6-phosphate dehydrogenase (G6PDH) in 5 mM sodium citrate)	BD Gentest	IV.3.2. IV.3.3.

Table III.1: (Continued)

Chemical / reagent	Supplier	Section(s)
Cyclodextrins		
Carboxymethyl- β -cyclodextrin (CM- β -CD)	Cyclolab	IV.2.2.
Carboxymethyl- γ -cyclodextrin (CM- γ -CD)	Cyclolab	IV.1.4.
Heptakis-(2,3,6-tri-O-methyl)- β -cyclodextrin (TM- β -CD)	Fluka	IV.2.3.
Highly sulfated β -cyclodextrin (HS- β -CD), 20% m/v aqueous solution	Beckman Coulter	IV.1.1. IV.1.2. IV.1.3. IV.2.1. IV.3.2. IV.3.3.
General chemicals		
Acetic acid	Scharlau	IV.1.4.
Ammonium acetate	Scharlau	IV.1.4.
Boric acid	Scharlau	IV.3.1.
Dimethyl sulfoxide (DMSO)	Scharlau	IV.1.4.
Hydrochloric acid 37%	Scharlau	IV.2.2. IV.2.3.
Magnesium sulfate heptahydrate	Scharlau	IV.3.1.
Methanol	Scharlau	IV. -all-
Potassium dihydrogen phosphate	Panreac	IV.2.2. IV.2.3.
Potassium hydroxide, pellets	Panreac	IV.2.2. IV.2.3.
Sodium dihydrogen phosphate dihydrate	Fluka	IV.1.1. IV.1.2. IV.1.3. IV.2.1. IV.3.1. IV.3.2. IV.3.3.
Sodium hydroxide, pellets	Scharlau	IV. -all-
Tris-(hydroxymethyl)-aminomethane (Tris)	Scharlau	IV.2.2. IV.2.3.

*Kindly donated by the mentioned pharmaceutical laboratory.

Location of the suppliers:

- Acros Organics (Geel, Belgium)
- Alter (Madrid, Spain)
- Astra Zeneca (Cheshire, United Kingdom)
- Aventis Pharma (Madrid, Spain)
- BD Gentest (Erembodegem, Belgium)
- Beckman Coulter (Fullerton, CA, USA)
- Ciba Geigy (Barcelona, Spain)
- Cyclolab (Budapest, Hungary)
- Fluka (Buchs, Switzerland)
- Guinama (Valencia, Spain)
- ICI Farma (Madrid, Spain)
- Italfarmaco (Madrid, Spain)
- Miquel-Otsuka (Barcelona, Spain)
- Novartis (Nyon, Switzerland)
- Panreac (Barcelona, Spain)
- Rhone-Poulenc (Madrid, Spain)
- Scharlau (Barcelona, Spain)
- Sigma (St. Louis, MO, USA)
- Squibb (Barcelona, Spain)
- VUB: Vrije Universiteit Brussel (Brussels, Belgium)
- Zeneca Farma (Madrid, Spain)

III.3. Experimental procedures

III.3.1. Capillary conditioning

The activation of new capillaries was a standard procedure applied in all cases. It consisted on 15 min rinse with 1 M NaOH at 60 °C, followed by 10 min rinse with deionized water at 25 °C and 10 min rinse with the corresponding BGE at working temperature. The pressure applied in all rinsing steps was 20 psi.

In order to achieve repeatable results in CE different cleaning procedures have been employed in this Thesis depending on the application and the capillary length, but all of them comprised rinsing the capillary in four steps: (i) deionized water, (ii) NaOH, (iii) deionized water and (iv) BGE.

When proteins were injected into the capillary (protein binding and metabolism studies), a 1 M NaOH solution was employed in order to prevent their adsorption to the capillary wall, which may result in high variability in migration times and peak shapes. For the rest of applications, the concentration of NaOH was 0.1 M. An extra rinse with MeOH was added to the NACE experiences before the BGE rinse.

III.3.2. Procedure for the chiral separation of xenobiotics

The chiral separations performed in this Thesis have been done by different modalities of EKC, using neutral or anionic cyclodextrins as chiral selectors and the partial or complete filling techniques, where the separation BGE vials remain free of chiral selector. In those cases the capillary was (partially or completely) filled with a solution of the CD in the BGE, followed by hydrodynamic injection of the racemic xenobiotic. Only in the NACE application (section IV.1.4), the cyclodextrin had to be added also to the separation vials (conventional EKC mode), in order to enhance the interaction between the racemic drugs and the chiral selector, which is disfavored in organic media. Then, the separations have been performed in normal polarity by applying different voltages. In some cases, the separation was performed by applying both voltage and a little pressure, in order to shorten migration times and improve peaks shape.

Table III.2 summarizes the general experimental conditions employed in this Thesis for the chiral separation of xenobiotics. More details about each xenobiotic enantioseparation can be found in the corresponding studies in section IV.

Table III.2: General conditions employed for the enantioseparation of xenobiotics.

Chiral selector	TM- β -CD (neutral), CM- β -CD, CM- γ -CD and HS- β -CD (anionic)
BGE	Tris or phosphate buffers, pH 6.0-8.8 (aqueous CE) DMSO/MeOH with NH ₄ Ac and HAc (NACE)
CD injection	Variable pressure/time combinations for PFT. 10 psi/1 min for CFT.
Drug injection	Hydrodynamic (0.5 psi/5s)
Capillary temperature	15-45 °C
Separation voltage	15-30 kV (normal polarity)
Separation pressure	0-0.4 psi
Detection wavelength	200-220 nm (aqueous CE), 270 nm (NACE)

III.3.3. Procedure for protein binding studies

The evaluation of the enantioselective binding of xenobiotics to HSA and total plasma proteins has been performed by ultrafiltration. With this purpose, different mixtures containing the racemic xenobiotic and HSA or human sera in different concentration ranges have been prepared in microvials (total mixture volume: 500 μ L).

Samples were incubated at 36.5 °C in a thermostated bath during 30 min, in order to reach the binding equilibrium, and then ultrafiltered through cellulose membranes using commercial filtration devices in a thermostated centrifuge at 9000 rpm during 30 min. The ultrafiltered fraction (unbound fraction of the drug) was directly injected in the CE system using for each xenobiotic its optimum

separation conditions. Figure III.1 shows a scheme of the procedure employed in this Thesis for protein binding studies.

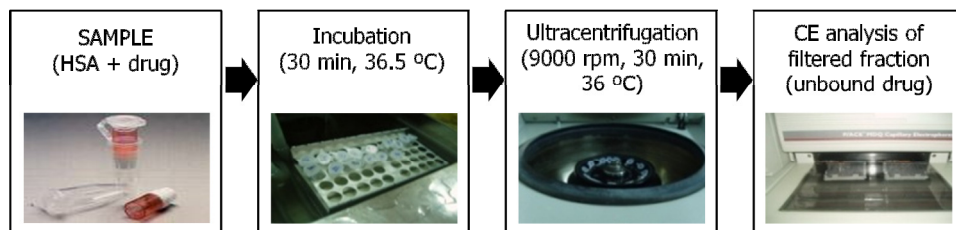


Figure III.1: UF-EKC procedure for the evaluation of enantioselective protein binding of drugs.

The calculation of the concentration of drug in the unbound fraction was done by interpolating the experimental peak area in calibration curves previously obtained for each enantiomer. When some non-specific adsorption of the xenobiotic onto the filtration devices was observed, the calibration curves were prepared following the same experimental procedure in order to correct the effect of this non-specific adsorption.

III.3.4. Procedure for electrophoretically mediated microanalysis

The fundamentals of EMMA have been widely discussed in the introduction of this Thesis. This technique consists on the use of the electrophoretic capillary simultaneously as a microreactor and as a separation column, so the mixture, incubation and separation can be performed in a unique, fully-automated step. As the enzymatic reaction takes part at a nanoscale, it is very important to adjust the incubation conditions in order to allow the reaction progress.

Two enzymatic reactions have been evaluated in this Thesis by EMMA: the hydrolysis of acetylthiocholine by AChE in order to evaluate AChE inhibitors and the enantioselective metabolism of chiral substrates by different isoforms of the

cytochrome P450. A general procedure was followed with individual conditions adapted for each reaction.

The selected modality was at-inlet EMMA, in which the substrates, enzymes and cofactors are successively injected in the inlet part of the capillary, mixed by simple diffusion, allowed to react during a given incubation time, and finally separated by CE. Table III.3 summarizes the experimental conditions employed for both enzymatic reactions, since the buffers, injection sequences, concentrations and incubation conditions may be individually selected. In the case of the evaluation of CYP metabolism, a chiral separation has been performed after the EMMA incubation, adapting separation conditions previously developed.

Table III.3: Experimental conditions employed in the EMMA assays performed in this Thesis.

	AChE	CYP450
Injection sequence	1) Water (2s) 2) 0.4 mg·mL ⁻¹ AChE (5s) 3) Substrate + inhibitor(5s) 4) 0.4 mg·mL ⁻¹ AChE (5s) 5) Water (2s) All steps at 50 mbar	1) Incubation buffer (20s) 2) CYP + Sol. B* (3s) 3) Substrate + Sol. A* (7s) 4) CYP + Sol. B* (3s) 5) Incubation buffer (10s) All steps at 0.5 psi
Incubation buffer	30 mM borate-phosphate, pH 8.0	100 mM potassium phosphate, pH 7.4
Incubation temperature	37 °C	37 °C
Incubation time	2 min	5 min
Background electrolyte	30 mM borate-phosphate, pH 8.0	50 mM sodium phosphate, pH 8.8
Separation voltage	15 kV	20 kV
Separation temperature	37 °C	25 °C

*Solutions A and B are the two parts of a NADPH regeneration system, that forms NADPH *in situ*. Their compositions are described in section III.2. NADPH is needed as a cofactor of the cytochrome P450 reaction, as stated in section I.1.1.3 (Eq. I.1).

III.4. Software and calculations

Effective electrophoretic mobilities were calculated in all cases using the following expression:

$$\mu_i = \frac{L \cdot l}{V} \left(\frac{1}{t_i} - \frac{1}{t_0} \right) \quad (\text{III.1})$$

where L is the total capillary length, l is the length of the capillary from the inlet end to the detector, V is the applied voltage, and t_i and t_0 are the measured migration times of the analyte and EOF marker, respectively.

Enantiomers resolution (R_s) was calculated as follows:

$$R_s = 1.18 \frac{t_2 - t_1}{w_1 + w_2} \quad (\text{III.2})$$

where t_1 and t_2 are, respectively, the migration times of the first and second eluted enantiomers, and w_1 and w_2 are their peak widths at 50% of peak height.

The following software has been used for data treatment and calculations:

- **Microsoft Excel**[®]: for data collecting and statistics.
- **Statgraphics**[®]: for fitting of non-linear models.
- **Matlab**[®]: for estimations of binding and kinetic constants.
- **The Unscrambler**[®]: for multivariate analysis.
- **Grapher**[®]: for representing x,y data.
- **Accelrys Draw**[®]: for drawing the chemical structures.



IV. RESULTS AND DISCUSSION

IV. RESULTS AND DISCUSSION

The results obtained in this Thesis have been grouped into three main blocks. The first one has been devoted to chiral separations of xenobiotics by CE, and includes theoretical studies about the chiral separation, an application to the determination of enantiomers in pharmaceutical samples, and a chiral NACE study. The second block includes enantioselective protein binding studies, where the binding of drugs to HSA and total plasma proteins has been evaluated by ultrafiltration followed by EKC-PFT enantioseparation. Finally, enzymatic studies by EMMA have been included in the third section, where EMMA methodologies, coupled or not with a posterior in-line enantioseparation of the studied drugs, have been developed and proposed as fast screening methods for the evaluation of drugs behavior in enzymatic reactions.

IV.1. Chiral separations of xenobiotics by capillary electrophoresis

As stated in the Introduction of this Thesis, one important application of CE is the chiral separation of small molecules (drugs and other xenobiotics) using different chiral selectors. The most widely used chiral selectors are cyclodextrins, due to their excellent enantioseparation abilities. In this Thesis, the CD of choice for enantioseparations is in most of the cases the HS- β -CD, an anionic cyclodextrin with an average content of 12 sulfate groups per molecule (Figure IV.1). Its high density of negative charge makes it an excellent chiral selector for neutral and positively charged compounds, since it remains anionic at a broad pH range.

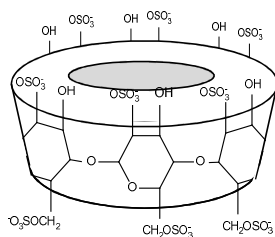


Figure IV.1: Structure of the HS- β -CD.

However, it may be taken into account that this is not a single-isomer cyclodextrin, but a mixture mainly composed of 12-sulfated isomers with identical mobilities. This feature, that is usually advantageous for enantioseparations due to the sum of different separation equilibria with each isomer, cannot be forgotten when mechanistic or modeling studies are performed.

The free enantiomers (usually positively charged for basic drugs) form complexes with the anionic CD with overall negative charge, and these negative complexes have opposite electrophoretic mobility to that of the enantiomers themselves. The different affinity of the enantiomers for the CD is usually responsible for their separation (thermodynamic enantioselectivity). When the amount of CD in the capillary is increased, the equilibrium between the free and complexed forms (Figure IV.2) is shifted to the enantiomer-CD complex, thus decreasing the effective mobilities of the enantiomers (sum of the mobilities of the free and complexed forms and the EOF mobility, see Eq. I.2) and increasing the migration times.

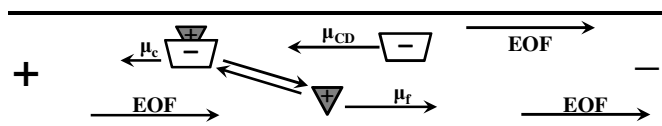


Figure IV.2: Schematic representation of the electrophoretic mobilities of the free enantiomers, the CD and their complexes, as well as the EOF mobility, in normal polarity.

Several variables influence the enantioseparation of compounds using cyclodextrins as chiral selectors. Some of them affect the equilibrium between the free and complexed forms of the enantiomers and others affect electrophoretic parameters that result in a modification on the enantioseparation. The main effects of the experimental variables on the enantioseparation of neutral and basic xenobiotics with CDs are discussed below, and some of them are shown in Figure IV.3.

The selection of the adequate cyclodextrin is usually a trial-and-error screening procedure, and, if some interaction between a concrete CD and the enantiomers is noticed, the study goes further into other experimental variables. It can be taken into account for the CD selection that charged CDs usually have stronger interaction with both neutral and charged compounds due to electrostatic forces that take part in the complexation equilibrium.

The cyclodextrin concentration and, in partial filling technique, the selector plug length, are both highly influential variables related to the amount of CD in the capillary. As explained above, an increase on the amount of CD in the capillary (higher concentration or longer SPL) favors the enantiomer-CD complexation and usually improves the enantioseparation (Figure IV.3a). With anionic CDs, the most usually employed in this Thesis, longer migration times are obtained due to the decrease of the enantiomers' effective mobility, so the CD concentration may be high enough to achieve complete enantioresolution but as low as possible to not increase the analysis time and also the analysis cost.

The pH of the BGE is also a very influential variable on the enantioseparation. It affects the magnitude of the EOF, so it influences considerably the effective mobilities of both the enantiomers and the CD. Working in normal polarity at pHs equal or higher than 6 usually allows that the enantiomer-CD complexes, negatively charged in most of the cases, reach the detector due to the EOF mobility (Figure IV.3b). On the other hand, the pH of the BGE affects not only the EOF but also the charge of the CD and enantiomers. The ideal situation for enhancing the interaction is that they have opposite charge, so the pH of the BGE can be adjusted with this purpose. The selection of the buffers that compose the BGE will be thus influenced by the working pH, since there may be selected a buffer whose pK_a is nearly the desired pH. It can be taken into account that higher buffer concentrations will diminish the electrophoretic and electroosmotic mobilities and will enlarge migration times, which can also affect the enantioresolution.

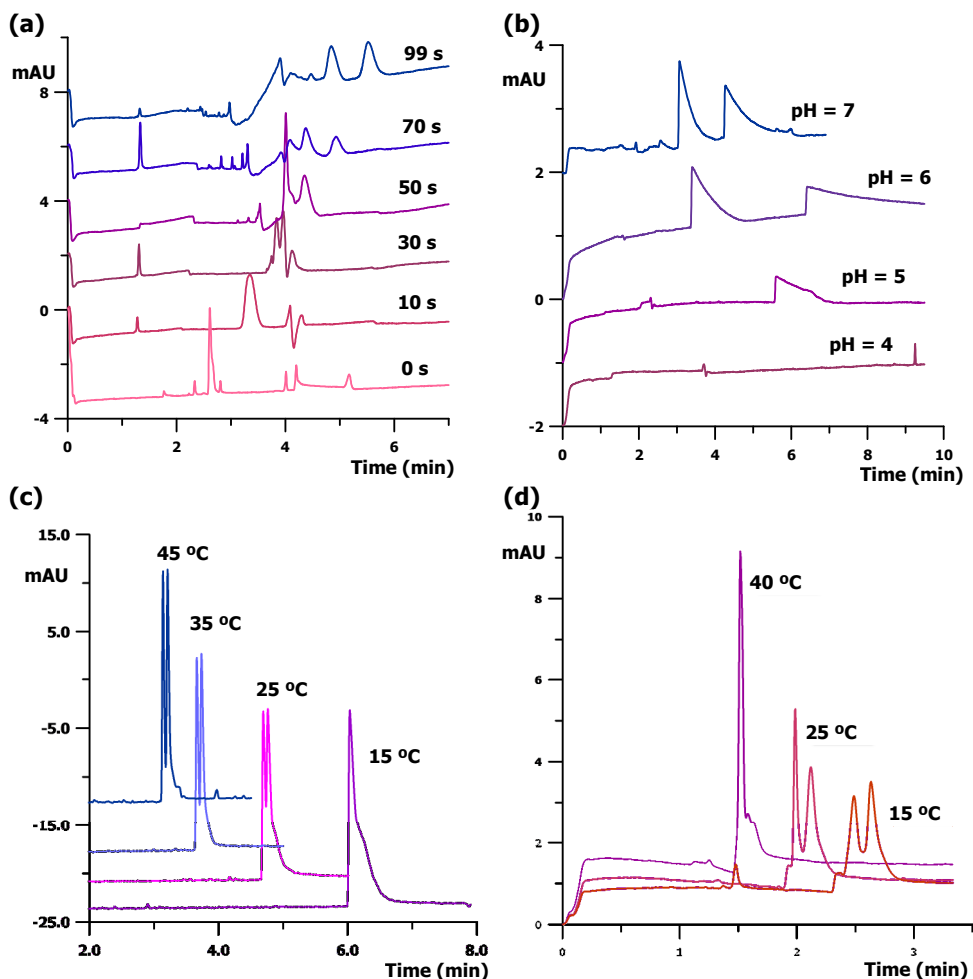


Figure IV.3: Overview of the effects of experimental variables on enantioseparation using CDs as chiral selectors. (a) Effect of the SPL on the separation of zopiclone enantiomers (BGE: 50 mM Tris at pH 6.0; 25 °C, 15 kV, chiral selector: 30 mM CM- β -CD, injected at 0.5 psi for different times). (b) Effect of the pH on the separation of fluoxetine enantiomers (BGE: 30 mM phosphate, 25 °C, 15 kV, chiral selector: 0.25% HS- β -CD injected at 5 psi/1min). (c) Effect of the temperature on the enantioseparation of nomifensine (BGE: 50 mM Tris at pH 6.0; 15 kV, chiral selector: 30 mM TM- β -CD injected at 10 psi/1 min). (d) Effect of the temperature on the separation of viloxazine enantiomers (BGE: 30 mM phosphate at pH 7.0; 25 °C, 15 kV, chiral selector: 1% HS- β -CD injected at 5 psi/1 min).

Temperature has a big influence on the enantiomers mobility (Figures IV.3c and d). Higher temperatures decrease the BGE viscosity, thus increasing the velocity of the EOF and decreasing all the migration times. As a consequence of the faster migration, usually R_s values are lower at high temperatures because the two peaks are closer (Figure IV.3d). Also, temperature affects the equilibrium of the enantiomer-CD complexation, so it can strongly affect the enantioseparation. This effect, related to the specific complexation equilibrium, will vary between molecules and should be checked individually.

Finally, the voltage applied for the separations affects the migration times and also the peaks efficiency. Higher voltages will decrease the migration times, so the enantiomers will be closer. However, if they gain in efficiency the R_s can improve. This will depend on the individual situation.

In this Thesis, the enantioseparation of several neutral and basic xenobiotics has been performed using different neutral and anionic cyclodextrins as chiral selectors. The effects explained above have been taking into account in order to achieve good resolution of the enantiomers. Table IV.1 summarizes the selected experimental conditions for the enantioseparation of compounds in each case and the R_s values obtained.

Table IV.1: Overview of all the enantioseparations performed in this Thesis.

Compound	Chiral selector	BGE	T (°C)	V (kV)	R_s
Benalaxyl	0.5% HS- β -CD	50 mM NaH ₂ PO ₄ , pH 7	40	15	4.1
Brompheniramine	0.25% HS- β -CD	50 mM NaH ₂ PO ₄ , pH 7	25	20	1.4
Bupivacaine	1.5% HS- β -CD	50 mM NaH ₂ PO ₄ , pH 7	15	15	1.6
Bupropion	1% HS- β -CD	30 mM NaH ₂ PO ₄ , pH 7	25	15	6.1
Carbinoxamine	0.25% HS- β -CD	50 mM NaH ₂ PO ₄ , pH 7	25	20	14.5
Chlorcyclizine	0.25% HS- β -CD	50 mM NaH ₂ PO ₄ , pH 7	25	20	3.1
Chlorpheniramine	0.25% HS- β -CD	50 mM NaH ₂ PO ₄ , pH 7	25	20	8.1
Clemastine	0.25% HS- β -CD	50 mM NaH ₂ PO ₄ , pH 7	25	20	1.5

Table IV.1: (Continued)

Compound	Chiral selector	BGE	T (°C)	V (kV)	<i>R_s</i>
Dimethindene	1% HS-β-CD	30 mM NaH ₂ PO ₄ , pH 7	35	15	10.2
Doxylamine	1% HS-β-CD	50 mM NaH ₂ PO ₄ , pH 7	25	20	5.5
Ethopropazine	0.25% HS-β-CD	50 mM NaH ₂ PO ₄ , pH 7	25	20	5.7
Fenfluramine	40 mM CM-γ-CD	125 mM NH ₄ Ac, 0.5 M HAc in DMSO	15	30	1.2
Fluoxetine	0.1% HS-β-CD	30 mM NaH ₂ PO ₄ , pH 7	35	15	9.2
Hexaconazole	2% HS-β-CD	50 mM NaH ₂ PO ₄ , pH 7	40	15	1.7
Hydroxyzine	0.25% HS-β-CD	50 mM NaH ₂ PO ₄ , pH 7	25	20	3.0
Imazalil	0.5% HS-β-CD	50 mM NaH ₂ PO ₄ , pH 7	40	15	3.7
Mepivacaine	1.5% HS-β-CD	50 mM NaH ₂ PO ₄ , pH 7	15	15	2.8
Nomifensine	0.1% HS-β-CD	30 mM NaH ₂ PO ₄ , pH 7	35	15	29.4
	30 mM TM-β-CD	50 mM Tris, pH 6	50	15	1.7
Norfluoxetine	1.25% HS-β-CD	50 mM NaH ₂ PO ₄ , pH 8.8	25	20	— ^a
Norverapamil	2.5% HS-β-CD	50 mM NaH ₂ PO ₄ , pH 8.8	25	20	— ^a
Orphenadrine	0.25% HS-β-CD	50 mM NaH ₂ PO ₄ , pH 7	35	15	5.8
Oxprenolol	1% HS-β-CD	50 mM NaH ₂ PO ₄ , pH 7	25	20	3.0
Penconazole	2% HS-β-CD	50 mM NaH ₂ PO ₄ , pH 7	25	15	2.1
Phenindamine	0.25% HS-β-CD	50 mM NaH ₂ PO ₄ , pH 7	25	20	22.3
Pindolol	1% HS-β-CD	50 mM NaH ₂ PO ₄ , pH 7	25	20	2.5
	40 mM CM-γ-CD	125 mM NH ₄ Ac, 0.5 M HAc in DMSO/MeOH 70:30	15	30	2.0
Prilocaine	1% HS-β-CD	50 mM NaH ₂ PO ₄ , pH 6	35	15	3.5
Promethazine	0.25% HS-β-CD	50 mM NaH ₂ PO ₄ , pH 7	15	15	3.2
Propanocaine	0.4% HS-β-CD	50 mM NaH ₂ PO ₄ , pH 6	25	15	4.1
Sotalol	1% HS-β-CD	50 mM NaH ₂ PO ₄ , pH 7	25	20	2.6
Trimeprazine	0.25% HS-β-CD	50 mM NaH ₂ PO ₄ , pH 7	25	20	1.9

Table IV.1: (Continued)

Compound	Chiral selector	BGE	T (°C)	V (kV)	<i>Rs</i>
Verapamil	2.5% HS- β -CD	50 mM NaH ₂ PO ₄ , pH 8.8	25	20	— ^a
	40 mM CM- γ -CD	125 mM NH ₄ Ac, 1 M HAc in DMSO/MeOH 80:20	15	30	1.5
Viloxazine	1% HS- β -CD	30 mM NaH ₂ PO ₄ , pH 7	15	15	3.0
Zopiclone	30 mM CM- β -CD	50 mM Tris, pH 6	25	15	2.1

^aIn the separation of drugs and metabolites together, *Rs* between enantiomers was not calculated because drug and metabolite enantiomers were interspersed. However, there was complete resolution of the four peaks in all cases.

Four studies have been included in this section, covering different topics related to chiral separations by CE. The first and second ones are theoretical studies about the use of HS- β -CD as chiral selector, concerning the binding mechanisms responsible for the enantioseparation and a quantitative structure-property relationship (QSPR) model to predict the ability of this CD to separate the enantiomers of new compounds in certain conditions. The third study is an application of the enantioseparation to the chiral analysis of commercial pharmaceutical formulations of the antidepressant fluoxetine. The last one is an approach to the use of a non-common solvent (DMSO) for NACE enantioseparations.

IV.1.1. Characterizing the interaction between enantiomers of eight psychoactive drugs and highly sulfated- β -cyclodextrin by counter-current capillary electrophoresis (Paper I)

In this work, apparent binding constants have been calculated for the interaction between HS- β -CD and the enantiomers of eight psychoactive drugs. The calculation of these binding constants provides information about the affinity of the CD for these types of compounds and can help to better understand the mechanisms responsible for the enantioseparation.

The most common situation when binding studies are performed is to carry out the chiral separation in conventional EKC, including the CD in the BGE and filling the capillary and the separation vials with it. In this case, the mathematical models described in section I.3.2.3 of this Thesis, developed by Wren and Rowe in 1992 (Wren and Rowe, 1992), are adequate for the estimation of binding constants. In PFT (Amini *et al.*, 1999a; Amini *et al.*, 1999b) apparent binding constants have been evaluated by varying the plug length of the chiral selector and studying the effect of the selector plug length on the enantiomers mobility. These models are more complex and require the estimation of the capillary fraction filled with the selector, since the mobility of the enantiomers is a sum of their mobility in the separation zone and their mobility in the rest of the capillary (filled only with BGE).

In this Thesis we have performed the binding studies using CFT, which allows saving a considerable amount of CD with respect to the conventional EKC but does not have the complicated mathematic treatment described for the estimation of binding constants by PFT in the case of the enantiomers do not leave the CD zone during their migration to the detector, since all the enantiomers migration takes part in the separation zone.

By estimation of the EOF mobility ($3.88\text{-}5.99 \cdot 10^{-8} \text{ m}^2 \cdot \text{V}^{-1} \cdot \text{s}^{-1}$) at working conditions (30 mM phosphate buffer, pH 7.0, 15 kV and normal polarity), and comparing it with the CD electrophoretic mobility ($-3.33 \cdot 10^{-8} \text{ m}^2 \cdot \text{V}^{-1} \cdot \text{s}^{-1}$, published by Chen and coworkers (Chen *et al.*, 2001)), we have concluded that the EOF will slowly push the CD to the detector. Also, as the studied compounds are basic (pK_a values between 8.1 and 9.7) and thus positively charged at the working pH, they migrate faster than the CD and do not leave the CD zone during the electrophoretic development (see Figure IV.2 for a schematic view of all the electrophoretic mobilities). So, the data treatment can be the same as in EKC and the considerations applied to PFT over the migration of the enantiomers in two different capillary zones, with and without chiral selector, are not necessary.

Another consideration that should be taken into account is the fact, previously commented, that the HS- β -CD is a mixture of 12-sulfated isomers, and individual

equilibriums with each isomer will take place. The mathematical model for multi-CD systems (Dubský *et al.*, 2010) proving that the mixture behaves like a single CD is similar to that described by Wren and Rowe:

$$\mu_i = \frac{\mu_i^0 + \mu_i^{CD} K_i' [CD]}{1 + K_i' [CD]} \quad (\text{IV.1})$$

where [CD] is the total HS- β -CD concentration and K_i' and μ_i^{CD} are the overall apparent binding constants and the overall limit mobilities, respectively, defined as:

$$K_i' = \sum_1^q \chi^q K_i^q \quad (\text{IV.2})$$

$$\mu_i^{CD} = \frac{\sum_q \chi^q K_i^q \mu_i^q}{K_i'} \quad (\text{IV.3})$$

where χ^q is the molar fraction of the q th selector isomer in the mixture, K_i^q is the individual apparent complexation constant with the i th enantiomer ($i = 1$ or 2) and q th isomer of CD, and μ_i^q is the individual mobility of the i th enantiomer- q th CD complex.

In order to estimate K' and μ^{CD} values, the effective mobility of the enantiomers, obtained using eight CD concentrations between 0 and 2%, was fitted to the CD concentration using the non-linear model of Eq. IV.1. Three capillary temperatures (15, 25 and 35 °C) have been used and a fitted model was obtained for each capillary temperature. The models obtained at 35 °C for the eight drugs studied (bupropion (BUP), dimethindene (DIM), fluoxetine (FLX), nomifensine (NMF), orphenadrine (ORP), promethazine (PRO), terfenadine (TER) and viloxazine (VLX)) can be seen in Figure IV.4, and the corresponding estimated values in Table IV.2. Similar relationships were obtained at 15 and 25 °C (see Paper I). In all cases, the fitted models showed good determination coefficients ($R^2 > 0.99$).

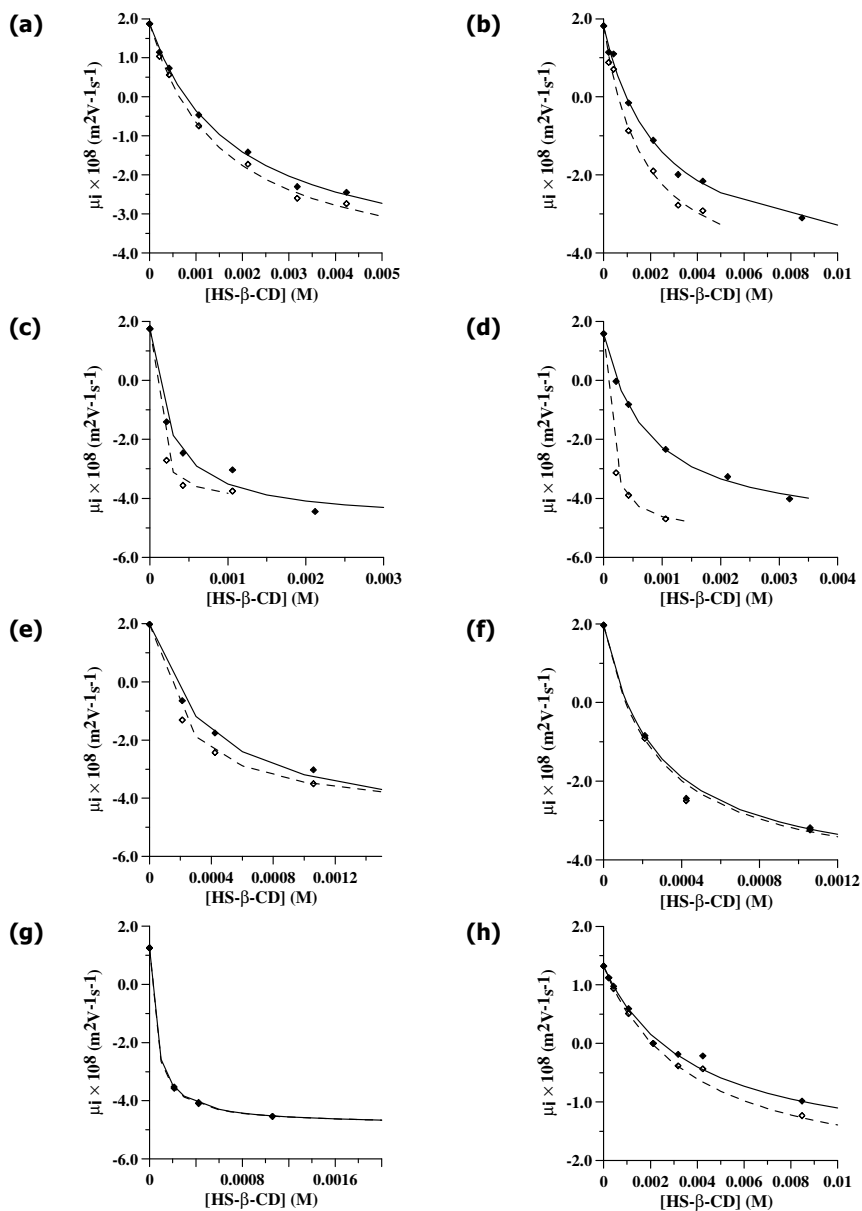


Figure IV.4: Non-linear models for the enantioselective binding constants at 35 °C of the eight drugs studied: (a) BUP, (b) DIM, (c) FLX, (d) NMF, (e) ORP, (f) PRO, (g) TER and (h) VLX (E1, \blacklozenge , solid line; E2, \diamond , dashed line).

Table IV.2: Interaction parameters for the enantiomers of the eight studied chiral drugs at 35 °C.

Drug	K_1 (M ⁻¹)	K_2 (M ⁻¹)	α_t	$\mu_1^{CD} \cdot 10^8$ (m ² ·V ⁻¹ ·s ⁻¹)	$\mu_2^{CD} \cdot 10^8$ (m ² ·V ⁻¹ ·s ⁻¹)	α_e
BUP	620 ± 70	710 ± 70	1.2	-3.9 ± 0.3	-4.1 ± 0.2	1.1
DIM	460 ± 50	660 ± 100	1.2	-4.1 ± 0.3	-4.5 ± 0.4	1.1
FLX	4500 ± 1200	16000 ± 4000	3.6	-4.5 ± 0.4	-4.1 ± 0.2	0.9
NMF	1470 ± 110	10700 ± 600	7.3	-4.74 ± 0.16	-5.06 ± 0.08	1.1
ORP	2900 ± 200	4930 ± 90	1.7	-4.74 ± 0.17	-4.43 ± 0.04	0.9
PRO	2000 ± 200	2100 ± 200	1.1	-4.3 ± 0.2	-4.3 ± 0.2	1.0
TER	17700 ± 600	18800 ± 300	1.1	-4.69 ± 0.02	-4.68 ± 0.02	1.0
VLX	310 ± 40	310 ± 40	1.0	-1.7 ± 0.2	-2.1 ± 0.2	1.2

As can be seen in Table IV.2, the highest binding constants were obtained for terfenadine, but with very low enantioselectivity values. The large size of this molecule may prevent its inclusion in the CD cavity, where the enantioselectivity occurs, also explaining its low R_s (< 1.5) in all cases. On the other hand, also high binding constants were obtained for fluoxetine and nomifensine, in this case with high thermodynamic enantioselectivities. R_s values for both drugs were also high (between 5.1 and 11.1 for FLX, and between 11.6 and 34.1 for NMF). High R_s values ($R_s \gg 1.5$) were found in all cases except terfenadine. The K' values obtained here were similar or higher than those found in the literature for this CD (Vaccher *et al.*, 2005, Lipka *et al.*, 2007), suggesting that it interacts strongly with the studied compounds.

Two possible mechanisms can be responsible for the enantioselectivity: one related to the differences between the apparent binding constants of the enantiomers (thermodynamic enantioselectivity, $\alpha_t = K'_2/K'_1$), and other to the differences on their overall limit mobilities (electrophoretic enantioselectivity, $\alpha_e = \mu_2^{CD}/\mu_1^{CD}$). A quantitative relationship between these enantioselectivities (not previously reported in the literature) is described here by means of Eq. IV.4:

$$\alpha_e = \frac{\mu_2^{CD}}{\mu_1^{CD}} = \frac{\sum_q \chi^q K_2^q \mu_2^q}{\sum_q \chi^q K_1^q \mu_1^q} \frac{1}{\alpha_t} \quad (\text{IV.4})$$

We have also estimated both enantioselectivities and we can conclude that the mechanism mainly responsible for these enantioseparations is the thermodynamic one, with values far from 1 in most of the cases, and specially high for nomifensine and fluoxetine (see Table IV.2). The electrophoretic selectivity, despite having less influence in most of the drugs, is the responsible for the enantioseparation of viloxazine, showing that when no (or little) thermodynamic enantioselectivity exists chiral separation is also possible. In conclusion, the enantioseparation of these basic drugs with HS- β -CD in EKC-CFT responds to a mixed mechanism in which thermodynamic enantioselectivity plays the major role but electrophoretic enantioselectivity has also a certain contribution.

As the binding constants and enantioselectivities were evaluated at three different temperatures, we can also see the effect of temperature on them. As a general trend, K' values decreased with higher temperatures. For example, for the first enantiomer of bupropion K' were 670, 630 and 620 M^{-1} with 15, 25 and 35°C, while for its second enantiomer they were 790, 740 and 710 M^{-1} , respectively. On the other hand, enantioselectivity values α_t and α_e practically did not change with temperature, except for nomifensine and fluoxetine. For these compounds, the quantitative relationship expected from Eq. IV.4 can be observed: α_t (as R_S) increases with temperature while α_e shows the opposite trend.

From the overall apparent binding constants and limit mobilities, the optimum [CD] for each enantioseparation, defined as the [CD] that provides the highest mobility difference between enantiomers, can be estimated using the following equation (Dubský *et al.*, 2010):

$$[CD]_{opt} = - \frac{\Delta_\mu \pm \sqrt{\Delta_\mu^2 - \frac{1}{K^\eta} \Delta_{\mu K} \widetilde{\Delta_{\mu K}}}}{\widetilde{\Delta_{\mu K}}} \quad (\text{IV.5})$$

where $\Delta_\mu = \mu_2^{r,CD} - \mu_1^{r,CD}$ (where $\mu_j^{r,CD} = \mu_j^{CD} - \mu_j^0$), $\Delta_{\mu K} = \mu_2^{r,CD} K'_2 - \mu_1^{r,CD} K'_1$, $\widetilde{\Delta_{\mu K}} = \mu_2^{r,CD} K'_1 - \mu_1^{r,CD} K'_2$, and $K^\eta = K'_1 K'_2$.

In the cases where the thermodynamic mechanism is responsible for separation and considering the limit mobilities of two enantiomers identical ($\mu_1^{CD} = \mu_2^{CD}$), Eq. IV.5 can be simplified to:

$$[CD]_{opt} = \frac{1}{\sqrt{K'_1 \cdot K'_2}} \quad (IV.6)$$

Both estimations have been done in this work, and the optimum CD concentrations obtained at 35 °C for the eight studied drugs are shown in Table IV.3. The same study for 15 and 25 °C can be found in Paper I.

Table IV.3: Optimum CD concentrations estimated for the enantioseparation of eight psychoactive drugs at 35 °C *via* two different equations.

Drug	[CD] _{opt} (m/v)	
	Eq. IV.5	Eq. IV.6
BUP	0.59	0.36
DIM	0.62	0.43
FLX	0.02	0.03
NMF	0.06	0.06
ORP	0.05	0.06
PRO	0.12	0.12
TER	0.01	0.01
VLX	–	0.76

In general, values obtained with both equations are relatively similar, confirming the major contribution of thermodynamic enantioselectivity to the enantioseparation. More differences between both values were found for the compounds that interact weakly with the CD (BUP, DIM and VLX). For viloxazine no estimation was possible using Eq. IV.5, suggesting that no optimum concentration exists and confirming that in this case electrophoretic enantioselectivity is responsible for the enantioseparation.

IV.1.2. Modeling the chiral resolution ability of highly sulfated β -cyclodextrin for basic compounds in electrokinetic chromatography (Paper II)

The development of methods for enantioseparation of chiral xenobiotics usually implies expensive and time-consuming trial-and-error procedures. However, interesting information for future researchers could be whether chiral compounds will be suitable for being enantioseparated with a concrete chiral selector. In this work, we have modeled the enantioresolution ability of the HS- β -CD, which has proved to be a good chiral selector for basic compounds, in order to establish a relationship between structural properties of new candidate compounds and their theoretical enantioseparation with HS- β -CD.

With this purpose, a simple QSPR model has been performed, based on easily available structural properties of forty selected compounds (34 drugs and 6 pesticides, see Table IV.4), and their enantioresolution under relatively similar EKC-CFT conditions with HS- β -CD (BGEs 30 or 50 mM phosphate buffers, with pH values between 7.0 and 8.8; CD concentrations between 0.25 and 2% (m/v), voltages of 15-20 kV and capillary temperatures between 25 and 40 °C). *R_s* data were obtained experimentally for this model using an EKC-CFT screening procedure or taken from some previously published papers of our research group. In that screening, the experimental conditions were as follows: BGE, 50 mM phosphate buffer, pH 7.0; capillary temperature 25 °C, voltage 20 kV and 1% HS- β -CD injected at 10 psi/1 min (filled capillary). For those cases that showed a strong interaction with the CD, no peaks were seen with the 1% HS- β -CD, so the injection was repeated using a 0.25% HS- β -CD solution.

Table IV.4: Compounds included in the QSPR model performed, numbered as they appear in the model. Their categorical *Rs* values, as well as the values of the four variables selected in the final model (*IgD*, *PSA*, *HBD* and *HBA*), are also included.

Name	Number	<i>Rs</i>	<i>IgD</i>	<i>PSA</i>	<i>HBD</i>	<i>HBA</i>
Brompheniramine	1	2	1.3	16.1	0	2
Carbinoxamine	2	2	1.4	25.4	0	3
Clemastine	3	2	2.7	12.5	0	2
Chlorcyclizine	4	2	2.9	6.5	0	2
Chlorpheniramine	5	2	1.0	16.1	0	2
Dimetindene	6	2	1.7	16.1	0	2
Doxylamine	7	2	1.1	25.4	0	3
Hydroxyzine	8	2	2.3	35.9	1	4
Orphenadrine	9	2	2.0	12.5	0	2
Phenindamine	10	2	2.7	3.2	0	1
Terfenadine	11	0	3.6	43.7	2	3
Methotrimeprazine	12	0	3.0	41.0	0	3
Ethopropazine	13	2	3.6	31.8	0	2
Promethazine	14	2	3.4	31.8	0	2
Trimeprazine	15	2	3.1	31.8	0	2
Acebutolol	16	0	-0.3	87.7	3	6
Atenolol	17	0	-1.8	84.6	4	5
Carteolol	18	0	-0.7	70.6	3	5
Timolol	19	0	-0.6	107.9	2	7
Metoprolol	20	1	-0.5	50.7	2	4
Propranolol	21	1	0.8	41.5	2	3
Pindolol	22	2	-0.5	57.3	3	4
Oxprenolol	23	2	0.1	50.7	2	4
Sotalol	24	2	-1.7	86.8	3	5
Nomifensine	25	2	0.3	29.3	2	2
Bupropion	26	2	2.1	29.1	1	4
Viloxazine	27	2	0.1	39.7	1	4
Fluoxetine	28	2	1.4	21.3	1	2
Imazalil	29	2	3.5	27.1	0	3

Table IV.4: (Continued)

Name	Number	<i>Rs</i>	<i>IgD</i>	<i>PSA</i>	<i>HBD</i>	<i>HBA</i>
Benalaxyl	30	2	3.3	46.6	0	4
Hexaconazole	31	2	3.9	50.9	1	4
Penconazole	32	2	4.6	76.4	0	3
Cyproconazole	33	1	2.8	50.9	1	4
Myclobutanil	34	1	3.1	54.5	0	4
Catechin	35	2	0.6	110.4	5	6
Verapamil	36	2	2.5	64.0	0	6
Prilocaine	37	2	1.6	41.1	2	3
Mepivacaine	38	2	1.3	32.3	1	3
Bupivacaine	39	-	2.9	32.3	1	3
Propanocaine	40	2	2.3	29.5	0	3

Due to the partially different conditions of the *Rs* data, we decided to treat them not as quantitative but as categorical (*Rs* = 0 for non-resolved enantiomers; *Rs* = 1 for partial resolution and *Rs* = 2 for completely resolved enantiomers). 15 structural variables, taken from the ChemSpider chemical structure database (ChemSpider, 2013), were used as **X**-matrix: **x**₁: logarithm of octanol–water partition coefficient (*IgP*), **x**₂: *IgP* estimated at pH 7.4 (*IgD*), **x**₃: polar surface area (*PSA*), **x**₄ and **x**₅: hydrogen bond donors (*HBD*) and acceptors (*HBA*), **x**₆: polarizability (*POL*), **x**₇: molar refractivity (*MR*), **x**₈: molar volume (*MV*), **x**₉: molecular surface area (*MSA*), **x**₁₀: van der Waals Volume (*VM*), **x**₁₁: dreiding energy (*DE*), **x**₁₂: orbital electronegativity of the chiral carbon atom (*OEC*), **x**₁₃: molecular mass (*MM*), **x**₁₄: maximal projection area (*MA*) and **x**₁₅: rotatable bonds (*RB*). The model was performed using the Unscrambler[®] software and a simple decision-making strategy.

A principal component analysis (PCA) was initially performed on the structure parameters (**X**-matrix), in order to detect highly influential compounds that could be eliminated from the further regression model. Leave-one-out cross-validation was used as validation strategy. Instead of *k*_s (suggested by the software) a manual selection of the optimum number of principal components (PCs) (*k*_o) was performed.

It was set to 2, coinciding with the first local maximum explained \mathbf{X} -variance in cross-validation (EV_{CV}), 60.7%. The corresponding explained variance (EV) was 72.6%.

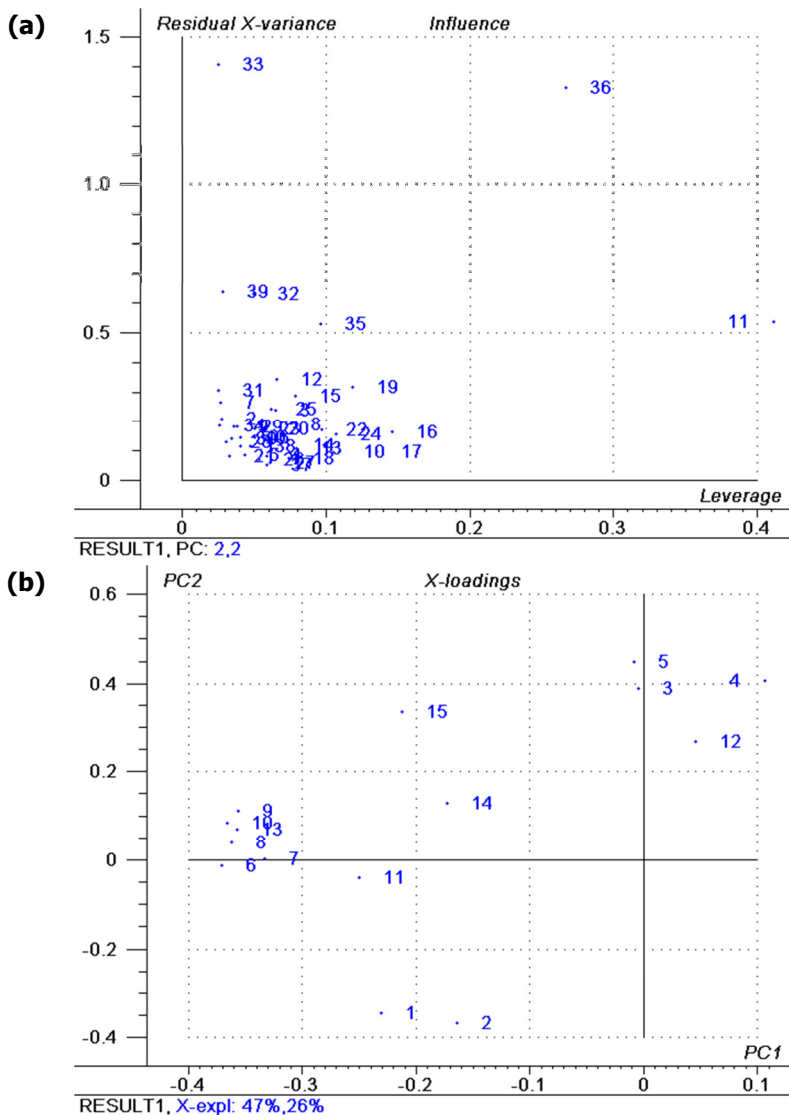


Figure IV.5: PCA (a) influence and (b) X-loadings plots corresponding to the 2-PC model performed.

Figure IV.5 shows the influence and loading plots for the 2-PC model. The influence plot (residual \mathbf{X} -variance *vs.* leverage) is used to detect atypical data, potential outliers of the model. As can be seen, a compact group with low-leverage and low-residual is observed, and compounds 36 and 11 appear as highly influential on the latent structure (high-leverage high-residual). Other less influential compounds are 33 (high-residual) and 32, 35 and 39 with medium-residual values. All these atypical compounds present a non-similar structural parameters profile and should be taken into account in the model development.

The loadings plot shows the distribution of variables over the 2 PCs. It can be seen in this plot that variables 6, 7, 8, 9, 10, 11, 13 and 14 are highly correlated, all forming low angles respect to the PC1 axis, which indicates that these variables provide redundant information.

A discriminant-partial least squares analysis over a single response variable (DPLS1) was performed, using the categorical R_s (\mathbf{y} -vector) and the structure data (\mathbf{X} -matrix). 39 compounds were used as calibration set, excluding bupivacaine that was subsequently predicted once an optimum model was obtained.

A sequential model simplification was carried out, both eliminating outlier compounds and non-significant variables. The objectives for the selected model were:

- An ideal number (k_i) of latent variables (LV); in this case $k_i = 1$, since there is a single response variable (R_s).
- A predictive power (Pp) equal or higher than 55%.
- All variables being significant (scaled regression coefficients, $\mathbf{b} \pm \mathbf{U}(\mathbf{b})$, not crossing the "0" axis).

Four plots of the DPLS1 analysis were chosen to help in the decision-making process (Figure IV.6): (a) Scaled \mathbf{b} -coefficients of \mathbf{X} -variables, plus their uncertainty limits, $\mathbf{b} \pm \mathbf{U}(\mathbf{b})$, for model stability evaluation. (b) Bi-plot of LV_2 *vs.* LV_1 , showing both scores (compounds) and loadings (variables), thus their relative "correlation". (c) EV and EV_{CV} bars for global model performance. (d) Validation plot, showing predicted *vs.*

measured y -values (both calibration and crossvalidation ones; y and y_{CV} data, respectively, for each compound).

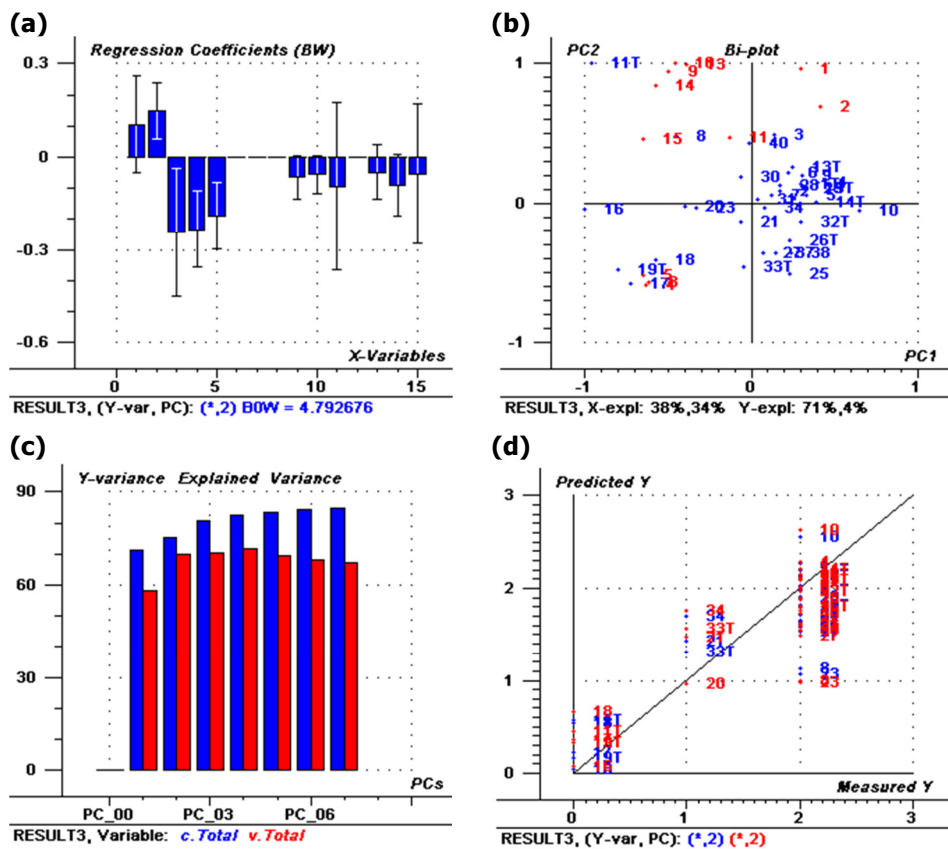


Figure IV.6: Plots corresponding to one of the simplification steps of the DPLS1 model performed. (a) Scaled **b**-coefficients of **X**-variables, plus their uncertainty limits, $\mathbf{b} \pm \mathbf{U}(\mathbf{b})$. (b) Bi-plot of LV_2 vs. LV_1 , showing both scores (compounds) and loadings (variables). (c) EV and EV_{CV} bars for global model performance. (d) Validation plot, showing predicted vs. measured y -values.

In successive steps, the model was simplified by applying two rules: the elimination of outlier compounds that were badly predicted, and the elimination of non-

significant variables (removing up to 3 variables if the predictive power of the model was less than 55%, or selecting only the significant variables if the Pp was adequate and $k_i = 1$).

For example, in the scaled **b**-coefficients plot of Fig. IV.6, it can be seen that only 4 variables are significant: IgD (x_2), PSA (x_3), HBD (x_4) and HBA (x_5). So, in this simplification step all the others were eliminated. It can be seen also in the validation plot that the model discriminates between the $R_s = 0$ and the $R_s > 0$ groups, which is an indication of the usefulness of the model. The plots corresponding to the final model, obtained after 7 simplification steps, are shown in Figure IV.7, which fits all the above mentioned objectives: $k_i = 1$, $EV = 72.4\%$, $Pp = 67.2\%$ and all variables significant.

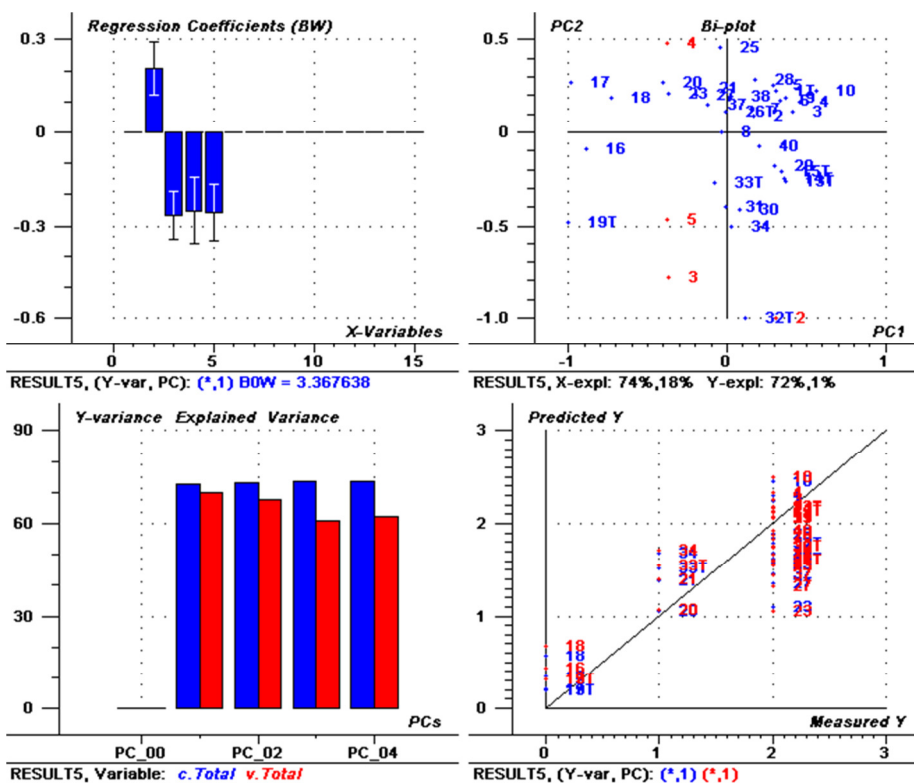


Figure IV.7: Plots corresponding to the final DPLS1 model performed.

De-scaled regression coefficients (**b**) were obtained from this DPLS1 model to derive a practical explicit model, which allows simply predicting a categorical R_s with the HS- β -CD from 4 structural properties:

$$R_s = 2.354 + 0.095I_gD - 0.008PSA - 0.159HBD - 0.137HBA$$

This model was used to predict R_s for bupivacaine, obtaining a categorical value of 1.8. This $1 < R_s < 2$ value suggests that enantioresolution is possible, but probably under specific experimental conditions. So, we propose the use of a pre-optimized experimental design (Box-Behnken) for a multivariate optimization of the three most influential EKC variables on the chiral separation (CD concentration, pH of the BGE and temperature). The Box-Behnken design for three experimental factors includes 15 experiments with three levels for each experimental factor (in this work, [HS- β -CD] 0.5-1.5%, pH 6.0-8.0 and temperature 15-35 °C) and three replicates of the central point.

A PLS2 model was performed using the experimental variables (CD concentration, pH of the BGE and temperature) as **X**-matrix and two response variables: R_s and t_{E2} (migration time of the second eluted enantiomer, to control the analysis time). As before, explicit equations for the estimation of R_s and t_{E2} were obtained from the de-scaled coefficients:

$$R_s = 3.497 + 0.269CD - 0.034T - 0.268pH$$

$$t_{E2} = 14.05 + 1.96CD - 0.247T - 0.149pH$$

As expected, CD is positively correlated with both response variables, while pH and T are negatively correlated. These effects can be easily explained from an electrophoretic point of view taking into account the separation mechanism, which implies the formation of anionic inclusion complexes with the cyclodextrin. Higher CD concentrations lead to longer migration times, because the equilibrium of the free-complexed drug is shifted to the complexed form (see Fig. IV.2); a higher R_s is reasonable because the complexed form is who migrates enantioselectively. For the increase of T , shorter migration times are logical for both enantiomers due to the decrease of viscosity of the BGE and the consequent increase of current. Therefore,

if both enantiomers migrate faster, less R_s is coherent. The same effect is observed with the pH, since higher pH implies higher EOF mobility, accelerating the migration of both enantiomers and decreasing the R_s value.

With these equations, simulated R_s and t_{E2} data could be generated in order to select the optimum experimental conditions (R_s around 2 with a short analysis time). In this work, simulations were performed for predicting the enantioresolution of bupivacaine: different values were given to the variables CD , T and pH , and R_s and t_{E2} were estimated from the explicit equations previously obtained. As an example, for $CD = 2\%$ (m/v), $T = 15$ °C and $pH = 6$, R_s is estimated as 1.92 and t_{E2} as 13.4 min, which is a good combination to be verified experimentally. So, these conditions could be selected to attempt the enantioseparation of bupivacaine.

IV.1.3. Determination of fluoxetine enantiomers in pharmaceutical formulations by electrokinetic chromatography-counter current technique (Paper III)

Fluoxetine is a selective serotonin-reuptake inhibitor, widely employed around the world as an antidepressant, but also indicated for other psychiatric disorders such as obsessive compulsive disorder or bulimia nervosa. Despite it is used as a racemate, stereospecificity associated with its interactions with the serotonin-reuptake carrier has been described. Methods for its chiral analysis become thus important for the pharmaceutical industry. In this work, an enantioselective method for the analysis of fluoxetine enantiomers in pharmaceuticals by EKC-counter current technique using HS- β -CD as chiral selector has been developed. It was optimized for a matrix including an interfering compound and applied to the analysis of three pharmaceutical formulations. Two of the samples were fluoxetine pills (Fluoxetina Teva[®] and Fluoxetina Mabo[®]) and the third one (Prozac[®]) was presented in tablets. The procedure for the analysis of samples is schematically shown in Figure IV.8.



Figure IV.8: Scheme of the experimental procedure used for the chiral analysis of fluoxetine in pharmaceutical formulations by EKC-CFT.

In preliminary studies, the following EKC-CFT conditions (previously developed by our research group) were tested here for the pharmaceutical samples: effective capillary length: 21 cm; BGE: 30 mM phosphate buffer, pH 7.0; 0.25% HS- β -CD injected at 2 psi/1 min; capillary temperature 30 °C and separation voltage 15 kV (with a little pressure of 0.3 psi in order to improve peak shapes). Using these conditions, which allow the chiral separation of fluoxetine with HS- β -CD in less than 4 minutes, an interference peak overlapped with the first enantiomer in Prozac[®] samples (Figure IV.9a).

Modifications in separation conditions were tested to improve the separation and efficiency of the electrophoretic peaks, trying to avoid this interference. For this purpose, voltages ranged between 5 and 25 kV were assayed using as BGE a 30 mM phosphate solution at pH 7.0, 7.5 and 8.0, and in all experiences 0.25% HS- β -CD.

As expected, an increased voltage yielded shorter migration times and higher efficiencies and resolution. However, the generation of Joule heat may limit the theoretical gain in resolution and efficiency with voltage. For fluoxetine, migration times of both enantiomers became shorter at higher voltages while resolution slightly decreased, being $R_s > 1.8$ in all cases. An increased voltage had also a good effect on the enantioseparation between the first eluted enantiomer and the interference peak, so 25 kV was selected as the separation voltage. On the other hand, the increase on pH values had no significant influence on migration times, but improved the resolution and in most cases the efficiency. Moreover, the application

of a pressure of 0.3 psi to the inlet vial during the electrophoretic processes led to higher efficiency, with an improvement in peak shapes.

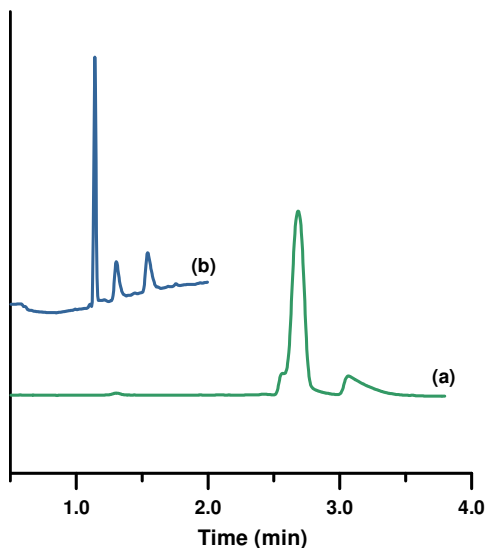


Figure IV.9: Electropherograms corresponding to the enantioseparation of fluoxetine in Prozac[®] samples (a) before and (b) after the optimization of the separation conditions.

From the results obtained, an applied voltage of 25 kV, a pressure of 0.3 psi and a 30 mM phosphate solution at pH 8.0 as BGE were selected. Using these conditions, complete enantioseparation of fluoxetine ($R_s = 2.4$) was achieved in less than 2 min (see Figure IV.9b). These separation conditions were adequate also for the analysis of the other pharmaceutical formulations (Fluoxetina Teva[®] and Fluoxetina Mabo[®]).

Once the separation conditions were selected, a partial validation of the method was performed, taking into account the features recommended by the International Conference on Harmonization (ICH) for analytical methods, and the requirements of the US Pharmacopeia. For the quantification of the analyte in the major-minor concentration level (this case), the ICH recommends to study the following features in a partial validation: confirmation of analyte identity (specificity), accuracy (or

recovery), precision (preferable in intermediate precision conditions) and linearity (in the practical range; the full linear range is not mandatory). Here, the confirmation of analyte identity was performed by recording the spectra along peak elution. The accuracy, precision and linearity results are shown in Table IV.5. As can be seen in this table, good analytical features were obtained, following the criteria of the Spanish accreditation entity, ENAC, for linearity ($R^2 > 0.995$ for chromatographic and related techniques), and the requirements of the US Pharmacopeia for recovery (85-115%). For all samples, analyzed with only a single replicate, which is the most common situation in testing laboratories, the content of racemic fluoxetine was within specifications of the US Pharmacopeia ($\pm 15\%$ criterion), and stereoisomer ratios were around 1 (Table IV.6).

Table IV.5: Main analytical features of the proposed chiral method.

Features	Fluoxetine-E1	Fluoxetine-E2
Linearity		
Linear range	5-50 mg·L ⁻¹	5-50 mg·L ⁻¹
Linear equation (determination coefficient, R^2)	$y = 112.83 + 54.44x$ (0.996)	$y = 97.12 + 49.27x$ (0.996)
Precision (n = 3)		
Sample result	11.8 ± 1.7 mg	11.1 ± 1.9 mg
Intermediate precision (RSD)	14.8%	17.3%
Accuracy (fortification assay)		
Intermediate recovery	92 ± 13	105 ± 6

Table IV.6: Results of the sample analysis of three pharmaceutical formulations containing racemic fluoxetine (labeled content: 20 mg).

Pharmaceutical	Rac-Fluoxetine	Fluoxetine-E1	Fluoxetine-E2	Stereoisomer ratio (E1/E2)
Fluoxetina Mabo®	21.0 mg	10.6 mg	10.4 mg	1.02
Prozac®	20.1 mg	9.0 mg	11.1 mg	0.82
Fluoxetina Teva®	21.4 mg	11.0 mg	10.4 mg	1.06

IV.1.4. Chiral separations by non-aqueous capillary electrophoresis in DMSO-based background electrolytes (Paper IV)

This work, performed in the Katholieke Universiteit of Leuven, responded to the interest on developing non-aqueous systems that could be able to dissolve new active pharmaceutical ingredients (APIs) which are non-soluble in aqueous systems and could be also non-soluble in methanolic mediums. DMSO is presented as an alternative to alcohols in chiral NACE, and a univariate optimization of the chiral separation is performed. In this case, the individual study of variables is considered interesting because there is still a certain lack of knowledge on the behavior of NACE systems.

The main advantages of DMSO that make it a promising solvent for NACE are its high dielectric constant, low toxicity and lack of volatility and hazardousness. Alcoholic BGEs are usually volatile, and this may affect the BGE composition and cause current breakdowns. In this work, current was highly stable in all cases.

Chiral separation of three drugs (verapamil, pindolol and fenfluramine) was performed, using a DMSO-based BGE and CM- γ -CD as chiral selector. A small percentage of methanol was added to the BGE in order to increase the current and facilitate the dissolution of the electrolytes, ammonium acetate and acetic acid. So, initial experimental conditions were: BGE, DMSO-MeOH 80:20, with 50 mM NH₄Ac, 1 M HAc and 40 mM CM- γ -CD; capillary temperature 25 °C and applied voltage 20 kV. With these conditions, partial resolutions of the three drugs were achieved, so they were adjusted in order to improve enantioseparations. The effects of separation temperature and voltage as well as the concentration of all the BGE components on the drugs enantioresolution were studied individually and combined in order to obtain the best separation conditions. It may be taken into account that enantioseparations in DMSO media are *a priori* disfavored due to the weak intermolecular interactions between chiral selectors and enantiomers in these organic media.

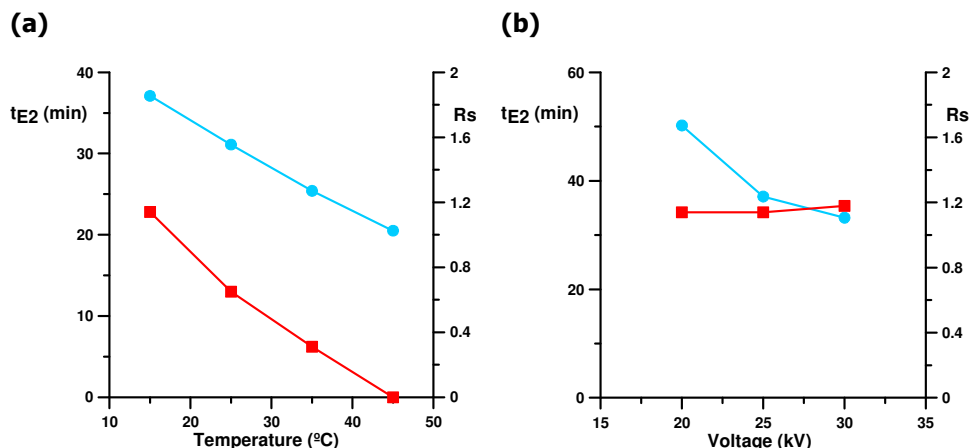


Figure IV.10: Effect of (a) temperature and (b) voltage on the enantioseparation (■) and migration time of the second eluted enantiomer (●) of verapamil by chiral NACE. Other experimental conditions: BGE DMSO/MeOH 80:20, 50 mM NH_4Ac , 1 M HAc, 40 mM CM- γ -CD. Voltage in (a): 25 kV. Temperature in (b): 15 °C.

The capillary temperature was ranged between 15 and 45 °C. Higher temperatures led in all cases to shorter migration times and, as a consequence, worse enantioresolutions, as can be seen in Figure IV.10a for the enantioseparation of verapamil. Consequently, despite analysis times were longer, the lowest possible temperature was selected in all cases (15 °C). On the other hand, the increase on separation voltage (range: 20-30 kV) decreased the migration times, which usually decreases enantioresolution, and improved the peaks efficiency, which usually improves the R_s , thus the R_s values were practically not affected by the voltage due to the combination of both effects, as can be seen for verapamil in Figure IV.10b. The highest possible voltage (30 kV) was selected here as best option because it provided the shortest analysis times.

The HS- β -CD concentration in the BGE was ranged between 10 and 70 mM. This uses to be the most influential variable on enantioseparations, since, as has been previously described, the complexation between the CD and the enantiomers is responsible for the chiral separation. Here, a maximum R_s value was observed for

the three drugs studied at about 40 mM (slightly better 50 mM for verapamil, but 40 mM was enough), and higher concentrations provided worse enantioresolutions (Figure IV.11).

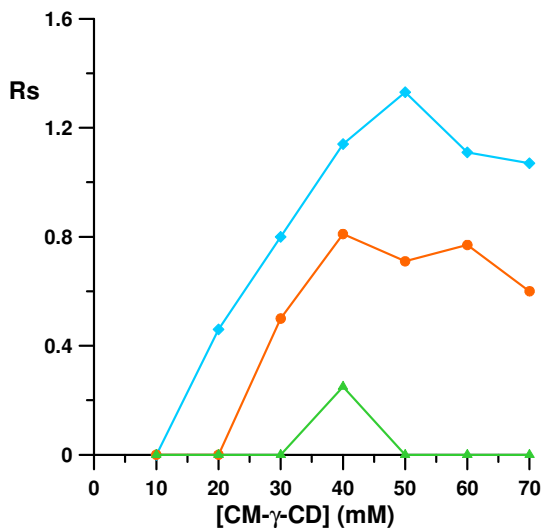


Figure IV.11: Effect of the CM- γ -CD concentration on the enantioseparation of (\blacklozenge) verapamil, (\bullet) pindolol and (\blacktriangle) fenfluramine.

The physicochemical properties of DMSO and MeOH are quite different: MeOH has lower dielectric constant (ϵ), much lower viscosity (η), lower boiling point, and lower autoprotolysis constant (pK_{auto}), which implies that more ions in solution will be found in methanolic BGEs. So, the percentage of MeOH will modify considerably the physicochemical properties of the BGE and will strongly affect the enantioseparation. In this work, since our main aim was to employ a DMSO-based BGE, the percentage of MeOH was varied from 0 to 30%, so the main component of the BGE was DMSO in all conditions.

A decrease in MeOH percentage increases the migration times of all compounds. In the case of verapamil best R_s is obtained with 20% MeOH, so it is selected as optimum. For pindolol there is a clear decrease in R_s when the MeOH percentage is

decreased so 30% is selected as best option since it combines better R_s with shorter migration time. The case of fenfluramine is the opposite; the split of peaks is larger without MeOH so a pure DMSO BGE is selected as best option.

The differences between the three compounds in the optimum MeOH percentage should be due to a dual mechanism that affects the enantioresolution: on one hand, the increase in MeOH increases the ϵ/η ratio of the BGE, which is a measure of the speed of the analysis, and decreases in consequence the migration times, so, if peaks migrate faster, less R_s can be expected *a priori* (this is the case of fenfluramine). On the other hand, as DMSO is an aprotic solvent, the increase of MeOH can increase the ionization degree of the drugs, enhancing the interaction with the anionic CD (the case of pindolol). For verapamil, both opposite effects lead to an intermediate BGE composition (DMSO/MeOH 80:20) as the best option.

The NH_4Ac concentration (25-125 mM in this work) showed a notable effect on the R_s . The increase on NH_4Ac concentration, despite increasing the current, led to longer migration times, due to a decrease on the electrophoretic and electroosmotic mobilities, which is perhaps more important here than in aqueous media. Considerably better enantioselectivities were found with high NH_4Ac concentrations, so 125 mM was selected for all the enantioseparations. The HAc concentration (0.5-1.5 M) had slight effect on the enantioseparation; 1 M was selected for pindolol and fenfluramine and 0.5 M for verapamil, because these conditions provided in each case slightly better separations. The final conditions selected, as well as the corresponding electropherograms, can be found in Table IV.7.

Table IV.7: Final separation conditions in chiral NACE for the three drugs studied.

	Verapamil	Pindolol	Fenfluramine
T (°C)	15	15	15
V (kV)	30	30	30
[CM-γ-CD] (mM)	40	40	40
%MeOH	20	30	0
[NH₄Ac] (mM)	125	125	125
[HAc] (M)	1	0.5	0.5
<i>Rs</i>	1.5	2.0	1.2
<i>t</i>_{E2} (min)	43	25	42
Current (μA)	25	29	17

Electropherogram

IV.2. Study of enantioselective binding of drugs to plasma proteins

As stated in the introduction of this Thesis, HSA is the most abundant protein in human plasma (60% of the protein content, with a plasmatic concentration of 35-45 g·L⁻¹). It binds a wide number of xenobiotics with a certain degree of enantioselectivity in most of the cases. Consequently, the knowledge about the binding of xenobiotics to HSA is interesting from a pharmacokinetic point of view, since most of the interactions and displacements of protein binding will take place with the HSA molecule, and can be enantioselective.

The protein binding of drugs is a well-known pharmacokinetic parameter which has to be evaluated during the drug development process. However, in most of the cases, no enantioselective information can be found in the literature for the protein binding of chiral drugs. Thus, the development of methodologies for the *in vitro* evaluation of enantioselective protein binding is an interesting field in bioanalytical chemistry. Moreover, an adequate mathematical treatment of the experimental data is important in order to obtain accurate estimations.

In this section, the evaluation of enantioselective binding of drugs to HSA and total plasma proteins is described in three studies about this topic. The first one, concerning the binding of the antidepressant fluoxetine to HSA, points out some weak aspects of the experimental methodologies and mathematical models previously published for the estimation of protein binding, and proposes a novel strategy for a reliable binding affinity evaluation. The second and third studies evaluate the binding of the hypnotic drug zopiclone and the antidepressant nomifensine to HSA and total plasma proteins, using the new mathematical approaches discussed in the first one.

IV.2.1. Evaluation of enantioselective binding of fluoxetine to human serum albumin by ultrafiltration and CE – Experimental design and quality considerations (Paper V)

In this work a discussion concerning the different experimental designs and mathematical approaches to HSA binding estimations is performed, using the HSA binding of the antidepressant fluoxetine as an example. The methodology used for the protein binding study is ultrafiltration followed by chiral separation of the unbound fraction by EKC-CFT with HS- β -CD as chiral selector. The experimental details are described in the Methodology section of this Thesis. Figure IV.12 shows the electropherogram corresponding to the chiral separation of fluoxetine enantiomers in a standard solution and in an ultrafiltrate (unbound fraction).

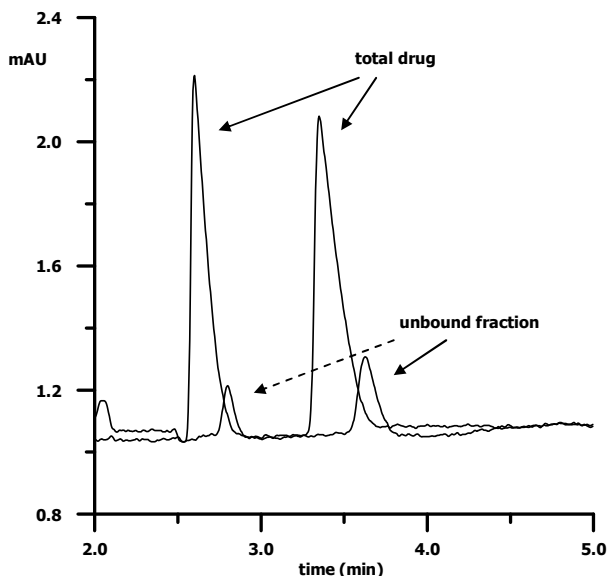


Figure IV.12: Electropherograms corresponding to a sample containing 200 μM racemic FLX (total drug) and the unbound fraction after ultrafiltration. Experimental conditions: BGE 30 mM phosphate, pH 7.0. 0.25% HS- β -CD as chiral selector, rinsed 2 psi/1 min. Separation at 30 $^{\circ}\text{C}$, 15 kV + 0.3 psi.

The first consideration that should be taken into account is that the *in vitro* system used for the binding study must simulate, as well as possible, the *in vivo* situation in order to obtain reliable estimates. Estimations done far from physiological conditions could provide results far from the real situation. Based on literature information about the steady-state concentration (C_{ss}) of fluoxetine in human plasma (around 0.2 μM of racemic FLX in a normal dosage situation) and the albumin plasmatic concentration (500-600 μM), an estimation of the *in vivo* D/P ratio was performed (D : total drug concentration; P : total protein concentration), showing that in a physiological normal situation $D/P \ll 1$.

From the general model for binding constants estimation (Eq. I.8), which considers that the protein molecule can have m kinds of binding sites with n sites of each kind, it is very difficult to estimate reliable affinity constants or apparent stoichiometries of

the binding process, due to its complexity. Thus, simplifications of Eq. I.8 become necessary, considering $m = 2$ (Eq. I.9) or $m = 1$ (Eq. I.10). These 4- and 2-parameter equations are simpler than the general model, but it may be taken into account that the assumptions performed ($m = 1$ or 2) should be checked for consistent estimations. *In vivo*, where $D \ll P$, the most probable situation is that the drug only binds to a kind of binding site in the protein, so $m = 1$. Furthermore, as there is a considerable excess of protein over the amount of drug in plasma, the stoichiometry of the binding will probably be 1:1 (only one molecule of drug *per* molecule of protein), so $n_1 = 1$. If the *in vitro* model tries to assembly the *in vivo* conditions and keeps the D/P ratio low enough, these assumptions can be also done *in vitro* and simplify the calculations considerably without losing reliability.

Experimental designs, defining the concentration ranges of D and P and the number of concentration levels, may thus be planned taking into account this consideration. There can be found in the literature experiments that use a fixed P level and different D levels in a broad range that covers several orders of magnitude. The main drawback of these designs is that they do not keep the D/P ratio < 1 , using frequently $D > P$ in some points. In contrast, we propose to perform two experimental designs, one keeping constant the concentration of protein and varying the drug (the most usual design) and other keeping the concentration of drug and varying the HSA level. The aim of performing two experimental designs is to have independent results and control the possible effect of varying the P -concentration on the estimations. In this work, we have performed both designs keeping the D/P ratio ≤ 0.5 and adjusting the lowest D levels taking into account the approximate quantification limits for d_{E1} and d_{E2} . So, in the P -constant design, D was ranged between 100 and 200 μM ($P = 475 \mu\text{M}$), and in the D -constant design, P was between 250 and 500 μM ($D = 125 \mu\text{M}$). All mixtures have been prepared and evaluated in duplicate in order to control (and eliminate, if necessary) atypical experimental data.

Prior to K_I estimations, outliers' identification and elimination is necessary since outlier values can considerably affect the K_I estimates. A possibility is to inspect directly the experimental data (d values) but it is preferable to evaluate outliers directly on the K_I estimates. With this purpose, we propose to perform individual estimations of K_I from each d - D - P data, via Eq. IV.7 (which provisionally assumes $n_I = 1$, this may be confirmed later):

$$K_1 = \frac{1}{d} \cdot \frac{r}{1-r} \tag{IV.7}$$

and check which K_I or $\log K_I$ values are far from the average value or median. This has been done in this work using the Grubbs test, a suitable approach to evaluate one (single) or two (double) extreme data. Here, the application of the Grubbs test ($\alpha = 2.5\%$, 2 tails) confirmed that the point ID = 13 was an outlier (see Figure IV.13), so it was eliminated from further estimations. No other points were considered as outliers by applying this test.

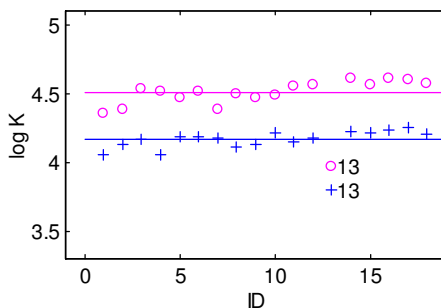


Figure IV.13: Log K_I values estimated for E1 (●) and E2 (+) from Eq. IV.7 using individual d - D - P data corresponding to the fluoxetine-HSA binding. Horizontal lines indicate the averaged values (after elimination of point ID = 13).

In Figure IV.13 it can also be observed that no significant differences exist between the estimation of K_I via a P -constant design (points ID = 1-10) or a D -constant one (points ID = 11-18). So, it can be concluded that the usual P -constant design should

be enough to provide reliable estimates if P is near physiological values and the D/P ratio is kept in its adequate range.

In this work, different equations have been checked and compared in terms of quality of estimations and robustness, in order to obtain a reliable estimation of the enantioselective protein binding and also to provide a working protocol for future protein binding estimations.

Eq. IV.7 allows performing individual K_I estimations from independent d - D - P data. This is interesting also because it allows performing an estimation of the uncertainty of K_I estimates. The only consideration that should be taken into account is that the assumption $n_i = 1$ must be confirmed to accept the data from Eq. IV.7 (despite it is the most probable situation in our experimental design). In order to confirm this assumption two possibilities are proposed. The first one is a linear equation derived from Eq. IV.7:

$$\log \frac{r}{1-r} = \log K_1 + \log(d) \quad (\text{IV.8})$$

With this equation, plotting $\log(r/(1-r))$ vs. $\log(d)$, slope = 1 verifies the assumption $n_i = 1$. Here, slopes of 1.0 and 1.1 were obtained for E1 and E2 respectively using data from the P -constant design, and 1.1 and 0.9 with data from the D -constant design, thus confirming that $n_i = 1$ and the validity of Eq. IV.7.

The other possibility proposed for the confirmation of the $n_i = 1$ assumption is the use of a 2-parameter model developed by a former member of our research group: a non-linear equation derived from Eq. I.10, in which d is a dependent variable of D and P (Martínez-Pla et al., 2004). Here, n_i and K_I can be estimated using non-linear approaches; however, several sets of values can be found (same problem as in Eq. I.10):

$$d = \frac{-(1 - K_1 D + n_1 K_1 P) \pm \sqrt{(1 - K_1 D + n_1 K_1 P)^2 + 4 K_1 D}}{2 K_1} \quad (\text{IV.9})$$

This problem is less relevant here, since Eq. IV.9 is proposed only with checking purposes and the estimations of K_I (and subsequently n_i) are derived from Eq. IV.7.

Eq. IV.9 is an alternative to the most popular linear approaches (Eqs. I.11-13, in Table I.2) which could provide inconsistent results, especially with short D -ranges (as in the experimental design proposed here in order to keep $D/P < 0.5$). Here the linear models have been also evaluated by adjusting data of E2 (P -constant design) to Eqs. I.11-13, obtaining inconsistent and erratic values. Log K_I and n_I values estimated from the Klotz plot (Eq. I.11) were 3.7 and 2.0, and from Scatchard (Eq. I.12) and y -reciprocal (Eq. I.13) plots the estimates were 3.5 and 4.1, and 3.9 and 1.5, respectively. Also, as these estimations are done from the slope and intercept of the linear models, the elimination of one point will have important consequences on the estimates, which lack of any robustness.

It may be taken into account that Eq. IV.9 requires a concrete experimental design in order to adjust d vs. D or d vs. P , keeping constant the other variable (Fig. IV.14a). However, estimations can be performed with all the joined data (d vs. D and P) by plotting a response surface (Fig. IV.14b).

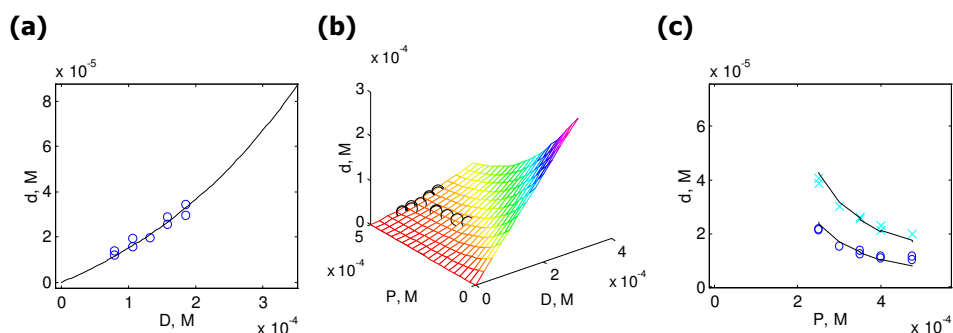


Figure IV.14: Three different plots derived from Eq. IV.9: (a) d vs. D plot (P -constant design, data from E2), (b) response surface plot (d vs. D and P , data from E2) and (c) d vs. P plots (D -constant design) adjusted simultaneously for both enantiomers using a competitive model (○, E1; ×, E2).

All these estimations have been performed considering an independent model where each enantiomer binds independently to the HSA molecule, thus not affecting the binding of the other one. On the other hand, a competitive model, where both

enantiomers compete for the free binding sites and consequently the binding of one enantiomer will be affected by the binding of the other one, can be also considered. From these two possibilities, the most probable when low D/P ratios are used is the independent one, since the amount of HSA is quite bigger and each enantiomer will easily find free binding sites. Nevertheless, in this work both possibilities are considered.

The competitive model is a modification of Eq. IV.9 which considers the concentrations of both enantiomers in the mixture (Eqs. IV.10 and IV.11 for estimating K_{E1} and K_{E2} , respectively):

$$d_{E1} = \frac{-(1 - K_{E1}D + n_1K_{E1}P + K_{E2}d_{E2}) \pm \sqrt{(1 - K_{E1}D + n_1K_{E1}P + K_{E2}d_{E2})^2 + 4K_1D}}{2K_{E1}} \quad (\text{IV.10})$$

$$d_{E2} = \frac{-(1 - K_{E2}D + n_1K_{E2}P + K_{E1}d_{E1}) \pm \sqrt{(1 - K_{E2}D + n_1K_{E2}P + K_{E1}d_{E1})^2 + 4K_1D}}{2K_{E2}} \quad (\text{IV.11})$$

In order to avoid bad estimations of the parameters by using these equations separately, a SIMPLEX algorithm that simultaneously optimizes both equations has been designed. The corresponding d vs. P plots for both enantiomers are shown in Fig. IV.14c. Table IV.8 summarizes all the $\log K_i$ estimates obtained in this work using the different equations proposed.

Table IV.8: Log K_i estimated values obtained with the different mathematical models proposed.

Model	Eq.	Conditions	$\log K_{E1}$	$\log K_{E2}$
Independent	IV.7	All data	4.51 ± 0.08	4.17 ± 0.06
	IV.9	P-constant	4.47	4.15
		D-constant	4.57	4.20
		All data	4.53	4.18
Competitive	IV.10 and 11	P-constant	4.67	4.37
	IV.10 and 11	D-constant	4.87	4.52

As can be noticed from Table IV.8, no differences were found between the estimations performed with the independent and competitive models for the fluoxetine-HSA binding, suggesting that, as expected, at low D/P ratios no competition between the enantiomers takes place and independent estimations *via* Eqs. IV.7 and IV.9 are enough to obtain reliable binding constants.

From the results obtained in this work a quality protocol for performing enantiomer-protein binding studies is proposed in order to obtain robust estimates in future protein binding studies. This protocol includes the following steps:

- (i) Elimination of outliers (Eq. IV.7)
- (ii) Verification of $n_I = 1$ (Eq. IV.8) and consequent acceptance of the K_{E1} and K_{E2} estimates of Eq. IV.7.
- (iii) Estimation of K_{E1} and K_{E2} *via* Eqs. IV.7 and IV.9 (independent model) or *via* Eqs. IV.10 and IV.11 (competitive model, less usual in the proposed experimental design).

On the other hand, the enantioselectivity degree (ES) is an important parameter of the enantiomer-binding studies that can be estimated from the ratio K_{E1}/K_{E2} . ES for fluoxetine enantiomers has been estimated as 2.20 using data from the independent model and 2.14 using data from the competitive one, so the binding of FLX enantiomers to HSA can be considered enantioselective.

Finally, other parameter that is interesting from a pharmacokinetic point of view is the percentage of protein binding ($PB\%$), which may be estimated at physiological conditions. It can be calculated as:

$$PB\% = \frac{D - d}{D} \cdot 100 \quad (IV.12)$$

which is an expression analogue to Eq. I.7.

From the D and P physiological levels found in the literature, d was estimated *via* Eq. IV.9 and used for the calculation of $PB\%$. $PB\%$ estimates were 95.2 and 90.0% for E1 and E2, respectively. These values are consistent with that reported for racemic FLX (94.75%).

IV.2.2. On the zopiclone enantioselective binding to human albumin and plasma proteins. An electrokinetic chromatography approach (Paper VI)

Zopiclone is a non-benzodiazepine hypnotic drug used for the treatment of insomnia. It increases the inhibitor effect of the neurotransmitter GABA (γ -aminobutyric acid) by binding to the GABA_A channel. It has been demonstrated that the hypnotic activity resides in the S-enantiomer, while R-zopiclone has no effect. Consequently eszopiclone, a new drug consisting on the pure S-enantiomer, has been recently commercialized.

Information about plasma protein binding of zopiclone is available in the literature, but there are considerable differences between the previously published results (*PB%* varying from 45 to 85% for the racemate, and only one enantioselective estimation but using experimental conditions very far from physiological ones). So, a reliable *in vitro* estimation of the enantioselective binding of zopiclone to HSA and other plasma proteins results interesting since there may be differences between the pharmacokinetics of the enantiomers.

The evaluation of enantioselective protein binding of zopiclone has been performed by ultrafiltration followed by chiral separation of the unbound fraction by EKC-PFT (the same methodology described before for fluoxetine). Here, the chiral separation has been carried out with CM- β -CD, an anionic cyclodextrin which strongly interacts with basic compounds like zopiclone ($pK_a = 6.9$).

Initially, the effect of some experimental conditions on the chiral EKC-PFT separation has been studied. A preliminary study of the pH and BGE composition showed that best resolution, signal-to-noise ratio and analysis time were obtained using 50 mM Tris at pH 6.0 over other buffers such as citrate, 2-(N-morpholino)ethanesulfonic acid (MES) or phosphate.

Figure IV.15 shows the effects of the CM- β -CD concentration and the SPL on the enantioseparation of zopiclone. As shown in Fig. IV.15a, an increase on the CD concentration increases the migration time and enhances the resolution. With 20 mM CM- β -CD the enantiomers are completely separated, but the first one overlaps with a

change in the baseline signal that could hamper its measurement. 30 mM CM- β -CD provides the best results in terms of resolution, migration times and peaks shape, so this concentration is selected for further studies. The effect of the SPL, which is shown in Fig. IV.15b, is very similar to that of the CD concentration. Larger amounts of CD injected in the capillary lead to longer migration times and better R_s values. Complete enantioresolution is reached with an injection of 30 mM CM- β -CD at 0.5 psi/99s, so this SPL is selected.

Temperature is considered a key parameter in the chiral separation because it can affect peaks efficiency, BGE viscosity and the enantiomer-chiral selector interaction, consequently modifying the chiral resolution. Temperatures of 15, 25 and 40 °C were tested, using the previously selected conditions of CM- β -CD concentration (30 mM) and SPL (0.5 psi/99s). A decrease in migration times of the enantiomers and EOF upon increasing the temperature was observed, due to the decrease of the BGE viscosity and also to changes in the enantiomers-CD interaction. The reduction of migration times resulted in a decrease in the R_s of enantiomers, being the R_s values of 2.8, 2.4 and 1.7 for 15, 25 and 40 °C respectively. In all cases complete resolution of the enantiomers was achieved, so a capillary temperature of 25 °C was selected for the enantioseparations.

Previously, in Paper V, we have demonstrated that the use of a P -constant design with the D/P ratio kept lower than 0.5 is adequate to obtain reliable estimates of the HSA-enantiomers affinity constants. In this work, for the evaluation of the enantioselective protein binding of zopiclone to HSA, an experimental design with a constant P value near the physiological concentration (450 μ M) and 5 D levels in a short D -concentration interval (100-200 μ M, 3 independent replicates of each level, total 15 individual samples) was used. The D/P ratios were from 0.22 to 0.44, in all cases lower than 0.5.

In order to estimate the enantioselectivity and protein binding of zopiclone to HSA, a previously described protocol was used (see section IV.2.1), including the identification and elimination of outliers, the estimation of K_I values for each enantiomer and the verification of the $n_I = 1$ approach *via* different equations.

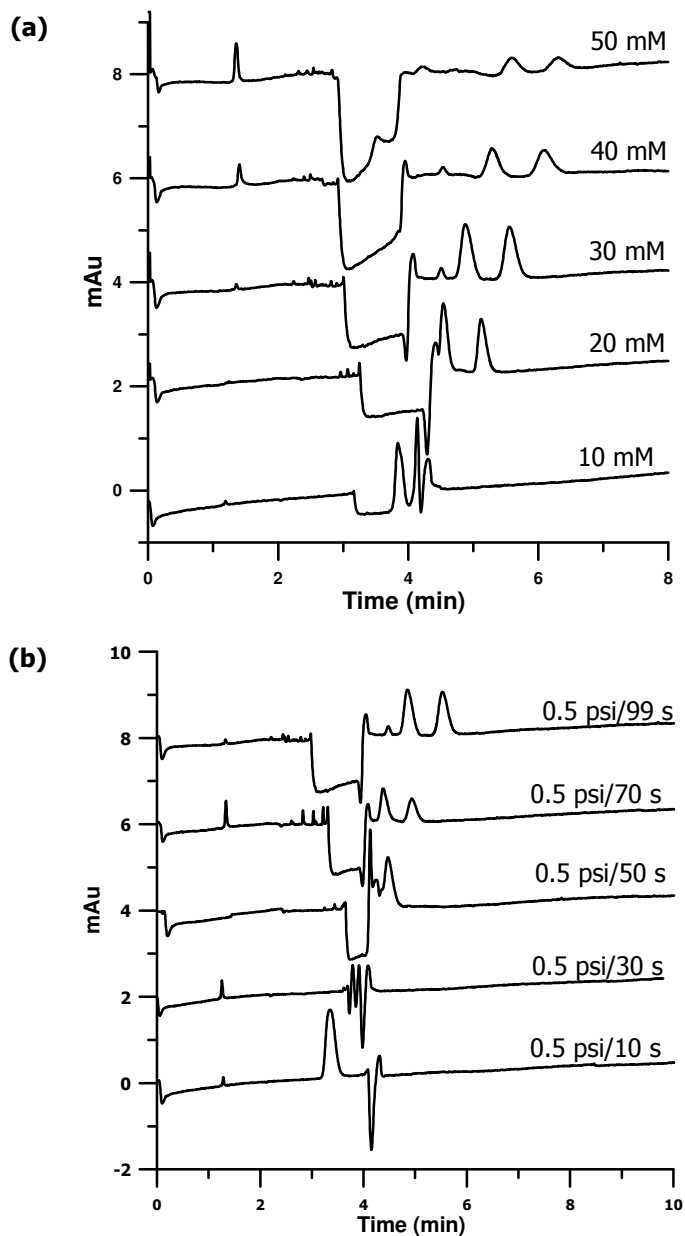


Figure IV.15: Effect of (a) CM- β -CD concentration and (b) SPL on the separation of zopiclone enantiomers by EKC-PFT. Other experimental conditions: BGE 50 mM Tris, pH 6.0. Separation at 25 °C, 15 kV.

Outlier experimental data were eliminated here using a *z*-score approach, which is a robust alternative to other tests for outliers. This is a convenient method for data that are expected to follow a near-normal distribution but are suspected to contain a small proportion of errors. A robust estimation of the *z*-score has been performed by using the median and *MADe* (more robust statistics than those commonly used, mean and standard deviation), for each log K_{1i} estimate obtained from Eq. IV.7:

$$z_i = \frac{\log K_{1i} - \text{median}}{MADe} \quad (\text{IV.13})$$

Habitually, $z_i > 3$ are considered unsatisfactory, while $z_i > 2$ are considered doubtful values. A fixed criterion of $z_i > 2.5$ was used in this work to eliminate a point in a round. After elimination of one or more outlier values, new median and *MADe* estimations are performed *via* Eq. IV.7 and the *z*-score test is repeated since no outliers are found. The final log K_I estimates for each enantiomer are shown as median \pm *MADe* (see Table IV.9).

After outliers elimination, Eq. IV.9 was used to confirm $n_I = 1$ for both enantiomers and to estimate also K_I . Log K_I estimates obtained using Eq. IV.7 and Eq. IV.9 are shown in Table IV.9.

Table IV.9: Protein binding parameters estimated for the enantioselective zopiclone-HSA binding.

Enantiomer	log K_I (Eq. IV.7)	log K_I (Eq. IV.9)	<i>PB</i> %	<i>ES</i>
S-zopiclone	3.38 \pm 0.14	3.37	47	1.95
R-zopiclone	3.09 \pm 0.19	3.14	36	

As can be seen in Table IV.9, the estimations of log K_I obtained by using both equations are very similar. This fact confirmed that estimations made using Eq. IV.7 could be considered acceptable values. In addition the estimation from Eq. IV.7 increases the control over individual data allowing the application of univariate statistics instead of a regression model with a single estimation.

The percentage of protein binding has been calculated here considering $D = 0.2 \mu\text{M}$ and $P = 600 \mu\text{M}$ (physiological conditions estimated in the fluoxetine study) and using Eq. IV.12. The values obtained are also shown in Table IV.9, as well as the enantioselectivity obtained as $K_{i,S}/K_{i,R}$. From the obtained ES value, around 2, it can be concluded that S-zopiclone has higher affinity to the HSA molecule than its antipode.

Finally, an estimation of the binding of zopiclone enantiomers to all the plasma proteins was performed using lyophilized human sera. For this purpose, samples containing racemic zopiclone and plasma with a relationship aqueous/plasma solution 100:300 (v/v) were prepared in triplicate and analyzed following the UF and EKC-PFT methodology described. $PB\%$ of 45 ± 3 and 49 ± 6 were found for S- and R-ZPC, respectively, values which agree with the $PB\%$ found in the literature for racemic zopiclone, 45% (Gaillot *et al.*, 1983; Spanish Drug Agency, 2011). Comparing these results with those obtained for HSA, we can conclude that the S-enantiomer mainly binds to HSA while R-zopiclone binds also to other plasma proteins.

IV.2.3. Electrokinetic chromatographic estimation of the enantioselective binding of nomifensine to human serum albumin and total plasma proteins (Paper VII)

Nomifensine is an isoquinoline derivative that prevents dopamine reuptake into synaptosomes. It is now mainly used in scientific research as a model of dopamine reuptake inhibitors, after its withdrawal as antidepressant in 1986. A clinical application of nomifensine in Parkinson's disease (PD) study and diagnosis has been described. PD can be evaluated by studying the dopamine pathways using positron emission tomography (PET) with different tracers to image the presynaptic and postsynaptic sites of dopaminergic system. PET can also contribute to the differential diagnosis of PD when clinical features are not clear. One of the tracers that have been used for presynaptic assessment is [^{11}C]nomifensine, which inhibits the reuptake of the released dopamine by blocking the dopamine reuptake sites

(dopamine transporters, DATs) in presynaptic nerve terminals. The use of nomifensine as PET tracer is affected by its distribution between blood and central nervous system, where protein binding plays an important role. So, the study of its enantioselective protein binding may be helpful in this context, since differences between the DAT-blocking activities of the enantiomers have been reported in the literature.

In this work, the enantioselective binding of nomifensine to HSA and total plasma proteins has been evaluated using the methodology and equations previously described. The separation of nomifensine enantiomers has been performed by EKC-CFT using TM- β -CD, a neutral cyclodextrin, as chiral selector. A minimum R_s of 1.7 was obtained for nomifensine enantiomers, in migration times around 3 min. Figure IV.16 shows the electropherograms obtained under the selected experimental conditions.

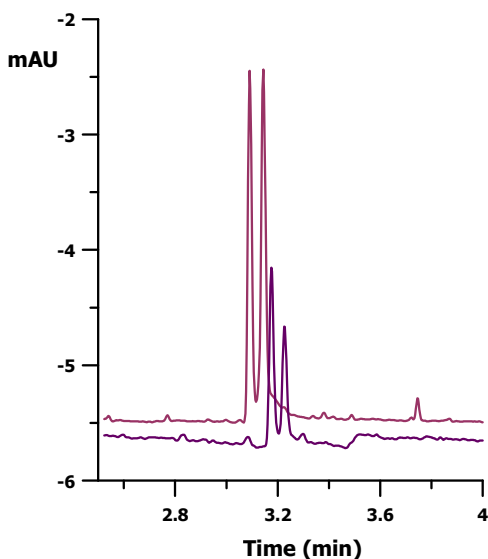


Figure IV.16: Enantioseparation of nomifensine enantiomers in a standard solution (pink) and in an ultrafiltrate (unbound fraction, purple) by EKC-CFT. Experimental conditions: 50 mM Tris buffer at pH 6.0 as BGE, 30 mM TM- β -CD in BGE injected at 10 psi/1 min, separation voltage 15 kV and capillary temperature 50 °C.

A P -constant experimental design was used for the evaluation of nomifensine-HSA enantioselective binding, keeping the D/P ratio < 0.5 . P was fixed near the physiological concentration and D was varied between 70 and 200 μM of each enantiomer (5 concentration levels, 3 replicates *per* level). The inter-day repeatability was controlled by repeating the complete experimental design in two independent working sessions. The previously described z -score approach has been applied here for the elimination of outlier values, combining data from both working sessions for the calculation of the median K_I and its $MADe$.

After outliers elimination, the robust log K_I estimates via Eq. IV.7 (median $\pm MADe$) were 3.24 ± 0.10 and 3.67 ± 0.08 for E1 and E2, respectively. The assumption $n_I = 1$ of Eq. IV.7 was confirmed by the estimation of K_I and n_I via Eq. IV.9. A SIMPLEX search was started with $n_I = 1$ and $\log K_I = 4$, allowing only integer n_I values. These log K_I estimates were 3.23 ± 0.11 and 3.64 ± 0.09 for E1 and E2, respectively, which are in agreement with the values calculated from Eq. IV.7. Also, the n_I estimated value was 1 for both enantiomers, verifying the assumption. It may be noticed that these uncertainties have been obtained under intermediate precision conditions (two independent working sessions).

Enantioselectivity, defined as the ratio between affinity constants (K_{E2}/K_{E1}), was estimated as 2.7 ± 0.1 , indicating higher affinity of the second eluted enantiomer for the HSA molecule. However, as the difference between the log K_I values of the enantiomers was not so high, this enantioselectivity was checked through hypothesis testing. Statistical comparison of log K_{E1} and log K_{E2} , using both a parametric test for means and a non-parametric one for medians, indicated significant differences ($p < 0.05$) between the averaged affinity estimates, so significant enantioselectivity was demonstrated. The same result was obtained by comparing the ES value with 1.

The estimation of enantioselective $PB\%$ to the HSA molecule at the physiological level was performed with Eq. IV.12. Also the enantioselective $PB\%$ to total plasma proteins was calculated by incubating racemic nomifensine with human sera and applying the same methodology described for HSA (UF followed by chiral EKC-CFT).

The results for the protein binding of nomifensine enantiomers to HSA and total plasma proteins are shown in Table IV.10.

Table IV.10: *PB%* estimates for nomifensine enantiomers to human serum albumin and total plasma proteins.

	<i>PB%</i> (E1)	<i>PB%</i> (E2)
To HSA	40 ± 5	63 ± 4
To plasma proteins	58 ± 7	64 ± 4

From the *PB%* estimates shown in Table IV.10, we can see that probably the first eluted enantiomer binds not only to HSA but also to other plasma proteins. However, the role of HSA is the most important in its protein binding. For E2, the values of *PB%* obtained for HSA and total plasma proteins are similar, so this enantiomer binds *a priori* only to HSA.

IV.3. Study of enzymatic reactions by capillary electrophoresis

Several diseases are caused by enzymatic disorders (excess or lack of activity, bad regulation, bad expression...) and consequently enzymes are a common target of drugs. Every year new candidate drugs are evaluated as inhibitors, substrates or modulators of different enzymes, and with this purpose screening methods are required in the pharmaceutical industry. As stated in the Introduction of this Thesis, CE in the EMMA modality is a good technique for high-throughput screening due to its speediness, ease of automation and extremely low consumption of reagents and enzymes (usually very expensive). Also, CE offers the possibility of coupling chiral analysis of substrates, inhibitors or metabolites to the EMMA assay, thus providing enantioselective information about the enzymatic reaction.

The present section of this Thesis deals with two different in-capillary enzymatic reactions that have been evaluated using the EMMA methodology: the degradation of acetylthiocholine by the enzyme acetylcholinesterase (Paper VIII) and the

enantioselective metabolism of verapamil and fluoxetine by two different isoforms of the cytochrome P450, CYP3A4 and CYP2D6 (Papers IX and X respectively). In EMMA all the reagents are introduced sequentially in the capillary, which acts simultaneously as a micro-reactor and as a separation system. The reaction takes place in a nanoliter scale, which has the previously commented advantage of extremely low consumption of expensive reagents, but the disadvantage of being difficult to control and measure. Extensive experimental work is required in order to optimize and control all the variables that affect an EMMA reaction and its subsequent separation by electrophoresis.

IV.3.1: Screening of acetylcholinesterase inhibitors by CE after enzymatic reaction at capillary inlet (Paper VIII)

AChE is a hydrolytic enzyme that catalyzes the degradation of the neurotransmitter acetylcholine (ACh) in the central nervous system. The decrease of ACh level in the synaptic spaces has been related to the Alzheimer's disease, so a possibility for its treatment is the inhibition of the AChE activity, in order to increase these ACh levels. The activity of some AChE inhibitors has been evaluated here with the aim of developing a fast and fully automated method for high-throughput screening of possible new candidate drugs.

In order to choose the best EMMA conditions for the proposed method, tacrine, whose activity as AChE inhibitor is well-known, was selected as model compound for the optimization process. The experimental conditions for the enzymatic assay were taken from literature (Tang *et al.*, 2007) (see Methodology section) and the progress of the enzymatic reaction was measured using the peak area of the formed product thiocholine (TCh) at 230 nm.

After some attempts with the plug-plug EMMA mode, where the injected plugs are mixed by application of a small voltage, we noticed a high variability in the results that was not corrected with the addition of an internal standard (alprenolol). So, we attributed the variability to the mixing procedure and decided to change to the at-inlet EMMA mode, where the mixing takes part by simple diffusion of the injected

plugs. A sandwich at-inlet EMMA procedure was proposed, introducing the substrate solution, with or without inhibitor, between two enzyme plugs. Two water plugs were injected before and after the reaction mixture in order to stack the reagents in a capillary zone, and the reagents were allowed to mix and react during a fixed waiting time. Figure IV.17 shows the typical electropherograms obtained after the AChE enzymatic reaction with and without the inhibitor edrophonium. In absence of the inhibitor (blue line), all the substrate is converted to TCh and the AThCh peak does not appear, while in presence of 100 μM edrophonium (red line) the formed product diminishes and the substrate peak appears indicating an incomplete substrate-product conversion.

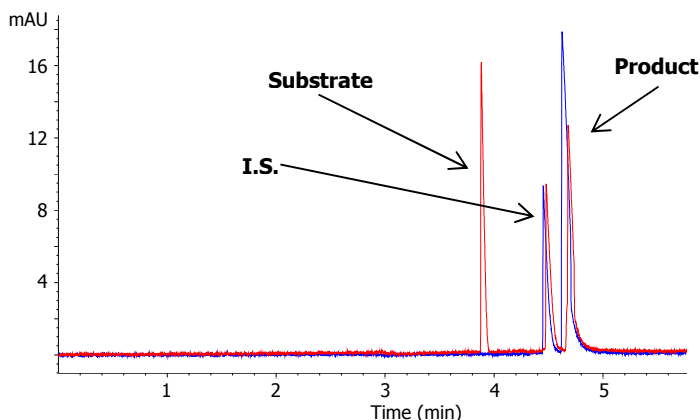


Figure IV.17: Electropherograms corresponding to the AChE enzymatic reaction in absence (blue line) and presence (red line) of the inhibitor edrophonium. Experimental conditions: 0.4 $\text{mg}\cdot\text{mL}^{-1}$ AChE, 10 mM AThCh with 20 mM MgSO_4 , 30 mM borate-phosphate buffer, pH 8.0 as BGE (the same buffer as for the enzymatic reaction), capillary temperature 37 $^\circ\text{C}$ and separation voltage 15 kV.

The incubation time is an important variable that should be studied in at-inlet EMMA, since during this time the enzyme and substrate plugs are mixed by simple diffusion and react in the capillary. A very short time will not allow the reaction to take part, but a very long one has the disadvantages of peaks diffusion and longer analysis

time, which is an important drawback for screening procedures. Figure IV.18 shows the effect of the incubation time on the inhibition of AChE. As can be seen, maximum inhibition percentage was achieved after two minutes of incubation, so this time was selected for further experiences.

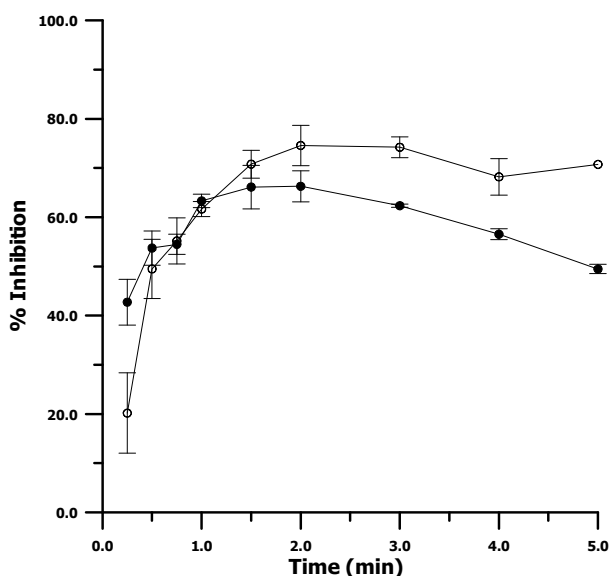


Figure IV.18: Effect of the incubation time on the percentage of inhibition using tacrine (●) 5 μM and (○) 10 μM . Experimental conditions as described in Fig. IV.17.

In order to obtain accurate kinetic data, it may be taken into account that the mixing of different plugs leads to a dilution of the substrate in the reaction zone. In this work, we have estimated a dilution factor that relates the actual substrate concentration in the reaction zone and the substrate concentration in the injected solution. With this purpose, an inhibition plot of tacrine was constructed in order to obtain its IC_{50} value, by performing assays in the tacrine range 10^{-3} - 10^3 μM (other conditions previously described). The IC_{50} value obtained in this work (9.16 μM) was compared with those reported in the literature using the reference method for AChE inhibition, named Ellman method (around 0.25 μM ; Andrisano *et al.*, 2001).

Assuming the reported IC_{50} as reference true value, a dilution factor (f) of 0.03 was estimated and then applied to all calculations.

Taking into account the dilution at the capillary inlet to correct both the substrate and the inhibitor concentrations the general model for enzyme inhibition (Eq. I.19) can be rewritten as:

$$V_0 = \frac{\left(\frac{1}{\alpha'}\right)V_{max}[S]}{\left(\frac{\alpha}{\alpha'}\right)\frac{1}{f}K_M + \alpha'[S]} = \frac{a[S]}{b + [S]} \quad (IV.14)$$

K_i could be determined by plotting the ratio of the fitted parameters (b/a) against the inhibitor injected concentration, as the ratio of the replot intercept to the replot slope, combining Eq. IV.14 with the definitions of α and α' (Eqs. I.20 and I.21):

$$\frac{b}{a} = \frac{K_M}{V_{max}} \frac{1}{f} \alpha = \frac{K_M}{V_{max}} \frac{1}{f} + \frac{K_M}{V_{max}} \frac{1}{K_i} [I] \quad (IV.15)$$

In order to study the applicability of the proposed methodology the inhibition potency of tacrine and other known AChE inhibitors was evaluated. With this purpose, the reaction was performed using different substrate and inhibitor concentrations. Firstly, K_i values for tacrine and edrophonium were estimated from Eqs. IV.14 and IV.15. The obtained values were 0.138 ± 0.012 and $3.3 \pm 0.2 \mu\text{M}$ for tacrine and edrophonium, respectively, in agreement with those reported using the Ellman official method.

Once inhibition constants were obtained, the inhibition mechanisms of tacrine and edrophonium were qualitatively evaluated. With this purpose, Lineweaver-Burk plots (the linear form of the Michaelis-Menten equation, Eq. I.19, conveniently modified for inhibition studies) were constructed for different inhibitor concentrations of both drugs (Figure IV.19).

In the Lineweaver-Burk plot, the slope represents the ratio K_m/V_{max} and the intercept is $1/V_{max}$. So, the change on slopes and intercepts with different inhibitor concentrations provides information about the inhibition mechanism.

For tacrine, both the slope and the intercept increase with higher inhibitor concentration, so the V_{max} is decreased and the K_m is increased. This behavior corresponds to a mixed inhibition mechanism, which affects both to the K_m and V_{max} . On the other hand, the plot of edrophonium shows increasing slopes but unvaried intercepts, which means that the V_{max} remains constant and the K_m increases. This is a typical plot of competitive inhibition.

These results well reflect the relative potency of the inhibitors and their mechanism of action, suggesting that this assay could be suitable for the first screening of new potential AChE inhibitors.

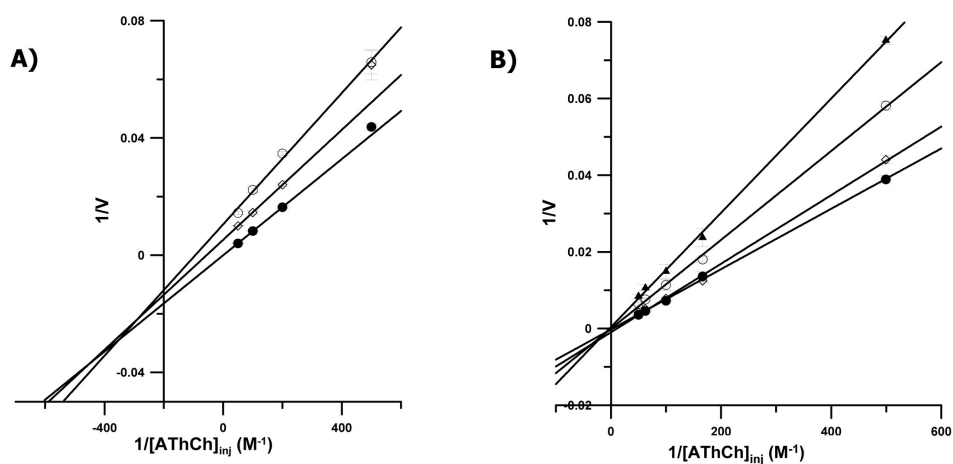


Figure IV.19: Lineweaver-Burk plots for the enzymatic reaction of AChE inhibited by (●) 0 μM , (◇) 5 μM and (○) 10 μM tacrine (A) and (●) 0 μM , (◇) 10 μM , (○) 50 μM and (▲) 100 μM edrophonium (B).

IC_{50} values, a measure of the inhibitory potency, were also obtained for edrophonium and neostigmine. With this purpose increasing inhibitor concentrations (10^{-3} - 10^3 μM) were injected using a fixed AThCh concentration of 10 mM. Both inhibition plots, as well as the IC_{50} values obtained, are shown in Figure IV.20.

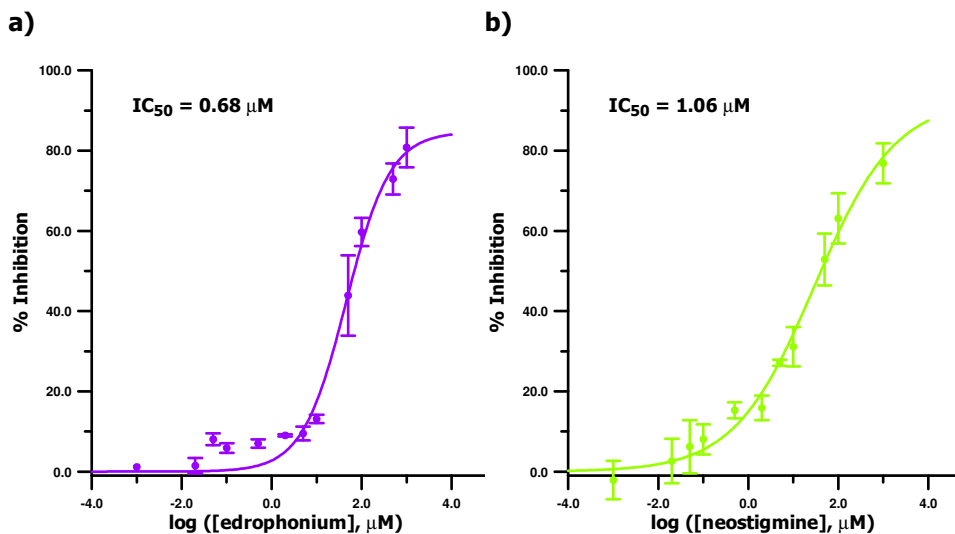


Figure IV.20: Inhibition plots for (a) edrophonium and (b) neostigmine. Experimental conditions as described in Fig. IV.17.

Finally, a method for a fast screening of potential new AChE inhibitors is proposed. This method consists on using the methodology previously described with fixed concentrations of 10 mM AThCh and 10 μM inhibitor, and calculating the inhibition percent of the candidate molecule at that concentration. This screening has been performed here for five known AChE inhibitors, thus providing information about their relative potency. The results of the screening are summarized in Table IV.11.

Table IV.11: Inhibitor screening results.

Compound	% of inhibition
Tacrine	54.2
Edrophonium	33.7
Neostigmine	31.1
Pyridostigmine	6.1
Eserine	20.1

According to the results shown in Table IV.11, the order of inhibitory potency was tacrine > edrophonium > neostigmine > eserine > pyridostigmine. The screening methodology developed and applied here has proved to be useful for the *in vitro* evaluation of AChE inhibitors (or new candidates) in terms of their K_i , inhibition mechanism or inhibitory potency.

IV.3.2. In-line capillary electrophoretic evaluation of the enantioselective metabolism of verapamil by cytochrome P3A4 (Paper IX)

Other application of EMMA, very interesting from a pharmacokinetic point of view, is the evaluation of drugs metabolism by individual enzymatic systems. The metabolism of a drug by different enzymes influences its plasmatic levels, half-life and disposition for reaching target organs and systems. This information should be estimated for candidate compounds in a fast and non-expensive way, being EMMA a good alternative for this purpose due to its previously commented features as screening procedure.

In this work, the enantioselective metabolism of verapamil by CYP3A4, the major CYP isoform in humans, is evaluated. Verapamil, a Ca^{+2} -channel blocker with anti-arrhythmic activity, is a model compound for several metabolic studies. EMMA reaction conditions and the separation and verapamil and norverapamil enantiomers by means of HS- β -CD and the partial filling technique were optimized.

The oxidation of drugs by the CYP450 system (Eq. I.1, Introduction) requires NADPH as a cofactor. Theoretically, NADPH is consumed in the enzymatic reaction and forms the oxidized product, NADP^+ , in a molar equivalence with the substrate-product conversion. So, many authors have used in EMMA the $\text{NADP}^+/\text{NADPH}$ system to evaluate the reaction turnover by quantifying the NADPH depletion or the NADP^+ formation. This approach is not useful for evaluating enantioselective metabolism but, as it is supposed to be the easiest way of measuring metabolic reactions, we tried to start the EMMA study with it. Very erratic results were obtained, suggesting that the formation of NADP^+ was due not only to the enzymatic

reaction but also to other possible effects, and we decided to study carefully the behavior of the NADP⁺/NADPH system.

One of the main drawbacks of the commercially available NADPH (powder) is its lack of stability. It has been reported in the literature that a considerable amount of NADP⁺ and other degradation products is non-specifically formed in a NADPH solution (Zhang *et al.*, 2006). So, in order to evaluate if the NADP⁺ formation was really due to the metabolism of verapamil by CYP3A4, the area of NADP⁺ was measured after incubation in at-inlet EMMA conditions with and without verapamil (Figure IV.21).

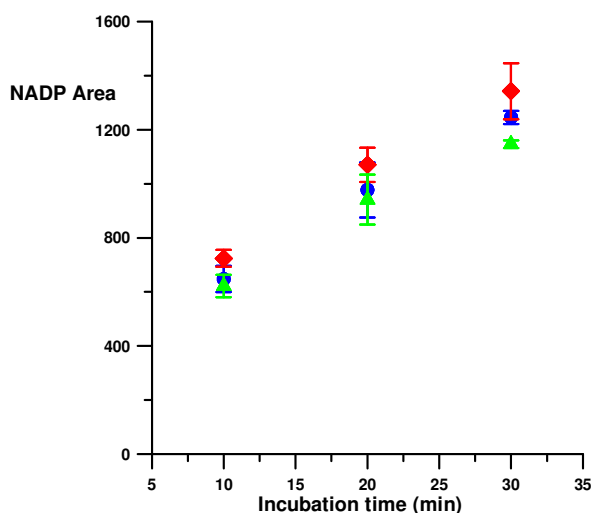


Figure IV.21: Effect of the incubation time on the NADP⁺ formation at different verapamil concentrations: (●) 0 μM, (◆) 100 μM and (▲) 200 μM. Experimental conditions as described in the Methodology section (Table III.3), but adding NADPH to the substrate solution instead of using solutions A and B.

This figure shows that at longer incubation times the formation of NADP⁺ is increased, as expected. However, no significant differences are observed between the NADP⁺ formation without and with verapamil (100 or 200 μM) in the reaction

mixture, suggesting that the NADP^+ formation corresponds to a non-specific degradation of the NADPH. So, this system was discarded for the quantification of the reaction turnover and a NADPH regenerating system (two independent solutions that form NADPH *in situ*, see Methodology section) was used for further studies in order to avoid problems related to the NADPH stability.

Firstly, the plug-plug and the at-inlet EMMA modes were assayed. Best results were obtained using the at-inlet mode, so a “sandwich” injection similar to that used in the AChE study, with a substrate plug between two enzyme plugs, was proposed. Two plugs of incubation buffer were added before and after the “sandwich” plugs in order to give to the enzyme its adequate reaction medium. The scheme of the EMMA configuration used in these studies is shown in Figure IV.22.

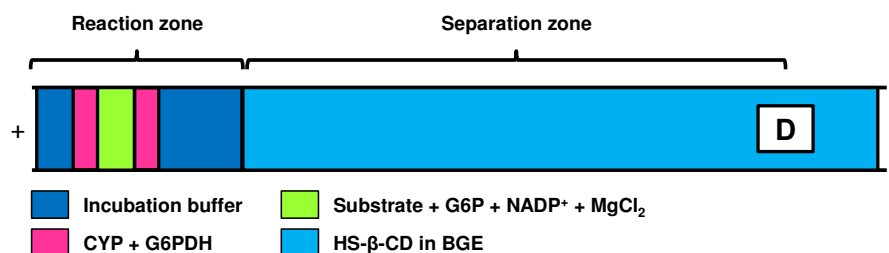


Figure IV.22: Scheme of the reaction and separation zones in the proposed enantioselective EMMA assay.

Two different zones can be distinguished in the capillary: the separation zone filled with a HS-β-CD solution in the BGE and the reaction zone, at the inlet part, where all the plugs of the EMMA sequence are injected and left to mix and react during a fixed incubation time. In these conditions, the mixture of reagents is due both to longitudinal and transverse diffusion. After reaction, a voltage is applied for the separation of substrates, products and enzymes.

The NADPH regenerating system employed in this work comprises two solutions (A and B) that allow the *in situ* NADPH formation. Solution A contains G6P, NADP^+ and

MgCl₂ and solution B contains G6PDH. When these solutions are put into contact, the G6PDH oxidizes G6P and forms NADPH, which can act as cofactor for the CYP3A4 reaction. Two configurations were tested for the inclusion of these solutions in the CYP and substrate vials. In the first one, both solutions A and B were included in the substrate vial, to form NADPH before the injection in the CE system. This strategy allows the immediate starting of the reaction due to the fact that the NADPH formed is present when the CYP and verapamil plugs contact in the capillary, but it presents the disadvantage of a possible degradation of NADPH. The other configuration studied consisted on the in-line formation of NADPH by the inclusion of solution B in the CYP vial and solution A in the verapamil vial, which allows always the presence of native NADPH but can retard the beginning of the enzymatic CYP reaction. Both configurations lead to the same metabolite (norverapamil) formation in short incubation times, so the in-line formation of NADPH was selected in order to preserve NADPH from degradation (see the solutions composition in Fig. IV.22).

With the aim of having a good reaction turnover in the shortest possible incubation time, we have optimized the in-capillary incubation time and the substrate injection. With this purpose, 200 μM verapamil solutions were incubated changing the incubation times or the substrate plugs, and keeping the other experimental conditions as described in the Methodology section. These experiences were carried out in achiral mode, without chiral selector in the separation zone, using separation conditions taken from literature (Zhang *et al.*, 2005): 50 mM sodium phosphate at pH 8.8 as BGE, capillary temperature 25 °C and separation voltage 20 kV.

The optimum incubation time depends on the enzyme and the concrete conditions of the assay, and it may be taken into account the linear range of each enzyme, since at longer incubation times they lose activity. Here, incubation times between 1 and 30 minutes were tested, based on the specifications of the commercial CYP and the previously published papers concerning this topic. The formation of the major product, norverapamil, was selected as response variable. From 1 to 5 min it increased considerably, but from 5 to 30 there was only a slight increase in the amount of norverapamil formed. Also, at longer incubation times there was an

important peak broadening due to the diffusion, so 5 min was selected as the best incubation time for further studies.

The length of the substrate plug (substrate injection) may be adjusted to maximize the reaction turnover but taking into account that very large plugs will not allow a complete mixing of the substrate with the enzyme. Here, three substrate plugs of 3, 5 and 7 s were tested (with a fixed pressure of 0.5 psi), and it was seen that the area of norverapamil formed was larger with the 7 s injection, so this injection plug was selected for the substrate.

Once the EMMA conditions were fixed, the EMMA assay was coupled to the enantioseparation of verapamil and norverapamil in order to measure the enantioselective metabolism of verapamil by CYP3A4. Using the same BGE and conditions, HS- β -CD was tested as chiral selector due to its widely proved good enantioseparation abilities, using the partial filling technique. Solutions of 0.25-2.5% (m/v) HS- β -CD in the BGE were tested. With 0.25% CD, no separation of verapamil and norverapamil enantiomers was achieved. Using 2% HS- β -CD each pair of enantiomers was separated but S-norverapamil and R-verapamil overlapped. A 2.5% CD solution provided good enantioseparation of the four peaks with migration times of 18.2, 19.9, 20.6 and 21.5 min for S-verapamil, S-norverapamil, R-verapamil and R-norverapamil, respectively. In order to shorten these migration times, a little pressure of 0.2 psi was added to the separation voltages and the new migration times were 9.8, 10.5, 10.8 and 11.2 min, respectively. The separation of the four peaks as well as the NADP⁺ and NADPH can be seen in Figure IV.23. Using the selected conditions the total analysis time (including preconditioning, injection, incubation and separation) was less than 35 min/sample.

The developed methodology was applied to estimate the kinetic Michaelis-Menten parameters for the metabolism of verapamil enantiomers by CYP3A4. With this purpose, six solutions containing verapamil in the concentration range 20-200 μ M (10-100 μ M of each enantiomer) were prepared in duplicate. The experiment was repeated in two different days in order to estimate the uncertainty under intermediate precision conditions. In order to obtain the verapamil peaks in the

same diffusion conditions as in the enzymatic assay, calibration curves for quantifying verapamil enantiomers were prepared in both sessions following the proposed methodology. Solution A was not included to avoid the advance of the enzymatic reaction, and corrected peak area was used as response variable. The quantification of the reaction turnover was done considering the consumption of verapamil enantiomers, so these results correspond to the overall metabolism of verapamil by CYP3A4 and not only to the norverapamil formation. Table IV.12 shows the calibration statistics obtained for each enantiomer in both working sessions together with their confidence intervals. As can be seen, adequate regression coefficients were obtained in all cases. Calculations for each experimental data set were done using its corresponding calibration curve.

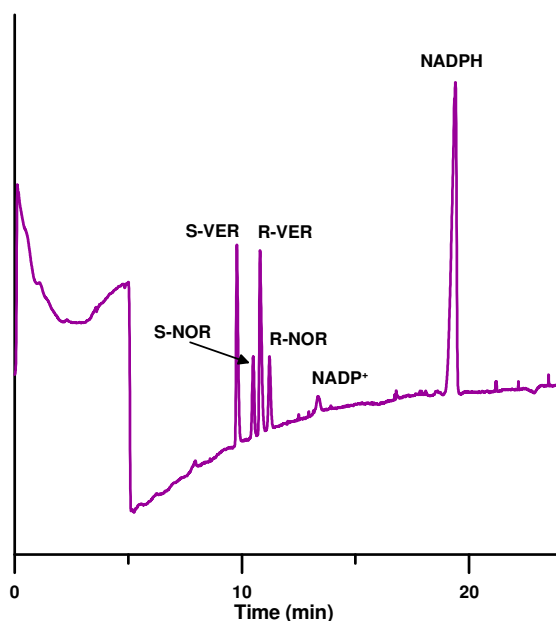


Figure IV.23: Electropherogram corresponding to the separation of the components of the proposed EMMA assay (VER: verapamil; NOR: norverapamil). EMMA conditions: incubation buffer 100 mM potassium phosphate, pH 7.4; 200 nM CYP3A4; capillary temperature 37 °C and injection sequence as described in Table III.3 and in Fig. IV.22).

Table IV.12: Calibration statistics for S- and R-verapamil.

		$b_0 \pm ts$	$b_1 \pm ts$	R^2
Session 1	S-VER	-50 ± 80	15.9 ± 0.8	0.996
	R-VER	-40 ± 80	13.8 ± 0.8	0.994
Session 2	S-VER	-1 ± 60	20.1 ± 0.6	0.998
	R-VER	-1 ± 60	19.2 ± 0.6	0.997

b_0 , intercept; b_1 , slope; ts , confidence interval at the 95% probability level; R^2 , determination coefficient.

In order to calculate the velocity rate data the amount of moles of verapamil transformed was estimated by calculating the injected volume of substrate *via* the following equation:

$$Vol = \frac{\Delta P \cdot d^4 \cdot \pi \cdot t}{128 \cdot \eta \cdot L} \quad (IV.16)$$

where Vol (m^3) is the injected volume, ΔP (Pa) is the applied pressure, d (m) is the internal diameter of the capillary, t (s) is the duration of pressure application, η (Pa·s) is the viscosity of the injected solution and L (m) is the total capillary length.

Velocity rate data (expressed in $pmol \cdot min^{-1} \cdot (pmol \text{ CYP})^{-1}$) were plotted thus *vs.* the initial enantiomer substrate concentration, $[S]$ (μM), combining data from both experimental sessions (Michaelis-Menten plot, Eq. I.17). So, these results become more realistic than those obtained from a single experiment. Figure IV.24 shows the Michaelis-Menten plots for the metabolism of both verapamil enantiomers by CYP3A4. From the non-linear fitting of experimental data to the Michaelis-Menten equation K_m and V_{max} were estimated. K_m values were 51 ± 9 and $47 \pm 9 \mu M$ for S- and R-verapamil, respectively, while V_{max} estimates were 22 ± 2 and $21 \pm 2 pmol \cdot min^{-1} \cdot (pmol \text{ CYP})^{-1}$, respectively. The enantioselectivity, calculated as the ratio between the V_{max} values of both enantiomers, was 1.08 in favour of the S-enantiomer, which is slightly more metabolized than the R one.

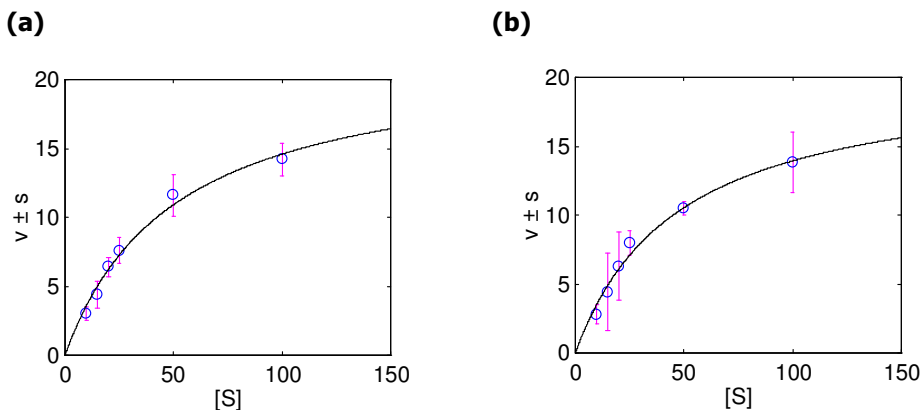


Figure IV.24: Michaelis-Menten plots for the metabolism of (a) S-verapamil and (b) R-verapamil by CYP3A4.

An interesting parameter from a pharmacokinetic point of view is the intrinsic clearance, defined as the amount of plasma from which a xenobiotic is removed in a certain time. It reflects the capacity of the body to remove a xenobiotic. The *in vitro* intrinsic clearance Cl_i can be estimated from the K_m and V_{max} values as V_{max}/K_m . Here, Cl_i values were estimated as 55 ± 10 and $55 \pm 11 \text{ mL} \cdot \text{min}^{-1} \cdot (\text{mg CYP})^{-1}$ for S- and R-verapamil, respectively. These values are in agreement with those found in the literature (Kroemer *et al.*, 1992).

IV.3.3. Fast evaluation of enantioselective drug metabolism by electrophoretically mediated microanalysis: application to fluoxetine metabolism by cytochrome P2D6 (Paper X)

In this work, the methodology developed in the previous paper for the enantioselective evaluation of drugs metabolism, that joins an EMMA assay for the enzymatic reaction and a chiral separation of drug and metabolite by EKC-PFT, is applied to the study of fluoxetine metabolism by CYP2D6 (another isoform of cytochrome P450).

For this purpose, the conditions proposed in the previous paper were applied to carry out the EMMA enzymatic reaction (see Fig. IV.22 and Methodology section). Conditions for the enantioseparation of fluoxetine and its metabolite norfluoxetine were adjusted to achieve adequate chiral resolution. Based on previous experiences, concentrations of HS- β -CD (prepared in the BGE 50 mM sodium phosphate at pH 8.8) in the range 0.1-1.25% (m/v) were assayed and a pressure of 0.4 psi was applied during separation.

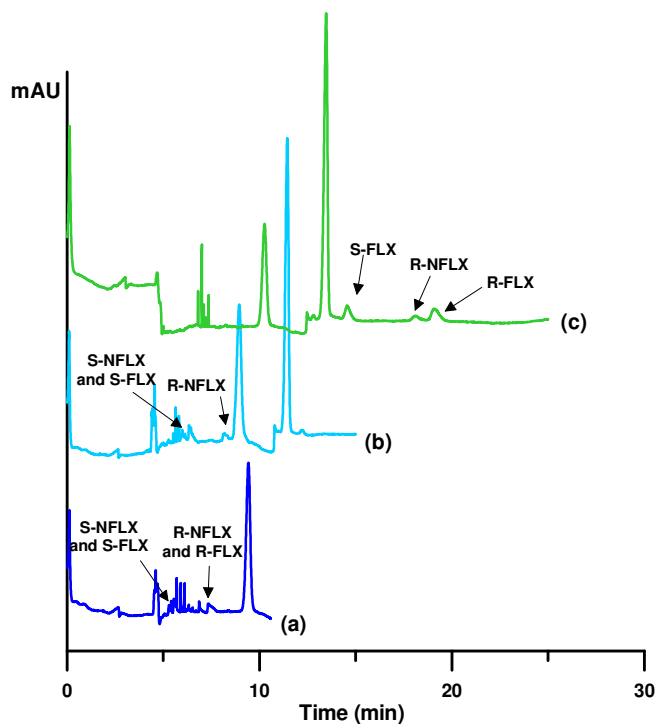


Figure IV.24: Electropherograms corresponding to the separation of the reaction mixture using different HS- β -CD concentrations: (a) 0.1%, (b) 0.15% and (c) 0.5%. Experimental conditions: BGE, 50 mM sodium phosphate at pH 8.8, 25 $^{\circ}$ C, 20 kV.

Figure IV.24 shows some of the results obtained using different HS- β -CD concentrations. As can be seen, with 0.1% HS- β -CD (a) the enantiomers of fluoxetine and norfluoxetine were separated but they overlapped with the peaks

corresponding to the CYP2D6. With 0.15% HS- β -CD (b) the peak of R-fluoxetine overlaps with the NADP⁺ peak (see Figure IV.26 for all peaks identification). Increasing the CD concentration to 0.5%, the fluoxetine and norfluoxetine enantiomers migrate after the NADP⁺/NADPH system, but S-norfluoxetine overlaps with the NADPH peak. Finally, with a HS- β -CD concentration of 1.25% (m/v) all the peaks in the reaction mixture were baseline resolved and fluoxetine enantiomers able to be quantified. The electropherogram corresponding to the final separation conditions is shown in Figure IV.26.

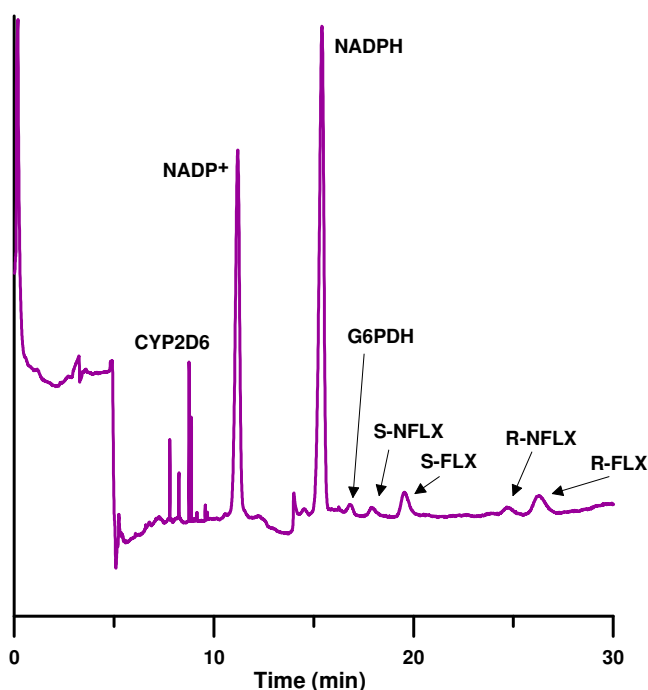


Figure IV.26: Electropherogram showing the separation of the reaction mixture with 1.25% HS- β -CD. Other experimental conditions as described in Fig. IV.25.

Once the separation conditions were adjusted, an experimental design was planned in order to obtain the Michaelis-Menten plots for the enantioselective fluoxetine metabolism by CYP2D6. The EMMA assay was carried out with seven concentration

levels of racemic fluoxetine in the range 10-200 μM , each one with two independent replicates. The complete experiment was repeated in two days in order to obtain the data under intermediate precision conditions. All data were used together for estimations.

The interday precision of the proposed methodology was evaluated. Averaged intermediate precision results for peak areas of calibration curves and samples were 9 and 16%, which can be considered acceptable taking into account the low concentrations used and the intrinsic variability of enzymatic reactions.

Velocity rate data were adjusted to the Michaelis-Menten equation (Eq. I.17) for each fluoxetine enantiomer employing a Marquardt algorithm. The corresponding Michaelis-Menten plots for S- and R-fluoxetine are shown in Figure IV.27.

From these plots, kinetic parameters for the metabolism of both enantiomers have been estimated. K_m values (mean \pm SD) were 30 ± 3 and 39 ± 5 μM for S- and R-fluoxetine, respectively. V_{max} estimates were 28.6 ± 1.2 $\text{pmol}\cdot\text{min}^{-1}\cdot(\text{pmol CYP})^{-1}$ (3630 ± 150 $\text{pmol}\cdot\text{min}^{-1}\cdot(\text{mg CYP})^{-1}$) and 34 ± 2 $\text{pmol}\cdot\text{min}^{-1}\cdot(\text{pmol CYP})^{-1}$ (4300 ± 200 $\text{pmol}\cdot\text{min}^{-1}\cdot(\text{mg CYP})^{-1}$) for S- and R-fluoxetine, respectively. These results show a slight enantioselectivity in favor of R-fluoxetine, estimated as the ratio between their V_{max} values (V_{max-R}/V_{max-S}) and giving a value of 1.18. Considerable differences between these results and those reported in the literature in a previous study of enantioselective metabolism of fluoxetine by CYP2D6 (Margolis *et al.*, 2000) were found. These differences can be attributed to the different enzyme sources and experimental methodologies, which strongly affect the estimations.

The *in vitro* intrinsic clearance has been estimated here as V_{max}/K_m and the values obtained were 121 ± 13 $\text{mL}\cdot\text{min}^{-1}\cdot(\text{mg CYP})^{-1}$ and 111 ± 16 $\text{mL}\cdot\text{min}^{-1}\cdot(\text{mg CYP})^{-1}$ for S- and R-fluoxetine, respectively.

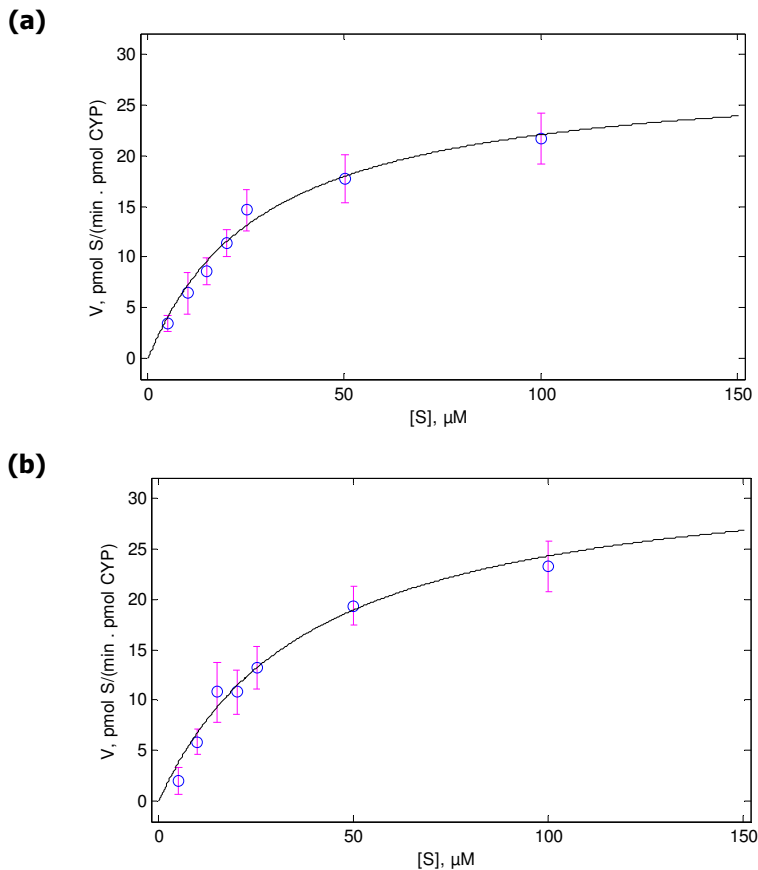


Figure IV.27: Michaelis-Menten plots for the metabolism of (a) S-fluoxetine and (b) R-fluoxetine by CYP2D6.

Finally, in order to check a possible interaction between the enantiomers in their metabolism, an experiment was carried out incubating only a single enantiomer, R-fluoxetine. The kinetic parameters obtained were: K_m $38 \pm 9 \mu\text{M}$ and V_{max} $33 \pm 4 \text{ pmol} \cdot \text{min}^{-1} \cdot (\text{pmol CYP})^{-1}$. The differences with the estimates obtained using the racemate were very low (1.6% for K_m and 3.9% for V_{max}) so we can conclude that the use of a racemate for the evaluation of enantioselective metabolism of a drug provides the same results than the use of single enantiomers, with the advantage of that no single enantiomers are needed.



V. CONCLUSIONS

V. CONCLUSIONS

This Thesis deals with two important application fields of capillary electrophoresis: chiral analysis and bioanalytical applications. The advantages of CE for these applications have been extensively proved along the research papers discussed here. Fast, economic and fully automated methods have been developed and applied to chiral separations and enantioselective evaluation of pharmacokinetic and pharmacodynamic properties of drugs. The most relevant conclusions that can be extracted from this work are summarized here:

- HS- β -CD has proved to be an excellent chiral selector for neutral and basic compounds. It has provided good enantioresolution values for most of the chiral compounds tested, using the partial and complete filling techniques. The enantioseparations performed with HS- β -CD have been successfully applied to the analysis of pharmaceutical samples, the analysis of ultrafiltrates from protein-drug mixtures and coupled to EMMA assays.
- Apparent binding constants between drugs and the HS- β -CD, calculated using non-linear regression, show that a strong interaction takes place between the HS- β -CD and the enantiomers of the eight psychoactive drugs studied. It has been demonstrated that enantioseparation with this CD is due to two different mechanisms, thermodynamic (the most usual) and electrophoretic enantioselectivity (less common but also enough to provide complete enantioresolution).
- The use of complete filling technique instead of conventional EKC is proposed for the evaluation of enantiomer-chiral selector binding constants. Its main advantage is a saving on chiral selector of about 99%. Except for the NACE application, all the enantioseparations in this Thesis have been performed by CFT or PFT, being the consumption of cyclodextrins extremely low.
- A relationship between some structural properties of basic xenobiotics and their enantioresolution with HS- β -CD, established by multivariate analysis, shows the ability of this CD as chiral selector. The most influential structural properties on the enantioresolution with HS- β -CD are *IgD*, *PSA*, *HBD* and *HBA*. From these

properties, predictions of categorical resolutions can be done via a simple direct equation developed in this Thesis.

- DMSO has proved to be an alternative for chiral NACE when the commonly used alcoholic BGEs could not be used due to volatility, solubility or current breakdown problems. CM- γ -CD has been successfully employed as chiral selector in NACE in a DMSO-based background electrolyte, with stable currents during all the electrophoretic developments. Despite the weaker selector-selectand interactions compared with aqueous media, baseline resolutions were achieved suggesting that the BGEs proposed in this work can be used in chiral NACE.
- A robust mathematical data treatment for the evaluation of protein binding is proposed, avoiding inconsistent equations that have been used in the past. The new protocol including outliers' identification and elimination, estimation of affinity constants with their uncertainty and verification of some assumptions done about the binding process also provides some quality suggestions about adequate conditions for the experimental design.
- The enantioselective binding of fluoxetine to HSA and of zopiclone and nomifensine to HSA and total plasma proteins has been evaluated in this Thesis *via* ultrafiltration and chiral EKC, using the experimental design and protocol developed here. In all cases, a certain degree of enantioselectivity has been found in their binding with the HSA molecule.
- An EMMA methodology for the screening of AChE inhibitors has been developed. This methodology allows obtaining inhibition constants, IC_{50} estimations and to determine the mechanism of the inhibition. Experimental conditions for screening new candidate drugs are established, with the percent of inhibition as measure of the inhibitor potency. The proposed methodology is applied to the screening of five known AChE inhibitors, being the order of their inhibitor potencies: tacrine > edrophonium > neostigmine > eserine > pyridostigmine.
- The EMMA procedure and the chiral separation by EKC-PFT have been combined in order to develop a methodology that allows the enantioselective estimation of drugs metabolism by different isoforms of the cytochrome P450. Some

experimental variables of the EMMA procedure, as well as the enantioseparations with HS- β -CD, have been adjusted in order to obtain a fast, simple and fully automated methodology with an extremely low consumption of enzymes, substrates and chiral selectors (usually expensive). The complete method, including capillary preconditioning, injection, incubation and chiral separation takes less than 35 min.

- Michaelis-Menten parameters, estimated for the metabolism of verapamil enantiomers by CYP3A4 and fluoxetine enantiomers by CYP2D6, show in both cases a slight enantioselectivity in the metabolism process. From the kinetic data an estimation of the *in vitro* intrinsic clearance has been performed also for the enantiomers of both drugs.

The results obtained in this Thesis show that capillary electrophoresis can be a powerful technique for all the studies that may be performed in the pre-clinical stages of the development of new drugs. Methods for the chiral analysis of new molecules can be easily developed using the prediction model of enantioresolution performed for HS- β -CD. EMMA has good features for the fast screening of candidate drugs in terms of their pharmacological activity, and also for evaluating relevant pharmacokinetic properties such as their metabolism by enzymatic systems. In combination with UF, chiral EKC provides accurate estimations of the enantioselective protein binding of drugs. In summary, the *in vitro* procedures developed in this Thesis provide an overview of the potential behavior of new molecules in their interaction with live systems, which is valuable information in order to save effort and money with *in vivo* studies.



VI. REFERENCES

VI. REFERENCES

- Afshar, M., Thormann, W. (2006) Capillary electrophoretic investigation of the enantioselective metabolism of propafenone by human cytochrome P-450 SUPERSOMES: Evidence for atypical kinetics by CYP2D6 and CYP3A4. *Electrophoresis* 27, 1526-1536.
- Ahuja, S., Jimidar, M.I. (2008) *Capillary electrophoresis methods for pharmaceutical analysis*. Elsevier, USA.
- Al Azzam, K.M., Saad, B., Aboul-Enein, H.Y. (2010) Determination of the binding constants of modafinil enantiomers with sulfated β -cyclodextrin chiral selector by capillary electrophoresis using three different linear plotting models. *Electrophoresis* 31, 2957-2963.
- Amini, A., Beijersten, I., Petterson, C., Westerlund, D. (1996) Enantiomeric separation of local anesthetic drugs by micellar electrokinetic capillary chromatography with taurodeoxycholate as chiral selector. *Journal of Chromatography A* 737, 301-313.
- Amini, A., Merclin, N., Bastami, S., Westerlund D. (1999a) Determination of association constants between enantiomers of orciprenaline and methyl- β -cyclodextrin as chiral selector by capillary zone electrophoresis using a partial filling technique. *Electrophoresis* 20, 180-188.
- Amini, A., Paulsen-Sörman, U. (1997) Enantioseparation of local anesthetic drugs by capillary zone electrophoresis with cyclodextrins as chiral selectors using a partial filling technique. *Electrophoresis* 18, 1019-1025.
- Amini, A., Paulsen-Sörman, U., Westerlund D. (1999b) Principle and applications of the partial filling technique in capillary electrophoresis. *Chromatographia* 50, 497-596.
- Amini, A., Petterson, C., Westerlund, D. (1997) Enantioresolution of disopyramide by capillary affinity electrokinetic chromatography with human α_1 -

- acid glycoprotein (AGP) as chiral selector applying a partial filling technique. *Electrophoresis* 18, 950-957.
- Andrisano, V., Bartolini, M., Gotti, R., Cavrini, V., Felix, G. (2001) Determination of inhibitors' potency (IC_{50}) by a direct high-performance liquid chromatographic method on an immobilised acetylcholinesterase column. *Journal of Chromatography B* 753, 375-383.
 - Ascoli, G.A., Domenici, E., Bertucci, C. (2006) Drug binding to human serum albumin: Abridged review of results obtained with high-performance liquid chromatography and circular dichroism. *Chirality* 18, 667-679.
 - BD Gentest Tissue Fractions Brochure. (2010). Available in: http://www.bdbiosciences.com/documents/tissue_fractions_brochure.pdf [accessed February 2013]
 - Borgstrom, L., Nyberg, L., Jonsson, S., Linberg, C., Paulson, J. (1989) Pharmacokinetic evaluation in man of terbutaline given as separate enantiomers and as a racemate. *British Journal of Clinical Pharmacology* 27, 49-56.
 - Brandon, E.F.A., Raap, C.D., Meijermann, I., Beijnen, J.H., Schellens, J.H.M. (2003) An update on in vitro test methods in human hepatic drug biotransformation research: pros and cons. *Toxicology and Applied Pharmacology* 189, 233-246.
 - Brauer, R.W., Pessotti, R.L., Pizzolato, P. (1959) Isolated rat liver preparation: bile production and other basic properties. *Proceedings of the Society for Experimental Biology and Medicine* 78, 174-181.
 - Brocks, D.R. (2006) Drug disposition in three dimensions: an update on stereoselectivity in pharmacokinetics. *Biopharmaceutics and Drug Disposition* 27, 387-406.
 - Caillet, C., Chauvelot-Moachon, L., Montastruc, J.L., Bagheri, H. (2012) Safety profile of enantiomers vs. racemic mixtures: it's the same? *British Journal of Clinical Pharmacology* 74, 886-889.

- Carter, D.C., Ho, H.X. (1994) Structure of serum albumin. *Advances in Protein Chemistry* 45, 153-203.
- Cashman, J.R. (1989) Enantioselective N-oxygenation of verapamil by the hepatic flavin-containing monooxygenase. *Molecular Pharmacology* 36, 497-503.
- Cashman, J.R., Celestial, J.R., Leach, A.R. (1992) Enantioselective N-oxygenation of chlorpheniramine by the flavin-containing monooxygenase from hog liver. *Xenobiotica* 22, 459-469.
- Chang, C., Wang, X., Bai, H., Liu, H. (2012) Applications of nanomaterials in enantioseparation and related techniques. *Trends in Analytical Chemistry* 39, 195-206.
- Chankvetadze, B. (2007) Enantioseparations by using capillary electrophoretic techniques. The story of 20 and a few more years ago. *Journal of Chromatography A* 1168, 45-70.
- Chankvetadze, B., Blaschke, G. (2001) Enantioseparations in capillary electromigration techniques: Recent developments and future trends. *Journal of Chromatography A* 906, 309-363.
- Chankvetadze, B., Burjanadze, N., Bergenthal, D., Blaschke, G. (1999) Potential of flow-counterbalanced capillary electrophoresis for analytical and micropreparative separations. *Electrophoresis* 20, 2680-2685.
- Chankvetadze, B., Endresz, G., Blaschke, G. (1994) About some aspects of the use of charged cyclodextrins for capillary electrophoresis enantioseparation. *Electrophoresis* 15, 804-807.
- ChemSpider database: <http://www.chemspider.com> [accessed July 2013]
- Chen, F.T.A., Shen, G., Evangelista, R.A. (2001) Characterization of highly sulfated cyclodextrins. *Journal of Chromatography A* 924, 523-532.
- Chuang, V.T.G., Otagiri, M. (2006) Stereoselective binding of human serum albumin. *Chirality* 18, 159-166.

- Cooper, M.A. (2002) Optical biosensors in drug discovery. *Nature Reviews Drug Discovery* 1, 515-528.
- Copeland, R.A. (2005) Evaluation of enzyme inhibitors in drug discovery. John Wiley and Sons, New Jersey, USA.
- Cserhádi, C. (2008) New applications of cyclodextrins in electrically driven chromatographic systems: a review. *Biomedical Chromatography* 22, 563-571.
- Cucinotta, V., Contino, A., Guffrida, A., Maccarrone, G., Messina, M. (2010) Application of charged single isomer derivatives of cyclodextrins in capillary electrophoresis for chiral analysis. *Journal of Chromatography A* 1217, 953-967.
- Del Bubba, M., Checchini, L., Lepri, L. (2013) Thin-layer chromatography enantioseparations on chiral stationary phases: a review. *Analytical and Bioanalytical Chemistry* 405, 533-554.
- Dey, J., Mohanty, A., Roy, S., Khatua, D. (2004) Cationic vesicles as chiral selectors for enantioseparation of nonsteroidal antiinflammatory drugs by micellar electrokinetic chromatography. *Journal of Chromatography A* 1048, 127-132.
- Doménech Berrozpe, J., Martínez Lanao, J., Plá Delfina, J.M. (1998) *Biofarmacia y Farmacocinética. Volumen II: Biofarmacia. Editorial Síntesis, Madrid, Spain.*
- Dong, X.L., Wu, R.A., Dong, J., Wu, M.H., Zhu, Y., Zou, H.F. (2008) A mesoporous silica nanoparticles immobilized open-tubular capillary column with a coating of cellulose tris(3,5-dimethylphenyl-carbamate) for enantioseparation in CEC. *Electrophoresis* 2008, 29, 3933-3940.
- Dubský, P., Svobodová, J., Tesařová, E., Gaš, B. (2010) Enhanced selectivity in CZE multi-chiral selector enantioseparation systems: proposed separation mechanism. *Electrophoresis* 31, 1453-1441.
- Duffus, J.H., Nordberg, M., Templeton, D.M. (2007) Glossary of terms used in toxicology, 2nd edition (IUPAC recommendations 2007). *Pure and Applied Chemistry* 79, 1153-1344.

- Eichelbaum, M., Mikus, G., Vogelsang, B. (1984) Pharmacokinetics of (+), (-) and (\pm)-verapamil after intravenous administration. *British Journal of Clinical Pharmacology* 18, 733-740.
- Escuder-Gilabert, L., Martínez-Gómez, M.A., Villanueva-Camañas, R.M., Sagrado, S., Medina-Hernández, M.J. (2009) Microseparation techniques for the study of the enantioselectivity of drug-plasma protein binding. *Biomedical Chromatography* 23, 225-238.
- European Medicines Agency. (1993) Investigation of Chiral Active Substances. Available in:
http://www.ema.europa.eu/docs/en_GB/document_library/Scientific_guideline/2009/09/WC500002816.pdf [accessed February 2013]
- Evans, G. (2004) *A handbook of Bioanalysis and Drug Metabolism*. CRC press, USA.
- Fan, Y., Scriba, G.K.E. (2010) Advances in-capillary electrophoretic enzyme assays. *Journal of Pharmaceutical and Biomedical Analysis* 53, 1076-1090.
- Fielding, L., Rutherford, S., Fletcher, D. (2005) Determination of protein-ligand binding affinity by NMR: observations from serum albumin model systems. *Magnetic Resonance in Chemistry* 43, 463-470.
- Food and Drug Administration. (1992) Development of New Stereoisomeric Drugs. Available in:
<http://www.fda.gov/drugs/guidancecomplianceregulatoryinformation/guidances/ucm122883.htm> [accessed February 2013]
- Forsberg, E.M., Green, J.R.A., Brennan, J.D. (2011) Continuous flow immobilized enzyme reactor-tandem mass spectrometry for screening of AChE inhibitors in complex mixtures. *Analytical Chemistry* 83, 5230-5236.
- Foulon, C., Danel, C., Vaccher, M.P., Bonte, J.P., Vaccher, C., Goossens, J.F. (2004) Chiral separation of N-imidazole derivatives, aromatase inhibitors, by

- cyclodextrin-capillary zone electrophoresis. Mechanism of enantioselective recognition. *Electrophoresis* 25, 2735-2744.
- Gaillot, J., Houghton, G.W., Marc Aurele, J., Dreyfus, J.F. (1983) Pharmacokinetics and metabolism of zopiclone. *Pharmacology* 27, 76-91.
 - Gálvez-Llompарт, M., Zanni, R., Romualdi, P., García-Doménech, R. (2013) Selection of nutraceutical compounds as COX inhibitors by molecular topology. *Medicinal Chemistry Research* 22, 3466-3477.
 - Gasser, R., Funk, C., Matzinger, P., Klemisch, W., Viger-Chougnnet, A. (1999) Use of transgenic cell lines in mechanistic studies of drug metabolism. *Toxicology in Vitro* 13, 625-632.
 - Gil-Av, E., Feibush, B., Charles-Sigler, R. (1966) Separation of enantiomers by gas liquid chromatography with an optically active stationary phase. *Tetrahedron Letters* 7, 1009-1015.
 - Gordon Gibson, G., Skett, P. (2001) *Introduction to drug metabolism*, 3rd edition. Cengage Learning, UK.
 - Gübitz, G., Schmid, M.G. (2008) Chiral separations by capillary electromigration techniques. *Journal of Chromatography A* 1204, 140-156.
 - Guo, Z., Du, Y., Liu, X.B., Ng, S.C., Chen, Y., Yang, Y.H. (2010) Enantioselectively controlled release of chiral drug (metoprolol) using chiral mesoporous silica materials. *Nanotechnology* 21, 165103.
 - Hage, D.S., Sengupta A. (1999) Characterization of the binding of digitoxin and acetyldigitoxin to human serum albumin by high-performance affinity chromatography. *Journal of Chromatography B* 724, 91-100.
 - Hage, D.S., Sengupta, A. (1998) Studies of protein binding to nonpolar solutes by using zonal elution and High Performance Affinity Chromatography: Interactions of cis- and trans-clomiphene with human serum albumin in the presence of β -cyclodextrin. *Analytical Chemistry* 70, 4602-4609.

- Hai, X., Adams, E., Hoogmartens, J., Van Schepdael, A. (2009) Enantioselective in-line and off-line CE methods for the kinetic study on cimetidine and its chiral metabolites with reference to flavin-containing monooxygenase genetic isoforms. *Electrophoresis* 30, 1248-1257.
- Hai, X., Yang, B., Van Schepdael, A. (2012) Recent developments and applications of EMMA in enzymatic and derivatization reactions. *Electrophoresis* 33, 211-227.
- Hariparsad, N., Sane, R.S., Strom, S.C., Desai, P.B. (2006) In vitro methods in human drug biotransformation research: implications for cancer chemotherapy. *Toxicology in Vitro* 20, 135-153.
- He, X.M., Carter, D.C. (1992) Atomic structure and chemistry of human serum albumin. *Nature* 358, 209-215.
- Healey, R., Ghanem, A. (2013) An insight to chiral monolith for enantioselective nano and micro HPLC: Preparation and applications. *Chirality* 25, 314-323.
- Hendel, J., Brodthages, H. (1984) Entero-hepatic cycling of methotrexate estimated by use of the D-isomer as a reference marker. *European Journal of Clinical Pharmacology* 26, 103-107.
- Hengstler, J.G., Utesch, D., Steinberg, P., Platt, K.L., Diener, B., Ringel, M., Swales, N., Fischer, T., Biefang, K., Gerl, M., Böttger, T., Oesch, F. (2000) Cryopreserved primary hepatocytes as a constantly available in vitro model for the evaluation of human and animal drug metabolism and enzyme induction. *Drug Metabolism Reviews* 32, 81-118.
- Hsiao, J.Y., Wu, S.H., Ding, W.H. (2006) Application of cyclodextrin-mediated capillary electrophoresis to simultaneously determine the apparent binding constants and thermodynamic parameters of naphthalenesulfonate derivatives. *Talanta* 68, 1252-1258.

- Huang, Z., Roy, P., Waxman, D.J. (2000) Role of human liver microsomal CYP 3A4 and CYP 2B6 in catalyzing N-dichloroethylation of cyclophosphamide and ifosfamide. *Biochemical Pharmacology* 59, 961-972.
- Jáč, P., Scriba, G.K.E. (2013) Recent advances in electrodriven separations. *Journal of Separation Science* 36, 52-74.
- Jansson, R., Malm, M., Roth, C., Ashton, M. (2008) Enantioselective and nonlinear intestinal absorption of eflornithine in the rat. *Antimicrobial Agents and Chemotherapy* 52, 2842-2848.
- Jiang, T.F., Liang, T.T., Wang, Y.H., Zhang, W.H., Lv, Z.H. (2013) Immobilized capillary tyrosinase microreactor for inhibitor screening in natural extracts by capillary electrophoresis. *Journal of Pharmaceutical and Biomedical Analysis* 84, 36-40.
- Jorgenson, J.W., Lukacs, K.D. (1981) Zone electrophoresis in open-tubular glass capillaries. *Analytical Chemistry* 53, 1298-1302.
- Kahle, K.A., Foley, J.P. (2007) Review of aqueous chiral electrokinetic chromatography (EKC) with an emphasis on chiral microemulsion EKC. *Electrophoresis* 28, 2503-2526.
- Katrahalli, U., Jaldappagari, S., Kalanur, S.S. (2010) Probing the binding of fluoxetine hydrochloride to human serum albumin by multispectroscopic techniques. *Spectrochimica Acta Part A* 75, 314-319.
- Kikura-Hanajiri, R., Kawamura, M., Miyajima, A., Sunouchi, M., Goda, Y. (2011) Chiral analyses of dextromethorphan/levomethorphan and their metabolites in rat and human samples using LC-MS/MS. *Analytical and Bioanalytical Chemistry* 400, 165-174.
- Kirsty, J., McLean, D., Clift, D., Lewis, G., Sabri, M., Balding, P.R., Sutcliffe, M.J., Leys, D., Munro, A.W. (2006) The preponderance of P450s in the *Mycobacterium tuberculosis* genome. *Trends in Microbiology* 14, 220-228.

- Klegerisa A., Maguireb, J., McGeer, P.L. (2004) S- but not R-enantiomers of flurbiprofen and ibuprofen reduce human microglial and THP-1 cell neurotoxicity. *Journal of Neuroimmunology* 152, 73-77.
- Kroemer, H.K., Echizen, H., Heidemann, H., Eichelbaum, M. (1992) Predictability of the in vivo metabolism of verapamil from in vitro data: contribution of individual metabolic pathways and stereoselective aspects. *Journal of Pharmacology and Experimental Therapeutics* 260, 1052-1057.
- Kuhn R., Hoffstetter-Kuhn, S. (1993) *Capillary Electrophoresis: Principles and practice*. Springer Laboratory, Germany.
- Kumar, N., Sharma, U., Singh, C., Singh, B. (2012) Thalidomide: chemistry, therapeutic potential and oxidative stress induced teratogenicity. *Current Topics in Medicinal Chemistry* 12, 1436-1455.
- Kurz, H. (1986) Methodological problems in Drug Binding Studies, in: *Drug Protein Binding*, Praeger Publishers, New York, USA, pp 70-92.
- Kwong, T.C. (1985) Free drug measurements: methodology and clinical significance. *Clinica Chimica Acta* 151, 193-216.
- Lämmerhofer, M. (2010) Chiral recognition by enantioselective liquid chromatography: Mechanisms and modern chiral stationary phases. *Journal of Chromatography A* 1217, 814-856.
- Lanchote, V.L., Takayanagui, O.M., Mateus, F.H. (2004) Enantioselective renal excretion of albendazole metabolites in patients with neurocysticercosis. *Chirality* 16, 520-525.
- Lázaro E., Lowe, P.J., Briand X., Faller, B. (2008) New approach to measure protein binding based on a parallel artificial membrane assay and human serum albumin. *Journal of Medicinal Chemistry* 51, 2009-2017.
- Lee, E.J.D., Williams, K.M. (1990) Chirality: clinical pharmacokinetics and pharmacodynamic considerations. *Clinical Pharmacokinetics* 18, 339-345.

- Leonard, B., Taylor, D. (2010) Escitalopram-translating molecular properties into clinical benefit: reviewing the evidence in major depression. *Journal of Psychopharmacology* 24, 1143–1152.
- Lewis, D.F.V. (2003) P450 structures and oxidative metabolism of xenobiotics. *Pharmacogenomics* 4, 387-395.
- Lewis, D.F.V. (2004) 57 varieties: the human cytochromes P450. *Pharmacogenomics* 5, 305-318.
- Li, H.F., Zeng, H.L., Chen, Z.F., Lin, J.M. (2009) Chip-based enantioselective open-tubular capillary electrochromatography using bovine serum albumin-gold nanoparticle conjugates as the stationary phase. *Electrophoresis* 30, 1022-1029.
- Li, M., Liu, X., Jiang, F.Y., Guo, L.P., Yang, L. (2011) Enantioselective open-tubular capillary electrochromatography using cyclodextrin-modified gold nanoparticles as stationary phase. *Journal of Chromatography A* 1218, 3725-3729.
- Lima, J.J., Boudoulas, H., Shields, B.J. (1985) Stereoselective pharmacokinetics of disopyramide enantiomers in man. *Drug Metabolism and Disposition* 13, 572-577.
- Lin, C.C., Li, Y.T., Chen, S.H. (2003) Recent progress in pharmacokinetic applications of capillary electrophoresis. *Electrophoresis* 24, 4106-4115.
- Lipka, E., Danel, C., Orhan, H., Bonte, J.P., Vaccher, C. (2007) Chiral resolution of melatonergic ligands by EKC using highly sulfated CDs. *Electrophoresis* 228, 3915-3921.
- Machour, N., Place, J., Tron, F., Charlionet, R., Morin, C., Desbene, A., Desbene, P.L. (2005) Analysis of virtual two-dimensional gels based upon affinity capillary electrophoresis hyphenated to ion trap-mass spectrometry. *Electrophoresis* 26, 1466-1475.

- Margolis, J.M., O'Donell, J.P., Mankowski, D.C., Ekins, S., Scott Obach, R. (2000) (R)-, (S)-, and racemic fluoxetine N-demethylation by human cytochrome P450 enzymes. *Drug Metabolism and Disposition* 28, 1187-1191.
- Martín-Biosca Y., García-Ruiz C., Marina M.L. (2001) Enantiomeric separation of chiral phenoxy acid herbicides by electrokinetic chromatography. Application to the determination of analyte-selector apparent binding constants for enantiomers. *Electrophoresis* 22, 3216-3225.
- Martínez-Gómez, M.A., Villanueva-Camañas, R.M., Sagrado, S., Medina-Hernández, M.J. (2007a) Evaluation of enantioselective binding of basic drugs to plasma by ACE. *Electrophoresis* 28, 3056-3063.
- Martínez-Gómez, M.A., Villanueva-Camañas, R.M., Sagrado, S., Medina-Hernández, M.J. (2007b) Evaluation of enantioselective binding of antihistamines to human serum albumin by ACE. *Electrophoresis* 28, 2635-2643.
- Martínez Gómez, M.A. (2007c) Evaluación de la interacción de fármacos básicos con las proteínas plasmáticas mediante electroforesis capilar. Estudios de enantioselectividad y aplicaciones analíticas. Tesis Doctoral, Universidad de Valencia.
- Martínez-Gómez, M.A., Sagrado, S., Villanueva-Camañas, R.M., Medina-Hernández, M.J. (2007d) Enantiomeric quality control of antihistamines in pharmaceuticals by affinity electrokinetic chromatography with human serum albumin as chiral selector. *Analytica Chimica Acta* 592, 202–209.
- Martínez-Pla, J.J., Martínez-Gómez, M.A., Martín-Biosca, Y., Sagrado, S., Villanueva-Camañas, R.M., Medina-Hernández, M.J. (2004) High-throughput capillary electrophoresis frontal analysis method for the study of drug interactions with human serum albumin at near-physiological conditions. *Electrophoresis* 25, 3176-3185.
- Matthijs, N., Van Hemelryck, S., Maftouh, M., Massart, D.L., Vander Heyden, Y. (2004) Electrophoretic separation strategy for chiral pharmaceuticals using

- highly-sulfated and neutral cyclodextrins based dual selector systems. *Analytica Chimica Acta* 525, 247-263.
- Mehvar, R., Brocks, D.R. (2001) Stereospecific pharmacokinetics and pharmacodynamics of beta-adrenergic blockers in humans. *Journal of Pharmaceutical Science* 4, 185-200.
 - Mehvar, R., Brocks, D.R., Vakily, M. (2002) Impact of stereoselectivity on the pharmacokinetics and pharmacodynamics of antiarrhythmic drugs. *Clinical Pharmacokinetics* 41, 533-558.
 - Mischinger, H.J., Walsh, T.R., Liu, T., Rao, P.N., Rubin, R., Nakamura, K., Todo, S., Starzl, T.E. (1992) An improved technique for isolated perfusion of rat livers and an evaluation of perfusates. *Journal of Surgical Research* 53, 158-165.
 - Moliner-Martínez, Y., Cárdenas, S., Valcárcel, M. (2007) Evaluation of carbon nanostructures as chiral selectors for direct enantiomeric separation of ephedrines by EKC. *Electrophoresis* 28, 2573-2579.
 - Monti, J.M., Pandi-Perumal, S.R. (2007) Eszopiclone: its use in the treatment of insomnia. *Neuropsychiatric Disease and Treatment* 3, 441-453.
 - Nelson, D.L., Cox, M.M. (2006) *Lehninger principios de bioquímica*. 4th edition. Ediciones Omega, Barcelona, Spain.
 - Nishi, H., Fujuyama, T., Matsuo, M., Terabe, S. (1990) Chiral separation of diltiazem, trimetoquinol and related compounds by micellar electrokinetic chromatography with bile salts. *Journal of Chromatography A* 515, 233-243.
 - Okhonin, V., Liu, X., Krylov, S.N. (2005) Transverse diffusion of laminar flow profiles to produce capillary nanoreactors. *Analytical Chemistry* 77, 5925-5929.
 - Oravcová, J., Böhs, B., Lindner, W. (1996) Drug-protein binding studies. New trends in analytical and experimental methodology. *Journal of Chromatography B* 677, 1-28.

-
- Ortiz de Montellano, P.R. (2005) Cytochrome P450. Structure, mechanism and biochemistry. 3rd edition. Kluwer Academic/Plenum Publishers, New York, USA.
 - Rettie, A.E., Korzekwa, K.R., Kunze, K.L., Lawrence, R.F., Eddy, A.C., Aoyama, T., Gelboin, H.V., Gonzales, F.J., Trager, W.F. (1988) Hydroxylation of warfarin by human cDNA-expressed cytochrome P-450: a role for P-450 2C9 in the etiology of (S)-warfarin drug interactions. *Chemical Research in Toxicology* 28, 25-39.
 - Rocco, A., Maruška, A., Fanali, S. (2013) Enantiomeric separations by means of nano-LC. *Journal of Separation Science* 36, 421-444.
 - Rudaz, S., Le Saux, T., Prat, J., Gareil, P., Veuthey, J.L. (2004) Ultrashort partial filling technique in capillary electrophoresis for infinite resolution of tramadol enantiomers and its metabolites with highly sulfated cyclodextrins. *Electrophoresis* 25, 2761-2771.
 - Sánchez-Hernández, L., Crego, A.L., Marina, M.L., García-Ruiz, C. (2008) Sensitive chiral analysis by CE: An update. *Electrophoresis* 29, 237-251.
 - Sanders, B.D., Slotcavage, R.L., Scheerbaum, D.L., Kochansky, C.J., Strein T.G. (2005) Increasing the efficiency of in-capillary electrophoretically mediated microanalysis reactions via rapid polarity switching. *Analytical Chemistry* 77, 2332-2337.
 - Schmid, M., Gübitz, G. (2004) Use of chiral crown ethers in capillary electrophoresis. *Methods in Molecular Biology* 243, 317-321.
 - Schmid, M.G., Gübitz, G. (1996) Direct resolution of underivatized amino acids by capillary zone electrophoresis based on ligand exchange. *Enantiomer* 1, 23-27.
 - Schwaninger, A.E., Meyer, M.R., Zapp, J., Maurer, H.H. (2012) Investigations on the stereoselectivity of the phase II metabolism of the 3,4-methylenedioxyethylamphetamine (MDEA) metabolites 3,4-dihydroxyethylamphetamine (DHEA) and 4-hydroxy-3-methoxyethylamphetamine (HMEA). *Toxicology Letters* 212, 38-47.

- Scriba, G.K.E. (2008) Cyclodextrins in capillary electrophoresis enantioseparations – Recent developments and applications. *Journal of Separation Science* 31, 1991-2001.
- Scriba, G.K.E. (2011) Fundamental aspects of chiral electromigration techniques and application in pharmaceutical and biomedical analysis. *Journal of Pharmaceutical and Biomedical Analysis* 55, 688-701.
- Sengupta, A., Hage, D.S. (1999) Characterization of minor site probes for human serum albumin by high-performance affinity chromatography. *Analytical Chemistry* 71, 3821-3827.
- Shanmuganathan, M., Britz-McKibbin, P. (2013) High quality drug screening by capillary electrophoresis: A review. *Analytica Chimica Acta* 773, 24-36.
- Šoltés, L., Mach, M. (2002) Estimation of drug-protein binding parameters on assuming the validity of thermodynamic equilibrium. *Journal of Chromatography B* 768, 113-119.
- Spanish Drug Agency (Agencia Española del Medicamento). Available in: <http://www.aemps.es> [accessed March 2011]
- Sugio, S., Kashima, A., Mochizuki, S., Noda, M., Kobayashi, K. (1999) Crystal structure of human serum albumin at 2.5 Å resolution. *Protein Engineering* 12, 439-446.
- Sun, X.M., Gao, N., Jin, W.R. (2006) Monitoring yoctomole alkaline phosphatase by capillary electrophoresis with on-capillary catalysis-electrochemical detection. *Analytica Chimica Acta* 571, 30-33.
- Tang, Z.M., Wang, Z.Y., Kang, J.W. (2007) Screening of acetylcholinesterase inhibitors in natural extracts by CE with electrophoretically mediated microanalysis technique. *Electrophoresis* 28, 360-365.
- Terabe, S. (1989) Electrokinetic chromatography: An interface between electrophoresis and chromatography. *Trends in Analytical Chemistry* 8, 129-134.

- Terabe, S., Otsuka, K., Ichikawa, A., Tsuchiya, A., Ando, T. (1984) Electrokinetic separations with micellar solutions and open-tubular capillaries. *Analytical Chemistry* 56, 111-113.
- Terabe, S., Ozaki, H., Otsuka, K., Ando, T. (1985) Electrokinetic chromatography with 2-O-carboxymethyl- β -cyclodextrin as a moving "stationary" phase. *Journal of Chromatography* 332, 211-217.
- Thöm, H.A., Sjögren, E., Dickinson, P.A., Lennernäs, H. (2012) Binding processes determine the stereoselective intestinal and hepatic extraction of verapamil in vivo. *Molecular Pharmaceutics* 9, 3034–3045.
- Togami, K., Tosaki, Y., Chrono, S., Morimoto, K., Hayasaka, M., Tada, H. (2012) Enantioselective uptake of fexofenadine by Caco-2 cells as model intestinal epithelial cells. *Journal of Pharmacy and Pharmacology* 65, 22-29.
- Toon, S., Hopkins, K.J., Garstang, F.M., Rowland, M. (1987) Comparative effects of ranitidine and cimetidine on the pharmacokinetics and pharmacodynamics of warfarin in man. *European Journal of Clinical Pharmacology* 32, 165-172.
- Urban, P.L., Goodall, D.M., Bergström, E.T., Bruce, N.C. (2007) Electrophoretically mediated microanalysis of a nicotinamide adenine dinucleotide-dependent enzyme and its facile multiplexing using an active pixel sensor UV detector. *Journal of Chromatography A* 1162, 132-140.
- Vaccher, M.P., Lipka, E., Bonte, J.P., Foulon, C., Gossens, J.F., Vaccher C. (2005) Enantiomeric analysis of baclofen analogs by capillary zone electrophoresis, using highly sulfated cyclodextrins: inclusion ionization constant pK_a determination. *Electrophoresis* 26, 2974-2983.
- Valtcheva, L., Mohammad, J., Petterson, G., Hjertén, S. (1993) Chiral separation of β -blockers by high-performance capillary electrophoresis based on non-immobilized cellulase as enantioselective protein. *Journal of Chromatography* 638, 263-267.

- Van Dyck, S., Vissiers, S., Van Schepdael, A., Hoogmartens, J. (2003) Kinetic study of angiotensin converting enzyme activity by capillary electrophoresis after in-line reaction at the capillary inlet. *Journal of Chromatography A* 986, 303-311.
- Vuignier, K., Schappler, J., Veuthey, J.L., Carrupt, P.A., Martel, S. (2010) Drug-protein binding: a critical review of analytical tools. *Analytical and Bioanalytical Chemistry* 2010, 398, 53-66.
- Walle, T., Webb, J.G., Bagwell, E.E., Walle, U.K., Daniell, H.B., Gaffney, T.E. (1988) Stereoselective delivery and actions of beta-receptor antagonists. *Biochemical Pharmacology* 37, 115-124.
- Wang, T., Kang, J. (2009) Hexokinase inhibitor screening based on adenosine 5'-diphosphate determination by electrophoretically mediated microanalysis. *Electrophoresis* 30, 1349-1354.
- Ward, T.J., Farris, A.B. (2001) Chiral separations using the macrocyclic antibiotics: a review. *Journal of Chromatography A* 906, 73-89.
- Williams, P.A., Cosme, J., Ward, A., Angove, H.C., Vinkovic, D.M., Jhoti, H. (2003) Crystal structure of human cytochrome P450 2C9 with bound warfarin. *Nature* 424, 464-468.
- Wren, S.A.C., Rowe, R.C. (1992) Theoretical aspects of chiral separation in capillary electrophoresis. I. Initial evaluation of a model. *Journal of Chromatography A* 603, 235-241.
- Wu, S.H., Ding, W.H. (2005) Application of cyclodextrin-mediated capillary electrophoresis to determine the apparent binding constants and thermodynamic parameters of the alkylnaphtalene derivatives. *Electrophoresis* 26, 3528-3537.
- Yacobi, A., Levy, G. (1977) Protein binding of warfarin enantiomers in serum of humans and rats. *Journal of Pharmacokinetics and Biopharmaceutics* 5, 123-131.

- Yelekçi, K., Büyüktürk, B., Kayrak, N. (2013) In silico identification of novel and selective monoamine oxidase B inhibitors. *Journal of Neural Transmission* 120, 853-858.
- Yu, J.G., Huang, D.S, Huang, K.L., Hong, Y. (2011) Preparation of hydroxypropyl- β -cyclodextrin cross-linked multi-walled carbon nanotubes and their application in enantioseparation of clenbuterol. *Chinese Journal of Chemistry* 29, 893-897.
- Zhang, J., Ha, P.T.T., Lou, Y., Hoogmartens, J., Van Schepdael, A. (2005) Kinetic study of CYP3A4 activity on verapamil by capillary electrophoresis. *Journal of Pharmaceutical and Biomedical Analysis* 39, 612-617.
- Zhang, J., Hoogmartens, J., Van Schepdael, A. (2008) Kinetic study of cytochrome P450 by capillary electrophoretically mediated microanalysis. *Electrophoresis* 29, 3694-3700.
- Zhang, J., Lou, Y., Hoogmartens, J., Van Schepdael, A. (2006) Screening of drug metabolism by CE. *Electrophoresis* 27, 4827-4835.
- Zhao, L., Ai, P., Duan, A.H., Yuan, L.M. (2011) Analytical and Bioanalytical Chemistry 399, 143-147.
- Zhou, Q., Yan, X.F., Pan, W.S., Zeng, S. (2008) Is the required therapeutic effect always achieved by racemic switch of proton-pump inhibitors? *World Journal of Gastroenterology* 14, 2617-2619.
- Zhu, X., Lin, B., Jakob, A., Koppenhoefer, B. (1999) Study of enantioselective interactions between chiral drugs and serum albumin by capillary electrophoresis. *Electrophoresis* 20, 1869-1877.



Paper I

Characterizing the interaction between enantiomers of eight psychoactive drugs and highly sulfated- β -cyclodextrin by counter-current capillary electrophoresis

**L. Asensi-Bernardi, L. Escuder-Gilabert, Y. Martín-Biosca, S. Sagrado
and M.J. Medina-Hernández**

Biomedical Chromatography 2014, 28, 120-126

Characterizing the interaction between enantiomers of eight psychoactive drugs and highly sulfated- β -cyclodextrin by counter-current capillary electrophoresis

Lucía Asensi-Bernardi^a, Laura Escuder-Gilabert^a, Yolanda Martín-Biosca^a, Salvador Sagrado^{a,b} and María José Medina-Hernández^{a*}

ABSTRACT: The estimation of apparent binding constants and limit mobilities of the complexes of the enantiomers that characterize the interaction of enantiomers with chiral selectors, in this case highly sulfated β -cyclodextrin, was approached using a simple and economic electrophoretic modality, the complete filling technique (CFT) in counter-current mode. The enantiomers of eight psychoactive drugs, four antihistamines (dimethindene, promethazine, orphenadrine and terfenadine) and four antidepressants (bupropion, fluoxetine, nomifensine and viloxazine) were separated for the first time for this cyclodextrin (CD). Estimations of thermodynamic and electrophoretic enantioselectivities were also performed. Results indicate that, in general, thermodynamic enantioselectivity is the main component explaining the high resolution found, but also one case suggests that electrophoretic enantioselectivity itself is enough to obtain a satisfactory resolution. CFT results advantageous compared with conventional capillary electrophoresis (CE) and partial filling technique (PFT) for the study of the interaction between drugs and chiral selectors. It combines the use of a simple fitting model (as in CE), when the enantiomers do not exit the chiral selector plug during the separation (i.e. mobility of electroosmotic flow larger than mobility of CD), and drastic reduction of the consumption (and cost; ~99.7%) of the CD reagent (as in PFT) compared with the conventional CE. Copyright © 2013 John Wiley & Sons, Ltd.

Keywords: overall apparent binding constants; overall limit mobilities; thermodynamic and electrophoretic enantioselectivities; capillary electrophoresis; complete filling technique; highly sulfated β -cyclodextrin

Introduction

A research area of current interest is the development of stereoselective analytical methods able to determine the stereoisomer ratios in synthetic products, pharmaceutical formulations and biological samples owing to the high degree of stereoselectivity of pharmacological and pharmacokinetic processes (Scriba, 2011). Capillary electrophoresis (CE) is one of the most employed analytical techniques for chiral analysis, owing to its high efficacy, short analysis time, low reagent consumption and ease of automation (Chankvetadze, 2007).

Among the different chiral selectors used in CE, cyclodextrins (CDs) are widely used owing to the wide arsenal of CDs of different natures (native, derivatives, anionic, cationic or neutral) available, which enables chiral separation of a large number of chiral compounds. Characterizing the interactions of enantiomers with CDs is helpful in chiral separations research for a better understanding of the separation mechanism and molecular interactions and the prediction of migration behavior (Al Azzam *et al.*, 2010; Pang *et al.*, 2009; Chen and Weber, 2008). In these studies estimations of the association constants enantiomer-CD are performed. Such information is also valuable in studies where CDs are used as macromolecular hosts for explaining inclusion phenomena or encapsulation within CD nanocavities.

Direct enantioseparation with CE can be performed by adding a chiral selector to the background electrolyte (BGE). An alternative to this conventional technique is the use of partial (PFT) and

complete (CFT) filling techniques in which the capillary is (partially or totally, respectively) filled with chiral selector solution prior to injection of the analyte, while the BGE remains without chiral agent. PFT allows using chiral selectors to which given detectors have a significant response, as well as to avoid contamination of the ion-source when CE is coupled to mass spectrometry. The most important property of PFT and CFT, compared with the conventional technique, is its reduced expense owing to the drastic reduction of the chiral selector consumption (Amini *et al.*, 1999b; Chankvetadze and Blaschke, 2001). A special form of PFT and CFT, when the chiral selector and analyte possess opposite charges and move in the capillary

* Correspondence to: María José Medina-Hernández, Departamento de Química Analítica, Universidad de Valencia, Burjassot, Valencia, Spain. Email: maria.j.medina@uv.es

^a Departamento de Química Analítica, Universidad de Valencia, Burjassot, Valencia, Spain

^b Centro Interuniversitario de Reconocimiento Molecular y Desarrollo Tecnológico, Unidad mixta Universidad Politécnica de Valencia – Universidad de Valencia, Valencia, Spain

Abbreviations used: BGE, background electrolyte; CD, cyclodextrin; CE, capillary electrophoresis; CFT, complete filling technique; EOF, electroosmotic flow; HS-CD, highly sulfated cyclodextrins; PFT, partial filling technique.

in opposite direction, has been called counter-current separation (Chankvetadze *et al.*, 1994).

Highly sulfated cyclodextrins (HS-CDs) are a relatively recent family of CDs with good enantiomeric separation ability of numerous acidic, neutral and basic analytes (Perrin *et al.*, 2001; Matthijs *et al.*, 2002; Verleysen *et al.*, 1999; Chen *et al.*, 2001; Vescina *et al.*, 2002; Vaccher *et al.*, 2005; Rudaz *et al.*, 2004; Foulon *et al.*, 2002; Lipka *et al.*, 2007; Danel *et al.*, 2005). These CDs have a high density of negative charge in a broad pH range, so their electrophoretic mobility makes them adequate for counter-current separations. The opposite mobility of the analyte and the cyclodextrin greatly increases their interaction. In fact, it has been reported that maximum enantioselectivity values are obtained when analytes and CDs have opposite mobilities (Chankvetadze *et al.*, 1994; Rudaz *et al.*, 2003).

The aim of this study was to evaluate the enantioselective interaction data (affinity constants and mobilities of enantiomers, and thermodynamic and electrophoretic enantioselectivity values) of four antihistaminic and four antidepressant drugs with highly sulfated β -cyclodextrin (HS- β -CD), using advantageously counter-current CE-CFT, a modality not used before for this purpose. Using CFT could ensure that enantiomers do not exit to the CD plug during the electrophoretic separation, simplifying the calculations.

Materials and methods

Instrumentation

A Beckman P/ACE MDQ Capillary Electrophoresis System equipped with a DAD (Beckman Coulter, Fullerton, CA, USA) and 32Karat software version 8.0 was used throughout. A 50 μm inner diameter (i.d.) fused-silica capillary with total and effective lengths of 60.2 and 50 cm, respectively, was employed (Beckman Coulter, Fullerton, CA, USA). Electrophoretic solutions and samples were filtered through 0.45 μm pore size nylon membranes (Micron Separation, Westboro, MA, USA) and degassed in an ultrasonic bath (JP Selecta, Barcelona, Spain) prior to use. A Crison Micro pH 2000 pH meter from Crison Instruments (Barcelona, Spain) was employed to adjust the pH of buffer solutions.

Chemicals and solutions

All reagents were of analytical grade. $\text{NaH}_2\text{PO}_4 \cdot 2\text{H}_2\text{O}$ was from Fluka (Buchs, Switzerland); HS- β -CD (20% w/v) aqueous solution was purchased from Beckman Coulter (Fullerton, CA, USA); Ultra Clear TWF UV deionized water (SG Water, Barsbüttel, Germany) was used to prepare solutions.

Orphenadrine hydrochloride (ORP), terfenadine (TER), bupropion hydrochloride (BUP) and nomifensine maleate (NMF) were purchased from Sigma (St Louis, MO, USA). Promethazine hydrochloride was purchased from Guinama (Valencia, Spain). Dimethindene maleate (DIM) was kindly donated by Novartis (Madrid, Spain) and fluoxetine hydrochloride (FLX) by Alter (Madrid, Spain). Viloxazine (VLX) was also kindly donated by Astra Zeneca (Cheshire, UK).

BGE containing 30 mM phosphate at pH 7.0 was obtained by dissolving the appropriate amount of $\text{NaH}_2\text{PO}_4 \cdot 2\text{H}_2\text{O}$ in water and adjusting the pH with 1 M NaOH; 200 μM solutions of the racemic drugs were prepared in BGE to be injected into the electrophoretic system. These solutions were obtained by dilution from 1000 μM stock ones, prepared by weighing the appropriate

amount of each drug, dissolving it in the minimum volume of methanol necessary and bringing it to final volume with BGE. The small amount of methanol present in the final solutions was used as an electroosmotic flow (EOF) marker.

Methodology

In order to obtain good peak shapes and reproducible migration data, the capillary was conditioned prior to each injection. In all cases, the conditioning run included the following steps: (a) 1 min rinse with deionized water; (b) 2 min rinse with 0.1 M NaOH; (c) 1 min rinse with deionized water; and (d) 2 min rinse with BGE at 20 psi.

For the evaluation of the enantioselective interaction between psychoactive drugs and the HS- β -CD, chiral separation of the racemic drugs was carried out employing eight concentrations of HS- β -CD between 0 and 2% (0, 0.05, 0.1, 0.25, 0.5, 0.75, 1 and 2%), and three capillary temperatures (15, 25 and 35°C). Other working conditions were kept constant at following values: BGE, 30 mM phosphate at pH 7.0; applied voltage, 15 kV; CD injection, 10 psi per 2 min (filled capillary); analyte injection, 0.5 psi per 5 s; detection wavelength, 220 nm.

Software and calculations

Effective electrophoretic mobilities, μ_{eff} , were calculated from:

$$\mu_{\text{eff}} = \frac{L}{V} \left(\frac{1}{t_{\text{f}}} - \frac{1}{t_0} \right) \quad (1)$$

where L is the total capillary length, l the length of the capillary from the inlet end to the detector, V is the applied voltage, and t_{f} and t_0 are the measured migration times of the analyte and EOF marker, respectively. STATGRAPHICS® Plus 5.1 was employed for nonlinear fitting.

Results and discussion

Enantioseparation of psychoactive drugs

Figure 1 shows the chemical structures of the eight psychoactive drugs in study. Their pK_{a} values are between 8.1 and 9.7, so they are positively charged at working conditions (pH 7), leading to a high interaction with the anionic HS- β -CD favoured by their migration through the CD plug. Figure 1 also shows some electropherograms corresponding to the enantiomer resolution obtained under different experimental conditions. As can be observed in Fig. 1, except for terfenadine, baseline resolution was achieved for all the analytes studied and high R_{s} values were obtained. The R_{s} values obtained were similar to or higher than those reported in the literature for these compounds with other cyclodextrins, but obtained in most cases using higher CD concentrations than here (Castro-Puyana *et al.*, 2008; Van Eckhaut *et al.*, 2004; Matsunaga *et al.*, 2002; Inoue and Chang, 2003; Rudaz *et al.*, 2003; Bonato *et al.*, 2003; Perrin *et al.*, 2001; Li and Vigh, 2004; Asensi-Bernardi *et al.*, 2010; Yang *et al.*, 2005; Liao *et al.*, 2007; Chen *et al.*, 2002; Wei *et al.*, 2005).

Electroosmotic flow mobility (μ_{EOF}) in the working conditions was estimated as between 3.81×10^{-8} and $5.99 \times 10^{-8} \text{ m}^2 \text{ V}^{-1} \text{ s}^{-1}$ from experimental data. These values are higher than the opposite CD mobility (μ_{CD}), obtained from the literature ($-3.33 \times 10^{-8} \text{ m}^2 \text{ V}^{-1} \text{ s}^{-1}$; Chen *et al.*, 2001). EOF pushes the CD and its complexes to the

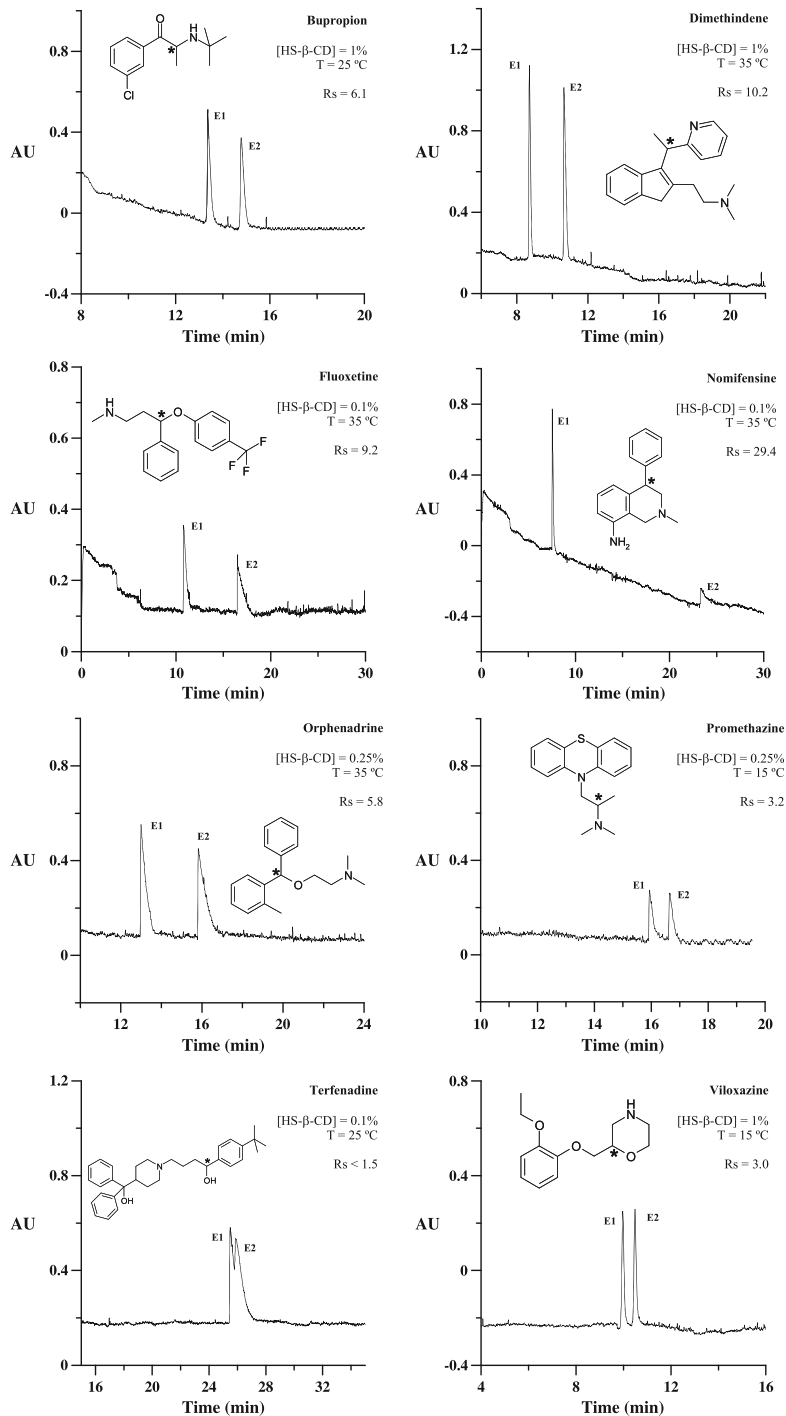


Figure 1. Electropherograms showing the chiral separation of each psychoactive drug, with the [CD] and temperature employed in each case. Other experimental conditions are: BGE, 30 mM phosphate buffer, pH 7.0; applied voltage, 15 kV.

detector, against their mobilities, whereas the free enantiomers migrate faster than the CD plug that is always inside it (an interesting feature; see below). The complexation equilibrium is shifted by the CD concentration and affects the effective mobility of the enantiomers, resulting in differences in the R_s and migration time values. For normal polarity, the enantiomer forming a more stable complex with HS- β -CD elutes second from the capillary.

The effect of HS- β -CD concentration and temperature on the enantiomeric resolution (R_s) was investigated. As can be expected, in all cases the increase in HS- β -CD concentration leads to longer analysis times and higher negative mobility of the enantiomers, owing to the negative charge of the formed complexes. In fact, for some drugs, the peak of the second enantiomer could not be seen after 50 min of voltage application. For all compounds R_s improved with higher CD concentrations. However, very different results were obtained for each compound, for example, the TER enantiomers were partially resolved ($R_s < 1.5$) for all the HS- β -CD concentrations assayed, while excellent resolution values ($R_s > 10$) were obtained for DIM, NMF and FLX at very low CD concentration. The increase in capillary temperature led to shorter analysis times whereas R_s increased for some compounds (e.g. NMF, FLX) and decreased for other ones (e.g. DIM, BUP). The different behaviors could be explained by the effects of temperature on peak efficiency, buffer viscosity or selector-selectand interactions (Martín-Biosca *et al.*, 2001).

Determination of interaction parameters for enantiomers

The commercial HS- β -CD used in the present study was a mixture mainly composed of 12-sulfated isomers with identical mobilities (Chen *et al.*, 2001; Rudaz *et al.*, 2004). For estimating the interaction parameters of enantiomers, we used the model describing CE enantioseparation with multi-CD systems proving that the mixture of HS- β -CDs behaves as only one CD (Dubský *et al.*, 2010). The model assumes that each individual analyte-CD interaction is fast and fully independent of other interactions; the analyte-CD ratio is 1:1 and the analyte concentration is low enough to not considerably change the concentration of free CDs. This provides an expression similar to the fundamental one introduced by Wren and Rowe (1992) for the multi HS- β -CD system:

$$\mu_i = \frac{\mu_i^0 + \mu_i^{\text{CD}} K'_i [\text{CD}]}{1 + K'_i [\text{CD}]} \quad (2)$$

where [CD] is the total concentration of HS- β -CD and K'_i and μ_i^{CD} are the overall apparent binding constants and the overall limit mobilities, respectively, defined as:

$$K'_i = \sum_1^q \chi^q K_i^q \quad (3)$$

$$\mu_i^{\text{CD}} = \frac{\sum_1^q \chi^q K_i^q \mu_i^q}{K'_i} \quad (4)$$

where χ^q is the molar fraction of the q th selector isomer in the mixture, K_i^q is the individual apparent complexation constant with the i th enantiomer ($i = 1$ or 2) and q th isomer of CD (Rudaz *et al.*, 2004; Dubský *et al.*, 2010), and μ_i^q is the individual mobility of the i th enantiomer- q th CD complex.

In PFT (Amini *et al.*, 1999a, 1999b), the effective electrophoretic mobility of the solute is the sum of its mobility within the plug (composed of the electrophoretic mobilities of the free and complexed solute) and outside the plug (in the BGE); in fact, apparent binding constants have been evaluated by varying the plug length (Amini and Westerlund, 1998; Amini *et al.*, 1999a, 1999b; Machour *et al.*, 2005; Ali *et al.*, 2003). This becomes unnecessary under the CFT $\mu_{\text{EOF}} > \mu_{\text{CD}}$ conditions used in this work, since the capillary is completely filled with the chiral selector and the enantiomers do not leave the CD plug during their migration. Thus, the extra PFT term, corresponding to mobility outside the plug, becomes zero in CFT and can be eliminated, simplifying the expression of the observed mobility. Consequently, in CFT equation (2) could be applied in order to evaluate K' (as in conventional CE).

On the other hand, in CFT (as in PFT), the change in the mobilities owing to differences in the buffer composition across the capillary during the separation process should be considered, which could provide possible variations of mobility during the separation (e.g. this justifies K' being named 'apparent'). However, results in the literature suggest that comparable mobilities are obtained in PFT and conventional CE (Amini *et al.*, 1999a, 1999b), which should be extrapolated to the intermediate CFT approach.

In order to estimate K' and μ_i^{CD} values, effective mobility of the enantiomers was fitted vs [CD] (in molar units on the basis of an average molar mass of 2360 g mol⁻¹ for a substitution degree of 12 sulfates mol⁻¹; Chen *et al.*, 2001) to equation (2). Nonlinear estimation was preferred instead of the most popular linear equations, owing to its expected higher robustness (Asensi-Bernardi *et al.*, 2010) and the possible lack of accuracy and precision of linear models owing to errors derived from variable transformation (Foulon *et al.*, 2004). The obtained fitted models have good correlation coefficients, $R^2 > 0.99$ in most of the cases, suggesting that equation (2) appropriately reflects the behavior of the compounds in the HS- β -CD system.

Two possible mechanisms or a combination of both can explain the differences in the effective mobilities of enantiomers in the presence of a chiral selector, which is the separation of enantiomers of a compound. The first one is related to the differences between the apparent binding constants of enantiomers (thermodynamic enantioselectivity $\alpha_i = K'_2/K'_1$). The second one is related to the differences in the overall limit mobilities of the complexes of the enantiomers (electrophoretic enantioselectivity ($\alpha_e = \mu_2^{\text{CD}}/\mu_1^{\text{CD}}$), or both of them (Dubský *et al.*, 2010). In this paper thermodynamic and electrophoretic enantioselectivity parameters were also estimated. Combining equations (3) and (4) a new relation between these enantioselectivity values, not previously reported in quantitative form, arises:

$$\alpha_e = \frac{\mu_2^{\text{CD}}}{\mu_1^{\text{CD}}} = \frac{\sum_1^q \chi^q K_2^q \mu_2^q}{\sum_1^q \chi^q K_1^q \mu_1^q} \frac{1}{\alpha_i} \quad (5)$$

Table 1 shows the estimated parameters of psychoactive drugs at three working temperatures. The highest binding constants were obtained for TER, but with very low values of enantioselectivity (thermodynamic and electrophoretic). The large size of this molecule may prevent its inclusion into the hydrophobic cavity of the cyclodextrin, where the enantiorecognition occurs,

Table 1. Interaction parameters for the enantiomers of the eight studied chiral drugs at three working temperatures, employing nonlinear fitting of equation (2). Estimated optimum [CD] according to equations (6) and (7). E_1 and E_2 correspond, respectively, to the first and second eluted enantiomer

Drug	Temperature (°C)	n	E_1	n	E_2	R_S range	K_1 (M^{-1})	K_2 (M^{-1})	$\alpha_t = K_2/K_1$	$\mu_1^{CD} \times 10^8$ ($m^2 V^{-1} s^{-1}$)	$\mu_2^{CD} \times 10^8$ ($m^2 V^{-1} s^{-1}$)	$\alpha_e = \mu_2^{CD}/\mu_1^{CD}$	[CD] _{opt} (% m/V), equation (6)	[CD] _{opt} (% m/V), equation (7)
BUP	15	7	7	1.8–8.8	670 ± 70	790 ± 70	1.2	-2.57 ± 0.16	-2.70 ± 0.13	1.1	0.49	0.32		
	25	7	7	1.5–6.1	630 ± 60	740 ± 70	1.2	-3.36 ± 0.19	-3.49 ± 0.17	1.0	0.48	0.35		
	35	7	7	1.3–4.1	620 ± 70	710 ± 70	1.2	-3.9 ± 0.3	-4.1 ± 0.2	1.0	0.59	0.36		
DIM	15	7	7	4.0–21.5	600 ± 100	980 ± 120	1.6	-2.6 ± 0.3	-2.92 ± 0.17	1.1	0.43	0.31		
	25	7	7	3.2–16.1	570 ± 70	860 ± 70	1.5	-3.2 ± 0.2	-3.58 ± 0.15	1.1	0.49	0.34		
	35	8	7	2.8–10.2	460 ± 50	660 ± 100	1.2	-4.1 ± 0.3	-4.5 ± 0.4	1.1	0.62	0.43		
FLX	15	5	4	5.1–5.4	6070 ± 100	14,000 ± 200	2.3	-3.282 ± 0.016	-3.371 ± 0.011	1.03	0.03	0.03		
	25	5	4	4.8–10.9	4490 ± 60	11,300 ± 1200	2.5	-4.25 ± 0.02	-4.18 ± 0.11	0.98	0.03	0.03		
	35	5	4	5.1–11.1	4500 ± 1200	16,000 ± 4000	3.6	-4.5 ± 0.4	-4.1 ± 0.2	0.91	0.02	0.03		
NMF	15	6	4	11.6–14.9	2800 ± 800	16,000 ± 35,000	5.7	-3.1 ± 0.4	-4 ± 2	1.3	0.04	0.04		
	25	6	3	11.0–19.9	1600 ± 90	11,800	7.4	-4.04 ± 0.09	-4.3	1.1	0.06	0.05		
	35	6	4	29.4–34.1	1470 ± 110	10,700 ± 600	7.3	-4.74 ± 0.16	-5.06 ± 0.08	1.1	0.06	0.06		
ORP	15	5	4	4.5–5.2	3770 ± 80	6600 ± 200	1.8	-3.28 ± 0.02	-3.34 ± 0.04	1.0	0.05	0.05		
	25	5	4	4.5–6.3	3300 ± 200	4770 ± 120	1.4	-4.09 ± 0.10	-4.32 ± 0.05	1.1	0.07	0.06		
	35	5	4	3.2–5.8	2900 ± 200	4930 ± 90	1.7	-4.74 ± 0.17	-4.43 ± 0.04	0.9	0.05	0.06		
PRO	15	6	6	1.7–6.4	2070 ± 130	2280 ± 150	1.1	-3.25 ± 0.09	-3.25 ± 0.08	1.0	0.11	0.11		
	25	5	5	1.4–2.7	1870 ± 140	1990 ± 150	1.1	-4.00 ± 0.11	-4.01 ± 0.11	1.0	0.13	0.13		
	35	4	4	1.3	2000 ± 200	2100 ± 200	1.1	-4.3 ± 0.2	-4.3 ± 0.2	1.0	0.12	0.12		
TER	15	4	4	< 1.5	31,000 ± 4000	34,000 ± 4000	1.1	-3.02 ± 0.04	-3.02 ± 0.04	1.0	0.01	0.01		
	25	4	4	< 1.5	20,000 ± 500	21,000 ± 500	1.1	-3.890 ± 0.017	-3.890 ± 0.013	1.0	0.01	0.01		
	35	4	4	< 1.5	17,700 ± 600	18,800 ± 300	1.1	-4.69 ± 0.02	-4.68 ± 0.02	1.0	0.01	0.01		
VLX	15	8	8	0.9–2.6	290 ± 30	300 ± 30	1.0	-1.44 ± 0.12	-1.69 ± 0.13	1.2	—	0.80		
	25	8	8	1.6–2.8	300 ± 50	310 ± 50	1.0	-1.6 ± 0.2	-1.9 ± 0.2	1.2	—	0.77		
	35	8	8	1.2–1.9	310 ± 40	310 ± 40	1.0	-1.7 ± 0.2	-2.1 ± 0.2	1.2	—	0.76		

n , E_1 , Number of data pairs (μ_i vs [CD]) employed for each nonlinear fitting; $n < 8$ indicates that at higher [CD] the enantiomers did not reach the detector in a 50 min run. R_S range, interval of resolution values obtained at different CD concentrations (see text for details). K_i , Binding constants ± standard error of estimates. α_t , Thermodynamic enantioselectivity. μ_i^{CD} , Complex limit mobility. α_e , Electrophoretic enantioselectivity. BUP, Bupropion hydrochloride; DIM, dimethindene maleate; FLX, fluoxetine hydrochloride; NMF, nomifensine maleate; ORP, orphenadrine hydrochloride; PRO, promethazine hydrochloride; TER, terfenadine; VLX, viloxazine.

also explaining the low R_s values obtained ($R_s < 1.5$). On the other hand, maximum α_t values were achieved for NMF (at 25°C), followed by FLX (at 35°C), which also exhibit relatively high K' values.

As can be observed in Table 1, except for VLX, α_t values were higher than those for α_e , which suggests that the thermodynamic mechanism plays a more important role in the enantiomeric separation of the studied compounds with the commercial HS- β -CD used in the present study. However, VLX is an example of how good enantioseparations ($R_s > 2$) can be achieved mainly owing to differences in overall limit mobilities of enantiomers ($\alpha_e = 1.2$), although this is a mixed effect [equation (5)].

Additionally, as can be seen in Table 1, the values of the binding constants decreased with increasing temperature, as a general trend. Exceptions to this trend could be attributed to the combination of low K_i -values and small differences in K_i and the K_i uncertainties. For compounds with lower affinity for the CD (BUP, DIM and VLX), minor differences were found at the three temperatures studied.

On the other hand, enantioselectivity values, α_t and α_e , practically do not change with temperature except for NMF and FLX. Precisely for these compounds, the quantitative relationship expected from equation (5) can be observed; α_t (as R_s) increases with the temperature, while α_e shows the opposite trend.

Although we have not found literature binding data for the analytes studied in this work, some reported values are available for other basic compounds (Vaccher *et al.*, 2005; Rudaz *et al.*, 2004; Foulon *et al.*, 2002; Lipka *et al.*, 2007; Danel *et al.*, 2005). The K' values of enantiomer-HS- β -CD in Table 1 are similar to or higher than those in the literature, confirming the extraordinarily good enantioseparation capabilities of this commercial mixture cyclodextrin.

The optimum [CD] for each separation, defined as the [CD] that provides the highest mobility difference between enantiomers (maximum $\Delta\mu$), can be estimated from the overall apparent binding constants in Table 1 by means of equation (6) (Dubský *et al.*, 2010).

$$[\text{CD}]_{\text{opt}} = -\frac{\Delta\mu \pm \sqrt{\Delta\mu^2 - \frac{1}{K^1} \Delta\mu K \Delta\mu K}}{\Delta\mu K} \quad (6)$$

where $\Delta\mu = \mu_2^{r,\text{CD}} - \mu_1^{r,\text{CD}}$ (where $\mu_i^{r,\text{CD}} = \mu_i^{\text{CD}} - \mu_i^0$), $\Delta\mu K = \mu_2^{r,\text{CD}} K'_2 - \mu_1^{r,\text{CD}} K'_1$, $\Delta\mu K = \mu_2^{r,\text{CD}} K'_1 - \mu_1^{r,\text{CD}} K'_2$, and $K^1 = K'_1 K'_2$. Where the thermodynamic mechanism is responsible for separation and considering the limit mobilities of two enantiomers identical ($\mu_1^{\text{CD}} = \mu_2^{\text{CD}}$), equation (6) could be simplified to obtain the simplest equation introduced by Wren and Rowe (1992):

$$[\text{CD}]_{\text{opt}} = \frac{1}{\sqrt{K'_1 \cdot K'_2}} \quad (7)$$

The estimated $[\text{CD}]_{\text{opt}}$ values using both equations (6) and (7) are also included in Table 1. In general, values obtained with both equations were similar, confirming a greater contribution of the thermodynamic mechanism in the enantioseparation of the drugs studied. The compounds that showed more differences (BUP, DIM and VLX) were those that interact more weakly with the cyclodextrin, particularly the last one, for which equation (6) results in negative solutions indicating that no optimum HS- β -CD concentration exists. This fact also confirms that for this compound the

differences between limit mobilities of two enantiomers are responsible for the enantioseparation.

Conclusions

HS- β -CD has proved to be an effective chiral selector for the separation of enantiomers of four antihistamines and four antidepressants by CE-CFT, since good resolutions have been achieved in most of the cases ($R_s > 1.5$ for seven of the studied compounds). The overall apparent binding constants, estimated by nonlinear fitting, indicate that these drugs interact strongly with the cyclodextrin. The thermodynamic mechanism plays a more important role in the enantiomeric separation, with high thermodynamic enantioselectivity particularly in the cases of nomifensine, fluoxetine and orphenadrine. Only in the case of viloxazine ($\alpha_t = 1$, $\alpha_e = 1.2$) is the electrophoretic enantioselective mechanism probably responsible for enantioseparation, providing also a good resolution. Matched with literature data for other basic compounds, comparable or higher binding constant and comparable or better resolution were observed with the compounds studied in this work, suggesting the adequacy of the CFT approach.

CFT is proposed as an advantageous alternative to conventional CE and PFT for the study of the interaction between drugs and chiral selectors. It has the advantage of PFT of reduced cost compared with conventional CE, but allows use of the simple model of CE, when the mobility of electroosmotic flow is larger than mobility of CD, thus the enantiomers do not exit the chiral selector plug during the separation. As an averaged estimation, the amount of CD solution needed for each injection is 2 mL in conventional CE and 5 μL in CFT. Assuming a cost of CD solutions of $\sim 0.5 \text{ mL}^{-1}$, the cost of each injection will be close to $\text{€}1$ for conventional CE, and only $\text{€}0.0025$ for CFT (saving 99.7%).

Along with its interest as separation mechanism key, the estimation of affinity constants characterizing the interactions of molecules with CDs is usual in biomedical processes, where CDs participate as macromolecular hosts, for explaining inclusion phenomena or encapsulation within CD nanocavities, useful for example in controlled release. However, in both research areas, there are still few chiral studies. The easy and economic method used here should promote the inclusion of the chiral component in these fields.

Acknowledgments

The authors acknowledge the University of Valencia (UV-INV-AE112-66280) for the financial support. L. Asensi-Bernardi acknowledges the Spanish Ministry of Education for her FPU pre-doctoral research grant (reference AP2010-1984). The authors declare no conflict of interest.

References

- Al Zazzam KM, Saad B and Aboul-Enein HY. Determination of the binding constants of modafinil enantiomers with sulfated β -cyclodextrin chiral selector by capillary electrophoresis using three different linear plotting models. *Electrophoresis* 2010; **31**: 2957–2963.
- Ali I, Gupta VK and Aboul-Enein HY. Chiral resolution of some environmental pollutants by capillary electrophoresis. *Electrophoresis* 2003; **24**: 1360–1374.
- Amini A and Westerlund D. Evaluation of association constants between drug enantiomers and human $\alpha 1$ -acid glycoprotein by applying a partial-filling technique in affinity capillary electrophoresis. *Analytical Chemistry* 1998; **70**: 1425–1430.

- Amini A, Merclin N, Bastami S and Westerlund D. Determination of association constants between enantiomers of orciprenaline and methyl- β -cyclodextrin as chiral selector by capillary zone electrophoresis using a partial filling technique. *Electrophoresis* 1999a; **20**: 180–188.
- Amini A, Paulsen-Sörman U and Westerlund D. Principle and applications of the partial filling technique in capillary electrophoresis. *Chromatographia* 1999b; **50**: 497–506.
- Asensi-Bernardi L, Martín-Biosca Y, Villanueva-Camañas RM, Medina-Hernández MJ and Sagrado S. Evaluation of enantioselective binding of fluoxetine to human serum albumin by ultrafiltration and CE – experimental design and quality considerations. *Electrophoresis* 2010; **31**: 3268–3280.
- Bonato PS, Jabor VAP, Paia FO and Lanchote VL. Chiral capillary electrophoretic separation of selected drugs and metabolites using sulfated β -cyclodextrin. *Journal of Liquid Chromatography and Related Technologies* 2003; **24**: 1115–1131.
- Castro-Puyana M, García MA and Marina ML. Enantiomeric separation of bupropion enantiomers by electrokinetic chromatography: quantitative analysis in pharmaceutical formulations. *Journal of Chromatography B* 2008; **875**: 260–265.
- Chankvetadze B. Enantioseparations by using capillary electrophoretic techniques. The story of 20 and a few more years. *Journal of Chromatography, A* 2007; **1168**: 45–70.
- Chankvetadze B and Blaschke G. Enantioseparations in capillary electromigration techniques: recent developments and future trends. *Journal of Chromatography, A* 2001; **906**: 309–363.
- Chankvetadze B, Endresz G and Blaschke G. About some aspects of the use of charged cyclodextrins for capillary electrophoresis enantio-separation. *Electrophoresis* 1994; **15**: 804–807.
- Chen FTA, Shen G and Evangelista RA. Characterization of highly sulfated cyclodextrins. *Journal of Chromatography, A* 2001; **924**: 523–532.
- Chen KH, Lin CE, Liao WS, Lin WY and Hsiao YY. Separation and migration behavior of structurally related phenothiazines in cyclodextrin-modified capillary zone electrophoresis. *Journal of Chromatography, A* 2002; **979**: 399–408.
- Chen Z and Weber SG. Determination of binding constants by affinity capillary electrophoresis, electrospray ionization mass spectrometry and phase-distribution methods. *Trends in Analytical Chemistry* 2008; **27**: 738–748.
- Danel C, Lipka E, Bonte JP, Goossens JF, Vaccher C and Foulon C. Enantioseparation of chiral N-imidazole derivatives by electrokinetic chromatography using highly sulfated cyclodextrins: mechanism of enantioselective recognition. *Electrophoresis* 2005; **26**: 3824–3832.
- Dubský P, Svobodová J, Tesárová E and Gaš B. Enhanced selectivity in CZE multi-chiral selector enantioseparation systems: proposed separation mechanism. *Electrophoresis* 2010; **31**: 1435–1441.
- Foulon C, Goossens JF, Fourmaintraux E, Bonte JP and Vaccher C. Chiral capillary electrophoretic determination of the enantiomeric purity of tetrahydronaphthalenic derivatives, melatoninergic ligands, using highly sulfated β -cyclodextrins. *Electrophoresis* 2002; **23**: 1121–1128.
- Foulon C, Danel C, Vaccher MP, Bonte JP, Vaccher C and Goossens JF. Chiral separation of N-imidazole derivatives, aromatase inhibitors, by cyclodextrin-capillary zone electrophoresis. Mechanism of enantioselective recognition. *Electrophoresis* 2004; **25**: 2735–2744.
- Inoue T and Chang JP. Chiral separation of fluoxetine and its analogs with charged cyclodextrins by capillary electrophoresis. *Journal of Liquid Chromatography and Related Technologies* 2003; **26**: 2351–2367.
- Li S and Vigh G. Single-isomer sulfated α -cyclodextrins for capillary electrophoresis: hexakis (2,3-di-O-methyl-6-O-sulfo)- α -cyclodextrin, synthesis, analytical characterization and initial screening tests. *Electrophoresis* 2004; **25**: 2657–2670.
- Liao WS, Lin CH, Chen CY, Kuo CM, Liu YC, Wu JC and Lin CE. Enantioseparation of phenothiazines in CD-modified CZE using single isomer sulfated CD as a chiral selector. *Electrophoresis* 2007; **28**: 3922–3929.
- Lipka E, Danel C, Orhan H, Bonte JP and Vaccher C. Chiral resolution of melatoninergic ligands by EKC using highly sulfated CDs. *Electrophoresis* 2007; **28**: 3915–3921.
- Machour N, Place J, Tron F, Charlonnet R, Morin C, Desbene A and Desbene PL. Analysis of virtual two-dimensional gels based upon affinity capillary electrophoresis hyperphenated to ion trap–mass spectrometry. *Electrophoresis* 2005; **26**: 1466–1475.
- Martin-Biosca Y, García-Ruiz C and Marina ML. Enantiomeric separation of chiral phenoxy acid herbicides by electrokinetic chromatography. Application to the determination of analyte-selector apparent binding constants for enantiomers. *Electrophoresis* 2001; **22**: 3216–3225.
- Matsunaga H, Tanimoto T and Haginaka J. Separation of basic drug enantiomers by capillary electrophoresis using methylated glucuronol glucosyl β -cyclodextrin as a chiral selector. *Journal of Separation Science* 2002; **25**: 1175–1182.
- Matthijs N, Perrin C, Maftouh M, Massart DL and Vander Heyden Y. Knowledge-based system for method development of chiral separations with capillary electrophoresis using highly-sulphated cyclodextrins. *Journal of Pharmaceutical and Biomedical Analysis* 2002; **27**: 515–529.
- Pang N, Zhang Z, Bai Y and Liu H. A study of the interaction between enantiomers of zolmitriptan and hydroxypropyl-beta-cyclodextrin by capillary electrophoresis. *Analytical and Bioanalytical Chemistry* 2009; **393**: 313–320.
- Perrin C, Vander-Heyden Y, Maftouh M and Massart DL. Rapid screening for chiral separations by short-end injection capillary electrophoresis using highly sulfated cyclodextrins as chiral selectors. *Electrophoresis* 2001; **22**: 3203–3215.
- Rudaz S, Callieri E, Geiser L, Cherkaoui S, Prat J and Veuthey JL. Infinite enantiomeric resolution of basic compounds using highly sulfated cyclodextrin as chiral selector in capillary electrophoresis. *Electrophoresis* 2003; **24**: 2633–2641.
- Rudaz S, Le Saux T, Prat J, Gareil P and Veuthey JL. Ultrashort partial filling technique in capillary electrophoresis for infinite resolution of tramadol enantiomers and its metabolites with highly sulfated cyclodextrins. *Electrophoresis* 2004; **25**: 2761–2771.
- Scriba GKE. Fundamental aspects of chiral electromigration techniques and application in pharmaceutical and biomedical analysis. *Journal of Pharmaceutical and Biomedical Analysis* 2011; **55**: 688–701.
- Vaccher MP, Lipka E, Bonte JP, Foulon C, Goossens JF and Vaccher C. Enantiomeric analysis of baclofen analogs by capillary zone electrophoresis, using highly sulfated cyclodextrins: inclusion ionization constant pK_a determination. *Electrophoresis* 2005; **26**: 2974–2983.
- Van Eckhaut A, Detaevier MR, Crommen J and Michotte Y. Differential effects of organic modifiers on the enantioseparation of dimetindene maleate with carboxymethyl- β -cyclodextrin in capillary electrophoresis. *Journal of Separation Science* 2004; **27**: 21–27.
- Verleysen K, Bosch TV and Sandra P. Comparison of highly sulfated α -, β -, and γ -cyclodextrins and 18-crown-6-tetracarboxylic acid for the enantiomeric separation of some amino acids and derivatives by capillary electrophoresis. *Electrophoresis* 1999; **20**: 2650–2655.
- Vescina MC, Fermier AM and Guo Y. Comparing cyclodextrin derivatives as chiral selectors for enantiomeric separation in capillary electrophoresis. *Journal of Chromatography, A* 2002; **973**: 187–196.
- Wei Y, Li J, Zhu C, Hao A and Zhao M. 2-O-(2-Hydroxybutyl)- β -cyclodextrin as a chiral selector for the capillary electrophoretic separation of chiral drugs. *Analytical Science* 2005; **21**: 959–962.
- Wren SAC and Rowe RC. Theoretical aspects of chiral separation in capillary electrophoresis. I. Initial evaluation of a model. *Journal of Chromatography, A* 1992; **603**: 235–241.
- Yang GS, Chen DM, Yang Y, Tang B, Gao JJ, Aboul-Enein HY and Koppenhoefer B. Enantioseparation of some clinically used drugs by capillary electrophoresis using sulfated β -cyclodextrin as a chiral selector. *Chromatographia* 2005; **62**: 441–445.

Paper II

**Modeling the chiral resolution ability of highly sulfated β -cyclodextrin
for basic compounds in electrokinetic chromatography**

**L. Asensi-Bernardi, L. Escuder-Gilabert, Y. Martín-Biosca, M.J. Medina-
Hernández and S. Sagrado**

Journal of Chromatography A 2013, 1308, 152-160



Modeling the chiral resolution ability of highly sulfated β -cyclodextrin for basic compounds in electrokinetic chromatography

L. Asensi-Bernardi^a, L. Escuder-Gilabert^a, Y. Martín-Biosca^a, M.J. Medina-Hernández^a, S. Sagrado^{a,b,*}

^a Departamento de Química Analítica, Universidad de Valencia, Burjassot, Valencia, Spain

^b Centro Interuniversitario de Reconocimiento Molecular y Desarrollo Tecnológico (IDM), Unidad Mixta Universidad Politécnica de Valencia-Universidad de Valencia, Spain

ARTICLE INFO

Article history:

Received 18 June 2013

Received in revised form 31 July 2013

Accepted 1 August 2013

Available online 6 August 2013

Keywords:

Electrokinetic chromatography

Highly sulfated β -cyclodextrin

Enantioresolution

Quantitative structure–property

relationships

Partial least squares

ABSTRACT

Despite the fact that extensive research in the field of enantioseparations by capillary electrophoresis has been carried out, it is difficult to predict whether a concrete chiral selector would be useful for the separation of a racemic compound. Hence, several experimental effort is necessary to test the abilities of individual chiral selectors, usually by trial and error procedures. Thus, the enantioseparation of a new racemate becomes a time- and money-consuming task. In this work, the ability of highly sulfated β -cyclodextrin (HS- β -CD) as chiral selector in electrokinetic chromatography (EKC) is modeled for the first time, using exclusively directly-available structural data of forty compounds (structurally unrelated basic drugs and pesticides). A discriminant partial least squares (PLS)-based quantitative structure–property relationship (QSPR) approach is simplified, resulting in a consistent, predictive and descriptive model. It is converted into an explicit equation able to predict the enantioresolution level (R_s) of new compounds, from four structure properties available in an on-line open database: logarithm of octanol–water partition coefficient estimated at pH 7.4 ($\lg D$), polar surface area (PSA), number of hydrogen bond donors (HBD) and acceptors (HBA). For the cases in which the model predicts good R_s only in concrete experimental conditions, a Box–Behnken experimental design is proposed for the fast PLS-based optimization of the most influential experimental variables: cyclodextrin concentration, temperature and pH.

© 2013 Elsevier B.V. All rights reserved.

1. Introduction

In the last years, chirality has become interesting for different industries related to chemistry, mainly the pharmaceutical and agrochemical ones [1]. Therefore, analytical methods for the determination of single enantiomers in different industrial and environmental samples are needed. The most often applied methods in chiral analysis are chromatographic and electrophoretic techniques. In the last ones, chiral selectors are usually included in the background electrolyte, in the so-called electrokinetic chromatography (EKC) mode [2].

Among the different chiral selectors used in EKC, cyclodextrins (CDs) are the most employed due to their good enantioselectivity, good water solubility, UV transparency, and the wide assortment of different neutral, cationic and anionic CDs with

different functional groups that can be employed [3]. Their structure, with a hydrophilic external surface and a hydrophobic cavity, allows the formation of diastereomeric complexes with a pair of enantiomers, which migrate at different velocities through the capillary allowing the enantioseparation. It has been reported that maximum enantioselectivities are achieved when analytes and CDs have opposite mobilities [4,5].

Highly sulfated β -cyclodextrin (HS- β -CD) is an anionic cyclodextrin with an average content of 12 sulfate groups per molecule [6]. Its high density of negative charge makes it an excellent chiral selector for neutral and positively charged compounds. However, in spite of its mainly good applicability for chiral separations, it is still difficult to predict its level of enantioselectivity (R_s) for a concrete compound.

In this context, mathematical models could help to save experimental effort, money and time, if previous R_s -related experimental information is available for a set of molecules. A regression-based quantitative structure–property relationship (QSPR) implies modeling a \mathbf{y} - \mathbf{X} relationship, where the vector \mathbf{y} represents a target property (response or dependent variable; e.g. R_s -related experimental values) and \mathbf{X} represents the matrix of descriptor variables

* Corresponding author at: Departamento de Química Analítica, Facultad de Farmacia, Universitat de Valencia, C/ Vicent Andrés Estellés s/n, E-46100 Burjassot, Valencia, Spain. Tel.: +34 963544878; fax: +34 963544953.

E-mail address: sagrado@uv.es (S. Sagrado).

(predictor or independent variables; e.g. structure information) when related by a particular regression algorithm, e.g. partial least squares (PLS). The \mathbf{y} - \mathbf{X} relationship can be expressed by their regression coefficients, \mathbf{b} [7,8]. Simultaneously, the predictive ability of the model can be assessed by analyzing the explained \mathbf{y} -variance (EV) and its cross-validated value (EV_{CV}), while the \mathbf{b} -coefficients can provide the descriptive ability if combined with uncertainty estimation, $\mathbf{b} \pm \mathbf{U}(\mathbf{b})$ (jack-knifing, as a part of the cross-validation process [7,9]). Thus, cross-validation becomes basic to assure reliability of future \mathbf{y} -estimations for new compounds [7,10].

Different strategies have been used in the literature for developing QSPR for modeling enantioresolution-related information in EKC [11–14]. In two of these works the response variable was the relative migration times to that of 6-aminonicotinic acid of 12 aromatic amino acids and alkyl esters of 2-phenylglycine, using (+)-18-crown-6-tetracarboxylic acid as chiral selector [11,12]. In the work by Beck et al. [13], enantiomers mobility differences for 13 β -blockers and tryptophan derivatives using sulfated polysaccharides as chiral selectors are used as response variable. At our knowledge, there is only one work that directly models the R_s parameter as a function of structural information (molecular mechanics/docking energy descriptors derived from a combination of several programs) for 12 structurally related triadimenol analogs using hydroxypropyl- γ -CD as chiral selector [14].

In this work, the ability of using HS- β -CD as chiral selector for enantioseparation in EKC of structurally unrelated basic compounds is modeled for the first time using exclusively directly-available structural data. A QSPR approach is simplified using categorized R_s -structure parameters of forty compounds (drugs and pesticides), based on discriminant PLS on one single response (DPLS1). The model is re-expressed for simplicity in the practical format ' $R_s = f(\text{selected parameters})$ '. Latent structure (consistent model complexity) as well as predictive and descriptive power criteria are incorporated to the decision making simplification process.

One particular aim of this work is to explore non-complex (clear for non-expert users) and easily available approaches. A single software/regression algorithm (PLS) and a single on-line (open) database (structure parameters) are used. The obtained R_s -explicit equation is applied to estimate the chiral resolution of bupivacaine. Further, a multivariate optimization including the standard Box-Behnken experimental design, followed by PLS2 on two response variables: R_s and analysis time, is used to derive again explicit equations for these two variables as a function of the methodological EKC variables: CD concentration, temperature and electrophoretic buffer pH. These equations are used to estimate the convenient separation conditions of bupivacaine.

2. Materials and methods

To facilitate the understanding of the statistical aspects, a complete list of abbreviations (including variables) has been included in Appendix A.

2.1. Instrumentation

A Beckman P/ACE MDQ Capillary Electrophoresis System equipped with a DAD (Beckman Coulter, Fullerton, CA, USA), and 32Karat software version 8.0 was used throughout. A 50 μm inner diameter (i.d.) fused-silica capillary with total and effective lengths of 60.2 and 50 cm, respectively, was employed (Beckman Coulter, Fullerton, CA, USA). Electrophoretic solutions and samples were filtered through 0.45 μm pore size nylon membranes (Micron Separation, Westboro, MA, USA) and degassed in an ultrasonic bath (JP Selecta, Barcelona, Spain) prior to use.

2.2. Chemicals and solutions

All reagents were of analytical grade. $\text{NaH}_2\text{PO}_4 \cdot 2\text{H}_2\text{O}$ was from Fluka (Buchs, Switzerland); HS- β -CD (20% m/v, average number of 12 sulfate groups per molecule) aqueous solution was purchased from Beckman Coulter (Fullerton, CA, USA); Ultra Clear TWF UV deionized water (SG Water, Barsbüttel, Germany) was used to prepare solutions.

Alprenolol hydrochloride, labetalol hydrochloride, pindolol, sotalol hydrochloride, etopropazine hydrochloride, metotrimeprazine maleate, trimeprazine hemi(+)-tartrate, brompheniramine maleate, carbinoxamine maleate, clemastine fumarate, chlorpheniramine maleate, chlorcyclizine hydrochloride, doxylamine succinate, hydroxyzine hydrochloride, and phenindamine tartrate were from Sigma (St. Louis, MO, USA). All the rest of drugs tested were kindly donated by several pharmaceutical laboratories: oxprenolol hydrochloride and metoprolol tartrate by Ciba Geigy (Barcelona, Spain); propranolol chlorhydrate by ICI Farma (Madrid, Spain); carteolol hydrochloride by Miquel-Otsuka (Barcelona, Spain); timolol maleate by Merck Sharp & Dohme (Madrid, Spain); acebutolol hydrochloride by Italfarmaco (Madrid, Spain); atenolol by Zeneca Farma (Madrid, Spain); celiprolol hydrochloride by Rhone-Poulenc Rorer (Madrid, Spain) and nadolol by Squibb (Barcelona, Spain). All racemic pesticides (benalaxyl, cyproconazole, hexaconazole, imazalil, myclobutanil and penconazole) were from Dr. Ehrenstoffer (Augsburg, Germany).

Background electrolyte (BGE) containing 50 mM phosphate at pH 7.0 was obtained by dissolving the appropriate amount of $\text{NaH}_2\text{PO}_4 \cdot 2\text{H}_2\text{O}$ in water and adjusting the pH with 1 M NaOH. 200 μM solutions of the racemic drugs and pesticides were prepared in BGE to be injected into the electrophoretic system.

2.3. Methodology for the chiral separation of compounds by EKC

Some of the categorical R_s data included in Table 1 were taken from previously published enantioseparations: fluoxetine (No 28 from Table 1) [15,16], catechin (No 35) [17], verapamil (No 36) [18] and several antihistamines and antidepressants (No 6, 9, 11, 14 and 25–28) [19]. For these compounds full resolution of enantiomers was obtained using 1% m/v HS- β -CD or lower concentrations. All the experiments were performed using phosphate buffer in a pH range of 7.0–8.8 and separation temperatures of 25–30 °C.

In order to obtain information about the enantioresolution of all the other compounds listed in Table 1 (No 1–5, 7, 8, 10, 12, 13, 15–24, 29–34 and 37–40) a screening EKC procedure was carried out in the following experimental conditions: BGE, 50 mM phosphate buffer at pH 7.0; capillary temperature, 25 °C; voltage, 20 kV (normal polarity). Previously to the compound injection, the capillary was completely filled with a 1% m/v HS- β -CD solution prepared in the BGE, by rinsing it at 10 psi for 1 min. In the cases with strong interaction with the HS- β -CD [19], no peaks were found with these conditions, so the experience was repeated using a 0.25% m/v HS- β -CD solution.

2.4. Software for calculations

The Unscrambler® v.9.2 multivariate analysis software version [20] is used for all calculations, based on principal component analysis (PCA) and PLS models. Two automatic default features of the software are used: (i) significant regression coefficients 'marked' when their uncertainty limits, i.e. scaled $\mathbf{b} \pm \mathbf{U}(\mathbf{b})$, do not cross the "0" axis and (ii) selected number of principal components (PCs) or latent variables (LVs) of the models (k), which is initially proposed by the software (k_s). Explicit equations, $\mathbf{y} = \mathbf{b}\mathbf{X}$, are obtained using de-scaled (raw) \mathbf{b} -coefficients to be multiplied

Table 1
Data. Compounds are identified by name, Chemspider identification number (ID) and numbered order (No). Variables are identified by a code, y = categorized Rs and x1–x15 for the abbreviated parameter name (see Section 2 for details). Note that x4, x6, x8 and x15 are non-continuous variables.

Name	ID	Var. ID	Rs	y	x1 lgP	x2 lgD	x3 PSA	x4 HBD	x5 HBA	x6 POL	x7 MR	x8 MIV ^b	x9 MSA	x10 WV ^b	x11 DE	x12 OEC	x13 MM	x14 MA	x15 RB	a
Brompheniramine	6573	1	2	3.2	1.3	16.1	0	2	33.1	83.6	25.22	432.6	265.1	47.7	8.6	319.2	78.7	5	(8)	
Carbinoxamine	2466	2	2	2.7	1.4	25.4	0	3	32.7	82.6	25.44	444.3	269.7	9.2	9.2	290.1	79.5	6	(9)	
Clemastine	25129	3	2	5.3	2.7	12.5	0	2	39.8	100.4	31.33	547.9	331.1	79.1	9.1	343.9	93.0	6	(1)	
Chlorcyclizine	2609	4	2	3.2	2.9	6.5	0	2	35.2	88.7	26.27	460.8	284.0	57.7	8.5	300.8	81.3	3	(6)	
Chlorpheniramine	2624	5	2	3.0	1.0	16.1	0	2	32.0	80.8	24.80	428.0	260.7	48.6	8.6	274.8	77.5	5	(7)	
Dimetindene	20541	6	2	3.9	1.7	16.1	0	2	36.6	92.2	27.44	483.5	294.5	67.4	8.2	292.4	89.6	5	(8)	
Doxylamine	3050	7	2	2.3	1.1	25.4	0	3	32.5	81.9	25.90	463.9	273.2	58.4	9.2	270.2	82.6	6	(9)	
Hydroxyzine	3531	8	2	2.3	2.3	35.9	1	4	42.0	105.9	31.71	579.6	352.8	68.1	8.5	374.0	105.1	9	(8)	
Orphenadrine	4440	9	2	3.3	2.0	12.5	0	2	33.4	84.4	26.55	467.0	277.2	58.2	9.0	269.0	80.2	6	(9)	
Phenindamine	10817	10	2	3.8	2.7	3.2	0	1	32.9	83.1	22.70	399.2	253.3	61.3	8.3	261.3	78.5	1	(9)	
Terfenadine	5212	11	0	5.6	3.6	43.7	2	3	57.2	144.3	43.35	797.9	483.9	152.2	8.7	471.7	133.6	11	(9)	
Methotrimiprazine	65239	12	0	4.9	3.0	41.0	0	3	39.3	99.1	29.18	518.6	314.0	78.4	7.8	328.5	86.7	5	(9)	
Ethopropazine	109488	13	2	5.9	3.6	31.8	0	2	38.5	97.1	28.43	500.4	305.1	83.7	8.2	312.4	86.9	5	(9)	
Promethazine	4758	14	2	4.9	3.4	31.8	0	2	34.8	87.8	25.13	439.3	271.0	75.6	8.2	284.4	82.3	3	(6)	
Trimetopazine	5373	15	2	5.0	3.1	31.8	0	2	36.7	92.5	26.78	469.4	287.7	73.8	7.8	298.4	80.2	4	(6)	
Acebutolol	1901	16	0	1.8	-0.3	87.7	3	6	37.5	94.7	30.07	559.9	332.1	52.9	8.8	336.4	108.8	10	(9)	
Atenolol	2162	17	0	0.3	-1.8	84.6	4	5	29.4	74.2	23.66	440.4	261.3	38.1	8.8	266.3	87.6	8	(9)	
Carteolol	2485	18	0	1.3	-0.7	70.6	3	5	32.3	81.4	25.86	482.8	284.7	52.1	8.8	292.4	89.4	6	(9)	
Timolol	31013	19	0	1.3	-0.6	107.9	2	7	32.6	82.2	25.85	498.0	292.1	54.9	8.8	316.4	85.4	7	(9)	
Metoprolol	4027	20	1	1.6	-0.5	50.7	2	4	30.6	77.1	25.87	474.7	274.2	39.7	8.8	267.4	91.6	10	(9)	
Propranolol	4777	21	1	2.9	0.8	41.5	2	3	31.3	78.9	23.72	426.9	257.6	43.3	8.8	259.3	85.3	7	(6)	
Pindolol	4662	22	2	-1.7	-0.5	57.3	3	4	29.1	73.4	21.55	399.5	238.8	45.7	8.8	247.3	83.6	7	(6)	
Oxprenolol	4470	23	2	2.2	0.1	50.7	2	4	30.5	76.8	25.52	443.8	266.8	38.0	8.8	265.3	90.2	10	(9)	
Sotalol	5063	24	2	0.2	-1.7	86.8	3	5	28.6	72.1	21.97	431.0	232.5	67.7	8.8	272.4	81.6	6	(5)	
Nonifensine	4371	25	2	1.0	0.3	29.3	2	2	29.9	75.4	21.38	374.7	233.6	49.1	8.4	238.3	73.2	2	(1)	
Bupropion	431	26	2	2.3	2.1	29.1	1	4	26.9	67.9	22.47	388.4	229.9	41.3	8.6	239.7	73.8	4	(7)	
Viloxazine	5464	27	2	1.2	0.1	39.7	1	4	26.0	65.6	22.35	391.6	229.5	36.9	8.9	237.3	73.1	5	(7)	
Fluoxetine	3269	28	2	3.9	1.4	21.3	1	2	31.7	79.9	26.67	449.6	274.2	50.4	8.8	309.3	81.5	6	(7)	
Imazalil	34116	29	2	3.6	3.5	27.1	0	3	31.5	79.4	24.07	382.9	247.4	48.6	8.9	296.0	79.9	6	(6)	
Benalaxyl	46525	30	2	3.3	3.3	46.6	0	4	37.7	95.0	28.77	520.1	314.6	68.3	9.0	325.0	86.5	7	(6)	
Hexaconazole	59833	31	2	3.9	3.9	50.9	1	4	32.7	82.4	24.16	432.9	267.3	50.6	9.0	314.2	76.5	7	(6)	
Penconazole	82796	32	2	4.6	4.6	76.4	0	3	30.3	76.4	22.28	389.7	241.4	43.3	8.3	284.2	70.6	5	(5)	
Cyproconazole	77706	33	1	2.8	2.8	50.9	1	4	31.7	79.9	21.99	422.0	258.8	176.8	8.0	291.8	68.9	6	(5)	
Myclobutanol	6096	34	1	3.1	3.1	54.5	0	4	33.1	83.5	24.79	423.8	261.6	55.0	8.9	288.1	81.5	6	(1)	
Catechin	8711	35	2	0.6	0.6	110.4	5	6	29.2	73.6	18.20	370.7	243.9	55.8	9.1	290.2	81.6	6	(1)	
Verapamil	2425	36	2	4.0	2.5	64.0	0	6	52.3	131.7	42.94	780.9	457.9	104.6	8.8	454.6	51.5	13	(1)	
Prilocaine	4737	37	2	2.0	1.6	41.1	2	3	26.7	67.4	21.40	387.3	227.1	36.6	8.7	220.0	73.9	5	(1)	
Mepivacaine	3922	38	2	1.8	1.3	32.3	1	3	29.6	74.7	22.86	423.6	250.4	56.9	8.8	246.3	72.5	2	(1)	
Bupivacaine	2380	39	-	3.3	2.9	32.3	1	3	35.1	35.1	27.92	515.4	301.6	61.9	8.8	288.4	89.9	5	(1)	
Propranolol	64696	40	2	4.8	2.3	29.5	0	3	37.3	94.0	29.50	522.7	313.3	73.6	8.9	311.0	90.0	9	(1)	

^a PSA and/or RB estimates from ChemAxon showing differences with ACD/Labs estimates (variables: x3 and x15). Cases showing high PSA-differences (i.e. compounds 12, 13, 14, 15 and 19), high RB-differences (i.e. compound 35) and both PSA- and RB-differences (i.e. compounds 22 and 24) were pre-classified as doubtful.

^b Apparently, variables x8 and x10 (MV from ACD/Labs and WV from ChemAxon) are estimates of the same parameter. In fact, although differences are observed for all the compounds, they show a high correlation. Only for compounds 35 (marked as doubtful in ^a) and 11 the differences are higher. For modeling purposes, we have processed these two variables as if they were independent.

by the original \mathbf{X} -variables, also provided by The Unscrambler[®], including the offset (b_0).

2.5. Procedure for QSPR. Simplification protocol

The ChemSpider chemical structure database [21] is used to obtain the values of variables for all compounds listed in Table 1. The selected 15 \mathbf{X} -variables include the properties: \mathbf{x}_1 : logarithm of octanol–water partition coefficient ($\lg P$), \mathbf{x}_2 : $\lg P$ estimated at pH 7.4 ($\lg D$), \mathbf{x}_3 : polar surface area (PSA), \mathbf{x}_4 and \mathbf{x}_5 : hydrogen bond donors (HBD) and acceptors (HBA), respectively, \mathbf{x}_6 : polarizability (POL), \mathbf{x}_7 : molar refractivity (MR), \mathbf{x}_8 : molar volume (MV), \mathbf{x}_9 : molecular surface area (MSA), \mathbf{x}_{10} : van der Waals volume (VV), \mathbf{x}_{11} : Dreiding energy (DE), \mathbf{x}_{12} : orbital electronegativity of the chiral carbon atom (OEC), \mathbf{x}_{13} : molecular mass (MM), \mathbf{x}_{14} : maximal projection area (MA) and \mathbf{x}_{15} : rotatable bonds (RB). Data in Table 1 correspond to predictions from two programs, ACD/Labs and ChemAxon, included in the database. Some compounds exhibiting different predictions over the variables PSA and/or RB from these programs were marked as doubtful (Table 1, footnote a).

A PCA is performed on the structure parameters in Table 1 (\mathbf{X} -matrix) using autoscaled data. Leave-one-out cross-validation is used as validation strategy. Instead of k_s (software), a manual selection of the optimum number of PCs (k_0) is performed. The k_0 value is set as the lowest k provoking the first (local) maximum or a nearly stabilization of EV_{CV} . The influence plot (residual variance vs leverage) is used to detect atypical data, ordering the compounds by their degree of influence on the \mathbf{X} latent structure: (i) high-leverage and high-residual (highly influential), (ii) high-leverage, (iii) high-residual, (iv) medium-residual; in all cases in relative terms, i.e. respect an eventual low-leverage and low-residual compact group of compounds.

Available enantiomeric resolution (R_s), in EKC using HS- β -CD, information for the compounds (excluding bupivacaine, No 39) is also incorporated in Table 1. Instead of using the (quantitative) R_s electrophoretic value, obtained in some cases under different experimental conditions, thus not directly comparable, the data were categorized as 0 (non-resolved enantiomers), 1 (partially resolved enantiomers) and 2 (fully resolved enantiomers).

A discriminant-PLS analysis over a single response variable (DPLS1) is performed, using the categorical R_s (\mathbf{y} -vector), and the structure data (\mathbf{X} -matrix; predictor variables). Thirty-nine compounds with complete \mathbf{y} - \mathbf{X} data (autoscaled) are used as calibration set (bupivacaine is excluded). A leave-one-out cross-validation is performed. Model simplification, including sequential elimination of potential 'justified outliers' and non-significant variables is applied, in view to obtain a simple representative model. On each simplification step, decisions are taken once the optimum number of LVs (k_0) is adjusted. Manual selection of k_0 value selection is performed based on the EV_{CV} -rule described in the PCA model.

To help in the sequential decision-making process, four plots are selected: (i) biplot of LV_2 vs. LV_1 , showing both scores (compounds) and loadings (parameters), thus their relative correlation. (ii) EV and EV_{CV} bars for global model performance. (iii) Validation plot, showing predicted vs. measured \mathbf{y} -values (both calibration and cross-validation ones; \mathbf{y} and \mathbf{y}_{CV} data, respectively, for each compound). (iv) Scaled \mathbf{b} -coefficients of \mathbf{X} -variables, plus their uncertainty limits, $\mathbf{b} \pm U(\mathbf{b})$, for model stability evaluation.

During the decision-making process, the representativeness of the DPLS1 model is assessed by examining three aspects: (i) the latent structure consistency: coincident k_0 and k_s values, but also close to the 'ideal' k -value (k_i), is considered an indicator of a well-defined latent structure. In this case, $k_i = 1$, since there is a single response variable (R_s). (ii) The predictive power: $Pp = 2EV_{CV} - EV$

[7]. $Pp \geq 55\%$ is considered acceptable for the discriminant model (instead of 60%, suggested for quantitative-PLS models [7]). (iii) The descriptive ability: a model with all the \mathbf{b} -coefficients significant is considered satisfactory (see Section 2.4, item i). According to this, the simplification of the DPLS1 model, involving both elimination of possible outliers and variables selection, is performed in successive steps. In every step the following rules are applied by order:

- Rule-1: eliminate doubtful compounds (Table 1) and/or highly influential (PCA influence plot) that appear misclassified in the validation plot.
- Rule-2: compare k_0 and k_s values against $k_i = 1$. Check the Pp estimation against the threshold value (55%). Decide the application of rule-2a or -2b accordingly.
- Rule-2a: if non-matching k -values ($k_0 \neq k_s$ and/or k_0 far from $k_i = 1$) and/or $Pp < 55\%$ are obtained, eliminate up to 3 non-significant \mathbf{X} -variables showing the lowest $b/U(b)$ ratios.
- Rule-2b: if matching adjusted k -values ($k_0 = k_s \sim 1$) and $Pp \geq 55\%$ are obtained, select only the 'marked' significant \mathbf{X} -variables.
- Stop criterion: the simplification process is stopped when none of the rules can be applied.

On the other hand, some undesirable situations observable in the bi-plot must be revised during this process, such as the occurrence of a doubtful or influential compound exclusively correlated with a single variable (the compound could be eliminated) or the presence of two highly correlated \mathbf{X} -variables (the variable showing the lowest $b/U(b)$ ratio could be eliminated).

2.6. Further use of categorical enantioresolution estimations

De-scaled PLS coefficients (Section 2.4) for the selected variables in Section 2.5 are then obtained to derive the explicit $\mathbf{y} = \mathbf{bX}$ equation (i.e. $R_s = f(\text{parameters})$; including an offset). It is then applied to estimate R_s for bupivacaine (No 39 in Table 1). In general, for $R_s \geq 2$ or well below 1, further studies are not considered. If $R_s \geq 2$, we suggest using the 1% m/v CD concentration, and, if no peaks are observed, decrease it to 0.25%. In the $\sim 1 < R_s < 2$ case (probable enantioresolution in particular conditions), or if convenient/desired, a standard Box–Behnken experimental design, using the methodological EKC variables concentration of CD (CD), temperature (T) and electrophoretic buffer pH (pH) as main factors, is performed. Using these factors as \mathbf{X} -data and two response variables, R_s and t_2 (the retention time of the second eluted enantiomer, thus the analysis time) as response \mathbf{Y} -matrix, a PLS2 is then applied. Again, de-scaled \mathbf{b} -coefficients are converted in two explicit equations for R_s and t_2 as a function of CD, T and pH . They are used to map simulated R_s - t_2 data, allowing the selection of convenient separation conditions satisfying $1.5 < R_s < 2$.

3. Results and discussion

3.1. Strategy selection

Among the structure of the solutes, R_s depends on electrophoretic factors. However, these factors should be more or less constant if the experimental conditions are similar (as in our case; see Section 2.3), so the structural properties of the molecules should be the discriminant factor providing (or not) enantioseparation. On the other hand, this is one of the reasons why we decided to treat the variable R_s as categorical instead of quantitative. Moreover, the use of different CD concentrations provides not directly comparable (numerical) R_s values, and this was the main reason why we decided to treat the variable R_s as categorical.

Set-of-variable rules, e.g. Lipinski's-like filters [21], or decision trees [22] could be used to roughly predict dicotomic (e.g. Yes/No) or categorical (e.g. 0, 1, 2, as in this case) response variables. Although these options are possible here, we have preferred to derive a predictive explicit equation, which is a practical option to easily automate future y -estimations. Obviously, such estimation, although numeric, should be seen as a rough enantioresolution level value. The classical tool for dealing with categorical response variables is discriminant analysis [23]. For instance, linear discriminant analysis (LDA) is quite popular, but it could fail if non-linear y - X relationships are present. Other options (including those using non-linear discriminant functions) are less common, unavailable in basic chemometric software packages or more difficult to understand or to use, thus, less operative in view of non-expert users.

On the contrary, PCA and PLS have become popular algorithms. The simplest and most common PLS algorithm, linear-PLS (the default option), is able to model some degree of y - X non-linearity (visible through their scores, \mathbf{u} - \mathbf{T}). DPLS1 is used as a conventional PLS, just assigning the categorical response variable (here, R_s) as y -variable. Since autoscaled data are used, scaled \mathbf{b} -coefficients, useful during the optimization step to analyze $\mathbf{b}/\mathbf{U}(\mathbf{b})$ data (Section 2.5), are initially obtained; but once an optimum model is selected, de-scaled coefficients can be easily obtained [7,9 and references therein]. Fortunately, all these tasks, applied here on Table 1 data (next section), can be performed with a single software [20], thus a practical equation able to provide y -estimates without the software. Variable selection (reduction) strategies, satisfying different objectives, are available in the literature [23]. Some software packages offer automatic tools for selecting variables for a multiple regression. These tools can be unfamiliar for many users, not user-friendly and/or insufficiently transparent, affecting the decision-making process. For instance, different strategies may provide different reduced models, particularly in complex situations (such as a discriminant problem). In addition, most of the automated approaches are aimed exclusively at obtaining the highest predictive ability, without taking into account the model stability [7,9,10]. Finally, none of the automatic approaches allows the elimination of compounds (e.g. doubtful or influential ones; as those present in Table 1) together with the variable reduction, thus increasing the risk of obtaining non-representative models.

Manual PLS compounds/variable simplification, following systematic rules, allows controlling the process, providing representative models and reliable future estimations (new compounds). A critical aspect to revise during model simplification is k since y -predictions and $\mathbf{b} \pm \mathbf{U}(\mathbf{b})$ outputs depend on such selection. Alternatively to automated k_s selection [20], inspection of the EV_{CV} (Section 2.5) allows a manual k_0 selection. Unfortunately, high k_s ($k_s \gg k_i = 1$) are common. In fact, during model simplification, a k_0 and k_s reduction (and approximation) should be expected, justifying rule 2a (Section 2.5). Note that high k -values could reveal the necessity to describe a non-representative connection between a given object (sometimes doubtful or influential) and a single variable.

Respect the multivariate experimental design/optimization process, response surface analysis is the classical option [23]. Again, software automatic analysis can be unfamiliar for some users and/or obscure, requiring moderate skills to perform the effects' analysis to deal with crossed effects (factors' multiplication) and nonlinearities (habitually incorporating the squared factors), mainly with two response variables (\mathbf{Y} data matrix), where complex functions are used. Again, in the last case, a simpler strategy is possible, PLS2, using only the main factors (i.e. experimental conditions) as \mathbf{X} data, partially accommodating the crossed and non-linear effects as a practical solution. The PLS-procedure is identical to the previously described, and in this case, model simplification is not

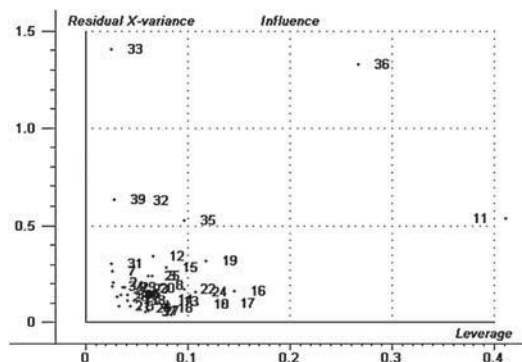


Fig. 1. The Unscrambler® screen for the PCA influence plot corresponding to a 2-PC model ($k_0 = 2$).

required. As before, the final output are two direct equations in the form $[R_s, t_2] = f(CD, T, pH)$ easy to be applied.

3.2. Modeling the X and y - X data

A preliminary PCA-inspection of the structure data (all compounds in Table 1) was performed as described in Section 2.5, using the autoscaled \mathbf{X} -data and leave-one-out cross-validation. The k_s value was 6, coinciding with the absolute maximum EV_{CV} values. However, k_0 was set to 2, coinciding with the first local maximum EV_{CV} (60.7%). The corresponding EV was 72.6%. Fig. 1 shows the influence plot for the 2-PC model. As can be observed, an almost compact group of objects with low-leverage and low-residual values is clearly observed ('similar group'). Compounds No 11 and 36 could be considered high-leverage and high-residual (highly influential on the latent structure). In fact, both compounds exhibit high negative scores in PC1, far from the rest of compounds that form a relatively homogeneous group in the PC1-PC2 score plot (not shown). Such influential effect was related to the high (or maximum) values of several variables in Table 1 for these two compounds. On the other hand, most of the $R_s = 2$ compounds show positive PC1 scores indicating that this PC is related with resolution. Other less influential compounds are No 33 (high-residual) and No 32, 35 and 39 with medium-residual values. All these atypical compounds present a 'dissimilar' molecular parameter profile and should be taken into account during the PLS stage. As expected, the loading plot (not shown) indicates that variables \mathbf{x}_8 and \mathbf{x}_{10} present a high correlation (see Table 1, footnote b) and also appear correlated with variables \mathbf{x}_6 , \mathbf{x}_7 , \mathbf{x}_9 , \mathbf{x}_{11} , \mathbf{x}_{13} and \mathbf{x}_{14} (all forming low angles respect to the PC1 axis), indicating redundant information.

Table 2 summarizes the simplification process of the DPLS1 model, following the rules/tests indicated in Section 2.5. Before stopping the process (step-7, Table 2), some relevant situations were found. In step-2, split of objects into $R_s = 0$ and $R_s > 0$ groups is observed in the validation plot, indicating the practical usefulness of the model. In step-5, a $k_0 = k_s = 2$ model, close to the ideal $k_i = 1$ situation (anticipated in Section 3.1), and with reasonable predictive ability (good EV and EV_{CV} combination, and then predictive power, $P_p > 55\%$) was obtained. In such conditions, direct selection of the four significant variables (\mathbf{x}_2 - \mathbf{x}_5 ; lgD , PSA , HBD and HBA) was decided (rule-2b). It was observed a clear correlation between variable \mathbf{x}_{14} and compound No 11 (particular, non-representative, situation warned in Sections 2.5 and 3.1), so the elimination of this variable caused the misclassification of that compound in step-6. Since compound No 11 was previously detected in PCA as highly influential, it was removed from the DPLS1 model (rule 1, step-7)

Table 2
DPLS1 simplification including the decision-making process.

Step	k_o (k_s) EV % (EV_{CV} %) Pp % (= $2EV_{CV} - EV$) [7]	Main observations (+) Positive output (-) Negative output suggesting new steps	Decision
1	2 (2) 46.5 (28.2) 9.9	(-) Misclassified compounds: 12 and 24 (badly predicted y and y_{CV}) and 36 (badly predicted y_{CV})	Rule 1: eliminate compounds 12 and 24 ^a and 36 ^b
2	2 (2) 63.7 (56.6) 49.5	(+) Separation of $Rs = 0$ and $Rs > 0$ groups in the validation plot (-) Non-significant regression coefficients (i.e. $\mathbf{b} \pm \mathbf{U}(\mathbf{b})$ includes 0) exist and poor predictive power ($Pp < 55$)	Rule 2a: eliminate \mathbf{x}_6 and \mathbf{x}_7^c
3	2 (2) 65.2 (57.1) 49.0	(-) Misclassified compounds: 22 and 35 (badly predicted y_{CV})	Rule 1: eliminate compounds 22 ^a and 35 ^a
4	2 (4) 74.0 (67.8) 61.6	(-) Non-significant regression coefficients (all $\mathbf{b} \pm \mathbf{U}(\mathbf{b})$ includes 0) (-) Non well-defined latent structure ($k_o \neq k_s$)	Rule 2a: eliminate \mathbf{x}_8 and \mathbf{x}_{12}^c
5	2 (2) 75.4 (69.8) 64.2	(+) Near adjusted ($k_o = k_s = 2 \sim k_i$) predictive model ($Pp > 55$) showing four significant variables: $\mathbf{x}_2 - \mathbf{x}_5$	Rule 2b: retain only $\mathbf{x}_2 - \mathbf{x}_5$
6	1 (1) 63.1 (60.4) 57.7	(+) Adjusted ($k_o = k_s = k_i = 1$) model (-) Misclassified compound 11 (badly predicted y and y_{CV})	Rule 1: Eliminate compound 11 ^b
7	1 (1) 72.4 (69.8) 67.2	(+) All doubtful/influential compounds are well predicted (+) Adjusted ($k_o = k_s = k_i = 1$) predictive model with good predictive power ($Pp > 55$) (+) Good descriptive power (the four variables are significant)	Stop criterion: select this model as the optimum

^a Doubtful compound in Table 1.

^b Highly influential compound in PCA.

^c Variables with the lowest $b/U(b)$.

providing finally the definitive DPLS1 model, fitting the stop criterion. It should be noted that the selected model is not able to separate completely all the calibration compounds with Rs 1 and 2, however this fact is less important in terms of usefulness, since the $Rs = 0$ compounds are well predicted.

The model selected should be seen as provisional, susceptible to change (improving its features) if new Rs -structure data can be incorporated in the future. However, currently, it represents a consistent ($k_o = k_s = k_i = 1$; the ideal situation), predictive (high variability of Rs is modeled, $EV = 72.4\%$; $Pp = 67.2\%$) and descriptive (all coefficients are significant; Fig. 2) model, thus satisfying the prefixed representativeness (Section 2.5), for a discriminant problem. Raw (de-scaled) coefficients were obtained from this DPLS1 model to derive the practical explicit model (Eq. 1):

$$Rs = 2.354 + 0.095lgD - 0.008PSA - 0.159HBD - 0.137HBA \quad (1)$$

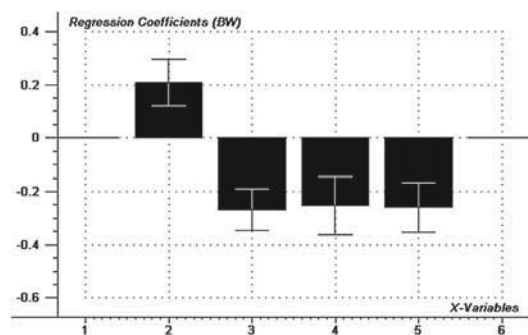


Fig. 2. The Unscrambler[®] screen showing the scaled \mathbf{b} -coefficients (weighted: BW) with uncertainty intervals, corresponding to the optimum DPLS1 model (Step-7, Table 2). \mathbf{X} -variables: 2, logarithm of octanol–water partition coefficient estimated at pH 7.4 (lgD); 3, polar surface area (PSA); 4 and 5, number of hydrogen bond donors (HBD) and acceptors (HBA), respectively.

Note that such de-scaled coefficients do not reveal the importance of the variables (as the scaled ones do). Concretely, Fig. 2 suggests a similar importance of PSA , HBD and HBA (negatively correlated with Rs) a slightly lower importance of lgD (positive correlation). This suggests that enantioresolution in the EKC-HS- β -CD system is favored by the pH-adjusted hydrophobicity of the molecule, but is not favored if the molecule presents high polar surface area (formed by polar atoms of the molecule) and high number of hydrogen-bonding formation functional groups.

Eq. (1) is ready to perform predictions of new molecules, from the on-line data of these selected variables, once they present consistent estimated parameters with non-influential PCA-behavior. Note that although Eq. (1) is linear (and simple), it comes from an intrinsic non-linear relationship (latent and more complex), as demonstrated in Fig. 3, which reveals the nature of the inner \mathbf{u} - \mathbf{T} scores relationship, corresponding to the optimum model in this work (step-7, Table 2). This plot also reveals the discrimination power of the proposed DPLS1 model. Note that this plot could serve

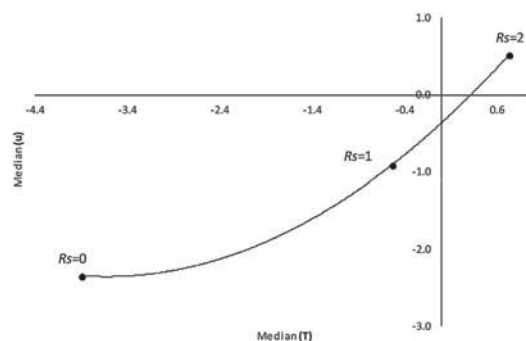


Fig. 3. Inner \mathbf{y} - \mathbf{X} PLS relationship. The median of \mathbf{u} - and \mathbf{T} -scores per Rs -category are calculated, and then, fitted using a quadratic model.

Table 3
Box–Behnken design for three factors showing the non-randomized coded factors levels distributed in 15 experiments (*Ne*). The corresponding experimental values were set form the range of factors (*CD*: 0.5–1.5% m/v, *T*: 15–35 °C and *pH* 6–8). Retention times for the first (*t1*) and second (*t2*) eluted enantiomers and *Rs* for each experiment are included. The experimental values *t2* and *Rs* were used as response variables.

<i>Ne</i>	<i>CD</i> (% m/v)		<i>T</i> (°C)		<i>pH</i>		<i>t1</i> (min)	<i>t2</i> (min)	<i>Rs</i>
	Code	Value	Code	Value	Code	Value			
1	-1	0.5	-1	15	0	7	11.54	11.8	1.38
2	-1	0.5	0	25	-1	6	7.64	7.73	0.87
3	-1	0.5	0	25	1	8	7.5	7.54	0.53
4	-1	0.5	1	35	0	7	6.5	6.54	0.95
5	0	1.0	-1	15	-1	6	10.58	10.75	1.91
6	0	1.0	-1	15	1	8	10.5	10.71	2.67
7	0	1.0	0	25	0	7	7.26	7.32	0.98
8	0	1.0	0	25	0	7	7.17	7.22	0.66
9	0	1.0	0	25	0	7	6.99	7.03	0.53
10	0	1.0	1	35	1	8	6.63	6.68	0.81
11	0	1.0	1	35	-1	6	6.6	6.69	1.05
12	1	1.5	-1	15	0	7	13.04	13.43	1.61
13	1	1.5	0	25	-1	6	10.66	10.97	1.77
14	1	1.5	0	25	1	8	9.43	9.62	1.00
15	1	1.5	1	35	0	7	7.22	7.37	0.57

as a criterion to compare different simplified models (outside the objective of the present work).

3.3. Application case: Optimization of EKC conditions for enantioresolution of bupivacaine.

Table 1 shows structure data for bupivacaine (*No* 39; with no *Rs* available). For this compound, Eq. 1 provides an estimation of $R_s = 1.8$ (this should not be seen as a metric value, but as an indicative value; e.g. $R_s > 1.5$ or $1 < R_s < 2$ and with the meaning of possible enantioresolution, but probably in particular experimental conditions, and pending from experimental confirmation). Optionally, a more sophisticated analysis could be performed with The Unscrambler® if the model (after step-7 in Table 2) is saved into the program. In that case, the software also provides a y -uncertainty ($U(y)$) for the estimation [9,20]; 1.8 ± 0.3 in this case, although less relevant here due to the categorized R_s used.

Although the R_s estimate is relatively high ($R_s > 1.5$), bupivacaine appeared as medium-residual in the PCA influence plot, and then some caution should be taken with such predictions. Thus, the $1 < R_s < 2$ situation indicated in Section 2.5 was considered, requiring a further experimental design. This is equivalent to assume possible difficulties for bupivacaine enantioresolution, i.e. its baseline resolution would require particular *CD*, *T* and *pH* conditions. Besides R_s , we preferred controlling also the analysis time, the variable *t2* (the migration time of the second eluted enantiomer), to make a more valuable decision. Pre-optimized experimental designs are the adequate option for multivariate optimization. An effective (with low-experiments) design is Box–Behnken [22,23]. For instance, the standard Box–Behnken design for three experimental factors (*CD*, *T*, *pH*) can be performed in 15 experiments, including three center points (replicated results). Table 3 shows the experimental conditions (coded and real factors' levels) and the EKC results, including the response variables (R_s and *t2*). The experiments were randomized, but for clarity, the intuitive *Ne* numbers in Table 3 were used to refer to the experiments. Fig. 4 shows the electropherogram corresponding to the enantioresolution of bupivacaine using the experimental conditions: 1.5% m/v HS- β -CD, 15 °C and *pH* 7.0 (Box–Behnken experimental point *Ne* = 12, Table 3). The experimental R_s was 1.61 while *t2* was 13.43 min.

A priori, an R_s –*t2* correlation could be expected. To check it, the experimental R_s vs. *t2* data in Table 3 were plotted (not shown) suggesting a positive correlation. A regression on the data reveals relevant information: (i) experiment *Ne* 6 (with the highest R_s value) exhibits a large residual, suggesting caution on this result

in the next stage; (ii) R^2 excluding *Ne* 6 data is 0.64 confirming the expected moderate correlation; in these cases PLS2 could be advantageous against PLS1 [24]. In addition, this plot indicated that complete resolution of bupivacaine enantiomers requires more than 10 min.

We are now interested in performing a rough response surface analysis, based only in the main factors and assuming some errors due to the relatively low number of experiments in the experimental design. However, approximate results should be sufficient for practical purposes. Initial PLS2 (15 experiments, **X**: *CD*, *T* and *pH*, **Y**: R_s and *t2*; autoscaled matrices) confirms that experiment *Ne* 6 is not adequate (low y and y_{CV} estimated values in the validation plot), suggesting an error during the experimental process resulting in a wrongly high R_s value. Again, to obtain a more representative model, this 'experiment' was excluded. The subsequent PLS2 shows reasonably good outputs (e.g. overall EV close to 70%). The impact of the factors (scaled coefficients values; not shown) suggests that *T* (negatively correlated with R_s and *t2*) is the most important factor. As expected, *CD* is positively correlated with both response

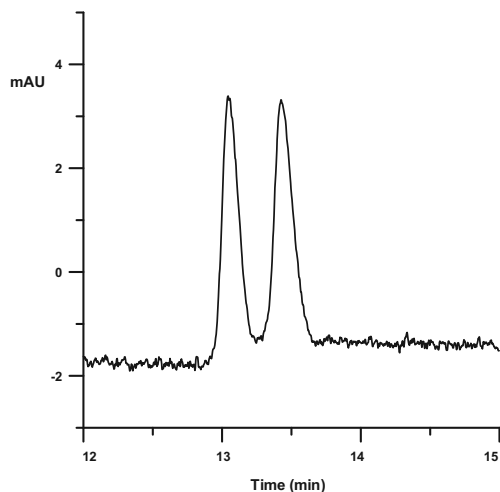


Fig. 4. Electropherogram corresponding to the enantioresolution of bupivacaine in one of the Box–Behnken experimental points (*Ne* = 12; Table 3). Experimental conditions: 1.5% HS- β -CD, 15 °C, *pH* 7.0.

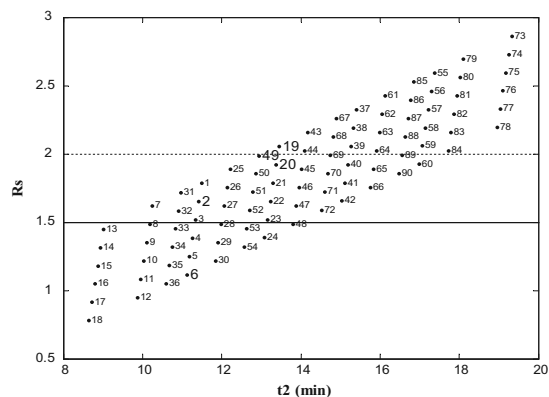


Fig. 5. Simulated R_s vs. t_2 map for bupivacaine from Eqs. (2a) and (2b) (results are identified by a simulation number, N_s). Simulated range for factors were, CD : 1–5%, T : 15–25 °C and pH 5.5–8. Some particular N_s are set in higher font-size (see Table 4 and related text for details). The minimum acceptable R_s (solid line) and a more secure value (dashed line) are included.

variables, while pH is negatively correlated. These effects can be easily explained from an electrophoretic point of view taking into account the separation mechanism, which implies the formation of anionic inclusion complexes with the cyclodextrin. The higher the CD , the longer the migration time, because the equilibrium of the free-complexed drug is shifted to the complexed form; a higher R_s is reasonable because the complexed form is who migrates enantioselectively. For the increase of T , shorter migration times are logical for both enantiomers due to the decrease of viscosity of the BGE and the consequent increase of current. Therefore, if both enantiomers migrate faster, less R_s is coherent. The same effect is observed with the pH , since higher pH implies higher EOF mobility, accelerating the migration of both enantiomers and decreasing the R_s value.

As before, two explicit equations, for R_s and t_2 , were obtained from the de-scaled regression coefficients:

$$R_s = 3.497 + 0.269CD - 0.034T - 0.268pH \quad (2a)$$

$$t_2 = 14.05 + 1.96CD - 0.247T - 0.149pH \quad (2b)$$

These equations were used to generate simulated R_s and t_2 data from a selected range of the factors, according to the previous derived importance of variables (extrapolation was accepted since only approximate values are searched). Fig. 5 shows the R_s – t_2 map generated for bupivacaine. Initially, only simulated numbers (N_s) above $R_s > 1.5$, but preferably $R_s \sim 2$ (more secure), are relevant, taking into account that they represent just simulated estimates from non-error free Eqs. (2a) and (2b). Some N_s data have been included in Table 4. Results from N_s 2 and 6 correspond to conditions already experimented in Table 3 (N_e 5 and 6, respectively). The case of N_s 6 (N_e 6) corresponds to the experimentally suspicious high- R_s value detected by PLS2, and eliminated there. In fact, the estimated R_s in Table 4 is 1.12 (<1.5, Fig. 5) confirming

Table 4
Selected simulated results identified by their simulation number (N_s). The response variables t_2 and R_s (mapped in Fig. 4) were predicted from Eqs. (2a) and (2b).

N_s	CD (% m/v)	T (°C)	pH	t_2 (min)	R_s
2	1	15	6	11.4	1.65
6	1	15	8	11.1	1.12
19	2	15	5.5	13.4	2.06
20	2	15	6	13.4	1.92
49	3	25	5.5	12.9	1.99

its error during the experimental design experiment. An eventual acceptance of the initial apparent good result ($R_s = 2.67$; Table 3) would lead to a waste of time when bupivacaine enantioseparation would be tried further. The estimated analysis time (t_2) is however similar to the experimental one.

In the case of N_s 2 (N_e 5), the experimental and estimated R_s values are different (1.96 and 1.65; Tables 3 and 4), but indicating $R_s > 1.5$ enantioresolution in these conditions ($CD = 1\%$ m/v, $T = 15$ °C and pH 6). Again, t_2 is quite similar in both tables. The advantage of deriving the map in Fig. 5 is the possibility of increasing the security for further enantioseparation, selecting simulated cases close to the $R_s = 2$ line. In this case, N_s cases with low t_2 are preferable (e.g. N_s 19, 20, 49). The simulated results for these three cases are shown in Table 4. The expected increase of analysis time respect the acceptable N_s 2 case is about 2 min. Since $R_s \sim 2$ in all these cases, it is preferable to choose the most practical conditions; for instance, case N_s 20 requires low CD and a pH 6, closer to the pK_a of phosphate (~ 7.2) used in the buffer, being therefore the best option.

4. Conclusions

Two simple enantioresolution models for the Electrokinetic chromatography-highly sulfated β -cyclodextrin (EKC-HS- β -CD) system are developed; one related exclusively to directly-available structural data of basic compounds and the other with experimental conditions. In the first case, an easily comprehensible PLS 'model simplification' protocol, involving manual sequential 'justified outliers' elimination and variable selection is proposed. This protocol is based on two rules and a stop criterion, providing the prefixed 'model representativeness' (i.e. latent structure consistency and predictive-descriptive power). In the second case, an easily comprehensible PLS-based 'multivariate optimization scheme', involving a standard experimental design and like-multiple response surface analysis, allows a map-based EKC experimental conditions selection. Both approaches and decision-making aspects proposed converges in a single software, easy to use with minor skills.

The modeling outputs define the ability of using HS- β -CD as chiral selector for enantioresolution in EKC for basic compounds and provide the key structure properties dominating their enantioresolution. A practical simple equation is provided ($R_s = 2.354 + 0.095IGD - 0.008PSA - 0.159HBD - 0.137HBA$) a priori estimate the enantioresolution level of a basic molecule in this system from the four-selected parameters available in an on-line database. Compounds with close estimated parameters in ChemSpider (from ACD/Labs and ChemAxon programs) and low influential in PCA respect the current latent structure fix the applicability of this equation. Since the model is trained using a heterogeneous data set of basic drugs and pesticides, no more limitations are expected using new data from basic compounds. Bupivacaine enantioresolution in this system (never been reported so far) is predicted with the equation, indicating probable enantioresolution in particular conditions. The further optimization scheme suggests good enantioresolution in approx. 12 min, under the following conditions: cyclodextrin concentration in the 1–2% m/v range, 15 °C and pH 6.

Conflict of interest

The authors declare no conflict of interest.

Acknowledgement

L. Asensi-Bernardi acknowledges the Spanish Ministry of Education for her FPU predoctoral scholarship (AP2010-1984).

Appendix A. List of chemometric abbreviations and variables used

b	Vector of regression coefficients relating y and X data. When scaled they explain the importance of the X -variables in predicting y
$b/U(b)$	Ratio between the regression coefficient and the estimated uncertainty value for a given variable of the X -matrix
b ± U(b)	Estimated uncertainty interval for b
CD	Cyclodextrin concentration. Factor used in the Box–Behnken design; one of the X -variables used in the PLS2 model for bupivacaine
DPLS1	Discriminant partial least squares on one single response (here <i>R_s</i> , categorical-enantioresolution)
EV	Explained y - or X -variance (in PLS and PCA, respectively)
EV _{CV}	EV in cross-validation
HBA	Number of hydrogen bond acceptors
HBD	Number of hydrogen bond donors
<i>k</i>	Number of principal component (PCs) of a PCA model or latent variables (LVs) of a PLS model (also called factors)
<i>k_i</i>	'Ideal' <i>k</i> -value. Here, <i>k_i</i> = 1, since there is a single response variable (categorical-enantioresolution, <i>R_s</i>)
<i>k₀</i>	Optimum <i>k</i> -value, manually selected as the lowest <i>k</i> provoking the first (local) maximum or a nearly stabilization of EV _{CV}
<i>k_s</i>	<i>k</i> -value initially proposed by the software (here The Unscrambler® [20])
LV	Latent variable of a PLS model
Ne	Number of experiment in the Box–Behnken experimental design of bupivacaine
No	Numbered order of compounds
Ns	Simulation number used in the optimization of EKC conditions for enantioresolution of bupivacaine
PC	Principal component of a PCA model
PCA	Principal component analysis
pH	Electrophoretic buffer pH. Factor used in the Box–Behnken design; one of the X -variables used in the PLS2 model for bupivacaine
PLS	Partial least squares
PLS2	Partial least squares on two response variables. Here <i>R_s</i> , enantioresolution, and <i>t₂</i> , migration time of the second eluted enantiomer for bupivacaine
Pp	Predictive power of the model. $Pp = 2 EV_{CV} - EV$ [7]
<i>R_s</i>	Enantioresolution
<i>T</i>	Separation temperature. Factor used in the Box–Behnken design; one of the X -variables used in the PLS2 model for bupivacaine
T	Score matrix corresponding to the X -matrix
<i>t₁</i>	Migration time of the first eluted enantiomer
<i>t₂</i>	Migration time of the second eluted enantiomer, thus the analysis time

u	Score vector corresponding to the y -vector
U(b)	Estimated uncertainty of b
X	Matrix of predictor or independent variables (here structural information of basic compounds)
x_i	Vectors used in the matrix- X
y	Vector of response or dependent variable (in DPLS1). Here the experimental <i>R_s</i> (categorized)
<i>y</i>	Predicted value of the response variable
<i>y_{CV}</i>	Predicted value of the response variable in cross-validation
Y	Matrix of responses or dependent variables (in PLS2). Here the experimental <i>R_s</i> (non-categorized) and <i>t₂</i> for bupivacaine

References

- [1] B. Chankvetadze, J. Chromatogr. A 1168 (2007) 45.
- [2] B. Chankvetadze, G. Blaschke, J. Chromatogr. A 906 (2001) 309.
- [3] T. Cserhádi, Biomed. Chromatogr. 22 (2008) 563.
- [4] L. Asensi-Bernardi, Y. Martín-Biosca, M.J. Medina-Hernández, S. Sagrado, J. Chromatogr. A 1218 (2011) 3111.
- [5] S. Rudaz, T. Le Saux, J. Prat, P. Gareil, J.L. Veuthey, Electrophoresis 25 (2004) 2761.
- [6] F.T.A. Chen, G. Shen, R.A. Evangelista, J. Chromatogr. A 924 (2001) 523.
- [7] S. Sagrado, M.T.D. Cronin, J. Chem. Inf. Model. 46 (2006) 1523.
- [8] T.W. Schultz, M.T.D. Cronin, Environ. Toxicol. Chem. 22 (2003) 599.
- [9] H. Martens, M. Martens, Multivariate Analysis of Quality. An Introduction, John Wiley & Sons, UK, 2001.
- [10] S. Sagrado, M.T.D. Cronin, Anal. Chim. Acta 609 (2008) 169.
- [11] H.-J. Park, Y. Choi, W. Lee, K.-R. Kim, Electrophoresis 25 (2004) 2755.
- [12] M. Goodarzi, M.P. Freitas, Sep. Purif. Technol. 68 (2009) 363.
- [13] G.M. Beck, S.H. Neau, A.J. Holder, J.N. Hemenway, Chirality 12 (2000) 688.
- [14] W. Li, G. Tan, L. Zhao, X. Chen, X. Zhang, Z. Zhu, Y. Chai, Anal. Chim. Acta 718 (2012) 138.
- [15] L. Asensi-Bernardi, Y. Martín-Biosca, R.M. Villanueva-Camañas, M.J. Medina-Hernández, S. Sagrado, Electrophoresis 31 (2010) 3268.
- [16] L. Asensi-Bernardi, Y. Martín-Biosca, E. Fornet-Herrero, S. Sagrado, M.J. Medina-Hernández, Biomed. Chromatogr. 27 (2013) 377.
- [17] M.I. Sabela, N.J. Gumede, L. Escuder-Gilabert, Y. Martín-Biosca, K. Bissety, M.J. Medina-Hernández, S. Sagrado, Anal. Bioanal. Chem. 402 (2012) 1899.
- [18] L. Asensi-Bernardi, Y. Martín-Biosca, L. Escuder-Gilabert, S. Sagrado, M.J. Medina-Hernández, J. Chromatogr. A 1298 (2013) 139.
- [19] L. Asensi-Bernardi, L. Escuder-Gilabert, Y. Martín-Biosca, S. Sagrado, M.J. Medina-Hernández, Biomed. Chromatogr. (2013), <http://dx.doi.org/10.1002/bmc.2935>.
- [20] <http://www.camo.com/> (accessed 31.07.2013).
- [21] <http://www.chemspider.com/> (accessed 31.07.2013).
- [22] M.A. Martínez-Gómez, R.M. Villanueva-Camañas, S. Sagrado, M.J. Medina-Hernández, Electrophoresis 27 (2006) 4364.
- [23] D.L. Massart, B.G.M. Vandeginste, L.M.C. Buydens, S. De Jong, P.J. Lewi, J. Smeyers-Berbeke, Handbook of Chemometrics and Qualimetrics, Part A, Elsevier, Amsterdam, 1997.
- [24] <http://www.eigenvector.com/> (accessed 31.07.2013).

Paper III

Determination of fluoxetine enantiomers in pharmaceutical formulations by electrokinetic chromatography-counter current technique

**L. Asensi-Bernardi, Y. Martín-Biosca, E. Fornet-Herrero, S. Sagrado and
M.J. Medina-Hernández**

Biomedical Chromatography 2013, 27, 377-381

Determination of fluoxetine enantiomers in pharmaceutical formulations by electrokinetic chromatography–counter current technique

Lucía Asensi-Bernardi^a, Yolanda Martín-Biosca^a, Eder Fornet-Herrero^a, Salvador Sagrado^{a,b} and María José Medina-Hernández^{a*}

ABSTRACT: In this work, an electrokinetic chromatography–counter current procedure for the separation of fluoxetine enantiomers using highly sulfated β -cyclodextrin was optimized and applied to the determination of the enantiomers in three pharmaceutical formulations according to the matrix features. Quality criteria were applied to facilitate its transferability to testing laboratories. Fluoxetine was used therapeutically as the racemate, although a stereospecificity associated with its interactions with the neuronal serotonin-uptake carrier was demonstrated. In this context, the development of enantioselective methods for the chiral analysis of pharmaceuticals allowing stereoisomer ratio estimations has increasing interest in pharmaceutical industry. The proposed method allows the quantification of both enantiomers in less than 2 min with high resolution ($R_s = 2.4$). Copyright © 2012 John Wiley & Sons, Ltd.

Keywords: fluoxetine; chiral analysis; pharmaceutical formulations; electrokinetic chromatography; highly sulfated β -cyclodextrin

Introduction

Psychoactive drugs are the most used drugs in our society. Antidepressants, hypnotics and other types are purchased every day by different kinds of patients. Usually, these drugs have been synthesized and commercialized as racemic forms, but today the industry is interested in the introduction of pure enantiomers in the pharmaceutical market. Owing to the high degree of stereoselectivity of pharmacological and pharmacokinetic processes, often one of the enantiomers is the most active while the other may produce side-effects and even toxicity in some cases. Consequently, the safety and efficiency of many racemic drugs could be improved with single-enantiomer formulations. Thus, there is a special interest in analytical methods able to determine the stereoisomer ratios in synthetic products, pharmaceutical formulations and biological samples (Scriba, 2011). At the level of formulations, the evaluation of such ratios in the manufacturing process and stability tests is a main objective.

Fluoxetine is a potent and selective inhibitor of the neuronal serotonin-uptake carrier. It is used therapeutically as a racemate, although a stereospecificity associated with its interactions with the serotonin-uptake carrier has been demonstrated (Robertson *et al.*, 1988). In fact, although the *S*- and *R*-fluoxetine are approximately equipotent in blocking serotonin reuptake, the enantiomers of the main *N*-demethylated metabolite, norfluoxetine, which are present in the circulation at higher concentrations than the parent drug, show marked differences in their pharmacological activity (Barclay *et al.*, 2011; Inoue and Chang, 2003; Desiderio *et al.*, 1999). Then, the determination of fluoxetine stereoisomer ratio in its pharmaceutical formulations becomes relevant.

Capillary electrophoresis (CE) is a powerful technique for enantiomer separations showing some advantages over HPLC that include the use of smaller amounts of sample and reagents, an increased separation efficiency, short analysis times and easy

conditioning of the column. One of the most common modes of chiral CE is electrokinetic chromatography (EKC) in the presence of a chiral selector in the background electrolyte (BGE). EKC has been widely employed for the separation of fluoxetine enantiomers with several anionic cyclodextrins, although no applications have been described for these separation methods (Inoue and Chang, 2003; Li *et al.*, 2003; Li and Vigh, 2004a, 2004b; Bonato *et al.*, 2001; Rudaz *et al.*, 2003; Perrin *et al.*, 2001).

Inoue and Chang (2003) achieved good resolutions with heptakis-(2,3-diacetyl-6-sulfato)- β -cyclodextrin (CD), sulfated- α -CD and heptakis-(2,3-dimethyl-6-sulfato)- β -CD in analysis times longer than 20 min. Li *et al.* (2003) employed carboxymethyl- β -CD with reverse polarity obtaining $R_s \approx 2$ in more than 30 min. Using sulfated- β -CD, good resolution was also obtained in 12 min (Bonato *et al.*, 2001). Li and Vigh (2004a, 2004b) synthesized hexakis(2,3-di-*O*-methyl-6-*O*-sulfo)- α -CD and hexakis(6-*O*-sulfo)- α -CD and applied them to the chiral separation of fluoxetine, achieving good resolutions in <5 min. The use of partial filling technique with highly sulfated γ -CD (HS- γ -CD) was also reported by Rudaz *et al.* (2003) in order to use mass spectrometry detection.

* Correspondence to: M. J. Medina-Hernández, Departamento de Química Analítica, Facultad de Farmacia, Universitat de Valencia, C/Vicent Andrés Estellés s/n, E-46100 Burjassot, Valencia, Spain. E-mail: maria.j.medina@uv.es

^a Departamento de Química Analítica, Facultad de Farmacia, Universidad de Valencia, Burjassot, Valencia, Spain

^b Centro Interuniversitario de Reconocimiento Molecular y Desarrollo Tecnológico, Unidad Mixta, Universidad Politécnica de Valencia-Universidad de Valencia, Spain

Abbreviations used: BGE, background electrolyte; CD, cyclodextrin; CE, capillary electrophoresis; EKC, electrokinetic chromatography; HS γ -CD, highly sulfated γ -CD.

In this case infinite enantioresolution was achieved, preventing the quantification of one of the enantiomers. These authors also proposed a reverse polarity methodology, which provided an excellent resolution in <10 min. With the same cyclodextrin Perrin *et al.* (2001) developed a short-end injection method with good features (R_s of 6.2 in 2 min). However, in this method the use of a high concentration of HS- γ -CD in the BGE increased the analysis cost. In a previous paper, our research group employed highly sulfated β -cyclodextrin (HS- β -CD) for the separation of fluoxetine enantiomers in order to evaluate the enantioselective binding of fluoxetine to human serum albumin, obtaining an R_s of 3.5 in ~4 min (Asensi-Bernardi *et al.*, 2010). In that case, there were no matrix interferences since the assay only required synthetic samples.

A recently published review shows the interest in capillary electrophoresis in the chiral analysis of pharmaceuticals (Suntornsuk, 2010). However, to our knowledge there are no CE methods reported for the pharmaceutical analysis of fluoxetine enantiomers and only LC methods with different chiral stationary phases (Olsen *et al.*, 1998) and a ^{19}F NMR spectroscopic method (Shamsipur *et al.*, 2007) have been described. With LC, the best results were for polysaccharide-based chiral stationary phases, resulting in adequate resolutions but higher retention times (>15 min). Separations were achieved in normal-phase LC, so an extraction step had to be added for analysis of pharmaceuticals (Olsen *et al.*, 1998), which are commonly water-soluble owing to their composition. The main inconvenience of the spectroscopic method is a high consumption of chiral selector, which increases the analysis cost.

In this work, an EKC methodology using the HS- β -CD in the counter-current modality has been developed for the chiral analysis of fluoxetine in pharmaceutical formulations, adapting the method optimization and the evaluation of fit-for-purpose features to commercial matrices. In this mode, the entire capillary is filled with a chiral selector, while the inlet and outlet vials are also free of chiral selector in partial-filling technique (Chankvetadze and Blaschke, 2001). The counter-current mobility of the anionic CD and oppositely charged analyte in the separation capillary allow complete enantioresolution using low concentrations of the chiral selector in very short analysis times (Rudaz *et al.*, 2004; Chen *et al.*, 2001). Under the selected conditions, fit-for-purpose analytical features of the developed method were evaluated and the chiral analysis of three pharmaceuticals containing racemic fluoxetine (Prozac[®], Fluoxetina Teva[®] and Fluoxetina Mabo[®]) was performed. The results obtained showed that the proposed methodology is adequate in terms of speed, cost, resolution power, precision and accuracy for the quality control of the enantiomeric composition of fluoxetine in pharmaceuticals. Transferability of the provided protocol to a laboratory with the ISO 17025 quality system implemented seems to be feasible.

Materials and methods

Instrumentation

A Beckman P/ACE MDQ Capillary Electrophoresis System with a diode array detector (Beckman Coulter, Fullerton, CA, USA), and 32Karat software version 8.0 was used throughout. A 50 μm inner diameter (i.d.) fused-silica capillary with total and effective lengths of 31.2 and 21 cm, respectively, was employed (Beckman Coulter, Fullerton, CA, USA). Electrophoretic solutions and samples were filtered through 0.45 μm pore size nylon membranes (Micron

Separation, Westboro, MA, USA) and degassed in an ultrasonic bath (JP Selecta, Barcelona, Spain) prior to use.

Chemicals

All reagents were of analytical grade. Sodium dihydrogen phosphate dihydrate was from Fluka (Buchs, Switzerland); highly sulfated- β -CD (HS- β -CD; 20% w/v) aqueous solution was purchased from Beckman Coulter (Fullerton, CA, USA). Racemic fluoxetine was kindly donated by Alter (Madrid, Spain). Ultra Clear TWF UV deionized water (SG Water, Barsbüttel, Germany) was used to prepare solutions. BGE containing 30 mM phosphate at pH 8.0 was obtained by dissolving the appropriate amount of sodium dihydrogen phosphate dihydrate in water and adjusting the pH with 1 M NaOH.

Methodology

Procedure for the preparation of standards and samples. A stock standard solution of racemic fluoxetine 200 mg/L was prepared in BGE. In order to obtain the calibration graphs, working solutions of fluoxetine containing between 10 and 50 mg/L of each enantiomer were obtained in duplicate by diluting the stock solution with BGE.

Samples were obtained from three pharmaceutical formulations containing racemic fluoxetine: Prozac[®] 20 mg (tablets), Fluoxetina Mabo[®] 20 mg (pills) and Fluoxetina Teva[®] 20 mg (pills). To prepare sample solutions, the content of five units was weighed, powdered (only for tablets) and mixed homogeneously. Then, the appropriate amount of the powder was weighed and dissolved in 100 mL of BGE by immersion in an ultrasonic bath (10 min), to achieve a final concentration of ~20 mg/L of each enantiomer.

Spiked samples were prepared in order to evaluate the accuracy of the method, by weighing and mixing homogeneously 0.9 g of sample powder and 0.1 g of standard fluoxetine. From these powder mixtures, solutions with a final concentration of ~40 mg/L of each enantiomer were prepared similarly to sample solutions.

Capillary conditioning. New capillaries were conditioned for a 15 min flush with 1 M NaOH at 60°C. Then they were rinsed for 5 min with deionized water and 10 min with separation buffer at 25°C. In order to obtain good peak shapes and reproducible migration data, the capillary was conditioned prior to each injection. In all cases, the conditioning run included the following steps: (1) 30 s rinse with deionized water; (2) 1 min rinse with 0.1 M NaOH; (3) 30 s rinse with deionized water; and (4) 1 min rinse with the separation buffer at 20 psi.

Procedure for the enantiomeric resolution of fluoxetine by EKC. A 30 mM phosphate solution of pH 8.0 was used as BGE. Fluoxetine standards and samples were injected hydrodynamically at 0.5 psi for 5 s. Before sample injection, the capillary was filled with a 0.25% HS- β -CD solution in BGE by applying 2 psi for 1 min. Separation was performed in normal polarity by applying 25 kV. In order to improve the peaks shape and decrease migration times, a 0.3 psi pressure was applied into the inlet vial throughout the analysis, because the combination of voltage and pressure in the CE separation gives higher efficiency. The capillary was thermostated at 30°C and the UV-detection wavelength was set at 200 nm.

Results and discussion

Development of an EKC chiral methodology

In preliminary studies, EKC conditions proposed in Asensi-Bernardi *et al.* (2010) (30 mM phosphate buffer at pH 7.0, 0.25% HS- β -CD, 30°C, 15 kV, with a little pressure of 0.3 psi applied to the inlet vial, and 220 nm as detection wavelength) were applied to the analysis of the pharmaceuticals in order to check their suitability in the present study. For this purpose, sample solutions with approximately 50 mg/L of racemic fluoxetine were prepared and injected into the electrophoretic system. Under these conditions, one of the pharmaceuticals (Prozac[®]) showed an interfering compound that co-eluted with the first enantiomer (E1), and prevented its quantification. Then, modifications in separation conditions were tested to improve the separation and efficiency of the electrophoretic peaks, trying to avoid this interference. For this purpose, voltages ranged between 5 and 25 kV were assayed using as BGE a 30 mM phosphate solution at pH 7.0, 7.5 and 8.0. In addition, the effect of the application of 0.3 psi to the inlet vial during the electrophoretic processes was also evaluated.

As expected, an increased voltage yielded shorter migration times and higher efficiencies and resolution (Heiger, 1992; Melanson *et al.*, 2001). However, the generation of Joule heat may limit the theoretical gain in resolution and efficiency with voltage. For fluoxetine, migration times of both enantiomers became shorter at higher voltages while resolution slightly decreased, being $R_s > 1.8$ in all cases. For E1, the increase of voltage provoked a decrease on efficiency at three pH values assayed. In the case of the second enantiomer, E2, similar behaviour was observed at pH 7.0 and 7.5. In contrast, the efficiency improved with the applied voltage for a pH buffer of 8.0. An increased voltage also had a good effect on the separation between E1 and the interference peak, so 25 kV was selected as the separation voltage.

On the other hand, the increase of pH values had no significant influence on migration times, but improved the resolution and in most cases the efficiency. Moreover, the application of a pressure of 0.3 psi to the inlet vial during the electrophoretic processes led to higher efficiency, with an improvement in peak shapes.

From the results obtained, an applied voltage of 25 kV, a pressure of 0.3 psi and a 30 mM phosphate solution at pH 8.0 as BGE were selected for the determination of fluoxetine enantiomers in pharmaceuticals. These conditions provided short analysis times (<2 min), high resolutions ($R_s = 2.4$) and good efficiencies for both enantiomers. Also the first enantiomer of Prozac[®] could be quantified without interferences using these working conditions, as can be seen in Fig. 1.

Application of the developed method to routine analysis of samples. Quality considerations

Accreditation entities, following ISO 17025 requirements, accept only validation obtained in accredited testing laboratories for auditing. This should be taken into account by research laboratories when developing analytical methods intended to become routine methods (Bisetty *et al.*, 2009). From a practical point of view, a partial-validation selecting the main fit-for-purpose features can be investigated as previous information for testing laboratories interested in an externally developed method. This fit-for-purpose selection should take into account the type of method (its objective) – in this case, the quantification of the analyte in a major–minor concentration level (one of the four

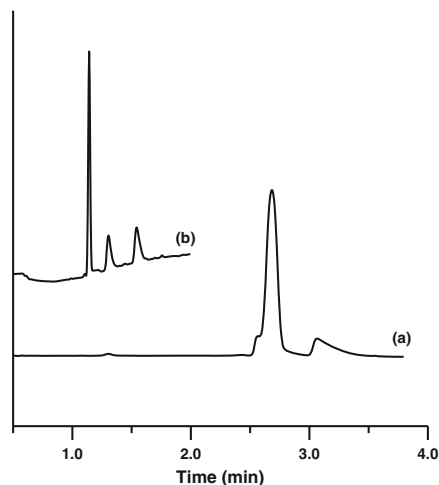


Figure 1. Electropherograms corresponding to the chiral analysis of Prozac[®] before (a) and after (b) the optimization of separation conditions performed to avoid interference. Experimental conditions are as described in the text.

categories from the International Conference on Harmonization (ICH) (Sagrado *et al.*, 2005). The features recommended for this ICH category are: confirmation of analyte identity (specificity), accuracy (or recovery), precision (preferably in intermediate precision conditions) and linearity (in the practical range; the full linear range estimation is not mandatory; Sagrado *et al.*, 2005). In the case of accuracy/precision, accreditation bodies demand experiments performed in presence of real matrices (e.g. the Spanish accreditation entity, ENAC). Other features, e.g. detection or quantification limits, were not considered, since they are not essential for this method-category. Anyway, if a full method validation is required by the accreditation body, this must be performed by the testing laboratory.

In this case, we adjusted the conditions to allow the determination of fluoxetine free of interferences from the matrix. Also, UV spectra recorded along peak elution were similar (not shown), indicating peak purity. Therefore, the confirmation of analyte identity could be considered guaranteed. Table 1 shows the results on linearity as well as precision (using samples of the pharmaceutical Fluoxetina Mabo[®]) and recovery (using samples of Fluoxetina Mabo[®] fortified with fluoxetine), in both cases, using data from intermediate precision conditions including data from three different working sessions, and three independent replicates in each session. Criteria for linearity (ENAC) and for recovery (*US Pharmacopeia*; Vila Jato, 2001) were used to contrast the results.

For practical reasons, most testing laboratories work during the routine phase, analyzing the samples only one time (single replicate; Bonet-Domingo *et al.*, 2007), performing new replicates for confirmation only if the result is out of the prefixed limits. Such practices are currently accepted by accreditation entities. On the other hand, a verification step is always required by these entities. Following this philosophy, a minimum-effort sequential protocol (including the previous acceptance criteria) is recommended for routine laboratories, before the analysis of samples: (1) method calibration (and application of the $R^2 > 0.995$ criterion for acceptance); (2) method verification by means of a fortification

Table 1. Main analytical features useful for partial validation following International Conference on Harmonization criteria (Sagrado *et al.*, 2005)

Features	Fluoxetine-E1	Fluoxetine-E2
<i>Linearity</i>		
Linear range	5–50 mg/L	5–50 mg/L
Order of magnitude ^a	1	1
Linear equation ^b	$y = 112.83 + 54.44x$	$y = 97.12 + 49.27x$
Determination coefficient (R^2) ^c	0.996	0.996
<i>Precision (sample analysis, n = 3^d)</i>		
Sample result	11.8 ± 1.7 mg	11.1 ± 1.9 mg
Intermediate precision (RSD)	14.8%	17.3%
<i>Accuracy (fortification assay, n = 3^d)</i>		
Intermediate recovery	92 ± 13	105 ± 6

^aAn order of magnitude >0.5 has been suggested for the concentration interval (Sagrado *et al.*, 2005).
^by = Corrected peak area.
^cThe current criteria used by ENAC for linearity (chromatography and related techniques) is $R^2 > 0.995$.
^dThe results are from three mean values in different sessions, each one estimated from three independent assays.

experiment, i.e. analyzing the sample and the spiked sample (and application of the recovery in the 85–115% criterion for acceptance; Sagrado *et al.*, 2005); and (3) first sample analysis [note that the sample results from the fortification experiment in (ii) can be used]; if the sample is within specifications, declare this status; otherwise, repeat the sample analysis and take the proper decision (e.g. if second analysis is outside specifications, declare this status for this sample).

Assuming that different samples must be analyzed, steps (2) and (3) will continue in the working session. Table 2 shows the starting application of this protocol, simulating the routine analysis phase with the three different formulations mentioned above. As can be observed for the three formulations assayed, the samples will be declared 'within specifications' according to the *US Pharmacopeia* criteria. Obviously, the testing laboratories could apply more complex protocols according with their internal Standard Operation Procedures.

Conclusions

In this work, an enantioselective method for the analysis of fluoxetine enantiomers in pharmaceuticals by counter-current

EKC has been developed, optimized for a matrix including an interfering compound and applied to the analysis of three pharmaceutical formulations. The developed method allows quantification of both enantiomers in <2 min with good resolution ($R_s = 2.4$) and low reagent consumption, and so has good features to be applied in routine laboratories – better than those reported in the literature. The proposed strategy is valid for research laboratories intending to develop new methods as well as for testing laboratories that must complete it with extra tasks. This paper can also help routine laboratories implementing quality systems to prepare their internal Standard Operation Procedures, based on the recommended protocol. In view of the current method evaluated in this work, we conclude that it can be considered provisionally fit for purpose with respect to the principal ICH features according to the method's objective. The results indicate that the method seems to be easily transferable since it fits currently accepted criteria.

Acknowledgments

The authors acknowledge the Generalitat Valenciana (GVA-COMP2011-002) and the University of Valencia (UV-INV-AE112-66280) for their financial support. L. Asensi-Bernardi

Table 2. Sample analysis of three pharmaceutical formulations according to the recommended protocol for testing laboratories^a. The results, expressed in milligrams, are for racemic fluoxetine (differences from the labeled value, 20 mg, are included) and its enantiomers

Pharmaceutical	Racemic fluoxetine (difference, %)	Fluoxetine-E1	Fluoxetine-E2	Stereoisomer ratio (E1/E2)
Fluoxetina Mabo [®]	21.0 (4.9) ^b	10.6	10.4	1.02
Prozac [®]	20.1 (0.5) ^b	9.0	11.1	0.81
Fluoxetina Teva [®]	21.4 (7.0) ^b	11.0	10.4	1.06

^aIn all cases, samples were analyzed after a calibration conform ($R^2 > 0.995$) and a verification conform (recovery in the 85–115% range). The verification was performed by analyzing the sample and a fortified sample. The result for the sample was used also for the sample analysis stage.

^bFor the three formulations, the samples will be declared 'within specifications' (differences in the ±15% interval). In this case they are also inside the expected range from the paired verification program of the AOAC, at the concentration level of this sample, ~0.0001 g/g ([–10, +7]%) (Sagrado *et al.*, 2005).

acknowledges the Spanish Ministry of Education for her FPU pre-doctoral research grant (AP2010-1984). The authors declare that there is no conflict of interest.

References

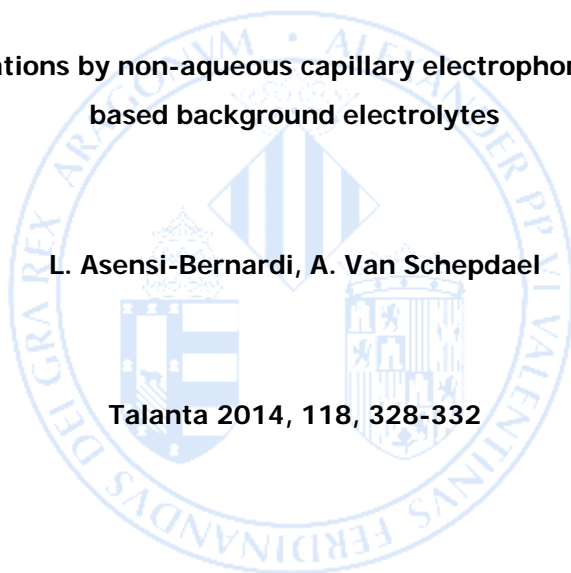
- Asensi-Bernardi L, Martín-Biosca Y, Villanueva-Camañas RM, Medina-Hernández MJ and Sagrado S. Evaluation of enantioselective binding of fluoxetine to human serum albumin by ultrafiltration and CE – experimental design and quality considerations. *Electrophoresis* 2010; **31**: 3268–3280.
- Barclay VKH, Tyrefors NL, Johansson IM and Petterson CE. Trace analysis of fluoxetine and its metabolite norfluoxetine. Part I: development of a chiral liquid chromatography–tandem mass spectrometry method for wastewater samples. *Journal of Chromatography. A* 2011; **1218**: 5587–5596.
- Bisetty K, Gumedde NJ, Escuder-Gilabert L and Sagrado S. Towards a quality guide to facilitate the transference of analytical methods from research to testing laboratories. A case study. *Journal of AOAC International* 2009; **92**: 1821–1832.
- Bonato PS, Jabor VAP, Paia FO and Lançote VL. Chiral capillary electrophoretic separation of selected drugs and metabolites using sulfated β -cyclodextrin. *Journal of Liquid Chromatography and Related Technologies* 2001; **24**: 1115–1131.
- Bonet-Domingo E, Grau-González S, Martín-Biosca Y, Medina-Hernández MJ and Sagrado S. Harmonized internal quality aspects of a multi-residue method for determination of forty-six semivolatiles compounds in water by stir-bar-sorptive extraction–thermal desorption gas chromatography–mass spectrometry. *Analytical and Bioanalytical Chemistry* 2007; **387**: 2537–2545.
- Chankvetadze B and Blaschke G. Enantioseparations in capillary electromigration techniques: recent developments and future trends. *Journal of Chromatography. A* 2001; **906**: 309–363.
- Chen FTA, Shen G and Evangelista RA. Characterization of highly sulfated cyclodextrins. *Journal of Chromatography. A* 2001; **924**: 523–532.
- Desiderio C, Rudaz S, Raggi MA and Fanali S. Enantiomeric separation of fluoxetine and norfluoxetine in plasma and serum samples with high detection sensitivity capillary electrophoresis. *Electrophoresis* 1999; **20**: 3432–3438.
- Heiger DN. *High Performance Capillary Electrophoresis – An Introduction*. Hewlett-Packard: France, 1992.
- Inoue T and Chang JP. Chiral separation of fluoxetine and its analogs with charged cyclodextrins by capillary electrophoresis. *Journal of Liquid Chromatography and Related Technologies* 2003; **26**: 2351–2367.
- Li H, Luo W, Hu X and Zhang H. Chiral resolution of basic pharmaceutical enantiomers by capillary zone electrophoresis. *Analytical Letters* 2003; **36**: 91–106.
- Li S and Vigh G. Single-isomer sulfated α -cyclodextrins for capillary electrophoresis: hexakis (2,3-di-O-methyl-6-O-sulfo)- α -cyclodextrin, synthesis, analytical characterization and initial screening tests. *Electrophoresis* 2004a; **25**: 2657–2670.
- Li S and Vigh G. Single-isomer sulfated α -cyclodextrins for capillary electrophoresis. Part 2: hexakis (6-O-sulfo)- α -cyclodextrin, synthesis, analytical characterization and initial screening tests. *Electrophoresis* 2004b; **25**: 1201–1210.
- Melanson JE, Barylak NE and Lucy CA. Dynamic capillary coatings for electroosmotic flow control in capillary electrophoresis. *Trends in Analytical Chemistry* 2001; **20**: 365–374.
- Olsen BA, Wirth DD and Larew JS. Determination of fluoxetine hydrochloride enantiomeric excess using high-performance liquid chromatography with chiral stationary phases. *Journal of Pharmaceutical and Biomedical Analysis* 1998; **17**: 623–630.
- Perrin C, Vander Heyden Y, Maftouh M and Massart DL. Rapid screening for chiral separations by short-end injection capillary electrophoresis using highly sulfated cyclodextrins as chiral selectors. *Electrophoresis* 2001; **22**: 3203–3215.
- Robertson DW, Krushinski JH, Fuller RW and Leander JD. Absolute configurations and pharmacological activities of the optical isomers of fluoxetine, a selective serotonin-uptake inhibitor. *Journal of Medicinal Chemistry* 1988; **31**: 1412–1417.
- Rudaz S, Calleri E, Geiser L, Cherkaoui S, Prat J and Veuthey JL. Infinite enantiomeric resolution of basic compounds using highly sulfated cyclodextrin as chiral selector in capillary electrophoresis. *Electrophoresis* 2003; **24**: 2633–2641.
- Rudaz S, Le Saux T, Prat J, Gareil P and Veuthey JL. Ultrashort partial filling technique in capillary electrophoresis for infinite resolution of tramadol enantiomers and its metabolites with highly sulfated cyclodextrins. *Electrophoresis* 2004; **25**: 2761–2771.
- Sagrado S, Bonet E, Medina MJ and Martín Y. *Manual práctico de calidad en los laboratorios. Enfoque ISO 17025*. AENOR: Spain, 2005.
- Scriba GKE. Fundamental aspects of chiral electromigration techniques and application in pharmaceutical and biomedical analysis. *Journal of Pharmaceutical and Biomedical Analysis* 2011; **55**: 688–701.
- Shamsipur M, Dasterjedi LS, Haghgoo S, Armspach D, Matt D and Aboul-Enen HY. Chiral selectors for enantioresolution and quantitation of the antidepressant drug fluoxetine in pharmaceutical formulations by ^{19}F NMR spectroscopic method. *Analytica Chimica Acta* 2007; **601**: 130–138.
- Suntornsuk L. Recent advances of capillary electrophoresis in pharmaceutical analysis. *Analytical and Bioanalytical Chemistry* 2010; **398**: 29–52.
- Vila Jato JL. *Tecnología Farmacéutica Volumen II: Formas farmacéuticas*. Síntesis: Spain, 2001.

Paper IV

Chiral separations by non-aqueous capillary electrophoresis in DMSO-based background electrolytes

L. Asensi-Bernardi, A. Van Schepdael

Talanta 2014, 118, 328-332





Chiral separations by non-aqueous capillary electrophoresis in DMSO-based background electrolytes

L. Asensi-Bernardi¹, A. Van Schepdael^{*}

Pharmaceutical Analysis, Department of Pharmaceutical and Pharmacological Sciences, KU Leuven, O&N 2, PB-923, Herestraat 49, B-3000 Leuven, Belgium

ARTICLE INFO

Article history:

Received 23 July 2013

Received in revised form

15 October 2013

Accepted 21 October 2013

Available online 26 October 2013

Keywords:

Carboxymethyl- γ -cyclodextrin

Chiral separation

DMSO

NACE

ABSTRACT

Capillary electrophoresis (CE) is a powerful technique for enantioseparations due to its high separation efficiency, high versatility, speed of analysis and low consumption of samples and reagents. Non-aqueous capillary electrophoresis (NACE) appears as a promising technique to perform enantioseparations when the drugs, chiral selectors or samples are non-water soluble. Chiral separations have been performed by NACE mainly using alcoholic solvents as BGEs, with problems of current breakdowns and changes in the BGE composition, due to their high volatility.

In this work, the suitability of DMSO as BGE in NACE has been evaluated. Different experimental variables affecting the enantioresolution of three drugs have been evaluated, finally achieving complete enantioresolution of two drugs (verapamil, $R_s=1.5$ and pindolol, $R_s=2.0$) and partial resolution of the third one (fenfluramine, $R_s=1.2$). DMSO has been demonstrated to be a good alternative to methanolic BGEs in NACE.

© 2013 Elsevier B.V. All rights reserved.

1. Introduction

Up to 50% of the commercialized pharmacologically active compounds are chiral, and differences in the pharmacological activity and/or the pharmacokinetics of their enantiomers are possible, due to the interactions with biomacromolecules such as proteins, enzymes, receptors or carriers that are optically active [1]. Several drugs have been recently commercialized as pure enantiomers, after discovering that their pharmacological activity was, mainly or exclusively, due to one of the enantiomers [2–5]. Also, due to the potential differences between the activities of a pair of enantiomers, the regulatory authorities declare that enantioselective studies of all new drugs, including single enantiomers and racemates, are mandatory. For all these reasons, the development of methods for the chiral analysis of drugs is of growing interest for the pharmaceutical industry [6].

Capillary electrophoresis (CE) is a powerful technique for enantioseparations due to its intrinsic characteristics such as high separation efficiency, high versatility, speed of analysis, low consumption of samples and reagents and low environmental impact [7]. The most common modality of CE employed for enantioseparations is electrokinetic chromatography (EKC), in which a chiral selector is added to the background electrolyte (BGE) and acts as a

pseudostationary phase. Usually, BGEs are aqueous and the chiral selectors employed are water soluble.

On the other hand, many candidate drugs are non-water soluble. This is actually one of the biggest problems for the pharmaceutical industry these days: the low solubility and dissolution rate of new pharmacologically active compounds. Alternatives to the classical EKC have been proposed in order to perform the chiral analysis of non-water soluble compounds: micellar electrokinetic chromatography (MEKC) and non-aqueous capillary electrophoresis (NACE) [8]. The use of non-aqueous solvents in CE (NACE) was introduced by Walbroehl and Jorgenson in 1984 [9] and the first chiral NACE application was presented in 1996 [10]. Chiral NACE can be considered as a complementary mode to aqueous separation since it facilitates the use of chiral selectors with a low solubility in water [11]. Another advantage is that the use of organic solvents enables poorly water soluble substances to be analyzed, and allows direct injection of organic extracts obtained after sample treatment [12]. The use of organic solvents in the background electrolyte (BGE) can enhance the resolution or the selectivity by tuning of the BGE composition, since different organic solvents have different acid–base behavior, which strongly affects the charge of the analytes, a key parameter for electrophoretic separations [8]. Also, the selector–selectand interactions are different depending on the solvent medium. Another advantage of NACE over aqueous CE is that low current values are obtained, so it is possible to apply high electric field strengths and high ionic strength buffers with no Joule heating, resulting in high separation efficiencies [8,12].

Several methods for the chiral separation by NACE have been published until now [11,13–19], mainly carried out in alcoholic and

^{*} Corresponding author. Tel.: +32 16 323443; fax: +32 16 323448.

E-mail address: ann.vanschepdael@pharm.kuleuven.be (A. Van Schepdael).

¹ Present address: Departamento de Química Analítica, Facultad de Farmacia, Universitat de València, C/Vicent Andrés Estellés s/n, E-46100 Burjassot, Valencia, Spain.

acetonitrile-based electrolytes, with the disadvantage of high volatility of the solvents which may affect the BGE composition during the run and cause current breakdowns. Also, methanol (MeOH) may be unable to assure the dissolution of poorly water-soluble and hydrophobic drugs. The use of dimethyl sulfoxide (DMSO) in NACE has been reported only a few times, mainly in chip-CE applications [20,21] and only in one case for a chiral separation [22], where few amino acids were partially or completely separated employing a cationic cyclodextrin. However, DMSO has good properties to be employed as a background electrolyte in NACE, since it has a high dielectric constant ($\epsilon=46.45$), and it is a non-toxic, non-hazardous, non-volatile solvent [20]. Also, the stability of samples in DMSO is higher than in alcoholic solvents due to its aprotic character. On the other hand, there is an important drawback of DMSO for chiral NACE: selector–selectand interactions, which are mainly intermolecular forces, are very weak in this medium, so achieving the enantioseparation may be difficult and a fine adjustment of the conditions becomes necessary.

In this work, the suitability of DMSO as BGE for performing chiral separations in NACE is evaluated, as an alternative that can be employed when the use of classical methanolic BGEs is not possible. An anionic cyclodextrin, carboxymethyl- γ -cyclodextrin (CM- γ -CD) has been employed as chiral selector, and the enantioseparation of three racemic drugs with different molecular sizes and functional groups (verapamil, pindolol and fenfluramine) has been studied. The influence of some experimental variables on the enantioseparation of these three drugs has been evaluated.

2. Materials and methods

2.1. Instrumentation

A Beckman P/ACE MDQ Capillary Electrophoresis System equipped with a diode array detector (Beckman Coulter, Fullerton, CA, USA), and 32Karat software version 8.0 was used throughout. A 75 μm inner diameter (i.d.) fused-silica capillary with total and effective lengths of 60.2 and 50 cm, respectively, was employed (Beckman Coulter, Fullerton, CA, USA). Detection wavelength was fixed at 270 nm due to the absorbance of UV light by DMSO at lower wavelengths (the cut-off wavelength for DMSO has been fixed around 260 nm in the literature). Sample tray temperature in the CE system was set at 20 °C for all experiments.

2.2. Chemicals and reagents

All reagents were of analytical grade. DMSO, MeOH, ammonium acetate (NH_4Ac), acetic acid (HAc) and sodium hydroxide (NaOH) were from Scharlau (Barcelona, Spain). Carboxymethyl- γ -cyclodextrin (average degree of substitution $\sim 3\text{--}5$, acidic form) was from Cyclolab (Budapest, Hungary). Fenfluramine hydrochloride and pindolol were kindly provided by Prof. Y. Vander Heyden, Vrije Universiteit Brussel, and verapamil hydrochloride by Prof. J. Crommen, University of Liège.

Background electrolytes were prepared by weighing or measuring the adequate amount of all the additives and bringing to final volume with DMSO. Stock solutions (1 mg mL^{-1}) of the racemic drugs were prepared by weighing the adequate amount of the drugs and bringing to 10 mL with DMSO. Working solutions (0.2 mg mL^{-1}) were prepared by dilutions of the stock solutions in DMSO. BGEs and drug solutions were stable at room temperature for at least 2 weeks. They were filtered through 0.45 μm pore size nylon membranes (Micron Separations, Westborough, MA, USA) prior to their injection in the CE system.

2.3. Methodology

2.3.1. Capillary conditioning

New capillaries were conditioned for 15 min by rinsing with 1 M NaOH at 60 °C. Then, they were rinsed for 5 min with deionized water and 10 min with BGE at 25 °C. At the beginning and end of each day, the capillary was rinsed with 1 M NaOH for 5 min, water for 5 min, and methanol for 5 min. Between runs, the capillary was rinsed for 2 min with methanol and 2 min with BGE. All steps were carried out at 20 psi.

2.3.2. Procedure for the study of enantioseparations by NACE

The initial composition of the background electrolyte was as follows: DMSO–MeOH 80:20, with 50 mM NH_4Ac , 1 M HAc and 40 mM CM- γ -CD. Initial experiments were carried out at 25 °C, applying a voltage of 20 kV (normal polarity). Experimental conditions for the enantioseparations were varied one by one, keeping the others at fixed values. After filling the capillary with the BGE, drug samples were injected hydrodynamically by applying 0.5 psi for 5 s. Separations were performed with normal polarity in all cases.

3. Results and discussion

The selection of initial conditions for the study (see Section 2.3.2.) was based on an overview of the literature about chiral NACE, in which buffering is done mainly using ammonium acetate/acetic acid systems. As we expected low current values and a possible lack of solubility of the buffer salts by using pure DMSO, a percentage of MeOH was added to the BGE. CM- γ -CD (acidic form) was selected as chiral selector due to its good solubility in the DMSO medium. It is important to use the acidic form of the CD because the sodium salt may be insoluble in non-aqueous solvents.

Using these initial conditions (BGE: DMSO–MeOH 80:20, with 50 mM NH_4Ac , 1 M HAc and 40 mM CM- γ -CD; capillary temperature, 25 °C and applied voltage, 20 kV), partial resolutions of 0.65 for verapamil (VER) and 0.69 for pindolol (PIN) were obtained. For fenfluramine (FEN), a little split of the peak was observed, but an R_s value could not be calculated. The calculation of R_s values was done using the following expression:

$$R_s = \frac{2(t_2 - t_1)}{W_2 + W_1} \quad (1)$$

where t_1 and t_2 are, respectively, the migration times of the first (E_1) and second (E_2) eluted enantiomers, and W_1 and W_2 are the peak widths at peak base.

An average current of $\sim 12.3\ \mu\text{A}$ was obtained with these conditions. The current was stable throughout the electrophoretic development.

A univariate optimization of the experimental conditions for the enantioseparation of three racemic drugs by NACE was carried out. This univariate procedure allows to see the effects of the different experimental variables one by one, and to better understand the mechanisms and effects responsible for the chiral separation. We consider that the study of the individual influences of variables in NACE is important, since there is still a lack of knowledge about the behavior of organic solvents and different buffer additives [12], and the way they can affect electrophoretic parameters such as peak efficiencies, selectivity or resolution. Also, as chiral NACE applications have been mainly studied with methanolic BGEs, the effects that could happen in a DMSO medium are still more unknown. So, taking as starting point the partial R_s obtained with the initial conditions, all experimental variables were adjusted in order to improve the R_s of enantiomers.

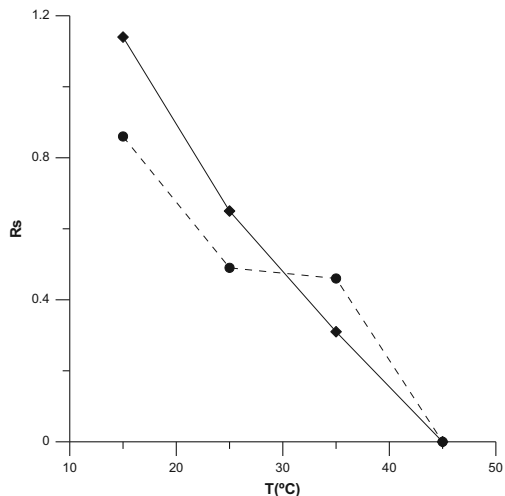


Fig. 1. Effect of the capillary temperature on the enantioresolution of VER (♦, solid line) and PIN (●, dashed line). Other experimental conditions: BGE DMSO–MeOH 80:20, 50 mM NH_4Ac , 1 M HAC, 40 mM CM- γ -CD, applied voltage 25 kV.

3.1. Effect of the capillary temperature

Capillary temperature is a key parameter for enantioseparations since it affects the mobility of the enantiomers and also the thermodynamic complexation equilibrium between the enantiomers and the chiral selector. In this work, capillary temperature was varied between 15 and 45 °C. As shown in Fig. 1 for VER and PIN, the enantioresolution of both drugs increases when the temperature is decreased. A similar effect was observed for FEN, with an increase in the peak split, but R_s values could not be calculated. This effect can be explained because a decrease in capillary temperature will increase the viscosity of the BGE, thus decreasing the mobility of the enantiomers and the EOF, with the consequence of higher R_s . Longer migration times are obtained in all cases with low temperatures: the migration time of the second enantiomer increases from 20.5 min at 45 °C to 37.1 min at 15 °C in the case of VER, from 16.6 (45 °C) to 28.6 min (15 °C) for PIN, and from 15.5 (45 °C) to 27.1 (15 °C) for FEN. A separation temperature of 15 °C was selected in all cases.

3.2. Effect of the separation voltage

As a consequence of the low currents obtained in NACE, high voltages can be employed thus improving the migration time of the enantiomers and the peaks' efficiency. Here the voltage ranged between 20 and 30 kV.

The increase in separation voltage considerably reduced the migration times of all the drugs, changing from 35–50 min with 20 kV to 23–33 min with 30 kV. This is due to the considerable increase of the current (from 8.2 μA at 20 kV to 12.6 μA at 30 kV). Also, the enantioresolution was slightly improved when higher voltages were employed. Fig. 2 shows the electropherograms corresponding to the separation of verapamil enantiomers at the three applied voltages, where the effect of the voltage on the R_s and migration time can be seen.

3.3. Effect of the CM- γ -CD concentration

The concentration of chiral selector is usually the most influential variable on enantioseparations. When cyclodextrins are employed as

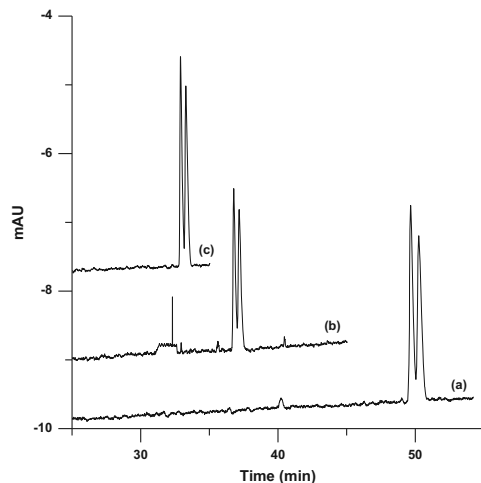


Fig. 2. Electropherograms corresponding to the enantioresolution of VER at three separation voltages: 20 kV (a), 25 kV (b) and 30 kV (c). Capillary temperature: 15 °C. Other experimental conditions as in Fig. 1.

chiral selectors, the separation mechanism is the formation of inclusion complexes of the enantiomers in the hydrophobic cavity of the cyclodextrin. The complexation equilibrium is affected by the concentrations of both the drug enantiomers and the cyclodextrins, so an increase in the CD concentration will favor the formation of the diastereomeric complexes responsible for the chiral separation. This is especially important in NACE because the interaction between the enantiomers and the CD is less favoured in organic media than in water.

In this work, the concentration of CD is changed between 10 and 70 mM for all drugs. Fig. 3 shows the enantioresolution values obtained for VER, PIN and FEN with all the CD concentrations. As shown in the figure, 10 mM CM- γ -CD was too low to provide any enantioresolution of drugs. With 20 mM, a partial R_s value is obtained for VER, but still no R_s was found for PIN and FEN. The maximum R_s value was obtained for PIN and FEN with 40 mM CM- γ -CD, decreasing with higher CD concentrations. For VER, the R_s was slightly higher with 50 mM CM- γ -CD, but 40 mM was enough to provide good enantioresolution, especially when combined with the best conditions selected in other variables. So, as the CD concentration is the most critical variable in terms of analysis cost, 40 mM was selected as the best concentration for the three drugs studied.

3.4. Effect of the percentage of methanol

The physicochemical properties of DMSO and MeOH are quite different: MeOH has lower dielectric constant (ϵ), much lower viscosity (η), lower boiling point, and lower autoprotolysis constant (pK_{auto}), which implies that more ions in solution will be found in methanolic BGEs [8]. So, the percentage of MeOH will modify considerably the physicochemical properties of the BGE and will strongly affect the enantioresolution. In this work, since our main aim was to employ a DMSO-based BGE, the percentage of MeOH was varied from 0% to 30%, so the main component of the BGE was DMSO in all conditions.

A decrease in MeOH percentage increases the migration times of all compounds. In the case of VER, best R_s is obtained with 20% MeOH, so it is selected as optimum. For PIN, there is a clear decrease

in R_s when the MeOH percentage is decreased (Fig. 4(1)), so 30% is selected as best option since it combines better R_s with shorter migration time. The case of FEN (Fig. 4(2)) is the opposite; the split of peaks is larger without MeOH so a pure DMSO BGE is selected as best option.

The differences between the three compounds in the optimum MeOH percentage should be due to a dual mechanism that affects the enantioresolution: on the one hand, the increase in MeOH increases the ϵ/η ratio of the BGE, which is a measure of the speed of the analysis, and decreases in consequence the migration times, so, if peaks migrate faster, less R_s can be expected *a priori* (this is the case of FEN). On the other hand, as DMSO is an aprotic solvent, the increase of MeOH can increase the ionization degree of the drugs, enhancing the interaction with the anionic CD (the case of PIN). For VER, both opposite effects lead to an intermediate BGE composition (DMSO–MeOH 80:20) as the best option.

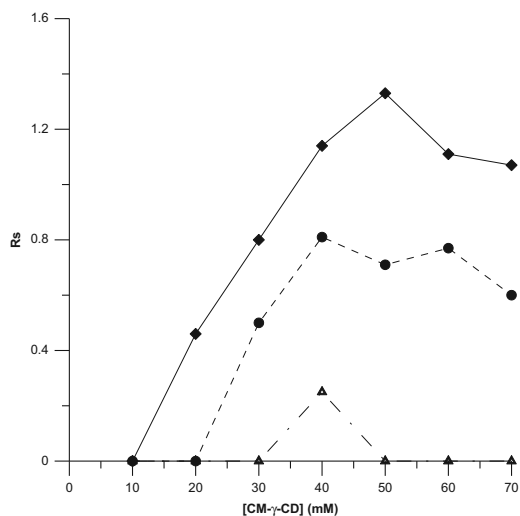


Fig. 3. Effect of CD concentration on the enantioresolution of VER (\blacklozenge , solid line), PIN (\bullet , dashed line) and FEN (\blacktriangle , semi-dashed line). Capillary temperature 15 °C, applied voltage 30 kV. Other experimental conditions as in Figs. 1 and 2.

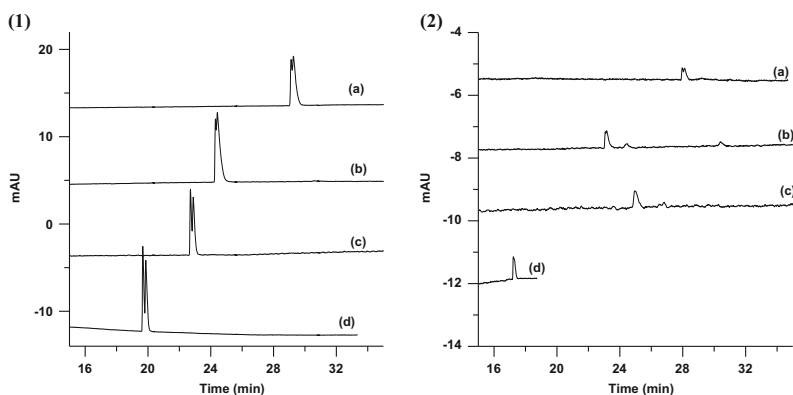


Fig. 4. Electropherograms corresponding to the enantioseparation of PIN (1) and FEN (2), with different MeOH percentages in the BGE: 0% (a), 10% (b), 20% (c) and 30% (d). [CM- γ -CD], 40 mM. Other experimental conditions as in Fig. 3.

3.5. Effect of the NH_4Ac and HAc concentration

The electrophoretic and electroosmotic mobilities are inversely proportional to the concentration of salts in the BGE [23], so longer

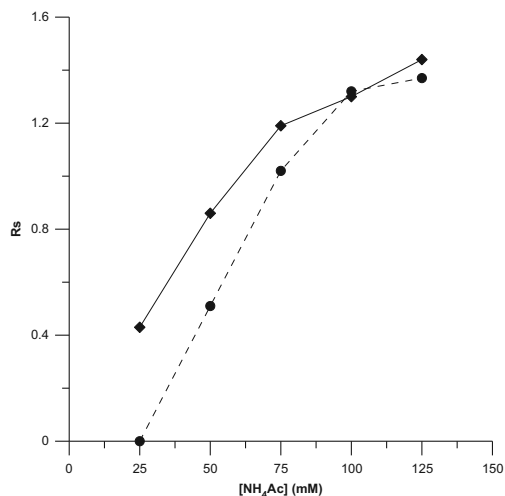


Fig. 5. Effect of $[\text{NH}_4\text{Ac}]$ on the enantioresolution of VER (\blacklozenge , solid line) and PIN (\bullet , dashed line). MeOH percentage: 20%. Other experimental conditions as in Fig. 4.

Table 1

Experimental conditions selected for the enantioseparation of each drug by NACE, and the corresponding electrophoretic parameters obtained in each case.

	VER	PIN	FEN
Temperature (°C)	15	15	15
Voltage (kV)	30	30	30
[CM- γ -CD] (mM)	40	40	40
% MeOH	20	30	0
$[\text{NH}_4\text{Ac}]$ (mM)	125	125	125
[HAc] (M)	1	0.5	0.5
R_s	1.5	2.0	1.2
Analysis time (min)	43	25	42
Current (μA)	25	29	17

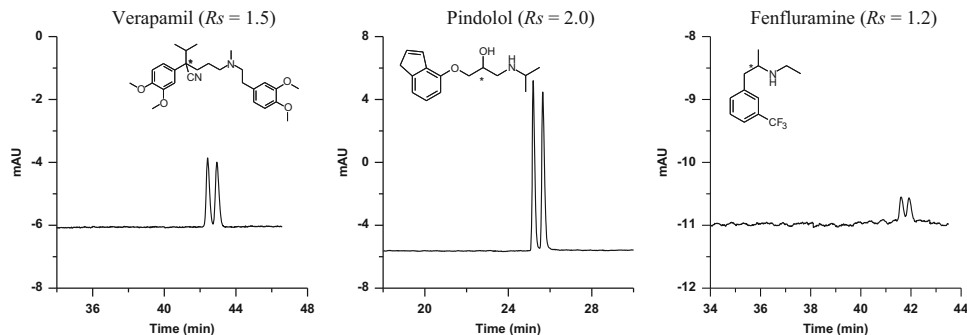


Fig. 6. Electropherograms corresponding to the selected enantioresolution conditions for VER, PIN and FEN. Experimental conditions detailed in Table 1.

migration times and better selectivities are expected when the buffer concentration is increased. The NH_4Ac concentration ranged in this work from 25 to 125 mM (a BGE without NH_4Ac was also tested, but no stable current was obtained). Better R_s values but longer migration times were obtained with higher NH_4Ac concentrations, as expected. Due to the notable improvement on the R_s of enantiomers (Fig. 5), 125 mM was selected as the best NH_4Ac concentration for all tested compounds.

The HAC concentration was varied between 0.5 and 1.5 M. The differences in HAC concentration did not affect so much the migration time and the resolution of enantiomers. Slightly better R_s values (or peak split, in the case of FEN) were found using 1 M HAC in the case of VER and 0.5 M for PIN and FEN, so these conditions were selected.

3.6. Selected conditions

Table 1 summarizes the experimental variables studied and the best conditions selected for the enantioresolution of VER, PIN and FEN in this DMSO-based NACE. It also shows the R_s values obtained for the three drugs, the analysis times of the three enantioresolutions (migration times of the second eluted enantiomers), and the current values obtained. As can be seen in Table 1, complete enantioresolution of VER and PIN and partial R_s of FEN were obtained. The electropherograms corresponding to these best experimental conditions are shown in Fig. 6, together with the chemical structures of the three drugs.

4. Conclusions

In this work, the suitability of DMSO to be employed as BGE in NACE has been evaluated. Different experimental conditions were tested in order to achieve the best enantioresolution conditions for three racemic drugs: verapamil, pindolol and fenfluramine. Complete enantioresolution was obtained for VER and PIN while a partial R_s value was obtained for FEN. Best enantioresolutions were obtained with low capillary temperatures, high separation voltages and high concentration of salts in the BGE, in general terms. For the other variables, individual effects may be considered. The analysis times were lower than 45 min in all cases (43 min for VER, 25 for PIN and 42 for FEN). These analysis times are *a priori* long for an electrophoretic separation, due to the high viscosity and relatively low ϵ/η ratio of DMSO, but are comparable

with chromatographic enantioresolutions performed with chiral stationary phases.

It is also remarkable that in all the tested experimental conditions current values were stable and there were no current breakdowns, so DMSO has proved to be a good solvent to be employed in NACE, combined (or not) with a small percentage of MeOH in order to modulate the physicochemical properties of the BGE. DMSO appears to be a good alternative for NACE when, due to solubility, stability or volatility problems, the common methanolic BGEs cannot be employed.

Acknowledgments

L. Asensi-Bernardi acknowledges the Spanish Ministry of Education for her predoctoral FPU scholarship (AP2010-1984).

References

- [1] J. Caldwell, J. Chromatogr. A 694 (1995) 39–48.
- [2] J.M. Monti, S.R. Pandi-Perumal, Neuropsychiatr. Dis. Treat. 4 (2007) 441–453.
- [3] A. Klegerisa, J. Maguire, P.L. McGeer, J. Neuroimmunol. 152 (2004) 73–77.
- [4] B. Leonard, D. Taylor, J. Psychopharmacol. 24 (2010) 1143–1152.
- [5] R. Kikura-Hanajiri, M. Kawamura, A. Miyajima, M. Sunouchi, Y. Goda, Anal. Bioanal. Chem. 400 (2011) 165–174.
- [6] G.K.E. Scriba, J. Pharm. Biomed. Anal. 55 (2011) 688–701.
- [7] B. Chankvetadze, G. Blaschke, J. Chromatogr. A 906 (2001) 309–363.
- [8] L. Geiser, J.-L. Veuthey, Electrophoresis 30 (2009) 36–49.
- [9] Y. Walbroehl, J.W. Jorgenson, J. Chromatogr. 315 (1984) 135–143.
- [10] F. Wang, M.G. Khaledi, Anal. Chem. 68 (1996) 3460–3467.
- [11] V. Maier, V. Ranc, M. Švidrnoch, J. Petr, J. Ševčík, E. Tesárová, D.W. Armstrong, J. Chromatogr. A 1237 (2012) 128–132.
- [12] M.-L. Riekkola, Electrophoresis 23 (2002) 3865–3883.
- [13] B. Chen, Y. Du, H. Wang, Electrophoresis 31 (2010) 371–377.
- [14] A. Rousseau, P. Chiap, R. Oprean, J. Crommen, M. Fillet, A.-C. Servais, Electrophoresis 30 (2009) 2862–2868.
- [15] A. Rousseau, M. Pedrini, P. Chiap, R. Ivanyi, J. Crommen, M. Fillet, A.-C. Servais, Electrophoresis 29 (2008) 3641–3648.
- [16] L. Huang, J. Lin, L. Xu, G. Chen, Electrophoresis 28 (2007) 2758–2764.
- [17] J. Olsson, F. Stegander, N. Marlin, H. Wan, L.G. Blomberg, J. Chromatogr. A 1129 (2006) 291–295.
- [18] M. Lämmerhofer, J. Chromatogr. A 1068 (2005) 3–30.
- [19] F. Wang, M.G. Khaledi, J. Chromatogr. A 875 (2000) 277–293.
- [20] N. Nuchtavorn, P. Smejal, M.C. Breadmore, R.M. Guijt, P. Doble, F. Bek, F. Foret, L. Suntornsuk, M. Macka, J. Chromatogr. A 1286 (2013) 216–221.
- [21] J. Wang, M. Pumera, Anal. Chem. 75 (2003) 341–345.
- [22] F. Wang, M.G. Khaledi, J. Chromatogr. A 817 (1998) 121–128.
- [23] G.M. Janini, H.J. Issaq, in: N.A. Guzmán (Ed.), Capillary Electrophoresis Technology, Marcel Dekker Inc., New York, 1993, pp. 119–160.

Paper V

Evaluation of enantioselective binding of fluoxetine to human serum albumin by ultrafiltration and CE – Experimental design and quality considerations

L. Asensi-Bernardi, Y. Martín-Biosca, R.M. Villanueva-Camañas, M.J. Medina-Hernández and S. Sagrado

Electrophoresis 2010, 31, 3268-3280

Lucía Asensi-Bernardi¹
Yolanda Martín-Biosca¹
Rosa María Villanueva-
Camañas¹
María José Medina-
Hernández¹
Salvador Sagrado Vives^{1,2}

¹Departamento de Química
Analítica, Facultad de Farmacia,
Universidad de Valencia,
Burjassot, Valencia, Spain
²Centro Interuniversitario de
Reconocimiento Molecular y
Desarrollo Tecnológico (IDM).
Unidad mixta Universidad
Politécnica de Valencia-
Universidad de Valencia, Spain

Received April 30, 2010
Revised June 10, 2010
Accepted June 10, 2010

Research Article

Evaluation of enantioselective binding of fluoxetine to human serum albumin by ultrafiltration and CE – Experimental design and quality considerations

Several pharmacokinetic processes are affected by enantioselectivity (ES). At the level of distribution, protein binding (PB) is one of the most important. The enantioselective binding of fluoxetine (FLX) to HSA has been evaluated in this work by ultrafiltration of FLX–HSA mixtures and chiral analysis of unbound fractions by EKC-CD. PB, affinity constants (K) and ES were obtained for both enantiomers of FLX. In order to improve the consistency of the estimations, the evaluation of affinity constants of each enantiomer was performed using two designs, one keeping constant the total concentration of protein and varying the total concentration of the enantiomers, and the other in the opposite way, in both cases *via* an unusual short-concentration interval strategy to assure model validity. Different mathematical approaches were compared and characterised and some of them, judged as the most consistent under the experimental conditions used, were selected to provide final estimates. Quality considerations include criteria for three critical aspects: (i) detecting/eliminating outliers, (ii) checking the number of binding sites in the protein and (iii) evaluating the robustness of each approach. The differences on estimates from the selected approaches were used as an uncertainty source to delimit the reported values. The ES of HSA for FLX enantiomers was approximate. Estimates include the assumptions of independent and competitive models. In the last case, a SIMPLEX function was designed capable of simultaneously optimizing the non-linear binding models for both enantiomers, thus improving the consistence of results.

Keywords:

EKC / Enantioselective binding / Fluoxetine / HSA / Quality protocol
DOI 10.1002/elps.201000250

1 Introduction

Drug action is the result of several pharmacokinetic and pharmacological processes. Most of them present a high degree of stereoselectivity, resulting in a difference between the activities of drug enantiomers [1]. Pharmacokinetic processes affected by enantioselectivity (ES) are drug absorption, distribution, metabolism and excretion. At the level of distribution, one important effect is the protein binding (PB). HSA is the most abundant protein in human plasma, and it presents a high degree of enantioselective

interaction with drugs [2]. Stereoselectivity in binding with HSA can have an important effect on the drug disposition such as first-pass metabolism, metabolic and renal clearance, and distribution to other compartments. Most of the interactions with the HSA occur at two well-defined regions of the HSA molecule, known as sites I and II [2–4].

When protein and racemic drugs interact, two diastereomeric adducts are formed with potential differences in the PB, which may result in different pharmacokinetic profiles for the individual enantiomers [5]. For the investigation of drug enantioselective binding, different approaches have been proposed. The majority of these methodologies include a first step in which the free drug fraction is separate from the bound drug once the drug-protein equilibrium has been reached using different techniques, such as the traditional equilibrium dialysis [3], ultracentrifugation [3] or ultrafiltration [4]. The second step includes chiral analysis of enantiomers in the unbound fraction using different techniques such as LC and CE and different chiral selectors, for instance using EKC [6].

From a pharmacokinetic point of view the estimation of the percentage of PB at physiological conditions is an important parameter. In the case of enantiomers, besides

Correspondence: Professor Salvador Sagrado Vives, Departamento de Química Analítica, Facultad de Farmacia, Universitat de Valencia, C/Vicent Andrés Estellés s/n, E-46100 Burjassot, Valencia, Spain
E-mail: sagrado@uv.es
Fax: +34-963544953

Abbreviations: C_{ss}, stationary state-plasmatic concentration; ES, enantioselectivity; FLX, fluoxetine; HS- β -CD, highly sulphated- β -CD; ID, identification number

their PB, it is also appropriate knowing the ES degree obtained, e.g. from their affinity constant K values. To obtain K it is necessary to assume a concrete binding model. Together with K , the model allows estimating the number of binding sites *per* protein molecule, n .

Psychoactive drugs are the most used drugs in our society. Antidepressants, hypnotics and many other families are purchased every day by different kinds of patients. Usually, these drugs have been synthesised and commercialised as racemic forms, but recently the industry is interested in the introduction of pure enantiomers in the pharmaceutical market. Pharmacokinetic and pharmacological properties of each enantiomer have to be studied nowadays for these drugs in pre-clinical phases. Fluoxetine (FLX) is a potent and selective inhibitor of the neuronal serotonin-uptake carrier and is a clinically effective antidepressant. FLX is used therapeutically as the racemate although a stereospecificity associated with its interactions with the serotonin-uptake carrier has been demonstrated [7]. Recently, the interaction between HSA and FLX has been studied by using different spectroscopic techniques, *viz.*, fluorescence, UV–vis absorption, circular dichroism and FTIR [8]. The reported value of binding constant, K , of FLX-HSA at 310°K (*i.e.* 36.84°C) was 1.45×10^3 ($\log K = 3.16$), while the number of binding sites, n , was almost equal to unity. The results correspond to an experimental design where HSA was kept constant at 2.5 μM and the drug was varied from 10 to 100 μM . The authors also used warfarin, ibuprofen and digitoxin as markers to locate the has-binding sites, I, II and III, respectively. They found that the drug competes with warfarin for site I in the protein (decreasing the K value for FLX, while it remained almost same in the presence of ibuprofen and digitoxin). So, they postulated that FLX is most likely bound to site I.

The interaction between small molecules and HSA is a complex process. Sometimes this point is disregarded and bad estimates are frequent [9]. In order to perform estimations, a model should be supposed, including some assumptions that should be verified (as far as possible). Also experimental conditions to *a priori* fit the assumptions should be selected. In this paper we have estimated the affinity constant of enantiomers of FLX for HSA. For this purpose, a methodology that includes the ultrafiltration of pre-equilibrated samples containing HSA and racemic FLX and the analysis of the unbound drug fraction by EKC with the highly sulphated- β -CD (HS- β -CD) as chiral selector, was applied. The affinity constants have been estimated using two experimental designs involving total enantiomer and HSA concentrations, selecting a short-concentration interval strategy in order to avoid conditions far from the physiological ones and trying to be consistent with the model assumptions. Different mathematical approaches were used evaluating their consistence. Quality considerations were included involving outliers identification/elimination, assumption verification and uncertainty estimation. The ES of HSA for FLX enantiomers as well as the PB percentage at physiological conditions were approximate.

2 Materials and methods

2.1 Instrumentation

A Beckman P/ACE MDQ Capillary Electrophoresis System equipped with a diode array detector (Beckman Coulter, Fullerton, CA, USA), and 32Karat software version 8.0 was used throughout. A 50 μm id fused-silica capillary with total and effective lengths of 31.5 and 21 cm, respectively, was employed (Beckman Coulter). Electrophoretic solutions and samples were filtered through 0.45 μm pore size nylon membranes (Micron Separation, Westboro, MA, USA) and degassed in an ultrasonic bath (JP Selecta, Barcelona, Spain) prior to use. A Crison Micro pH 2000 pHmeter from Crison Instruments (Barcelona, Spain) was employed to adjust the pH of buffer solutions.

A Selecta thermostatised bath (JP Selecta) was used for samples incubation. For the ultrafiltration of samples, Microcon YM-10 cellulose filters of a molecular weight of 10 000 MVCO (Millipore Corporation, Bedford, MA, USA) and a centrifuge Heraeus Biofuge Strate (Heraeus, Madrid, Spain) were used.

2.2 Chemicals and standard solutions

All reagents were of analytical grade. HSA fraction V was purchased from Sigma (St. Louis, MO, USA); sodium dihydrogen phosphate dihydrate from Fluka (Buchs, Switzerland); HS- β -CD (20% w/v) aqueous solution was purchased from Beckman Coulter; Racemic FLX was kindly donated by Alter (Madrid, Spain). Ultra Clear TWF UV deionised water (SG Water, Barsbüttel, Germany) was used to prepare solutions.

Separation buffer in EKC containing phosphate 30 mM at pH 7.0 was obtained by dissolving the appropriate amount of sodium dihydrogen phosphate dehydrate in water and adjusting the pH with 1 M NaOH. Similarly, phosphate buffer 67 mM of pH 7.4 was prepared for the study of binding to HSA. Aliquots of 1000 μM HSA stock solution were daily prepared by weighting the corresponding amount of protein powder and dissolving it with 67 mM phosphate buffer.

A stock standard solution of FLX 1000 μM was prepared in the separation buffer. In order to obtain the calibration graphs for the analysis of samples, working solutions of FLX containing different concentrations of enantiomers (between 25 and 250 μM of each enantiomer) were obtained in duplicate by diluting the stock standard solution with 30 mM phosphate buffer.

2.3 Methodology

2.3.1 Experimental designs

We have planned two experimental designs, one keeping the concentration of protein constant (P -constant) and varying

the concentration of FLX and the other one keeping the concentration of FLX, and therefore of their enantiomers, constant (*D*-constant) and varying concentration of protein (see Table 1). In both designs five concentration levels were used and two independent replicates *per* level, totalling 18 independent mixtures (two of them used in both designs).

2.3.2 Procedure for separation and analysis of unbound FLX fraction to HSA

Mixtures containing different FLX and HSA concentrations were prepared in duplicate by dilution of the stock solutions of drug and protein with phosphate buffer at 67 mM and pH 7.4. All these mixtures were allowed to reach equilibrium for 30 min in a water bath at 36.5°C and were filtered through cellulose filters by centrifugation at 9000 rpm for 30 min. Adsorption of the drug on the cellulose filters was observed, so the calibration standards were processed *via* the methodology used for samples, to account for this effect. The ultrafiltrate was directly injected into the EKC system.

2.3.3 Capillary conditioning

New capillaries were conditioned for 15 min flush with 1 M NaOH at 60°C. Then, they were rinsed for 5 min with

deionised water and 10 min with separation buffer at 25°C. In order to obtain good peak shapes and reproducible migration data, the capillary was conditioned prior to each injection. In all cases, the conditioning run included the following steps: (i) 30 s rinse with deionised water, (ii) 1 min rinse with 0.1 M NaOH and (iii) 30 s rinse with deionised water at 20 psi. Before chiral selector and sample injection the capillary was also rinsed with the separation buffer for 1 min at 20 psi.

2.3.4 Procedure for enantiomeric resolution of FLX by EKC and HS-β-CD as chiral selector

For all experiments, a 30 mM phosphate solution of pH 7.0 was used as electrophoretic buffer. A 0.25% HS-β-CD solution obtained from 20% w/v HS-β-CD by dilution with the separation buffer was used to carry out the enantio-resolution of FLX enantiomers. FLX solutions (ultrafiltrated fractions; calibration and mixture solutions) were injected hydrodynamically at 0.5 psi for 5 s. Before sample injection, the capillary was filled with the HS-β-CD solution by applying 2 psi for 1 min. Separation was performed in normal polarity by applying 15 kV. In order to improve the peaks shape and decrease migration times, a 0.3 psi pressure was applied into the inlet vial throughout the analysis. The capillary was thermostated at 30°C and the UV-detection wavelength was set at 220 nm. In order to avoid the effect of buffer depletion, buffer vials were changed after one run (in samples) and two runs (in calibration standards). Under the selected separation conditions a medium resolution of 3.5 was obtained for the FLX enantiomers (Fig. 1).

Table 1. Experimental data^{a)}

ID ^{b)}	<i>D</i> (μM)	<i>P</i> (μM)	<i>d</i> _{E1} (μM)	<i>d</i> _{E2} (μM)
<i>P</i> -constant design				
1	78.9	476.6	7.8	13.9
2			7.3	12.2
3	105.3		7.6	15.7
4			7.8	19.5
5	131.6		11.5	19.9
6			10.4	19.8
7	157.9		17.2	25.8
8			13.8	28.9
9	184.2		18.3	34.4
10			17.6	29.5
<i>D</i> -constant design				
11	131.6	250.9	21.8	40.7
12			21.4	38.9
13 ^{c)}		301.0		
14			15.3	30.2
15		351.2	13.7	26.0
16			12.6	25.4
17		401.4	10.8	21.1
18			11.5	23.0
19 ^{d)}		476.6	11.5	19.9
20 ^{d)}			10.4	19.8

a) Data were transformed to M units for calculations.

b) Identification number to refer to individual data along the text.

c) Data for ID = 13 was eliminated for the studies (see Section 3.3).

d) IDs 19 and 20 are repeated from IDs 5 and 6 data, used in both designs.

2.4 Software

Routines made/adapted in MATLAB[®] 4.2 were used for calculations. The results generated were verified using EXCEL[®] and STATGRAPHICS[®]. In some calculations a SIMPLEX algorithm routine was used (non-linear fitting).

3 Results and discussion

There are numerous papers concerning PB. Unfortunately, nomenclature is not uniform and sometimes ambiguous words or symbols are encountered, and some information remains unclear. To avoid this, Appendix A shows the nomenclature used along the text concerning the PB process (in some cases the general nomenclature, valid for molecules, was adapted to refer to enantiomers). It is also common in these studies using a single approach to perform the estimations, with little or null attention to its consistence. Appendix B shows the equations used for calculations, as well as comments related to the degree of consistency involving some assumptions to simplify them. In this sense, several assumptions are only consistent in the

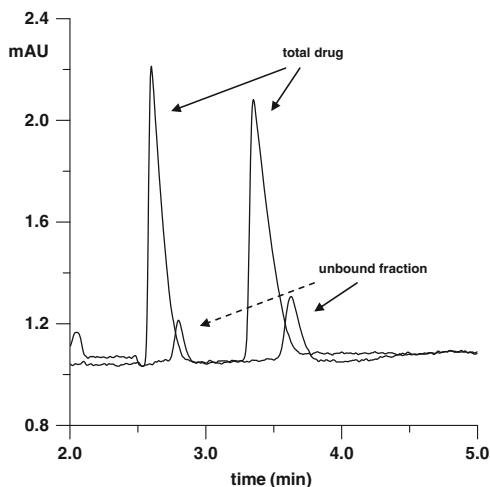


Figure 1. Electropherograms obtained for a sample containing racemic FLX (total drug) and the unbound fraction after FLX-HSA incubation and ultrafiltration processes (HSA 476.6 μM). The enantiomers concentration was 105.3 μM in both cases. Separation conditions: HS- β -CD 0.25% as chiral selector (rinsed at 2 psi for 1 min), 30 mM phosphate buffer, pH 7, 15 kV (+0.3 psi) and 30°C. The sample was injected hydrodynamically at 0.5 psi for 5 s.

case of low D values (*i.e.* low D/P ratios; an uncommon experimental situation in most papers), which habitually agrees with the physiological situation. We have first investigated the physiological concentrations of FLX and HSA. Appendix C shows some data related to FLX and HSA concerning the binding process.

3.1 Pharmacokinetic data and physiological conditions

Appendix C includes an in-house approximation of the drug stationary state-plasmatic concentration (C_{ss}), based on pharmacokinetic data for FLX. The approximated value of $C_{ss} \sim 0.2 \mu\text{M}$ (after normal dose) was obtained for the molecule (so a concentration of 0.1 μM would correspond to its enantiomers). This is consistent with published data for enantiomers of FLX. Plasmatic concentration of enantiomers of FLX, investigated in 131 adult patients receiving long-term FLX of 10–60 mg/day (mean, 24 ± 10 mg/day), provide mean values of 0.186 and 0.067 μM for S-FLX and R-FLX, respectively [10].

These results allow estimating D under physiological conditions, *i.e.* $D \sim 0.1 \mu\text{M}$ (for each enantiomer). Since $P \sim 600 \mu\text{M}$, the physiological D/P ratio could be established in < 0.0002 . The low D (and D/P ratio) suggests that several assumptions indicated in Appendix B should be satisfied at the physiological level, for instance, $m = 1$ to characterise the FLX–HSA binding interaction (Appendix B, footnote d).

From the available data of PB for FLX (PB $\sim 94.75\%$; Appendix C), which is assumed to correspond mainly to HSA under physiologic conditions, a value of K_1 could be estimate from Eq. (6a) (Appendix B). A value of $\log K_{FLX} = 4.78$ (for FLX, not their enantiomers) is obtained. The validity of Eq. (6a) (which assumes $K_1 d < 1$) could be assessed approximating the free FLX concentration (d_{FLX}), from PB and the physiological FLX concentration ($C_{ss} \sim 0.2 \times 10^{-6} \text{M}$), as indicated in Appendix C; $d_{FLX} \sim 1 \times 10^{-8} \text{M}$; then $K_{FLX} \times d_{FLX} \sim 0.00063 < 1$ (Error $\sim 0.06\%$; therefore the assumption is fulfilled). Note that the estimated $\log K_{FLX}$, 4.78, is more than one order of magnitude higher than the reported one, 3.16 [8], obtained under experimental conditions far from the physiological ones.

3.2 Experimental design and data

Numerous published papers use large-concentration ranges, under a single experimental design, for instance, fixing P and varying D along several of orders of magnitude. Large D -ranges partially reduce the impact of inconsistent approaches (*e.g.* Scatchard plot, [11] and references therein) on the estimates, but there is not guaranty on the unique-model validity (Appendix B) and implies working too far from the real physiological concentrations. For instance, experiments performed at $D/P > 1$ (in the opposite of physiological conditions) are habitual. An example is the data reported from FLX-HSA binding, using D/P ratios from 4 to 40 [8] (in contrast to the estimated D/P ratio < 0.0002 at physiological level, Section 3.1). On the other hand, some authors have reported the influence of binding parameter estimates with P [9, 12, 13]; accordingly, the use of P far from the physiological one could provide useless estimations.

We have adapted the concentrations to the instrument features, but trying to approximate as close as possible the physiological concentrations, as well as covering possible factor-effects on the estimates. Thus, we have established the following criteria: (i) Combining two experimental designs, P -constant (varying D) and D -constant (varying P), to have independent results and to control the possible P -concentration effect (ii) Fixing the concentration ranges keeping $D/P < 1$; in the P -constant design the minimum D was fixed taking into account the approximate quantification limit for d_1 and d_2 , while in the D -constant case, maximum P was fixed close the physiological concentration (in the hypoalbuminemia-normal levels frontier [14]).

Previous assays suggest that a value of $\sim 10 \mu\text{M}$ of racemic FLX (*i.e.* d_{FLX}) provides the minimum acceptable signals to quantify the enantiomers (note that this is just an approximation of the quantification limit). Employing $\log K_{FLX} \sim 4.78$ as a provisional estimation for FLX (Section 3.1), the total D_{FLX} could be estimated re-writing Eq. (4) (*i.e.* $D_{FLX} = f(d_{FLX}, P, K_{FLX})$, *e.g.* using $d_{FLX} = 10 \times 10^{-6} \text{M}$ and $P = 500 \times 10^{-6} \text{M}$ (selected as maximum P). The estimated minimum D_{FLX} was $\sim 200 \mu\text{M}$ for FLX, which imply a $D \sim 100 \mu\text{M}$ for each enantiomer.

We pre-selected a D -range from ~ 100 to ~ 200 μM in the P -constant design to avoid too high D/P ratios. To assure $D/P < 1$, the pre-selected P range was ~ 250 to ~ 500 μM in the D -constant design. Therefore we have imposed narrow experimental ranges for D and P , i.e. a short-concentration interval strategy. Such decisions imply to take cautions respect to the consistence of the Appendix B-approaches. Table 1 shows the final prepared concentrations (D and P , in μM units, although they were transformed in M units to used in the equation of Appendix B), as well as the measured ones (d_{E1} and d_{E2}). Since each of the five concentration levels *per* design has two independent replicates, we can control eventual atypical results. The final D/P ratio values in Table 1 vary from 0.17 to 0.52 (larger than the *in vivo* ones, but at least less than 1, contrasting with the general literature ones) and then, here, Appendix B assumptions could be reasonably fulfilled; for instance, $m = 1$ -model for the FLX-HSA interaction, since only at high concentration, a single drug may populate multiple sites ($m > 1$) on HSA [15].

3.3 Outlier identification/elimination

Examples in the literature indicate that an insufficient attention to possible outliers or their impact on the selected model estimations is practised. Experimental error in determining d (see for instance duplicate results in Table 1) has to be taken into account. Therefore, outliers' identification/elimination should be a previous basic task. One possible way to explore outliers could be inspecting the experimental data. For instance, Fig. 2, visualising the experimental designs, suggests

that points identification number (ID) = 13 have atypical d values for both enantiomers. However, since the objective of measuring the data is to estimate K_1 , outliers should be preferably inspected on it.

Let us suppose that $n_1 = 1$ (as a provisional assumption). In such case, K_1 could be estimated by Eq. (4) for each individual data. Those values relatively far from the average value (mean or the median of the estimates) could be potential outliers (e.g. to be submitted to an outliers' statistical analysis). Figure 3 illustrated such plot for both enantiomers, which clearly identifies the points ID = 13 for $E1$ and $E2$ as possible outliers. It should be taken into account that irrespective of $n_1 = 1$, this approach could be used to identify and eliminate outliers, at least in our short-concentration interval selection.

The Grubbs test is a suitable approach to evaluate one (single) or two (double) extreme data [16]. Application of the Grubbs test ($\alpha = 2.5\%$, 2 tails) confirmed that ID = 13 K_1 -estimates are outliers. After eliminating ID = 13 data, other extreme single (ID = 1) or double (ID 1 and 2) data, in the case of $E1$, or ID = 1 or ID 1 and 4 data, in the case of $E2$, were not outliers, according to the Grubbs criteria. For further studies the data corresponding to ID = 13 were eliminated (as indicated in Table 1).

3.4 Consistent and inconsistent/insecure approaches/estimates

Numerous literature results on PB estimations are obtained using one of the equations of Appendix B without checking

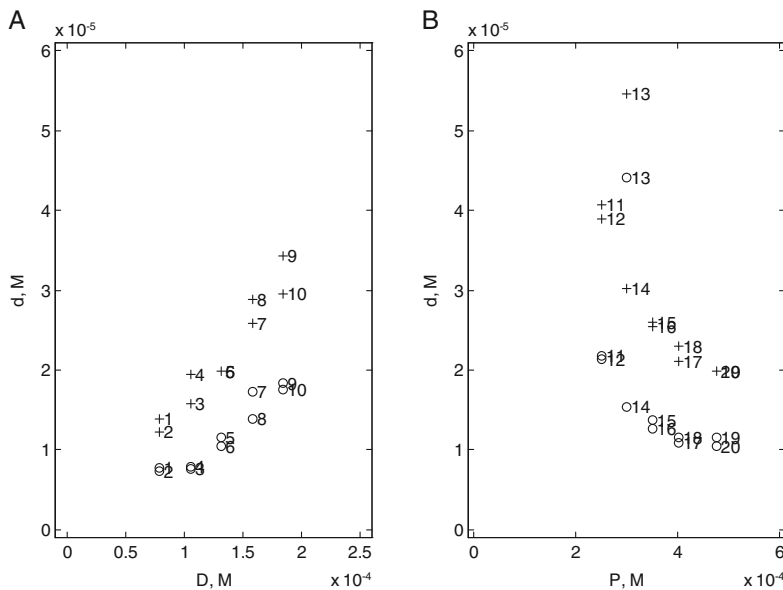


Figure 2. Experimental designs and results for each enantiomer: (A) P -constant design and (B) D -constant design, showing d_{E1} (o) and d_{E2} (+) versus D and P , respectively. The IDs represent duplicate experiments by five D and P levels for each experimental design. In all cases $D/P < 1$.

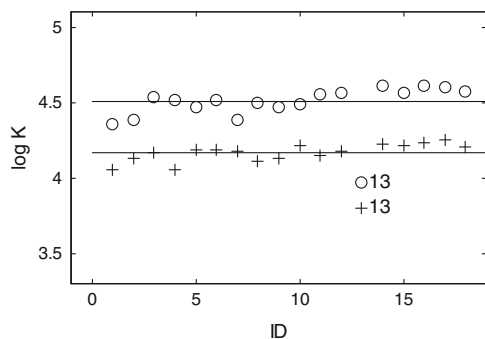


Figure 3. Estimated $\log K_1$ values for E1 (o) and E2 (+) based on Eq. (4) (i.e. assuming $n_1 = 1$; see Appendix B). ID 13 appears as an outlier. Horizontal lines indicate the mean value (after eliminating ID = 13 as well as the repeated IDs 19 and 20 data).

their consistence or robustness. Moreover, it could be considered that some published data are rough or even erroneous estimates [9]. Appendix B indicates some problems, intrinsic to the available equations, which may influence the estimates. Here, we have used all the approaches in Appendix B, evaluating the consistence of the results. Obviously the conclusions must be confined to the present experimental conditions.

From the experimental data, we have calculated d_{FLX} as the sum of d_{E1} and d_{E2} and used Eq. (6) to estimate K_{FLX} . The results ranged from 4.10 to 4.26 (excluding the result from ID = 13). These values are inconsistent since the $K_{\text{FLX}} d_{\text{FLX}} < 1$ assumption is not fulfilled (errors from -20 to -70%). Although Eq. (6) is not valid, due to the relatively low D/P (< 1) ratios used, the estimates are closer to $\log K_{\text{FLX}}$ estimated from PB% (4.78; Section 3.2) than that reported with $D/P > 1$ (3.16 [8]). In addition, Eq. (6) also would require checking the $n_1 = 1$ assumption, otherwise the estimate should be $[n_1, K_1]$ (Eq. (5), Appendix B).

In Section 3.3, Eq. (4) was just used for evaluating outliers assuming that $n_1 = 1$. In our opinion, at low D/P ratios, as occurs with $m = 1$ [15], $n_1 = 1$ should be considered the most probable situation, since the relatively high concentration of available binding sites. Also, $n_1 = 1$ was supported by previous experimental results for FLX [8]. Apart from this, assessing this assumption is appropriate to gain confidence respect to the K_1 -estimates acceptance from Eq. (4) approach. A feasible way could be using Eq. (4a), i.e. plotting $\log(r/(1-r))$ versus $\log(d)$ and checking the slope = 1 (verification criterion; Appendix B). Using the P -constant design (ID numbers 1–10) data in Table 1, the slope ($\pm 1/2$ CI 95%) values were 1.0 (± 0.3) and 1.1 (± 0.3), for E1 and E2, respectively; while using the D -constant design (ID numbers 11–20, except ID = 13) were 1.1 (± 0.3) and 0.9 (± 0.2). This means that the assumption $n_1 = 1$ can be accepted, giving also validity of $\log K_1$ estimations based on Eq. (4).

Table 2 shows the mean (\pm standard deviation) from 17 K_1 individual estimates (points ID 13, 19 and 20 were excluded). In our opinion, Eq. (4) is a robust option due to the number of data to obtain the mean (or median) and the possibility of controlling them. In contrast, caution must be taken to estimates from Eq. (4a) (i.e. $\log K_1$ as the intercept of the plot $\log(r/(1-r)) = \log K_1 + \log(d)$), because slightly slope deviations from unity could provide significant changes in the intercept, particularly for short-concentration interval strategies. For instance, the $\log K_1$ values corresponding to the above indicated linear regression slopes were: 4.55, 4.65, 4.85 and 3.54, respectively (the last value differs from the other ones). In the same way, elimination of any point has also notable impact of the estimate. Therefore Eq. (4a) is a risky non-robust solution to estimate K_1 values.

Equation (3d) is a non-linear alternative to the more popular linear approaches, Eq. (3a–c), to estimate two parameters: n_1 and K_1 . Table 2 shows the results of D - and P -constant designs for E1 and E2 enantiomers corresponding to Eq. (3d), when SIMPLEX algorithm includes the restriction of integer n_1 values (see Section 2). In all cases the $n_1 = 1$ result was found when 'starting values' for the SIMPLEX search were $n_1 = 1$, $\log K_1 = 5$ (e.g. based on results from Eq. (4) in Table 2). As expected, the $\log K_1$ agree well with those obtained from Eq. (4), suggesting that Eq. (3d) is a consistent approach. However this point deserves more attention. Figure 4 shows some results associated to enantiomer E2 (P -constant design data) based on Eq. (3d); the validation plot for d (Fig. 4A) and the d versus D plot (Fig. 4B) superimposing on it the fitted model (the best SIMPLEX solution). Both plots suggest adequate results, also supported by other available statistics, e.g. $R^2 = 0.92$. However, as indicated in Appendix B, several combinations of n_1 and K_1 could provide apparently good results. For instance, eliminating the restriction of integer n_1 values, provided $n_1 = 1.9$, $\log K_1 = 3.81$ and $R^2 = 0.93$ or using $n_1 = 3$ and $\log K_1 = 3$ as 'starting values' provided $n_1 = 8$, $\log K_1 = 3.13$ and $R^2 = 0.92$. This could introduce lack of confidence to the approach, so an independent estimation, or at least a verification, of n_1 becomes convenient (e.g. as that provided by Eq. (4a)).

Equations (3a–c) have recognised mathematical inconsistencies and their use is risky ([9, 13] and references therein); surprisingly, they are still commonly used, particularly the Scatchard plot (Eq. 3b). Figure 4C shows the corresponding linear plots to enantiomer E2 (P -constant design data) based on Eq. (3a–d). It can be observed that different dispersion degrees (then quality statistics) are observed between the approaches, which contrast to the fact that all are derived from Eq. (3) (as Eq. 3d). As consequence, estimates obtained also differ. For instance n_1 values were 2.0, 4.1 and 1.5 and $\log K_1$ 3.7, 3.5 and 3.9, from Eq. (3a), (3b) and (3c), respectively. As expected, inconsistent, erratic in this particular case, n_1 values are obtained. Also, it is evident that elimination of any data point will provide notable changes in the estimates (based on the slope and the intercept), and then a lack of robustness.

Table 2. Consistent results using some approaches of Appendix B

Model	Eq.	Conditions ^{a)}	Estimated parameters			
			n_1	$\log K_{E1}$	$\log K_{E2}$	Comments
Independent	4	All data	1 ^{b)}	4.51 ± 0.08	4.17 ± 0.06	Concrete <i>D-P</i> design unnecessary. Control on individual results. It allows an estimation of uncertainty
	3d	<i>P</i> -constant design	1 ^{c)}	4.47	4.15	Concrete <i>D-P</i> design necessary. Combining the estimates from designs an estimation of uncertainty is possible ^{d)} . It allows estimating <i>PB</i> ^{e)}
		<i>D</i> -constant design		4.57	4.20	
Competitive	3 (3d)	All data (joined designs)		4.53	4.18	Concrete <i>D-P</i> design unnecessary.
	3d1 and 3d2	<i>P</i> -constant design		4.67	4.37	Concrete <i>D-P</i> design necessary. Combining the estimates from designs and estimation of uncertainty is possible ^{f)}
		<i>D</i> -constant design		4.87	4.52	

a) When *D*-constant design (ID = 11–20) and joined designs (ID = 1–20) are used, the point ID = 13 was eliminated.

b) $n_1 = 1$ was prefixed and verified by means of Eq. (4a). $\log K_1$ Estimates make sense only if verification is satisfied.

c) n_1 was optimised by SIMPLEX but allowing only integer n_1 values (restriction). Starting values for SIMPLEX were $n_1 = 1$, $\log K_{E1} = 5$, $\log K_{E2} = 5$.

d) Mean (\pm standard deviation) was $4.52 (\pm 0.07)$ and $4.18 (\pm 0.04)$ for $\log K_{E1}$ and $\log K_{E2}$, respectively.

e) $PB = 100(1-d/D)$, where d could be estimated from Eq. (3d) once n_1 and K_1 have been estimated; e.g. to estimate *PB* at physiological conditions d could be estimated using in Eq. (3d) $P = 600 \cdot 10^{-6}$ M and $D = C_{ss}/2M$ (see Appendix C) and an average value of K_1 from Table 2 (here using $n_1 = 1$).

f) Mean (\pm standard deviation) was $4.77 (\pm 0.14)$ and $4.45 (\pm 0.11)$ for $\log K_{E1}$ and $\log K_{E2}$, respectively.

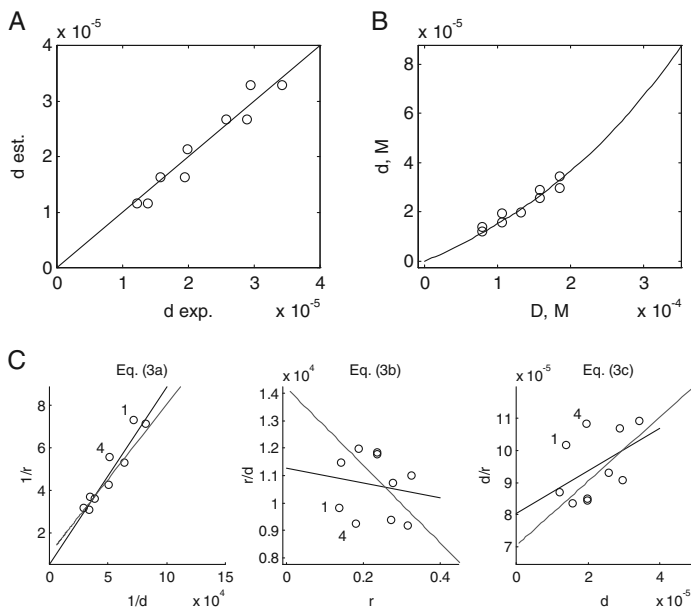


Figure 4. Results corresponding to *E2* using the *P*-constant design (IDs: 1–10): (A) Validation plot for *d* (estimated versus experimental) and (B) *d* versus *D* plot including the experimental data and the fitted model (solid line) using Eq. (3d) (optimised by SIMPLEX). (C) Linear plots (Eq. 3a–c) showing the experimental results (o) incorporating the linear fit (black line) as well as the linear model corresponding to the optimum estimates from Eq. (3d) (grey line). On these plots (named according to the equations) points IDs 1 and 4 have been labelled.

The black line in Fig. 4C is the linear fit of the data. We have also superimposed (grey line) the linear equation derived from the estimations based on Eq. (3d) ($n_1 = 1$ and $\log K_1 = 4.15$; see Table 2) for comparison. The Klotz plot ($1/r$ versus $1/d$, in which $n_1 = 1/\text{intercept}$) shows an apparent similar trend between the two lines. However, the slight difference is enough to move n_1 from 1 (Eq. 3d line) to 2

(Eq. 3a line). The other two plots reveal larger differences between the lines, due mainly to data points IDs 1 and 4. (Note that Fig. 3 reveals a certain atypical character to these points in comparison to the rest). After eliminating both points the aspect of Fig. 4C becomes more favourable (better agreement between lines), as well as the estimates, for instance, combining the estimations of Eq. (3a–c) we obtain,

mean \pm standard deviation, $n_1 = 1.1 \pm 0.2$ and $\log K_1 = 4.10 \pm 0.10$, values close to those in Table 2. In contrast, eliminating IDs 1 and 4 data does not affect markedly the $\log K_1$ estimate from Eq. (3d) (4.16 instead of 4.15 in Table 2). This indicates that Eq. (3d) is more robust than the linear ones. The use of two designs allows obtaining two estimates of $\log K_1$, then provides a source to estimate the involved uncertainty (see Table 2, footnote d). As suggests Fig. 4C, the use of Eq. (3a–c) could serve as an additional verification step, *i.e.* the eventual coincidence between linear plots lines and the corresponding from Eq. (3d) will indicate good data quality.

It is also possible to perform the calculation joining all the available data irrespective of the experimental design (for instance, in this case, joining the data from the two experimental designs) by means of Eq. (3) (or an equivalent form). One option is to employ again Eq. (3d) to fit entire response surfaces (*d*-*D*-*P* data) to the experimental data. Table 2 also includes these results, which are similar with the previous ones (in fact an average of them), suggesting that this direct approach is also consistent. Figure 5 shows the validation plot for *d* and the response surface optimised by SIMPLEX, corresponding to *E2*, showing the degree of fit to the experimental values superimposed. As expected, this approach is also robust, *i.e.* insensitive to elimination of data. For instance, elimination of data points IDs 1 and 4 provokes a negligible change in $\log K_1$ (from 4.179 to 4.184). In this case, only one estimate of $\log K_1$ is obtained, and then the possibility of directly obtaining uncertainty estimation is not feasible (see Table 2, footnote e).

In our opinion, at low *D/P* ratios the probability of competitive binding between enantiomers should be low, for the same reasons that $m = 1$ (and $n_1 = 1$) could be assumed, *i.e.* the high concentration of available binding sites. Only an increase of *D* (*e.g.* severe overdose situation) could vary this reasoning. For instance, in this case (*D/P* up 0.52), the competitive binding between enantiomers could not be absolutely avoided. A variant of Eq. (3d) allows evaluating competitive models, through Eq. (3d1) or (3d2) [6]. In order to avoid infra- or over-estimations on the parameters (by using only one of the equations) we have designed a

SIMPLEX algorithm that simultaneously optimises both equations. The conditions were the same as in previous results on Table 2. As an example, Fig. 6 shows the validation plot for *d* and the *d* versus *P* plot corresponding to both enantiomers (*D*-constant design). As before, the use of two designs allows obtaining two estimates of $\log K_1$ (see Table 2), then provides a source to estimate the involved uncertainty (Table 2, footnote e).

3.5 ES and PB at physiological conditions

An important aim of performing enantiomer-binding studies is estimating the ES degree, (see Appendix A), from K_{E1} and K_{E2} estimations. Let us accept the following quality protocol providing the Table 2 results:

- (i) Elimination of outliers (Eq. 4)
- (ii) Verification of $n_1 = 1$ (Eq. 4a) and consequent acceptance of K_{E1} and K_{E2} -estimates (Eq. 4).
- (iii) Estimation of K_{E1} and K_{E2} (Eq. 4, 3d and 3 by means of 3d, for an independent model, or Eq. 3d1 and 3d2, for a competitive model)
- (iv) Optionally, additional verification steps, *e.g.* comparison between linear, Eq. (3a–c) (including the eventual elimination of points), and non-linear, Eq. (3d) models, as in Fig. 4C.

We combined the mean estimates for each model-type in Table 2 to obtain the mean \pm standard deviation values for the estimates, from which ES was estimated (see Table 3).

A key parameter from a pharmacokinetic point of view is the estimation of the percentage of PB, at physiological conditions. Using the constants in Table 3 (independent model) and the selected physiological conditions, $D = 0.1 \times 10^{-6}$ M (see Section 3.1) and $P = 600 \times 10^{-6}$ M (see Appendix C), *d*, for each enantiomer were estimated, by means of Eq. (3d), and from them PB, as indicated in Table 2 (footnote e). PB estimates were 95.2 and 90.0% for *E1* and *E2*, respectively. These values are consistent with the reported in the literature for FLX (94.75%; Appendix C).

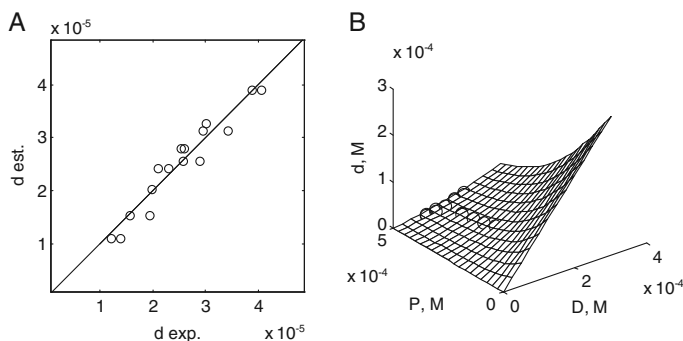


Figure 5. Results corresponding to *E2* using all the data (excluding IDs 13, 19 and 20): (A) Validation plot for *d* (estimated versus experimental) and (B) Response surface *d* versus *D* and *P* (from Eq. 3d, optimised by SIMPLEX) and experimental values superimposed.

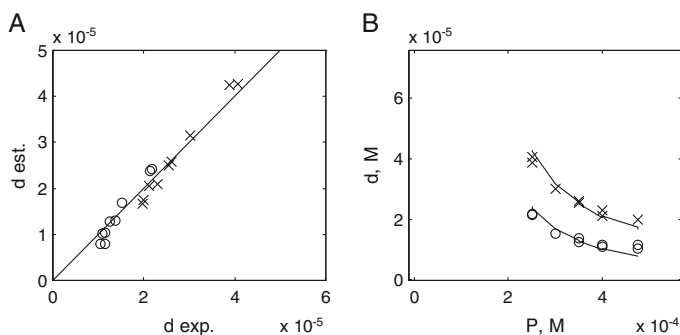


Figure 6. Results corresponding to E1 (o) and E2 (x) using the data corresponding to the *D*-constant design (IDs 11–20, except ID = 13): (A) Validation plot for *d* (estimated versus experimental) and (B) *d* versus *P* plot including the experimental data and the fitted model (line) using simultaneously Eq. (3d1) and (3d2) (optimised by SIMPLEX).

Table 3. Affinity constants of enantiomers of FLX and enantioselectivity to HSA from data in Table 2

Model type	K_{E1}, M^{-1}	K_{E2}, M^{-1}	ES
Independent	$(3.3 \pm 0.3) \times 10^4$	$(1.50 \pm 0.07) \times 10^4$	2.20
Competitive	$(6.0 \pm 1.9) \times 10^4$	$(2.8 \pm 0.6) \times 10^4$	2.14

Estimations at other desired *D*-*P* values (e.g. FLX overdose or hypoalbuminemia) would be possible.

3.6 Final remarks

Some additional technical details are: (i) the time of 30 min for equilibration was described as adequate in a previous paper [17]; (ii) due to experimental random errors and probably capillary-environment changes, e.g. punctual capillary wall modification caused by albumin adsorption, migration times exhibit little displacements between injections. This fact is visible in Fig. 1 and the effect was estimated (mean \pm standard deviation) from calibration data for E1 and E2 (2.7 ± 0.2 and 3.5 ± 0.2 min, respectively). However this does not affect the results based on areas; (iii) from the analytical point of view the method used was found adequate in terms of linearity and precision. Calibration lines for E1 and E2 were: Area = $-88.874 + 23.8005 \times d_{E1}$ and Area = $-65.8151 + 22.833 \times d_{E2}$, respectively, both models were significant ($p < 0.0001$; *F*-ANOVA = 1416.5 and 2168.10, respectively) and do not exhibit lack-of-fit ($p > 0.05$). The determination coefficients were adequate ($R^2 = 0.99_3$ and 0.99_5 , respectively). A precision study was performed joining the duplicate *d* data of both enantiomers (Table 1; excluding outliers and repeated data-pairs; ID = 13, 14 and 19, 20). The data were arranged into a 2×16 matrix, checked for homogeneity of variances (p (Cochran's *C* test) > 0.05) and submitted to ANOVA, to extract the relative standard deviation in repeatability conditions [18], *RSDr* = 8% (valid for the concentration interval studied; ~ 7 – $40 \mu M$).

Table 2 represents a selection of equations from Appendix B, according to their consistency and robustness

in the present experimental conditions. The low robustness exhibited by Eq. (4a) or (3a-c) is in part due to the low concentration interval used here. Obviously, large intervals would be beneficial not only for these equations, but also for Eq. (3d) (and 3d1 and 3d2), from a mathematical point of view. However a gain in robustness based on increasing of *D*- or *P*-ranges (e.g. adding higher *D* or lower *P* values) has the inconvenience of unfavourable *D/P* ratios (i.e. it becomes hard to guaranty the validity of the assumed model along the concentration interval) and, sometimes, it could be difficult to achieve (e.g. limited technical/instrumental factors). Therefore, the short-concentration interval strategy selected here should be seen as a cost-benefit option in terms of results quality and risk control. It demarcates the use of each of equation of Appendix B (estimation, verification, data consistence). The combination of reasonably robust equations and designs to increase the control of individual data compensates the mathematical problems. Moreover, since the opposite option, large-concentration interval approach, has been extensively used in the past, in our opinion, numerous published parameters should be taken with caution. Finally, in those cases that the n_1 estimate can not be assessed, it is preferable to report the binding capacity ($n_1 K_1$; Appendix A, Eq. 5 in Appendix B).

From the results obtained, some recommendations for authors (and an exigency for editors accepting papers on protein-binding) are:

- (i) The convenience of reporting the *D*-*P*-*d* data (as in Table 1), so other researchers could verify the estimations with alternative approaches (note that *n* and *K* estimations should be limited to the concrete *D*- or *P*-range used).
- (ii) The convenience of using alternative approaches to check for data quality and verification before publishing the estimates.

4 Concluding remarks

When performing PB studies (enantioselective, as in this case, or not) involving HSA, the mathematical approaches to

be selected should be consistent to the selected experimental design, since they have an effect on the robustness and reliability of the available equations. Factors to be considered include enantiomer (or drug) and protein concentrations, D and P , and then, their interval (which also affect the interval of other dependent/independent variables used, e.g. d or r data) and D/P ratios. When possible, assumptions should be *a priori* justified, but also verified. The approaches selected have consequences related to both accuracy and uncertainty of the estimates. Finally, data quality indicators should be considered (e.g. outliers).

In our opinion, the $m = 1$, but also $n_1 = 1$ and non-competitive model, assumptions for modelling the PB of most xenobiotics if favoured when experiments are performed with low D/P ratios; conditions consistent with the physiological levels of HSA and particularly many drugs after normal dosage. In such conditions, reliable results could be obtained using Eq. (4), if the slope of Eq. (4a) is statistically equal to 1 (particularly using the data corresponding to the central values of the individual log K_1 estimations from Eq. 4). Once $n_1 = 1$ is confirmed, Eq. (3d) or (3) (e.g. optimised by means of 3d) should alternatively provide consistent estimations.

From the results in this work, under physiological conditions or moderate overdose, the enantiomers of FLX exhibit fair ES ($ES \sim 2$) in favour of the first eluted enantiomer, which imply also a larger PB (95.2%) with respect to the less retained one (90.0%).

The authors acknowledge the Spanish Ministry of Science and Technology (MCYT), the European Regional Development Fund (ERDF) (project SAF2008-00859) for the financial support. Dr. Salvador Sagrado Vives acknowledges the South African-Spanish Bilateral Agreement of the National Research Foundation (NRF) South Africa, project UID 69160 and the Spanish Ministry of Science and Technology (MCYT) (project HS2008-0002).

The authors have declared no conflict of interest.

5 References

- [1] Brocks, D. R., *Biopharm. Drug Dispos.* 2006, 27, 387–406.
- [2] Ascoli, G. A., Domenici, E., Bertucci, C., *Chirality* 2006, 18, 667–679.
- [3] Kwong, T. C., *Clin. Chim. Acta* 1985, 151, 193–216.
- [4] Kurz, H., *Methodological Problems in Drug Binding Studies*, in: *Drug Protein Binding*, Praeger Publishers, New York 1986, pp. 70–92.
- [5] Chuang, V. T. G., Otagiri, M., *Chirality* 2006, 18, 159–166.
- [6] Martínez-Gómez, M. A., Villanueva-Camañas, R. M., Sagrado, S., Medina-Hernández, M. J., *Electrophoresis* 2007, 28, 2635–2643.
- [7] Robertson, D. W., Krushinski, J. H., Fuller, R. W., Leander, J. D., *J. Med. Chem.* 1988, 31, 1412–1417.
- [8] Katrahalli, U., Jaldappagari, S., Kalanur, S. S., *Spectrochim. Acta A* 2010, 75, 314–319.
- [9] Fielding, L., Rutherford, S., Fletcher, D., *Magn. Reson. Chem.* 2005, 43, 463–470.
- [10] Jannuzzi, G., Gatti, G., Magni, P., Spina, E. et al., *Ther. Drug Monit.* 2002, 24, 616–627.
- [11] Soltés, L., Mach, M., *J. Chromatogr. B* 2002, 768, 113–119.
- [12] Busch, M. H. A., Carels, L. B., Boelens, H. F. M., Kraak, J. C., Poppe, H., *J. Chromatogr. A* 1997, 777, 311–328.
- [13] Barri, T., Trtic-Petrovic, T., Karlsson, M., Jönsson, J. A., *J. Pharm. Biomed. Anal.* 2008, 48, 49–56.
- [14] Mehvar, R., *Am. J. Pharm. Educ.* 2005, 69, 1–8.
- [15] Kragh-Hansen, U., *Mol. Pharmacol.* 1988, 34, 160–171.
- [16] Massart, D. L., Vandeginste, B. G. M., Buydens, L. M. C., De Jong, S. et al., *Handbook of Chemometrics and Qualimetrics, Part A*, Elsevier, Amsterdam 1997.
- [17] Martínez-Gómez, M. A., Sagrado, S., Villanueva-Camañas, R. M., Medina-Hernández, M. J., *Electrophoresis* 2006, 27, 3410–3419.
- [18] Koyama, H., Sugioka, N., Uno, A., Mori, S., Nakajima, K., *Biopharm. Drug Dispos.* 1997, 18, 791–801.
- [19] Chen, J., Hage, D. S., *Anal. Chem.* 2006, 78, 2672–2683.
- [20] McDonnell, P. A., Caldwell, G. W., Masucci, J. A., *Electrophoresis* 1998, 19, 448–454.
- [21] Bisetty, K., Gumede, M. J., Escuder-Gilabert, L., Sagrado, S., *J. AOAC Int.* 2009 92 1821–1832.

Appendix A. Symbols (in alphabetic order) and nomenclature used for the xenobiotic - protein binding process

Symbol ^{a)}	Meaning	Comments
<i>b</i>	Bound concentration of xenobiotic after the equilibrium	It can be obtained from: $b = D - d$
<i>C_{ss}</i>	Plasmatic concentration (stationary state) of xenobiotic	Normally available as an interval (experimental) or estimated as an approximate value. Here, since <i>C_{ss}</i> was estimated for the racemic drug, <i>C_{ss}</i> /2 corresponds to enantiomers. It could be used to estimate <i>D</i> in physiological conditions
<i>D</i>	Total xenobiotic concentration	Designed variable (together with <i>P</i>). Finally, the experimental values (after preparation) are used in Appendix B. Here, <i>D</i> represents the total enantiomer concentration
<i>d</i>	Free (unbound) concentration of xenobiotic after the equilibrium	Normally, the measured variable after application of the analytical method (here EKC using a cyclodextrin as chiral selector). Here we use <i>d_{E1}</i> and <i>d_{E2}</i> for distinguishing <i>d</i> corresponding to the first and second eluted enantiomers (<i>E1</i> and <i>E2</i> , respectively)
<i>K</i> (<i>K₁</i>)	The affinity constant of the xenobiotic–protein interaction (in M ⁻¹ units). <i>K₁</i> refers to the main active site (with the highest <i>K</i> value)	The inverse of the dissociation constant, <i>K_D</i> ($K = 1/K_D$). Here we use <i>K_{E1}</i> , <i>K_{E2}</i> to differentiate <i>K₁</i> for <i>E1</i> and <i>E2</i> , respectively, allowing estimating the enantioselective binding as: $ES = K_{E1}/K_{E2}$
<i>m</i>	Number of classes of independent active sites in the protein	Each class of site (<i>i</i>) accounts for <i>n_i</i> binding sites
<i>n</i> (<i>n_i</i>)	Number of (equivalent) binding sites (of one class) per protein molecule. In this case only one class of site was considered with an apparent stoichiometry of <i>n_i</i>	It represents the apparent stoichiometry, thus, the number of xenobiotic molecules that could bind this site
<i>n.K</i> (<i>n_i K₁</i>)	Total binding capacity. In this case only one class of site was considered with a total binding capacity of <i>n_i.K₁</i>	This could be used when <i>n_i</i> estimation is not reliable
<i>P</i>	Total protein concentration	Designed variable (together with <i>D</i>). Finally, the experimental values (after preparation) are used in Appendix B
<i>PB</i>	Protein binding (bound fraction of xenobiotic) in percentage	It can be obtained from: $PB = 100 b/D$. It depends on <i>D</i> and <i>P</i> that should be reported when <i>PB</i> is estimated
<i>r</i>	Fraction of bound xenobiotic per molecule of protein	It can be obtained from: $r = b/P$

Other variables are defined in Appendix C. Concentrations must be set in M units to be used in Appendix B.

a) This nomenclature could represent any xenobiotic (e.g. a racemic drug or its enantiomers) interacting with proteins. In this work the symbols (and some of the comments) refer to an enantiomer of FLX and HSA as the protein. We have used sub-indexes when necessary, to specify the enantiomers (*E1*, *E2*) and the racemic drug (FLX).

Appendix B. Equations relating the experimental variables (see Appendix A), assuming independent (non-competitive) binding between E1 and E2 (except in footnote f). Non-specific and non-cooperative binding were assumed to be negligible. Although non-specific binding exists, this assumption could be reasonably valid for low D

Case (assumptions) and equations (Eq.)	Comments
m classes of independent active sites, each with n_i binding sites ^{a)} $r = \frac{b}{p} = \frac{D-d}{P} = \sum_{i=1}^m n_i \frac{K_i d}{1+K_i d}$	(1) 2.i)-parameter model (n_i and K_i). It could be difficult to obtain reliable estimations
$m = 2$ (two main classes of active sites) ^{b)} $r = \frac{b}{p} = \frac{D-d}{P} = n_1 \frac{K_1 d}{1+K_1 d} + n_2 \frac{K_2 d}{1+K_2 d}$	(2) 4-Parameter model (n_1, K_1, n_2 and K_2). It could be difficult to obtain reliable estimations
$m = 1$ (one main active site) ^{c)} $r = \frac{b}{p} = \frac{D-d}{P} = n_1 \frac{K_1 d}{1+K_1 d}$	(3) 2-Parameter model (n_1 and K_1). Data could be fitted using non-linear approaches, with some problems ^{d)}
$(1/r) = 1/n_1 + (1/n_1 K_1) (1/d)$ $(r/d) = n_1 K_1 - K_1 r$ $(d/r) = (1/n_1 K_1) + (1/n_1) d$	(3a) Linear forms of Eq. 3 (Klotz, Scatchard and γ -reciprocal plot). They have some important problems ^{e)} (3b) (3c)
$d = \frac{-(1-K_1 D + n_1 K_1 P) \pm \sqrt{(1-K_1 D + n_1 K_1 P)^2 + 4K_1 D}}{2K_1}$	(3d) d -Isolated (dependent variable) non-linear form of Eq. (3). Data could be fitted using non-linear approaches (e.g. SIMPLEX algorithm). It has some problems ^{d)} . A modification of this approach could be used for competitive binding between enantiomers ^{f)}
$m = 1; n_1 = 1$ (apparent stoichiometry = 1 ^{g)} $K_1 = \frac{1}{d} \frac{r}{1-r}$	(4) 1-Parameter model (K_1). Adapted from Eq. (3)
$m = 1; K_1 d < < 1^h)$ $n_1 \cdot K_1 = \frac{r}{d} = \frac{b}{Pd} = \frac{D-d}{Pd}$	(5) 1-Pseudo-parameter model ($[n_1, K_1]$; joining 2 parameters). Adapted from Eq. (3)
$m = 1, n_1 = 1^g; K_1 d < < 1^h)$ $K_1 = \frac{r}{d} = \frac{b}{Pd} = \frac{D-d}{Pd}$	(6) 1-Parameter model (K_1). Adapted from Eq. (3). It allows estimating K_1 from PB ⁱ⁾ .

a) For the site i , n_i represent the apparent site stoichiometry.

b) In HSA, among others, two high active sites, I and II, have been described (see Appendix C).

c) Most drugs are found to bind one site according to competitive studies using site-markers. For low D/P ratios (usual under *in vivo* conditions) only one site should be in fact occupied.

d) Different combination of n_1 and K_1 estimates (several local optima) are feasible. n_1 and K_1 are dependent estimates.

e) Mathematically inconsistent [11], since d is included as dependent and independent variable. n_1 and K_1 are dependent estimates. Imprecise data plus short-concentration intervals could provide unreliable estimations.

f) If competitive binding is assumed between two enantiomers (E1 and E2 compete for the same site class; in our opinion, this is less probable for low D/P ratios), the Eq. for E1 as a function of E2, and *vice versa*, are [6]:

$$d_{E1} = \frac{-(1 - K_{E1}D + n_1 K_{E1}P + K_{E2}d_{E2}) - \sqrt{(1 - K_{E1}D + n_1 K_{E1}P + K_{E2}d_{E2})^2 + 4K_{E1}D}}{2K_{E1}} \quad (3d1)$$

$$d_{E2} = \frac{-(1 - K_{E2}D + n_1 K_{E2}P + K_{E1}d_{E1}) - \sqrt{(1 - K_{E2}D + n_1 K_{E2}P + K_{E1}d_{E1})^2 + 4K_{E2}D}}{2K_{E2}} \quad (3d2)$$

g) This assumption should be assessed by, e.g. a linear plot derived from Eq. 4:

$$\log(r/(1-r)) = \log(b/(P-b)) = \log K_1 + \log(d) \quad (4a)$$

The plot of $\log(r/(1-r))$ versus $\log d$ provides a slope = 1-straight line (if $n_1 = 1$ is valid). In our opinion, low D/P ratios (usual under *in vivo* conditions) should favour it. Short-concentration intervals could complicate its use.

h) This assumption should be assessed once K_1 is estimated. Low d , e.g. low D/P ratios (usual under *in vivo* conditions), as well as a low K_1 (i.e. low PB), should favour it.

i) Combining PB definition and Eq. 6:

$$K_1 = \frac{PB}{(100 - PB)P} \quad (6a)$$

Appendix C. Data of the molecules concerning the binding process

Molecule/features	Information	Comments
FLX, CAS: 54910–89–3		
<i>MW</i>	309.3261 g/mol ^{a)}	Used for <i>C_{ss}</i> calculations
<i>MW</i> (FLX. HCl)	345.79 g/mol	Used for <i>D</i> calculations
PB	94.5% ^{a)} , 95% ^{b)}	PB ~ 94.75 %. From the PB definition, <i>d</i> could be estimated as: $d \sim D \times (100 - PB) / 100$
Absorption	72% ^{a)}	Approximate bioavailability, <i>f</i> ~ 0.72 (overestimated; FLX exhibits a first-pass hepatic effect)
Dose (dose-timing)	Up to 60 mg/day (e.g. once-daily) ^{b)}	<i>Dose</i> ~ 60 mg. Dose-timing, $\tau = 24$ h
Half life, <i>t</i> _{1/2}	1–3 days (24–72 h) ^{a)}	<i>t</i> _{1/2} ~ 48 h; approximate elimination constant, $K_{el} = \ln 2 / t_{1/2} \sim 0.0144 \text{ h}^{-1}$
Volume of distribution, <i>Vd</i>	20–40 L/kg ^{b)}	<i>Vd</i> ~ 30 L/kg; Human weight ~ 70 kg; <i>Vd</i> ~ 2100 L
Clearance, <i>Cl</i>		$Cl = K_{el} \times Vd \sim 30.24 \text{ L/h}$
<i>C_{ss}</i> (see Appendix A)	FLX exhibits a nonlinear kinetics	$C_{ss} \sim (f \text{ dose}) / (\tau Cl) \sim 0.06 \text{ mg/L}$; $C_{ss} \sim 0.2 \mu\text{M}$. (biased; this Eq. is valid for linear kinetics)
HSA, CAS: 9048-49-1 [9], [19], [20], [21] and references therein		
Average <i>MW</i>	66472.2 ^{a)}	Used for <i>P</i> calculations
Plasma concentration	530–750 μM (normal) ^{c)}	<i>P</i> ~ 600 μM (for normal physiological conditions)
Binding capability	Endogenous (fatty acids) and exogenous xenobiotics	Mainly neutral and acidic xenobiotics, but also basic hydrophobic ones (e.g. FLX ^{a)})
Specificity	Flexible, dynamic molecule with mobile regions able to specific binding	For most small molecules, a single-high affinity binding site (high- <i>K</i>) is usual. Other secondary lower- <i>K</i> sites (multiple binding) and non-specific interaction (low- <i>K</i> , $n > 1$), could be responsible of bad estimations, particularly for high <i>D/P</i>
Active sites	Main sites, so-called site I and II (Sudlow Scheme)	Sites I and II are dominated by hydrophobic interactions and to a lesser extent by structural factors. Other sites have been described (e.g. digitoxin site, so-called site III, or tamoxifen site, which exhibits allosteric interactions with site I)
Site I:	Unclear binding model (lack of specificity and competitive binding). Confusing results	Tight site for some drugs like warfarin, salicylate or sulphonamide. These molecules are typical site I markers for competitive studies. Examples of binding with medium log <i>K</i> values (4–5)
Site II:	Tight and specific binding model, usually with $n = 1$ stoichiometry	Typical ligands are diazepam, ibuprophen, naproxen, flufenamic acid or L-tryptophan as well as medium-chain fatty acids. Some of them are typical site II markers for competitive studies. Examples of competitive binding

a) Data from the DrugBank Database. <http://www.drugbank.ca/> (accessed 19-Feb-2010).

b) Data from the *Agencia Española del Medicamento* (Spanish Drug Agency) <https://sinaem4.agemed.es/consaem/especialidad.do?metodo=verFichaHtml&codigo=62643&fichaCompleta=S> (accessed 19-Feb-2010).

c) Clinically, hypoalbuminemia (up to ~*P*/2 of the normal level) is much more frequent than hyperalbuminemia [14]. *MW* molecular weight.

Paper VI

On the zopiclone enantioselective binding to human albumin and plasma proteins. An electrokinetic chromatography approach

L. Asensi-Bernardi, Y. Martín-Biosca, M.J. Medina-Hernández and S. Sagrado

Journal of Chromatography A 2011, 1218, 3111-3117



On the zopiclone enantioselective binding to human albumin and plasma proteins. An electrokinetic chromatography approach

L. Asensi-Bernardi^a, Y. Martín-Biosca^a, M.J. Medina-Hernández^a, S. Sagrado^{a,b,*}

^a Departamento de Química Analítica, Facultad de Farmacia, Universidad de Valencia, Burjassot, Valencia, Spain

^b Centro de Reconocimiento Molecular y Desarrollo Tecnológico (IDM), Unidad mixta Universidad Politécnica de Valencia-Universidad de Valencia, Spain

ARTICLE INFO

Article history:

Received 17 January 2011

Received in revised form 7 March 2011

Accepted 14 March 2011

Available online 21 March 2011

Keywords:

Zopiclone

EKC

Human serum albumin

Plasma proteins

Enantioselective binding

ABSTRACT

In this work, a methodology for the chiral separation of zopiclone (ZPC) by electrokinetic chromatography (EKC) using carboxymethylated- β -cyclodextrin as chiral selector has been developed and applied to the evaluation of the enantioselective binding of ZPC enantiomers to HSA and total plasma proteins. Two mathematical approaches were used to estimate protein binding (PB), affinity constants (K_1) and enantioselectivity (ES) for both enantiomers of ZPC. Contradictory results in the literature, mainly related to plasma protein binding reported data, suggest that this is an unresolved matter and that more information is needed. Discrepancies and coincidences with previous data are highlighted.

© 2011 Elsevier B.V. All rights reserved.

1. Introduction

Drug action is the result of a large number of pharmacological processes that take place in the living systems. It is well known that most of these processes present a high degree of enantioselectivity and thus, the pharmacological characteristics of chiral drugs often vary between enantiomers [1]. Consequently, in such cases, there is a special interest within pharmaceutical industry to develop optically pure drugs, like eszopiclone, the S(+)-enantiomer of zopiclone (ZPC) [2], once it has been demonstrated that it shares the pharmacological properties, whereas the R(–)-enantiomer has no hypnotic activity [3].

The investigation of enantioselectivity of drugs in their binding with human plasma proteins represents a great challenge in clinical pharmacology. When plasma proteins and racemic drugs interact, two diastereomeric adducts are formed with potential differences in their protein binding which may result in different pharmacokinetic profiles for the individual enantiomers [4]. For the investigation of drug enantioselective binding, different approaches have been proposed. The majority of these methodologies include a first step in which the free drug fraction is separated from the bound drug once the drug-protein equilibrium

has been reached using different techniques, such as the traditional equilibrium dialysis [5], ultracentrifugation [5] or ultrafiltration [6]. The second step includes chiral analysis of enantiomers, habitually on the unbound fraction. In this context, enantioseparation has become one of the most important fields of modern analytical and bioanalytical chemistry [7]. Different analytical techniques have been proposed for chiral drugs separation, such as high-performance chromatography (HPLC), gas chromatography, capillary electrophoresis or supercritical fluid chromatography [8].

Zopiclone is a non-benzodiazepine hypnotic drug used for treatment of insomnia. Its mechanism of action consists in binding to the GABA_A channel, increasing the inhibitor effect of GABA (the same mechanism of benzodiazepines). The separation of the enantiomers of ZPC has been achieved by different chromatographic and electrophoretic methods [9–24]. Chromatographic methods included different chiral stationary phases [9–14] using fluorimetric [9,10] or UV [14] detection, beta-cyclodextrin bonded phases [15,16] or mobile phases with cyclodextrins as chiral selectors [17]. Recently, the chiral separation for the quantitation of eszopiclone using LC–MS/MS and AGP chiral column was reported [18]. Enantioseparation of ZPC in CE has been obtained upon the addition of neutral cyclodextrins as β -cyclodextrin [19,20,22], γ -cyclodextrin [23], or hydroxypropyl- β -cyclodextrins [24] to the separation buffer. The use of cyclodextrin-modified gold nanoparticles (GNPs) was also recently reported [21].

Important differences in plasma protein binding (PB) values for racemic ZPC (45–85% [3,9,25–28]) have been published, suggesting that this information still deserves more attention. A value

* Corresponding author at: Departamento de Química Analítica, Facultad de Farmacia, Universitat de Valencia, C/Vicent Andrés Estellés s/n, E-46100 Burjassot, Valencia, Spain. Tel.: +34 963544878; fax: +34 963544953.

E-mail address: sagrado@uv.es (S. Sagrado).

45% is available from the Spanish Drug Agency [27] and figures in the well-known DrugBank database [28]. Only one reference provides plasma *PB* values for R- and S-ZPC (estimated at 4 °C) [9], and another one for S-ZPC (in vivo) [3]; differing in their values. Particular studies involving individual proteins are not available, except from [9]; however the reported data on *PB* to human serum albumin (HSA) (as well as α 1-acid glycoprotein, AGP) are too low compared with those encountered for plasma. These results, based on equilibrium dialysis at 4 °C and HPLC with chiral columns, also include affinity constant (K_1) to HSA for racemic ZPC and its enantiomers, from which an estimation of enantioselectivity to HSA (not reported by the authors in terms of a concrete value) can be derived. Both, the contradictory data and the lack of contrasted information on K_1 , particularly for ZPC enantiomers, point out the need to amplify this kind of studies in order to establish a more reliable ZPC enantioselectivity (*ES*).

In this paper, the enantioselective binding of ZPC to human serum albumin (HSA) and plasma proteins is evaluated. HSA is the most abundant protein in the circulatory system (i.e. with the largest complexation potential), moreover it exhibits the highest potential of enantiodifferentiation among the plasmatic proteins. The proposed methodology comprises the ultrafiltration of pre-equilibrated samples containing HSA (or human sera) and racemic drug and the enantiomeric resolution and analysis of the unbound fraction [6,29,30]. In order to evaluate the enantioselective binding of ZPC enantiomers, the electrokinetic chromatography (EKC)-partial filling technique (PFT) with the anionic carboxymethylated- β -cyclodextrin (CM- β -CD) as chiral selector was used. EKC-PFT, which involves the filling of a separation capillary only in part with a chiral selector, presents several advantages as the extremely low consumption of cyclodextrin, since the inlet and outlet vials of the separation system are free of chiral selector [8]. The use of a cyclodextrin as chiral selector was preferred here to HSA, used previously by our group (affinity EKC [29]), due to their broad spectrum of enantioselectivity and better electrophoretic features (signal-to-noise ratio, resolution, etc.).

2. Experimental

2.1. Instrumentation

A Beckman P/ACE MDQ Capillary Electrophoresis System equipped with a diode array detector (Beckman Coulter, Fullerton, CA, USA), and 32Karat software version 8.0 was used throughout. A 50 μ m inner diameter (i.d.) fused-silica capillary with total and effective lengths of 31.5 and 21 cm, respectively, was employed. Electrophoretic solutions and samples were filtered through 0.45 μ m pore size nylon membranes (Micron Separation, Westboro, MA, USA) and degassed in an ultrasonic bath (JP Selecta, Barcelona, Spain) prior to use. A Crison Micro pH 2000 pH meter from Crison Instruments (Barcelona, Spain) was employed to adjust the pH of buffer solutions.

A Selecta thermostated bath (JP Selecta, Barcelona, Spain) was used for samples incubation. For the ultrafiltration of samples, Microcon YM-10 cellulose filters of a molecular weight of 10,000 MWCO (Millipore Corporation, Bedford, MA, USA) and a centrifuge Heraeus Biofuge Strate (Heraeus, Madrid, Spain) were used.

2.2. Chemicals and standard solutions

All reagents were of analytical grade. Human serum albumin fraction V (HSA) and human sera were purchased from Sigma (St. Louis, MO, USA); sodium dihydrogen phosphate dihydrate from Fluka (Buchs, Switzerland); Tris-(hydroxymethyl)-aminomethane

(Tris) was from Scharlab (Barcelona, Spain), carboxymethylated- β -cyclodextrin was from Cyclolab (Budapest, Hungary). Racemic ZPC was kindly donated by Aventis Pharma (Madrid, Spain). Ultra Clear TWF UV deionized water (SG Water, Barsbüttel, Germany) was used to prepare solutions.

Separation buffer in EKC containing Tris 50 mM at pH 6.0 was obtained by dissolving the appropriate amount of Tris in water and adjusting the pH with 1 M HCl. For the incubation process (ZPC-HSA binding) phosphate buffer 67 mM of pH 7.4 was prepared by dissolving the appropriate amount of sodium dihydrogen phosphate dihydrate in water and adjusting the pH with 1 M NaOH. Stock solution of 100 mM CM- β -CD was prepared in the separation buffer. 1000 μ M ZPC and HSA stock solutions were daily prepared by weighting the corresponding amount of protein powder and dissolving it with the phosphate buffer.

2.3. Methodology

2.3.1. Capillary conditioning

New capillaries were conditioned for 15 min flush with 1 M NaOH at 60 °C [29,31]. This treatment removes adsorbates and refreshes the surface by deprotonation of the silanol groups. Then, they were rinsed for 5 min with deionized water and 10 min with separation buffer at 25 °C. In order to obtain good peak shapes and repeatable migration data, the capillary was conditioned prior to each injection. In all cases, the conditioning run included the following steps: (i) 1 min rinse with deionized water, (ii) 2 min rinse with 0.1 M NaOH, and (iii) 1 min rinse with deionized water at 20 psi. Before chiral selector and sample injection the capillary was also rinsed with the separation buffer for 2 min at 20 psi [31]. No drift in migration time and no peak broadening during a working session (suggesting that no protein adsorption occurred) were verified, indicating the adequacy of the protocol.

2.3.2. Procedure for the enantioseparation of ZPC by EKC using CM- β -CD

For all experiments, the Tris solution was used as electrophoretic buffer. A 30 mM CM- β -CD solution obtained by diluting the stock solution with the buffer was used. ZPC samples (ultrafiltrated fractions and standards) were injected hydrodynamically at 0.5 psi for 5 s. Before sample injection, the capillary was partially filled with the 30 mM CM- β -CD solution by applying 0.5 psi for 99 s. Separation was performed in normal polarity by applying 15 kV (higher voltage would give higher efficiency but also lower enantioresolution [31]). The capillary was thermostated at 25 °C and the UV-detection wavelength was set at 220 nm. The R and S enantiomers were identified by comparison between our *ES* data and the derived from [9] (see Section 3.3.3).

2.3.3. Procedure for the separation and analysis of unbound ZPC fraction to HSA and plasma proteins

We have planned an experimental design to study the binding of the enantiomers to HSA, keeping the concentration of protein nearly physiological values and varying the concentration of ZPC according to the detector capabilities. 5 concentration levels of ZPC were used with 3 independent replicates per level, totalling 15 independent mixtures for the studies with HSA. For the evaluation of the total plasma protein binding, 4 concentration levels of ZPC, with 3 independent replicates per level, totalling 12 samples, were used.

Mixtures containing different ZPC concentrations were prepared in triplicate by the dilution of the stock solutions of drug and protein with the phosphate buffer. HSA concentration was fixed at 475 μ M, and in the plasma samples the relation aqueous/plasma solution was 100/300 (v/v). All these mixtures were allowed to reach equilibrium for 30 min in a water bath at 36.5 °C and were

filtered through cellulose filters by centrifugation at 9000 rpm for 30 min. The ultrafiltrate was directly injected into the EKC system.

2.4. Software and calculations

From the experimental data, pseudoeffective (due to the partial filling technique) electrophoretic mobilities corrected for electroosmotic flow (EOF) variations were calculated according to the following equation:

$$\mu_i = \frac{Ll}{V} \left(\frac{1}{t_i} - \frac{1}{t_0} \right) \quad (1)$$

where L and l are the total capillary length and the length from the inlet to the detector, respectively, V the run voltage, t_i is the analyte migration time and t_0 is the migration time of methanol, used as non-interacting electroosmotic flow marker. Methanol is detected at 220 nm as a perturbation in the baseline due to a change in the refractive index. Enantiomeric resolution (R_S) was calculated according to:

$$R_S = \frac{1.18(t_2 - t_1)}{w_1 + w_2} \quad (2)$$

where t_1 and t_2 are the migration time of each enantiomer and w_1 and w_2 represent the peak widths at 50% peak heights.

For the ZPC–HSA binding study routines made/adapted in MATLAB® 4.2 were used for calculations. The results generated were verified using EXCEL® and STATGRAPHICS®. In some calculations a SIMPLEX algorithm routine was used (non-linear fitting). We have used two simplified approaches from the general protein-binding model considering m classes of independent active sites on HSA, each with n_i binding sites:

$$r = \frac{b}{P} = \frac{D-d}{P} = \sum_{i=1}^m n_i \frac{K_i d}{1 + K_i d} \quad (3)$$

In this equation, r is the fraction of bound enantiomer per molecule of protein, b is the bound concentration of enantiomer and P is the total protein concentration. D and d are the total and free enantiomer concentrations, respectively. All the concentrations must be expressed in molar units (M). For the site i , n_i represents the apparent site-stoichiometry. Eq. (3) assumes negligible non-specific and non-cooperative binding. Two simplified approaches were used here. The first simplified approach assumes $m = 1$ and $n_1 = 1$. Both assumptions should be reasonably valid for low D/P ratios (usual under in vivo conditions) [31], providing:

$$K_1 = \frac{1}{d} \frac{r}{1-r} \quad (4)$$

Eq. (4) is a 1-parameter model, allowing K_1 estimation for each individual D – P – d data and then serving as a source for outliers' identification [31]. To verify the previous approach, an alternative equation, assuming simply $m = 1$ was used, providing:

$$d = \frac{-(1 - K_1 D + n_1 K_1 P) + \sqrt{(1 - K_1 D + n_1 K_1 P)^2 + 4 K_1 D}}{2 K_1} \quad (5)$$

Eq. (5) is a d -isolated (dependent variable) non-linear form of Eq. (3) when $m = 1$. SIMPLEX optimization was used for estimating the parameters n_1 and K_1 , allowing integer n_1 values [31].

3. Results and discussion

3.1. Enantioseparation of ZPC by EKC

Enantioseparation of ZPC in CE has been reported using neutral cyclodextrins in the separation buffer [19,20,22–24]. Even though charged CDs were used initially for the enantioseparation of neutral

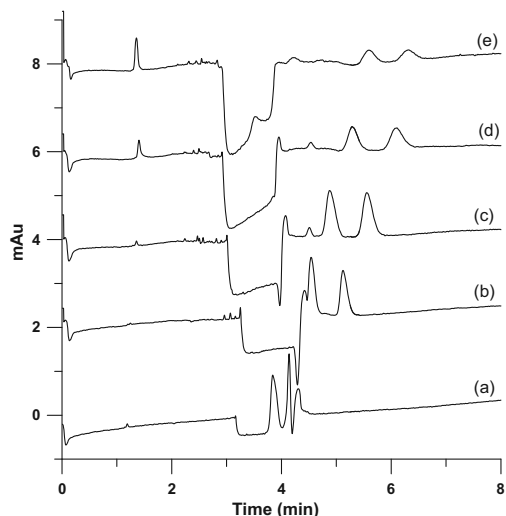


Fig. 1. Effect of the CM- β -CD concentration on the chiral separation of ZPC enantiomers. Electropherograms correspond to CM- β -CD at different concentration levels: (a) 10 mM, (b) 20 mM, (c) 30 mM, (d) 40 mM and (e) 50 mM. Other experimental conditions: ZPC 500 μ M, injected at 0.5 psi during 3 s, CD injection 0.5 psi/99 s, 50 mM Tris buffer at pH 6, 25 °C, 15 kV.

compounds they also have shown high enantioselectivity towards many basic and acidic compounds. It has been reported that maximum enantioselectivities are obtained when analytes and CDs have opposite mobilities [32–34], due to the counter-current mobility of the chiral selector and the selectand in the separation capillary [8]. In this paper the use of the anionic carboxymethylated- β -cyclodextrin (CM- β -CD) as chiral selector in EKC using the partial filling technique was evaluated accounting to the positive charge of ZPC in a wide pH range ($pK_a = 6.9$ [35]). The selection of the pH relied on a compromise between of EOF, chiral selector concentration and mobility of ZPC enantiomers, depending on the running buffer pH and driven by their respective pK_a . Initial experiments were carried out with different buffers (citrate, phosphate, Tris and 2-(N-morpholino)ethanesulfonic acid, MES) at pH values between 4 and 8. Among the buffers, Tris at pH 6 provided the best results in terms of resolution, signal-to-noise ratio and analysis time. This solution (50 mM) was selected as running buffer for the optimization process. In these conditions, cationic ZPC migrates through the selector plug allowing the interaction with the anionic CM- β -CD. Detection wavelength was fixed at 220 nm. Lower wavelengths (e.g. 200 and 210 nm were also tested) gave worse signal-to-noise ratio, probably due to the higher contribution of the absorbance of the selector. In these conditions, the initial experiments suggested that sufficient enantioresolution and relatively short analysis time could be achieved; thus we decided to simplify the study employing univariate optimization. The effect of CD concentration, selector plug length, and temperature on the enantioresolution was studied. Fig. 1 shows the effect of the concentration of CM- β -CD. Migration times of enantiomers increase as the CD concentration increases. The observed pseudoeffective electrophoretic mobilities are a combination of electrophoretic mobility of both free and complexed enantiomer. An increase of CD concentration in the capillary provides higher proportion of anionic complexes, increasing their negative electrophoretic mobility and shifting the peaks to longer migration times. As can be seen, complete separation was obtained using a 20 mM CM- β -CD concentration. An improvement in enan-

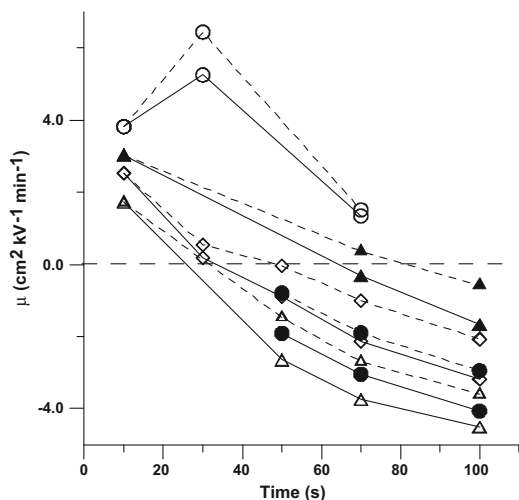


Fig. 2. Effect of the selector plug length on the pseudoeffective electrophoretic mobility S-ZPC (---) and R-ZPC (—) at different CM- β -CD concentrations: (○) 10 mM; (▲) 20 mM; (◇) 30 mM; (●) 40 mM; and (△) 50 mM. The solution of CM- β -CD was injected into the capillary by applying 0.5 psi for variable times. Other experimental conditions as in Fig. 1.

tioresolution upon increasing CM- β -CD concentration is observed, although the shape of the peaks also becomes poorer; probably due to the counter current mobilities of the enantiomers and the chiral selector and the fact that higher CD concentrations provide higher interaction degree (i.e. wider peaks).

When using the partial filling technique, one of the most influential parameters affecting the chiral separation is the amount (the selector plug length, SPL, and concentration) of chiral selector introduced into the capillary. To study this effect on the zopiclone enantioresolution the capillary was filled with increasing concentrations of CM- β -CD by applying 0.5 psi for 10, 30, 50, 70 or 99 s. Fig. 2 shows the SPL effect on the pseudoeffective electrophoretic mobility of both enantiomers, at different concentrations of cyclodextrin. A decrease in pseudoeffective electrophoretic mobility of each enantiomer (or an increase in negative mobility) and an improvement in enantioresolution are observed upon increasing the amount of cyclodextrin introduced into the capillary for all the concentrations assayed. Resolution applying 99 s was sufficiently adequate and higher SPL should provide an increase in the analysis time.

Temperature is considered a key parameter in the chiral separation because it can affect the peaks efficiency, the buffer viscosity and the compound-selector interaction, and consequently can modify the chiral resolution. In this work, temperatures of 15, 25 and 40 °C were tested filling the capillary with a 30 mM CM- β -CD solution (applying 0.5 psi for 99 s). It was observed a decrease in migration times of enantiomers and EOF upon increasing the temperature, both effects are due to a decrease on the viscosity of the running buffer and also to changes in solute-cyclodextrin binding constant. The reduction of migration times resulted in a decrease in the resolution of the enantiomers with increasing temperature (R_s values of 2.8, 2.4 and 1.7 were obtained for 15, 25 and 40 °C, respectively), although in all cases a complete chiral separation had been achieved.

From the results obtained the experimental conditions indicated in Section 2.3.2 were selected. Fig. 3 shows the electropherogram obtained with these conditions. As can be seen, a good resolution

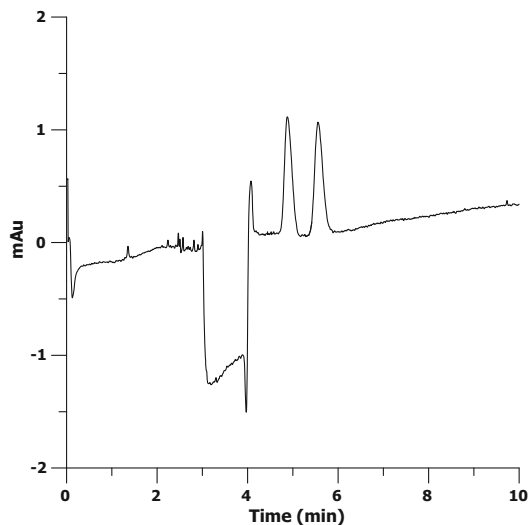


Fig. 3. Electropherogram of racemic ZPC (500 μ M) obtained under experimental conditions selected: fused silica capillary (50 μ m inner diameter, 31.5 cm total length, 21 cm effective length); Tris buffer (50 mM, pH 6); CM- β -CD 30 mM (injection 0.5 psi/99 s); capillary temperature 25 °C; separation voltage, 15 kV; absorbance detection at 220 nm.

was obtained for the ZPC enantiomers ($R_s = 2.1$) in an analysis time lower than 6 min.

3.2. Calibration

Calibration standard solutions containing racemic ZPC in the range 50–500 μ M were prepared in triplicate. Table 1 shows the regression statistics for the linear regression models, fitted using the least squares approach, for each enantiomer, using the peak area corrected by migration time (in order to compensate for velocity discrepancy between peaks) as dependent variable. It includes the intercept and slope together with their corresponding confidence intervals. These models were used to estimate d by interpolating the signals (peak area corrected by migration time) corresponding to ultrafiltrates from the ZPC-HSA mixtures.

3.3. Enantioselective binding to HSA and plasma proteins

Mixtures of racemic ZPC and HSA were designed keeping $D/P < 1$ to assure, as far as possible, model validity [31]. The minimum D ($\sim 100 \mu$ M) was fixed considering the approximate quantification limit for d , for both S- and R-enantiomers, d_S and d_R , respectively. P was fixed close the physiological concentration (in the hypoalbuminemia-normal levels frontier [36]). Table 2 shows the prepared concentrations (D and P , in μ M units, although they were transformed in M units for modelling), as well as the measured ones (d_S and d_R). The D/P ratios (from 0.22 to 0.44) should guarantee the

Table 1
Calibration model statistics^a for S- and R-ZPC under the selected separation conditions using peak area corrected by migration time as dependent variable.

	$b_0 \pm ts$	$b_1 \pm ts$	r
S-ZPC	60 \pm 40	2.4 \pm 0.2	0.993
R-ZPC	30 \pm 20	2.37 \pm 0.12	0.998

^a b_0 , intercept; b_1 , slope; ts , confidence interval at the 95% probability level; r , correlation coefficient.

Table 2

Experimental design and results. Experimental P was 449.1 μM . Data were transformed to M units for calculations. A robust z-score approach (applied to the corresponding independent K_1 estimates) was used to detect/eliminate outliers (see text for details).

D-level	ID	D (μM)	d_s (μM)	d_R (μM)
1	1	100.8	45.0	52.6
	2	100.8	^b	82.1
	3	100.8	50.3	63.2
2	4	126.0	^a	89.7
	5	126.0	^a	116.7
	6	126.0	73.8	89.3
3	7	151.2	76.7	104.9
	8	151.2	80.8	116.7
	9	151.2	96.5	97.7
4	10	176.4	101.4	127.6
	11	176.4	100.2	130.6
	12	176.4	91.1	111.2
5	13	201.6	97.7	115.4
	14	201.6	118.7	117.9
	15	201.6	91.5	103.6

^a Data eliminated in the first round.

^b Data eliminated in the second round.

assumptions made in Section 2.4; for instance, the $m = 1$ -model for the ZPC–HSA interaction, since only at high concentration, a single drug may populate multiple sites ($m > 1$) on HSA [31,37]. In Table 2, since each of the five D -concentration levels has three independent replicates, we can control atypical results.

3.3.1. Outlier identification/elimination in the HSA study

The z-score approach has been proposed as an alternative to other tests for outliers, as an automatic criterion [38]. Most tests for outliers depend on good estimates of dispersion, and become less reliable with real errors present. Robust statistics is a convenient method of handling results when they are expected to follow a near-normal distribution, but are suspected to contain a small proportion of errors which are not representative of the bulk of the data [39]. To gain in security, the *median* and *MADe* (a robust estimation of the standard deviation) were used to estimate a robust z-score, z_i for each independent $\log K_{1i}$ estimate, from Eq. (4) [31]:

$$z_i = \frac{\log K_{1i} - \text{median}}{\text{MADe}} \quad (7)$$

Habitually, $z_i > 3$ are considered unsatisfactory, while $z_i > 2$ are considered doubtful values. Here we have pre-fixed a $z_i > 2.5$ criterion to eliminate a point in a round (see Table 2). The final *median* and *MADe* are included in Table 3. It should be taken into account that irrespectively $n_1 = 1$ or not, this approach could be used to identify and eliminate outliers [31].

3.3.2. Affinity constants to HSA

In Section 3.3.1, Eq. (4) was only used for evaluating outliers assuming that $n_1 = 1$ (the most probable situation at low D/P ratio [31]), since the relatively high concentration of available binding sites. Table 3 provides a robust estimate of $\log K_1$ for the enantiomers based on Eq. (4). To verify the parameters n_1 and K_1 an

Table 3

Affinity constants of enantiomers of ZPC, protein-binding and enantioselectivity to HSA.

Enantiomer	$\log K_1^a$	PB^b	ES^c
S-ZPC	3.38 ± 0.14	47 ± 6	1.95
R-ZPC	3.09 ± 0.19	36 ± 8	

^a From data estimated from Eq. (4) (*median* \pm *MADe*; after outliers elimination).

^b Estimated at $D = 0.2 \mu\text{M}$ (total enantiomer concentration) and $P = 600 \mu\text{M}$.

^c From data estimated from the ratio between $K_{1,S-ZPC}$ ($\sim 2400 \text{M}^{-1}$) and $K_{1,R-ZPC}$ ($\sim 1230 \text{M}^{-1}$).

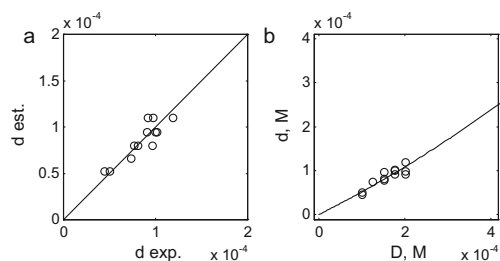


Fig. 4. Results corresponding to S-ZPC using all the data. (a) Validation plot for d (estimated vs. experimental) and (b) d vs. D plot and model (superimposed line; from Eq. (5), optimized by SIMPLEX).

approach based on non-linear fitting (using Eq. (5)) was used. This is an alternative to other more popular linear approaches having recognised mathematical inconsistencies and risks ([31,40,41] and references therein). SIMPLEX search was started with $n_1 = 1$, $\log K_1 = 4$ (based on results on Table 3), and only integer n_1 values were allowed. The $\log K_1$ estimates found were: 3.37 and 3.14 for S- and R-ZPC, respectively, which agree with values in Table 3. In addition, $n_1 = 1$ estimates were found for both enantiomers, verifying the assumption. As an example of the model adequacy, Fig. 4 shows some results associated to S-ZPC based on Eq. (5); the validation plot for d (Fig. 4a) and the d vs. D plot (Fig. 4b) superimposing on it the fitted model (the best SIMPLEX solution). This suggests that $\log K_1$ estimates in Table 3, including uncertainty (based on a minimum of 12 independent estimates) could be considered acceptable values.

3.3.3. Enantioselectivity and protein binding to HSA

We combined K_1 estimates for S- and R-ZPC to calculate the enantioselectivity of ZPC–HSA interaction ($ES = K_{1,S-ZPC}/K_{1,R-ZPC}$) which indicate a fair enantioselectivity degree ($ES \sim 2$), in favour to the first eluted enantiomer, S-ZPC (see Table 3). These results can be compared with the only previous available values, obtained using equilibrium dialysis at 4 °C [9], from which a quantitative estimation of enantioselectivity, not reported by the authors, can be derived ($ES = 524/293 = 1.8$). This value is similar to that obtained in the present work, supporting the fact that ZPC exhibit enantioselective binding to HSA. Attending to this agreement, enantiomers R (the second eluted enantiomer) and S (the first eluted one) were assigned. On the other hand, the reported affinity constants in [9] are notably lower than those encountered here (by a factor close to 4.4). This could be explained in terms of experimental conditions, mainly the incubation temperature.

A key parameter from a pharmacokinetic point of view is the estimation of the percentage of protein binding. By means of Eq. (5) and using the constants in Table 3 at prefixed (desired) D and P values, it is possible to estimate the corresponding d values, and from them, the PB according to:

$$PB = \frac{100(D - d)}{D} \quad (8)$$

Here we have assumed values consistent with physiological conditions, e.g. $D = 0.2 \times 10^{-6} \text{M}$ (see [42]) and $P = 600 \times 10^{-6} \text{M}$ (see Section 3.3). After d_s and d_R estimation, PB for each enantiomer was calculated (see Table 3). As expected (according to the K_1 values), binding percentages to HSA reported in [9], 23.9 ± 2.8 and 15.0 ± 3.5 for S- and R-ZPC, respectively, are lower than those found here (Table 3), but also too low (in our opinion) compared with those encountered for plasma by the authors.

Table 4

Plasma protein binding values for racemic ZPC and its enantiomers. Some available aspects that could potentially explain differences between results were included in footnotes.

PB% rac-ZPC	PB% S-ZPC	PB% R-ZPC	Ref.
45 ^a	–	–	Gaillot et al. [25]
78.7–91.2 ^{a,b}	–	–	Howard et al. [26]
79.3 ± 5.5 ^{b,c}	75.1 ± 2.1 ^{b,c}	86.8 ± 5.2 ^{b,c}	Fernandez et al. [9]
45 ^d	–	–	AEMPS [27] DrugBank [28]
–	52–59 ^d	–	DrugBank [28]
47 ± 4	45 ± 3	49 ± 6	This work

^a In vivo (presumably $D/P \ll 1$).

^b Equilibrium dialysis was used to separate free and bound ZPC fractions.

^c In vitro; plasma with EDTA or heparin as anticoagulant; incubation at 4 °C (24 h); $D/P = 0.00043$. The authors also reported other in vitro results but using citrate-phosphate-dextrose as alternative anticoagulant (38.0 ± 8.1, 31.8 ± 6.6, 42.5 ± 7.1, respectively) and in vivo estimates for R- and S-ZPC (86.76 and 79.17, respectively; presumably $D/P \ll 1$).

^d No references are provided (it is assumed the values comes from in vivo experiments; presumably $D/P \ll 1$).

3.3.4. Plasma protein binding

The total plasma protein binding was approximated for racemic ZPC and its enantiomers, using Eq. (8) according with our experimental data using human sera. These data were compared with previous values found in the literature (Table 4), illustrating that this was an unresolved matter. Our PB result on racemic ZPC is consistent with some reported ones [25,27,28], but differs from others [9,26]. In addition, our result for S-ZPC is reasonably close with the one reported from the pure enantiomer [3]. Comparing our results for plasma (Table 4) with those for HSA (Table 3), it seems that S-ZPC binds mainly to HSA, while R-ZPC binds also to other plasma proteins, but with a limited affinity compared to HSA. This also disagrees with the explanation provided in [9] forced by the large PB differences between HSA and AGP and plasma.

3.3.5. Final remarks

The protocol used, including (i) elimination of outliers (Eq. (4) + Eq. (7)) on K_1 direct individual estimations and (ii) verification of $n_1 = 1$ and K_1 (Eq. (5)) aims to provide a sufficient quality on the results. To gain in robustness we have avoided unfavourable D/P ratios (to guaranty the validity of the assumed model along the D -concentration interval), then using a short- D -concentration interval [31]. The estimations from Eq. (4) increase the control over individual data (here replicates at different D -concentration levels) allowing the application of univariate statistics instead off a regression model with a single estimation. It should be noted that using Eq. (4) (independent estimations were obtained) the D -range becomes irrelevant, i.e. the estimation is not based on regression where a short range would become problematic.

D , P or D/P information, as well as the experimental d -values and experimental details should be always clearly reported since it could condition the reported estimates (allowing appropriate comparison or even a different mathematical data treatment).

4. Conclusions

Due to its intrinsic characteristics such as high separation efficiencies, speed of analysis, low reagent consumption and small sample requirements, EKC, combined here with CM- β -CD using the partial filling technique, has been demonstrated to be adequate for the inexpensive chiral separation of ZPC enantiomers, allowing the evaluation of enantioselective binding of ZPC to HSA and total plasma proteins. The results suggest that S-ZPC exhibit more affinity (by a factor of 2) to HSA than R-ZPC. This work provides the second evidence of ZPC enantioselectivity to HSA, using an independent method with more favourable experimental conditions

respect to the physiological ones, and therefore serves to confirm the previous result. Our PB results (47 ± 4, 49 ± 6 and 45 ± 3% for racemic, R- and S-ZPC, respectively) agree with other reported values, supporting the idea that the protein binding of ZPC is in the ~45% level (e.g. the value that figures in the DrugBank database [28]) and not in the other reported level (~80%).

When performing protein binding studies (enantioselective, as in this case, or not) involving HSA, the mathematical approaches to be selected should be consistent to the selected experimental design. Factors to be considered include total enantiomer (or drug) and protein, D and P , concentration intervals used, which also affect the interval of other variables used, e.g. d or r data, and D/P ratios. When possible, model assumptions should be a priori justified, but also verified. The approaches selected have consequences related to both accuracy and uncertainty of the estimates. Finally, data quality indicators should be considered (e.g. outliers) and robust statistics are recommended.

Acknowledgments

The authors acknowledge the Spanish Ministry of Science and Innovation (MCINN), the European Regional Development Fund (ERDF) (project SAF2008-00859) for the financial support. Dr. Salvador Sagrado Vives acknowledges the South African–Spanish Bilateral Agreement of the National Research Foundation (NRF), South Africa, project UID 69160 and the Spanish Ministry of Science and Innovation (MCINN), project HS2008-0002 for the financial support. The authors declared no conflict of interest.

References

- [1] D.R. Brocks, *Biopharm. Drug Dispos.* 27 (2006) 387.
- [2] C. Höschl, J. Svestka, *Expert Rev. Neurother.* 8 (4) (2008) 537.
- [3] J.M. Monti, S.R. Pandi-Peruma, *Neuropsychiatr. Dis. Treat.* 3 (4) (2007) 441.
- [4] V.T.G. Chuang, M. Otigiri, *Chirality* 18 (2006) 159.
- [5] T.C. Kwong, *Clin. Chim. Acta* 151 (1985) 193.
- [6] H. Kurz, *Drug Protein Binding*, Praeger Publishers, New York, 1986, p. 70.
- [7] H. Wang, J.L. Gu, H.F. Hu, R.J. Dai, T.H. Ding, R.N. Fu, *Anal. Chim. Acta* 359 (1998) 39.
- [8] B. Chankvetadze, *J. Chromatogr. A* 1168 (2007) 45.
- [9] C. Fernandez, F. Gimenez, A. Thuillier, R. Farinotti, *Chirality* 11 (1999) 129.
- [10] C. Fernandez, P. Alet, C. Davrinche, J. Adrien, A. Thuillier, R. Farinotti, F. Gimenez, *J. Pharm. Pharmacol.* 54 (2002) 335.
- [11] C. Fernandez, F. Gimenez, B. Baune, V. Maradeix, A. Thuillier, *J. Chromatogr. Biomed. Appl.* 617 (1993) 271.
- [12] R.T. Foster, G. Caille, A.H. Ngoc, C.H. Lemko, R. Kherani, F.M. Pasutto, *J. Chromatogr. B* 658 (1994) 161.
- [13] C. Fernandez, B. Baune, F. Gimenez, A. Thuillier, R. Farinotti, *J. Chromatogr. Biomed. Appl.* 572 (1991) 195.
- [14] M.G. Gebauer, C.P. Alderman, *Biomed. Chromatogr.* 16 (2002) 241.
- [15] S. Piperaki, A. Tsantili-Kakoulidou, M. Parissi-Poulou, *Chirality* 7 (4) (1995) 257.
- [16] S. Piperaki, M. Parissi-Poulou, *J. Chromatogr. A* 729 (1996) 19.
- [17] K. Tang, Y. Chen, J. Liu, *Sep. Purif. Technol.* 62 (2008) 681.
- [18] M. Meng, L. Rohde, V. Čápka, S.J. Carter, P.K. Bennett, *J. Pharm. Biomed. Anal.* 53 (2010) 973.
- [19] G. Hempel, G. Blaschke, *J. Chromatogr. B* 675 (1996) 139.
- [20] B. Koppelhofer, U. Epperlein, B. Christian, B. Lin, Y. Ji, Y. Chen, *J. Chromatogr. A* 735 (1–2) (1996) 333.
- [21] L. Yang, C. Chen, X. Liu, J. Shi, G. Wang, L. Zhu, L. Guo, J.D. Glennon, N.M. Scully, B.E. Doherty, *Electrophoresis* 31 (2010) 1.
- [22] D. Blanco-Gomis, C. Botas-Velasco, I. Herrero-Sánchez, D. Gutiérrez Álvarez, *J. Liq. Chromatogr. Relat. Technol.* 32 (2009) 2654.
- [23] B. Koppelhofer, U. Epperlein, A. Jakob, S. Wuertner, Z. Xiaofeng, L. Bingcheng, *Chirality* 10 (1998) 548.
- [24] Z. Jiang, R. Thorogate, N.W. Smith, *J. Sep. Sci.* 31 (2008) 177.
- [25] J. Gaillot, G.W. Houghton, J. Marc Aurele, J.F. Dreyfus, *Pharmacology* 27 (1983) 76.
- [26] P.J. Howard, E. Mc Clean, J.W. Dundee, Br. *J. Clin. Pharmacol.* 21 (1986) P614.
- [27] Agencia Española del Medicamento (Spanish Drug Agency). Available from: http://sinaem4.aged.es/consaem/especialidad.do?metodo=verFichaWordPdf&codigo=58549&formato=p_d&formulario=FICHAS (accessed 04.03.11).
- [28] DrugBank Database: <http://www.drugbank.ca/drugs/> (accessed 04.03.11).
- [29] M.A. Martínez-Gómez, R.M. Villanueva-Camañas, S. Sagrado, M.J. Medina-Hernández, *Electrophoresis* 28 (2007) 2635.
- [30] L. Escuder-Gilbert, M.A. Martínez-Gómez, R.M. Villanueva-Camañas, S. Sagrado, M.J. Medina-Hernández, *Biomed. Chromatogr.* 23 (2009) 225.

- [31] L. Asensi-Bernardi, Y. Martín-Biosca, M.J. Medina-Hernández, S. Sagrado, *Electrophoresis* 31 (2010) 3268.
- [32] S. Rudaz, E. Calleri, L. Geiser, S. Cherkaoui, J. Prat, J.L. Veuthey, *Electrophoresis* 24 (2003) 2633.
- [33] S. Rudaz, T. Le Saux, J. Prat, P. Gareil, J.L. Veuthey, *Electrophoresis* 25 (2004) 2761.
- [34] C. Perrin, Y. Vander Heyden, M. Maftouth, D.L. Massart, *Electrophoresis* 22 (2001) 3202.
- [35] ChemIDPlus: <http://chem.sis.nlm.nih.gov/chemidplus/> (accessed 13.01.11).
- [36] R. Mehvar, *Am. J. Pharm. Educ.* 69 (article 103) (2005) 1.
- [37] U. Kragh-Hansen, *Mol. Pharmacol.* 34 (1988) 160.
- [38] K. Bisetty, N.J. Gumede, L. Escuder-Gilbert, S. Sagrado, *J. AOAC Int.* 92 (2009) 1821.
- [39] RobStat.xla 1.0, Robust statistic Toolkit. The Royal Society of Chemistry. AMC technical brief number 6.
- [40] L. Fielding, S. Rutherford, D. Fletcher, *Magn. Reson. Chem.* 43 (2005) 463.
- [41] T. Barri, T. Trtic-Petrovic, M. Karlsson, J.A. Jönsson, *J. Pharm. Biomed. Anal.* 48 (2008) 49.
- [42] R.V.S. Nirogi, V.N. Kandikere, K. Mudigonda, *Biomed. Chromatogr.* 20 (2006) 794.

Paper VII

Electrokinetic chromatographic estimation of the enantioselective binding of nomifensine to human serum albumin and total plasma proteins

L. Asensi-Bernardi, Y. Martín-Biosca, S. Sagrado and M.J. Medina-Hernández

Biomedical Chromatography 2012, 26, 1357-1363

Electrokinetic chromatographic estimation of the enantioselective binding of nomifensine to human serum albumin and total plasma proteins

Lucía Asensi-Bernardi^a, Yolanda Martín-Biosca^a, Salvador Sagrado^{a,b} and María J. Medina-Hernández^{a*}

ABSTRACT: This report is the first evidence of enantioselective binding of nomifensine to human serum albumin (HSA) and plasma proteins. The overall process with HSA included: (i) consistent experimental design along two independent sessions; (ii) incubation of nomifensine–HSA designed mixtures; (iii) ultrafiltration for separating the unbound enantiomers fraction; (iv) electrokinetic chromatography (EKC) using heptakis-2,3,6-tri-*O*-methyl- β -cyclodextrin as chiral selector to provide experimental data for enantiomers (first, E1, and second, E2, eluted ones); and (v) a recent direct equation allowing univariate tests and robust statistics to provide consistent parameters and uncertainty. A significant enantioselectivity to HSA (2.7 ± 0.1) was encountered, related to a 1:1 stoichiometry and log affinity constants of 3.24 ± 0.10 and 3.67 ± 0.08 for E1 and E2, respectively. The protein binding (PB) estimated at physiological concentration levels was 40 ± 5 and $63 \pm 4\%$ for E1 and E2, respectively. The use of synthetic human sera allowed *in vitro* estimation of the total plasma PB for the racemate ($61 \pm 5\%$; coincident with *in vivo* values), and its enantiomers (58 ± 7 and $64 \pm 4\%$ for E1 and E2, respectively). Comparison allowed the relative importance of HSA respect to other plasma proteins for binding nomifensine to be established. Copyright © 2012 John Wiley & Sons, Ltd.

Keywords: EKC; enantioselectivity; nomifensine; protein binding

Introduction

Pharmacokinetic *in vitro* studies are useful for pharmaceutical and biomedical industry, mainly in the preclinical phases of the development of new drugs. Pharmacokinetic studies of drugs involve processes like intestinal absorption, distribution between blood and tissues, metabolic reactions and elimination. All these processes affect the pharmacological activity, because only the fraction of the drug that can reach the target place is active. Owing to this influence, the development of powerful methodologies at the microscale level for the study of pharmacokinetic properties of drugs has become an important field in bioanalytical research. Most of the pharmacokinetic and pharmacological processes exhibit a high degree of enantioselectivity, owing to the characteristic chirality of biomolecules, and this results in differences between the pharmacological activities of drug enantiomers. In fact, very often one of them is most active while the other may produce side-effects and even toxicity in some cases (Asensi-Bernardi *et al.*, 2010). Therefore, investigation of the enantioselectivity of drugs in their pharmacokinetic and pharmacological properties represents a great challenge for clinical pharmacology (Escuder Gilabert *et al.*, 2009). Under pressure from authorities, there has been an increasing interest in development of rapid, efficient and sensitive analytical methods to control the chiral purity of drugs and for pharmacokinetic studies (Cherkaoui *et al.*, 2001). Protein binding is one of the most important parameters affecting drug distribution. Since only free drug is active, and can be metabolized or eliminated, drug–plasma protein complexes serve as reservoirs to supply free drug,

prolonging the duration of the drug action (Martínez-Gómez *et al.*, 2007). Human serum albumin (HSA) is the most abundant protein in human plasma, and it presents a high degree of enantioselectivity in its interaction with drugs (Ascoli *et al.*, 2006). Owing to this property, it has been widely used as chiral selector in chromatographic and electrophoretic methodologies (Millot, 2003; Zhu *et al.*, 1999; Domenici *et al.*, 1990; Zhang *et al.*, 1999; Lloyd *et al.*, 1995; Hjerten *et al.*, 1998).

The most important bioanalytical approaches to characterizing drug–protein binding have been recently reviewed, including a critical evaluation of their strengths and weaknesses (Vuignier *et al.*, 2010). A review of our group emphasized the microseparation techniques for evaluating the enantioselective binding of drugs to plasma proteins (Escuder Gilabert *et al.*, 2009). Most *in vitro* studies

* Correspondence to: María J. Medina-Hernández, Departamento de Química Analítica, Facultad de Farmacia, Universidad de Valencia, Burjassot, Valencia, Spain. E-mail: mariaj.medina@uv.es

^a Departamento de Química Analítica, Facultad de Farmacia, Universidad de Valencia, Burjassot, Valencia, Spain

^b Centro de Reconocimiento Molecular y Desarrollo Tecnológico (IDM), Unidad mixta Universidad Politécnica de Valencia-Universidad de Valencia

Abbreviations used: CD, cyclodextrins; EKC, electrokinetic chromatography; ES, enantioselectivity; HSA, human serum albumin; NMF, nomifensine; PB, protein binding; PET, positron emission tomography; TM- β -CD, heptakis-2,3,6-tri-*O*-methyl- β -cyclodextrin.

concerning a racemate involve two steps: separation of the free drug fraction from the bound drug once the drug–protein equilibrium has been reached, and chiral analysis of enantiomers, usually on the unbound fraction. For the first step, dialysis equilibrium (Kwong, 1985), ultracentrifugation (Kwong, 1985) and ultrafiltration (Kurz, 1986) have been frequently used. For the second step, various analytical techniques have been proposed, such as HPLC, GC, CE and supercritical fluid chromatography (Chankvetadze, 2007). In this field, CE is one of the most used techniques, owing to its high separation power, low amount of sample required (microvolumes), short analysis time and ease of automation (Zhu *et al.*, 1999; Lin *et al.*, 2003). One of the most common modes of chiral CE is EKC in the presence of a chiral selector in the BGE. In the EKC modality of partial filling technique, proposed by Valtcheva *et al.* (1993), the capillary is partially filled with the chiral selector solution, leaving all the rest, including the detection window, free of it. In this methodology the consumption of chiral selector per injection is minimized (from milliliters to nanoliters), achieving advantages from the analysis cost and environmental points of view. Among the different chiral selectors employed in CE (proteins, glycopeptides, polysaccharides, chiral surfactants, bile salts, etc.), cyclodextrins (CDs) are one of the most widely used, owing to their UV transparency, stability and broad enantioselective abilities for the various kinds of native and derivatized CDs available (Matthijs *et al.*, 2004).

While reports on biodifferentiation between enantiomers activity evidence the general importance of the field, the quantitative estimation of enantioselective binding of chiral compounds to HSA is an issue poorly treated in the literature. In most cases, incomplete data are provided with uncertain results (Asensi-Bernardi *et al.*, 2010; Fielding *et al.*, 2005, and references therein). Also, methodological drawbacks are encountered, suggesting that clearer information is needed. Quantitative enantioselectivity to HSA (of maximum interest from the distribution point of view), implies reliable affinity data for both enantiomers (constant and stoichiometry; two dependent parameters which must be solved from a single equation). This justifies the effort to minimize errors by the use of the racemate instead of the pure enantiomers, an optimized experimental design (favoring the model validity), a direct equation allowing a univariate data treatment (avoiding the reported inconsistencies/lack of robustness of regression/fitting strategies; Asensi-Bernardi *et al.*, 2010; Fielding *et al.*, 2005) or stoichiometry verification, to improve confidence. The conversion of the protein binding data analysis into a univariate problem, a very recent proposal in this area (Asensi-Bernardi *et al.*, 2010), allows a radical change in the data treatment possibilities (i.e. outlier checking, hypothesis testing, robust statistics, reliable uncertainty on the results). New examples are necessary to demonstrate its usefulness with respect the classical approaches (massively used in the past) that do not have these features.

Nomifensine (NMF) is an isoquinoline derivative that prevents dopamine reuptake into synaptosomes. The maleate was formerly used in the treatment of depression but it was withdrawn worldwide in 1986 owing to the risk of acute hemolytic anemia with intravascular hemolysis resulting from its use (Martindale, 1993). Nomifensine is now mainly used in scientific research as a model of dopamine reuptake inhibitors (Yorgason *et al.*, 2011; Stouffer *et al.*, 2011; Masana *et al.*, 2011; Hadjiconstantinou *et al.*, 2011), although a clinical application in Parkinson's disease study and diagnosis has been described (Sioka *et al.*, 2010). Parkinson's disease can be evaluated by studying the dopamine pathways using positron emission tomography (PET) with different tracers to image the presynaptic and postsynaptic sites of dopaminergic system. PET can also contribute to the differential diagnosis of Parkinson's

disease when clinical features are not clear. One of the tracers that have been used for presynaptic assessment is [11 C]nomifensine, which inhibits the reuptake of the released dopamine by blocking the dopamine reuptake sites (dopamine transporter) in presynaptic nerve terminals (Sioka *et al.*, 2010). The use of nomifensine as a PET tracer is affected by its distribution between blood and central nervous system, where protein binding plays an important role. Therefore, the study of its enantioselective protein binding may be helpful in this context, since differences between the dopamine transporter-blocking activities of the enantiomers have been shown in the literature (Vaugeois *et al.*, 1992; Schacht and Leven, 1984).

In this paper, nomifensine (racemate) serves as a test chiral compound to illustrate the applicability of an overall robust-univariate-stereoselective protein binding-approach, performed under intermediate precision conditions, forming the first evidence of its enantioselective binding to HSA and plasma proteins. This methodology includes the incubation of drug–protein mixtures at the microliter level, their ultrafiltration through cellulose filters and the chiral analysis of the unbound fraction by EKC-partial filling technique using heptakis-2,3,6-tri-O-methyl- β -cyclodextrin (TM- β -CD) as chiral selector. A recent mathematical approach of our group (Asensi-Bernardi *et al.*, 2010) was used to estimate affinity constants (K_1) and verify the stoichiometry (n_1), for both enantiomers of nomifensine, as well as to estimate their enantioselectivity (ES). Protein binding in percentage (PB) to HSA at physiological concentration levels and total plasma proteins were also estimated and compared with *in vivo* literature data.

Experimental

Instrumentation

A Beckman P/ACE MDQ capillary electrophoresis system equipped with a diode array detector (Beckman Coulter, Fullerton, CA, USA), and 32Karat software version 8.0 was used throughout. A 50 μ m inner diameter (i.d.) fused-silica capillary with total and effective lengths of 60.5 and 50 cm, respectively, was employed. Electrophoretic solutions and samples were filtered through 0.45 μ m pore size nylon membranes (Micron Separation, Westboro, MA, USA) and degassed in an ultrasonic bath (JP Selecta, Barcelona, Spain) prior to use. A Crison Micro pH 2000 pHmeter from Crison Instruments (Barcelona, Spain) was employed to adjust the pH of buffer solutions.

A Selecta thermostated bath (JP Selecta, Barcelona, Spain) was used for sample incubation. For the ultrafiltration of samples, Microcon YM-10 cellulose filters of a molecular weight of 10,000 MWCO (Millipore Corporation, Bedford, MA, USA) and a Heraeus Biofuge Strate centrifuge (Heraeus, Madrid, Spain) were used.

Chemicals and standard solutions

All reagents were of analytical grade. Human serum albumin fraction V and lyophilized human sera were purchased from Sigma (St Louis, MO, USA); sodium dihydrogen phosphate dihydrate and TM- β -CD were from Fluka (Buchs, Switzerland); Tris-(hydroxymethyl)-aminomethane (Tris) was from Scharlab (Barcelona, Spain). Racemic NMF was from Research Biochemicals International (Natick, USA). Ultra Clear TWF UV deionized water (SG Water, Barsbüttel, Germany) was used to prepare solutions.

Separation buffer in EKC containing Tris 50 mM at pH 6.0 was obtained by dissolving the appropriate amount of Tris in water and adjusting the pH with 1 M HCl. For the incubation process (NMF–HSA binding), 67 mM phosphate buffer was prepared and adjusted to pH 7.4 with 1 M NaOH. Stock solutions of 100 mM TM- β -CD and 1000 μ M NMF were prepared in

the separation buffer. A 1000 μM HSA stock solution was prepared daily by weighting the corresponding amount of protein powder and dissolving it with the phosphate buffer.

Capillary conditioning

New capillaries were conditioned using a 15 min flush with 1 M NaOH at 60 °C. Then, they were rinsed for 10 min with deionized water and 10 min with separation buffer at 25 °C. In order to obtain good peak shapes and reproducible migration data, the capillary was conditioned prior to each injection, and at the beginning and the end of the working session. In all cases, the conditioning run included the following steps: (i) 1 min rinse with deionized water; (ii) 2 min rinse with 0.1 M NaOH; and (iii) 1 min rinse with deionized water at 20 psi. Before chiral selector and sample injection the capillary was also rinsed with the separation buffer for 2 min at 20 psi.

Enantioseparation of NMF by EKC using TM- β -CD

For all experiments, the 50 mM Tris solution was used as electrophoretic buffer. A 30 mM TM- β -CD solution obtained by diluting the stock solution with the buffer was used as the chiral selector. NMF samples (ultrafiltrated fractions and standards) were injected hydrodynamically at 0.5 psi for 3 s. Before sample injection, the capillary was partially filled with the 30 mM TM- β -CD solution by applying 10 psi for 1 min. Separation was performed in normal polarity by applying 15 kV. The capillary was thermostated at 50 °C and the UV-detection wavelength was set at 220 nm. Under these conditions, a minimum resolution of 1.7 was obtained for the enantiomers of NMF.

Incubation, separation and analysis of unbound NMF fraction to HSA and plasma proteins

We planned an experimental design to study the binding of the enantiomers to HSA (or synthetic human sera), keeping the concentration of protein constant within the physiological range, varying the concentration of racemic NMF according to the detector capabilities and keeping an excess of protein respect to the enantiomer concentration. Five concentration levels of NMF were used with three independent replicates per level, totalling 15 independent mixtures for the studies with HSA. This experiment was repeated in two different working sessions (days). For the evaluation of the total plasma protein binding, four concentration levels of NMF, with three independent replicates per level, totalling 12 samples, were used. Mixtures were prepared by dilution of the stock solutions of drug and protein with the phosphate buffer. In the sera samples case, the relation aqueous/sera solution was 100/300 (v/v). All these mixtures were allowed to reach equilibrium for 30 min in a water bath at 36.5 °C and filtered through cellulose filters by centrifugation at 9000 rpm for 30 min. The ultrafiltrate was directly injected into the EKC system. Figure 1 shows the electropherograms of total and unbound fraction of NMF obtained in the EKC conditions previously specified.

Software and calculations

For the NMF-HSA binding study, routines made/adapted in MATLAB[®] 4.2 were used for calculations, and the results generated were verified using EXCEL[®] and STATGRAPHICS[®]. The mathematical aspects were previously described in detail (Asensi-Bernardi *et al.*, 2010, and references therein) and they are briefly described here. An accepted mathematical model describing the ligand-HSA interaction, applicable for each enantiomer in the case of a chiral molecule, considering m classes of independent active sites on HSA, each with n_i binding sites, is:

$$r = \frac{b}{P} = \frac{D-d}{P} = \sum_{i=1}^m n_i \frac{K_i d}{1 + K_i d} \quad (1)$$

In this equation, r is the fraction of bound enantiomer per molecule of protein, b is the bound concentration of enantiomer and P is the total protein concentration. D and d are the total and free enantiomer

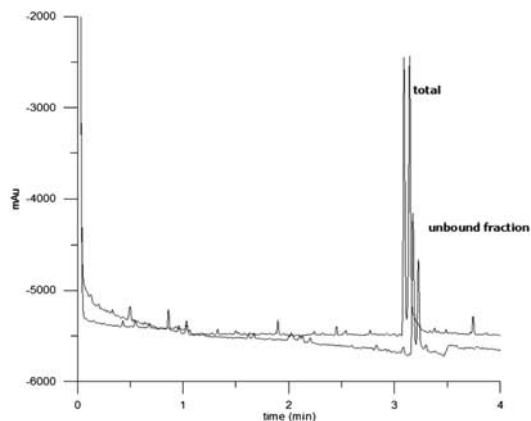


Figure 1. Electropherograms of total and unbound fraction of nomifensine, after incubation with human serum albumin and ultracentrifugation. Electrokinetic chromatography conditions specified in Experimental section.

concentrations, respectively. All the concentrations must be expressed in molar units (M). For the site i , n_i represents the apparent site stoichiometry. Two simplified approaches were used here. The first simplified approach assumes $m = 1$ and $n_1 = 1$. Both assumptions should be reasonably valid for low D/P ratios (usually under *in vivo* conditions), as well as the independent binding between enantiomers, since there is relatively high concentration of available binding sites (Asensi-Bernardi *et al.*, 2010), providing:

$$K_1 = \frac{1}{d} \frac{r}{1-r} \quad (2)$$

Equation (2) is a one-parameter model, allowing K_1 estimation for individual $D-P-d$ data and then serving as a source for outlier identification (Asensi-Bernardi *et al.*, 2010). To verify the previous approach an alternative equation, it was simply assumed that $m = 1$, providing:

$$d = \frac{-(1 - K_1 D + n_1 K_1 P) + \sqrt{(1 - K_1 D + n_1 K_1 P)^2 + 4 K_1 D}}{2 K_1} \quad (3)$$

Equation (3) is a d -isolated (dependent variable) nonlinear form of equation (1) when $m = 1$. SIMPLEX optimization (nonlinear fitting) was used for estimating the parameters n_1 and K_1 , allowing integer n_1 values (Asensi-Bernardi *et al.*, 2010).

Results and discussion

Calibration

Calibration standard solutions containing racemic NMF in the range 50–500 μM (25–250 μM of each enantiomer; the first, E1, and second, E2, eluted ones) were prepared in triplicate. The linear regression equations were

$$\text{corrected peak area} = (-16 \pm 14) + (4.27 \pm 0.09)[E1] (\mu\text{M}), R^2 = 0.993$$

$$\text{corrected peak area} = (-23 \pm 13) + (4.39 \pm 0.08)[E_2] \text{ } (\mu\text{M}), R^2 = 0.995$$

These calibration models were used to estimate d , by interpolating the analytical signals (corrected peak areas) corresponding to ultrafiltrates from the racemic NMF–HSA mixtures, providing the required D – P – d values.

Enantioselective binding to HSA and plasma proteins

Consistently with equation (2) suggestions, D and P (independent variables in the experimental design) concentration levels were designed keeping $D/P < 0.5$ as a prefixed rule, to ensure, as far as possible, model validity (Asensi-Bernardi *et al.*, 2010). The minimum D ($\sim 70 \mu\text{M}$) was fixed considering the adequate analytical signals for enantiomer quantification after the analysis of the ultrafiltrates (unbound fraction). P was fixed around the hypoalbuminemia–normal levels frontier (Asensi-Bernardi *et al.*, 2010). Table 1 shows the experimental values of D and P in the mixtures (in micromolar units, although they were transformed into molar units for modeling), as well as the measured ones, d_{E1} and d_{E2} . The D/P ratios (from 0.15 to 0.45) should guarantee the assumptions made above, for instance, the $m=1$ model for the NMF–HSA interaction, since only at high concentration may a single drug populate multiple sites on HSA (Asensi-Bernardi *et al.*, 2010; Kragh-Hansen, 1988). In Table 1, since each of the five D -concentration levels has three independent replicates in each of the two working sessions, we can control atypical results. Owing to the intermediate precision conditions of the study, which are unusual in this field, we can also control inter-day effect.

Outlier identification/elimination in the HSA study

We have proposed a Z -score approach as an alternative to other tests for outliers, as an automatic criterion (Bisetty *et al.*, 2009). Most tests for outliers depend on good estimates of dispersion, and become less reliable with real errors present. Robust statistics is a convenient method of handling results when they are expected to follow a near-normal distribution, but are suspected to contain a small proportion of errors that are not representative of the bulk of the data (RobStat.xla 1.0, 2002). The median and $MADe$ (a robust estimation of the standard deviation) were used to estimate a robust Z -score, Z_j for each independent $\log K_{1j}$ estimate from equation (2):

$$Z_j = (\log K_{1j} - \text{median}) / MADe \quad (4)$$

Normally, $Z_j > 3$ is considered unsatisfactory, while values of $Z_j > 2$ are considered dubious. Here we have pre-fixed a $Z_j > 2.5$ criterion to eliminate a point.

Data ID 9 and 19 (marked in Fig. 2) appear atypical for both enantiomers, which suggests errors in the overall sample process (other replicates at the same level were normal). These values were found to be outliers according to double Grubbs test ($\alpha = 2.5\%$, two tails) for $E1$, but not for $E2$ (although close to violating the critical value). The Z -score approach showed that data ID 9 and 19 had Z -scores, based on robust statistics, larger than 3 (unsatisfactory) for $E1$ and $E2$. The data were therefore considered inconsistent and eliminated from further analyses since there were two replicate data for the same D – P levels with consistent values. The median values (lines into Fig. 2) suggest a larger K_1 value for $E2$.

Table 1. Experimental design and results. Experimental p -values were $459.6 \mu\text{M}$ for the first working session (ID 1–15) and $459.9 \mu\text{M}$ for the second one (ID 16–27). Data were transformed to molar units for calculations. Outliers appear crossed out

D -Level	ID	D (μM)	d_{E1} (μM)	d_{E2} (μM)
1	1	70.0	35.6	22.1
	2	70.0	38.1	23.2
	3	70.0	45.6	27.5
2	4	105.0	61.2	37.2
	5	105.0	64.8	37.1
	6	105.0	57.3	33.6
3	7	140.0	84.3	51.5
	8	140.0	71.3	43.9
	9	140.0	42.2	33.4
4	10	174.9	118.6	75.8
	11	174.9	102.5	66.5
	12	174.9	125.4	77.8
5	13	209.9	145.1	105.6
	14	209.9	107.6	69.2
	15	209.9	118.0	80.3
1 ^a	16	70.0	43.9	25.2
2 ^a	17	105.0	56.6	47.9
3	18	105.0	63.5	36.6
	19	140.0	106.9	73.0
	20	140.0	81.2	52.4
4	21	140.0	80.3	47.6
	22	174.9	105.6	70.2
	23	174.9	104.0	71.9
5	24	174.9	113.1	73.8
	25	209.9	132.8	92.4
	26	209.9	129.5	81.1
	27	209.9	122.4	83.9

^aMissing data for D -levels 1 and 2 in the second working session are due to problems with the electrophoretic system.

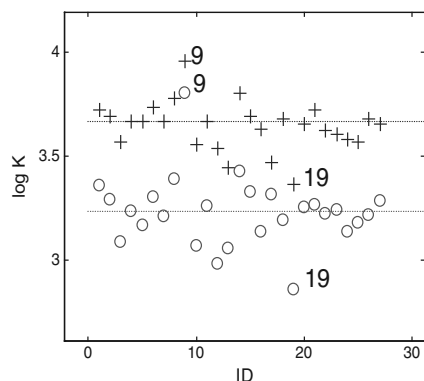


Figure 2. Estimated $\log K_1$ values for $E1$ (open circles) and $E2$ (crosses) based on equation (2). Points $ID = 9$ and 19 appear as atypical data (note they are one of three replicates for a given D – P level; see Table 1). Horizontal lines indicate the median value.

Estimation of affinity constants to HSA

Equation (2) was used above for evaluating outliers assuming that $n_1 = 1$ (the most probable situation at low D/P ratio; Asensi-Bernardi *et al.*, 2010), owing to the relatively high concentration of available binding sites. An initial robust estimate of $\log K_1$ for the enantiomers was provided based on equation (2). Initially, there was no reason to suspect that the data from a particular session were worse than the others, so, except the outliers, all the data were combined to derive the final affinity estimates. The $\log K_1$ robust estimates (median \pm MADe; Asensi-Bernardi *et al.*, 2010), after eliminating data ID 9 and 19, were 3.24 ± 0.10 and 3.67 ± 0.08 for E1 and E2, respectively.

To verify the parameters n_1 and K_1 , an approach based on nonlinear regression [using equation (3)] was used. A SIMPLEX search was started with $n_1 = 1$, $\log K_1 = 4$, and only integer n_1 values were allowed (Asensi-Bernardi *et al.*, 2010). The $\log K_1$ estimates found were 3.23 ± 0.11 and 3.64 ± 0.09 , respectively, which agree with the values obtained using equation (2). In addition, $n_1 = 1$ estimates were found for both enantiomers, verifying the assumption. As an example of the model adequacy, Fig. 3 shows some results associated to enantiomer E1 based on equation (3): the validation plot for d (Fig. 3a) and the response surface estimation by SIMPLEX (Fig. 3b). This suggests that $\log K_1$ estimates using equation (2), including their uncertainty (accounting for the overall process variability in intermediate precision conditions), could be considered acceptable values.

Enantioselectivity and protein binding to HSA

From K_1 estimates, the enantioselectivity (ES , estimated as K_{E2}/K_{E1}) could be obtained [note that, as K_1 , individual estimations of ES are possible using the equation (2) strategy]. The estimated ES was 2.7 ± 0.1 , indicating a fair enantioselectivity degree in favor of the second enantiomer eluted (E2). Figure 4 shows the box-and-whisker plots from the affinity (AF , in terms of $\log K_1$) and ES estimates, considering all the data (Fig. 4a) or two data sets corresponding to the independent working sessions (Fig. 4b). As can be seen in Fig. 4 (a), $\log K_1$ data for E1 and E2 exhibit similar dispersion with median and mean values almost coincident, while ES (combined data from E1 and E2) presents larger dispersion with an appreciable difference between the mean and median values. The K_1 estimates and the ES

obtained in the two working sessions are similar (Fig. 4b), suggesting that the data could be combined, providing more robust results.

Qualitatively, it was clear that E2 showed higher affinity to HSA than its antipode, so values of $ES > 1$ were obtained. However, since the $\log K_1$ differences were not too high, it was convenient to check this observation through hypothesis testing. Statistical comparison of $\log K_1$ paired data vectors of the enantiomers was performed. Both the parametric t -test for the means and the nonparametric ones for the medians (the sign test and the signed rank test) indicate significant differences ($p < 0.05$) between the averaged affinity estimates, so significant enantioselectivity was demonstrated. The same conclusion was encountered through the comparison between ES and the unity.

A key parameter from a pharmacokinetic point of view is the estimation of the percentage of protein binding. By means of equation (3) and using the estimated constants at prefixed (desired) D and P values, it is possible to estimate the corresponding d values, and from them, the PB according to:

$$PB = 100(D - d)/D \quad (5)$$

Here we have selected values consistent with physiological conditions, e.g. $D = 0.2 \times 10^{-6}$ M (Nirogi *et al.*, 2006) and $P = 600 \times 10^{-6}$ M (Asensi-Bernardi *et al.*, 2010). After d_{E1} and d_{E2} estimation, the PB for each NMF enantiomer was calculated. The estimated values were 40 ± 5 and $63 \pm 4\%$ for E1 and E2, respectively.

Plasma protein binding

The total plasma protein binding was estimated for racemic NMF and, for the first time, its enantiomers using synthetic human sera, using equation (5). The results for the racemate were compared with previous *in vivo* values found in the literature (Kellner *et al.*, 1977; Heptner *et al.*, 1978; Table 2). As can be seen, protein binding estimation agreed with the literature values. Plasma protein binding data can be compared with HSA data. In the case of E1 (PB to HSA, $40 \pm 5\%$) a contribution of other plasma proteins was expected according to the plasma PB ($58 \pm 7\%$), but not for E2 (PB $63 \pm 4\%$ and $64 \pm 4\%$ for HSA and plasma, respectively). Even for E1, the role of HSA is the most important.

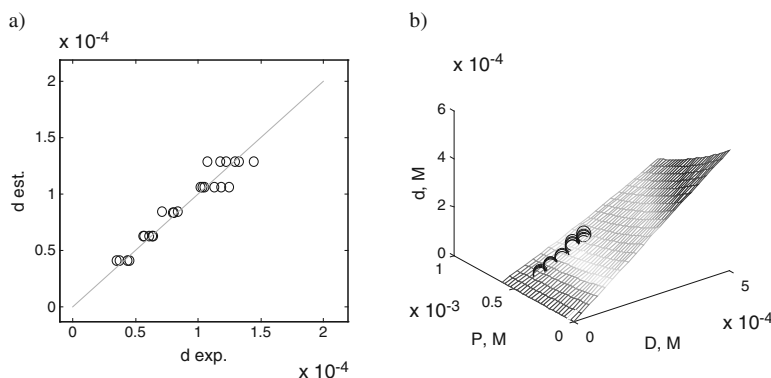


Figure 3. Results of the nonlinear approach corresponding to E1. Validation plot, d -estimated vs d -experimental (a) and response surface estimation (d - D - P plot) (b).

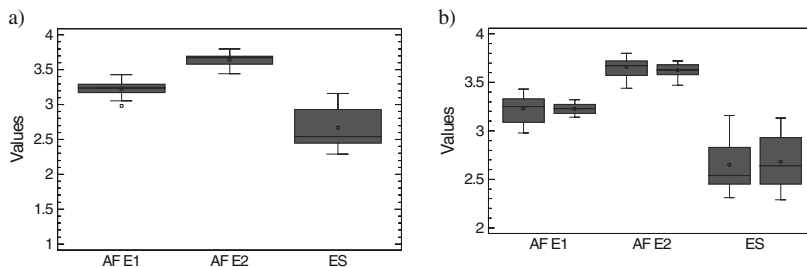


Figure 4. Box-and-whisker plots for affinity constants [affinity, AF , in terms of $\log K_1$ estimated by equation (2)] of nomifensine enantiomers (E1 and E2) and their enantioselectivities ($ES = K_{E2}/K_{E1}$), considering all the data (a) or two data sets considering the independent working sessions (b).

Table 2. Plasma protein binding values for racemic NMF and its enantiomers

Reference	PB% NMF-rac	PB% NMF-E1	PB% NMF-E2
This work (<i>in vitro</i> ; synthetic human sera)	61 ± 5	58 ± 7	64 ± 4
Kellner et al. (1977), <i>in vivo</i>	60	—	—
Heptner et al. (1978), <i>in vivo</i>	60	—	—

Conclusions

The *in vitro* incubation of racemic nomifensine with HSA or synthetic human sera in approximated physiological conditions followed by ultrafiltration and separation/determination of enantiomers by EKC-TM- β -CD-partial filling system makes it possible to access information unobtainable by *in vivo* experiments. Microvolumes of analyte, HSA and sera and nanovolumes of cyclodextrin per injection are enough to provide the results, which constitute the first evidence of enantioselective binding of nomifensine to HSA and plasma proteins. A significant enantioselectivity to HSA (2.7 ± 0.1) was encountered, consistent with a confirmed 1:1 stoichiometry and affinity constants ($\log K_1$ 3.24 ± 0.10 and 3.67 ± 0.08 for E1 and E2, respectively) and protein binding (40 ± 5 and 63 ± 4 for E1 and E2, respectively, at physiological concentration levels). PB results for the racemate-synthetic human were coincident with those available *in vivo*. Additionally, PB estimates for the enantiomers allowed the predominant role of HSA respect to the rest of plasma proteins to be established.

Consistency is favored by the direct simple strategy based on equation (2), an adaptation of the protein-binding data analysis into a univariate problem with intrinsic statistical advantages, as well as the elimination of outliers tools [equation (2)+equation (4)] and further verification of $n_1=1$ and K_1 [equation (3) and SIMPLEX]. Moreover low D/P ratios (to guarantee the validity of the assumed model along the D -concentration interval) contribute to the consistency. The proposed scheme favors control over the individual D - P - d data, here replicated at different D -concentration levels in two independent sessions (days), allowing reliable uncertainty estimations accounting for the intermediate precision conditions used.

Acknowledgments

The authors acknowledge the Spanish Ministry of Science and Innovation (MCINN), project SAF2008-00859, the South African-Spanish Bilateral Agreement of the National Research Foundation South Africa, project UID 69160, MCINN, project HS2008-0002, and the Generalitat Valenciana (GVACOMP2011-002) for financial support. L. Asensi-Bernardi acknowledges the Generalitat Valenciana for her pre-doctoral research grant (ACIF/2011/114). The authors declare that there is no conflict of interest.

References

- Ascoli G-A, Domenici E and Bertucci C. Drug binding to human serum albumin: Abridged review of results obtained with high-performance liquid chromatography and circular dichroism. *Chirality* 2006; **18**: 667–679.
- Asensi-Bernardi L, Martín-Biosca Y, Villanueva-Camañas RM, Medina-Hernández MJ and Sagrado S. Evaluation of the enantioselective binding of fluoxetine to human serum albumin by ultrafiltration and CE. Experimental design and quality considerations. *Electrophoresis* 2010; **31**: 3268–3280.
- Bisetty K, Gumede NJ, Escuder-Gilabert L and Sagrado S. Toward a quality guide to facilitate the transference of analytical methods from research to testing laboratories: a case study. *Journal of AOAC International* 2009; **92**: 1821–1832.
- Chankvetadze B. Enantioseparations by using capillary electrophoretic techniques. The story of 20 and a few more years. *Journal of Chromatography. A* 2007; **1168**: 45–70.
- Cherkaoui S, Rudaz S, Varesio E and Veuthey JL. On-line capillary electrophoresis-electrospray mass spectrometry for the stereoselective analysis of drugs and metabolites. *Electrophoresis* 2001; **22**: 3308–3315.
- Domenici E, Brett C, Salvadori P, Félix G, Cahagne I, Motellier S and Wainer IW. Synthesis and chromatographic properties of an HPLC chiral stationary phase based upon human serum albumin. *Chromatographia* 1990; **29**: 170–176.
- Escuder Gilabert L, Martínez Gómez MA, Villanueva-Camañas RM, Sagrado S and Medina-Hernández MJ. Microseparation techniques for the study of the enantioselectivity of drug-plasma protein binding. *Biomedical Chromatography* 2009; **23**: 225–238.
- Fielding L, Rutherford S and Fletcher D. Determination of protein-ligand binding affinity by NMR: Observations from serum albumin model systems. *Magnetic Resonance in Chemistry* 2005; **43**: 463.
- Hadjiconstantinou M, Duchemin A, Zhang H and Neff NH. Enhanced dopamine transporter function in striatum during nicotine withdrawal. *Synapse* 2011; **65**: 91–98.
- Heptner W, Hornke I and Cavagna F. Metabolism of nomifensine in man and animal species. *Arzneimittel-Forschung/Drug Research* 1978; **28**: 58–64.
- Hjerten S, Vegvari A, Srichaiyo T, Zhang HX, Ericson C and Eaker D. An approach to ideal separation media for (electro)chromatography. *Journal of Capillary Electrophoresis* 1998; **5**: 13–26.

- Kellner HM, Baeder C and Christ O. Kinetics and metabolism of nomifensine in animals. *British Journal of Clinical Pharmacology* 1977; **4**: 1095–1165.
- Kragh-Hansen U. Evidence for a large and flexible region of human serum albumin possessing high affinity binding sites for salicylate, warfarin, and other ligands. *Molecular Pharmacology* 1988; **34**: 160–171.
- Kurz H. Methodological problems in drug binding studies. In *Drug Protein Binding*. Praeger: New York, 1986; 70–92.
- Kwong TC. Free drug measurements: methodology and clinical significance. *Clinica Chimica Acta* 1985; **151**: 193–216.
- Lin CC, Li YT and Chen SH. Recent progress in pharmacokinetic applications of capillary electrophoresis. *Electrophoresis* 2003; **24**: 4106–4115.
- Lloyd DK, Li S and Ryan P. Protein chiral selectors in free-solution capillary electrophoresis and packed-capillary electrochromatography. *Journal of Chromatography. A* 1995; **694**: 285–296.
- Martindale. *The Extra Pharmacopoeia*, 30th edn. Pharmaceutical Press: London, 1993; 266.
- Martínez-Gómez MA, Carril-Avilés MM, Sagrado S, Villanueva-Camañas RM and Medina-Hernández MJ. Characterization of antihistamine–human serum protein interactions by capillary electrophoresis. *Journal of Chromatography. A* 2007; **1147**: 261–269.
- Masana M, Bortolozzi A and Artigas F. Selective enhancement of mesocortical dopaminergic transmission by noradrenergic drugs: Therapeutic opportunities in schizophrenia. *The International Journal of Neuropsychopharmacology* 2011; **14**: 53–68.
- Matthijs N, Van Hemelryck S, Maftouh M, Massart DL and Vander Heyden Y. Electrophoretic separation strategy for chiral pharmaceuticals using highly-sulfated and neutral cyclodextrins based dual selector systems. *Analytica Chimica Acta* 2004; **525**: 247–263.
- Millot MC. Separation of drug enantiomers by liquid chromatography and capillary electrophoresis, using immobilized proteins as chiral selectors. *Journal of Chromatography B* 2003; **797**: 131–159.
- Nirogi RVS, Kandikere VN and Mudigonda K. Quantitation of zopiclone and desmethylzopiclone in human plasma by high-performance liquid chromatography using fluorescence detection. *Biomedical Chromatography* 2006; **20**: 794–799.
- RobStat.xla 1.0. *Robust statistic Toolkit. AMC technical brief number 6*. The Royal Society of Chemistry: London, 2002.
- Schacht U and Leven M. Stereoselective inhibition of synaptosomal catecholamine uptake by nomifensine. *European Journal of Pharmacology* 1984; **98**: 275–277.
- Sioka C, Fotopoulos A and Kyritsis AP. Recent advances in PET imaging for evaluation of Parkinson's disease. *European Journal of Nuclear Medicine and Molecular Imaging* 2010; **37**: 1594–603.
- Stouffer MA, Ali S, Reith MEA, Patel JC, Sarti F, Carr KD and Rice ME. SKF-83566, a D1-dopamine receptor antagonist, inhibits the dopamine transporter. *Journal of Neurochemistry* 2011; **118**: 714–720.
- Valtcheva L, Mohammad J, Petterson G and Hjertén S. Chiral separation of β -blockers by high-performance capillary electrophoresis based on non-immobilized cellulose as enantioselective protein. *Journal of Chromatography. A* 1993; **638**: 263–267.
- Vaugeois JM, Bonnet JJ and Costentin J. In vivo labelling of the neuronal dopamine uptake complex in the mouse striatum by [3 H]GBR 12783. *European Journal of Pharmacology* 1992; **210**: 77–84.
- Vuignier K, Schappler J, Veuthey JL, Carrupt PA and Martel S. Drug–protein binding: a critical review of analytical tools. *Analytical and Bioanalytical Chemistry* 2010; **398**: 53–66.
- Yorgason JT, Jones SR and España RA. Low and high affinity dopamine transporter inhibitors block dopamine uptake within 5 sec of intravenous injection. *Neuroscience* 2011; **182**: 125–132.
- Zhang XX, Hong F, Chang WB, Ci YX and Ye YH. Enantiomeric separation of promethazine and D,L - α -amino- β -[4-(1,2-dihydro-2-oxo-quinoline)] propionic acid drugs by capillary zone electrophoresis using albumin as chiral selectors. *Analytica Chimica Acta* 1999; **392**: 175–181.
- Zhu X, Ding Y, Lin B, Jakob A and Koppenhoefer B. Study of enantioselective interactions between chiral drugs and serum albumin by capillary electrophoresis. *Electrophoresis* 1999; **20**: 1869–1877.

Paper VIII

**Screening of acetylcholinesterase inhibitors by CE after enzymatic
reaction at capillary inlet**

**Y. Martín-Biosca, L. Asensi-Bernardi, R.M. Villanueva-Camañas, S.
Sagrado and M.J. Medina-Hernández**

Journal of Separation Science 2009, 32, 1748-1756

Yolanda Martín-Biosca
Lucia Asensi-Bernardi
Rosa M. Villanueva-Camañas
Salvador Sagrado
María J. Medina-Hernández

Departamento Química Analítica,
Universitat de València, C/Vicente
Andrés Estellés s/n, Burjassot
(Valencia), Spain

Original Paper

Screening of acetylcholinesterase inhibitors by CE after enzymatic reaction at capillary inlet

In this study the development of a procedure based on capillary electrophoresis after enzymatic reaction at capillary inlet methodology for the screening and *in vitro* evaluation of the biological activity of acetylcholinesterase (AChE) inhibitors is presented. The progress of the enzymatic reaction of the hydrolysis of acetylthiocholine at pH 8 in the presence of AChE and the inhibitor studied is determined by measuring at 230 nm the peak area of the reaction product thiocholine (TCh). In the method employed the capillary was first filled with 30 mM borate-phosphate buffer (pH 8.0) and subsequently, plugs of: (i) water, (ii) AChE solution, (iii) substrate solution with or without inhibitor, (iv) AChE solution, and (v) water, were hydrodynamically injected into the capillary, and were allowed to stand (and react) during a waiting period of 2 min. The applicability of the proposed methodology to estimate different kinetic parameters of interest such as inhibition constants K_i , identification of inhibitory action mechanism and IC_{50} , is evaluated using compounds with known activity, tacrine edrophonium, and neostigmine. The results obtained are compared with bibliographic values and confirm the effectiveness of the methodology proposed. Finally a method for AChE inhibitor screening is proposed.

Keywords: Capillary electrophoresis / Enzymatic reaction in capillary / Screening of acetylcholinesterase inhibitors

Received: December 3, 2008; revised: December 23, 2008; accepted: February 24, 2009

DOI 10.1002/jssc.200800701

1 Introduction

The use of compounds to inhibit enzyme action is an important possibility for therapeutic intervention. Many drugs act by inhibiting specific enzymes which are associated with the disease process [1]. In this context, human acetylcholinesterase (AChE) is currently indicated as a target enzyme for drugs to be used in the treatment of Alzheimer's disease (AD), the most common form of dementia in the elderly. One important change observed in the brain of AD patients is a decrease in hippocampal and cortical levels of the neurotransmitter acetylcholine (ACh) by nearly 90%. This important decrease in ACh levels causes impairment in cognitive function [2]. Pharmacological treatment of AD is currently based on AChE inhibitors, such as tacrine, donepezil, rivastigmine, and galantamine which maintain high levels of ACh at the

muscarinic and nicotinic receptors in the central nervous system determining beneficial effects on cognitive, functional, and behavioral symptoms of the disease [3]. However, the adverse side effect of these drugs, often due to inhibition of peripheral AChE, limits their use [4]. For that reason, research on new inhibitors for the treatment of AD with improved pharmacological properties is currently in progress.

Preliminary studies in the discovery and development process of new drugs include the *in vitro* evaluation of the biological activity of the candidate compounds. For enzyme inhibitor screening, the most common approach is the measurement of the reduction of the enzyme activity in the presence of candidate compounds. For *in vitro* screening AChE inhibitors, the reaction of acetylthiocholine (ATHCh, substrate) at pH 8 in the presence of AChE (enzyme) and the inhibitor to form acetic acid and thiocholine (TCh, product of the enzymatic hydrolysis) is considered.

Several procedures for the evaluation of AChE activity have been described. These include static procedures such as the titration of the acid formed in the reaction [5], the use of radiolabeled ACh [6] or colorimetric methods using Ellman's reagent [7]. The latter method is the most widely used to measure the activity of AChE and its

Correspondence: Dr. María J. Medina-Hernández, Departamento Química Analítica, Universitat de València, C/Vicente Andrés Estellés s/n, E-46100 Burjassot (Valencia), Spain
E-mail: maria.j.medina@uv.es
Fax: +34-96-3544953

Abbreviations: ACh, acetylcholine; AChE, acetylcholinesterase; AD, Alzheimer's disease; ATHCh, acetylthiocholine; EMMA, electrophoretically mediated microanalysis; TCh, thiocholine

decrease in the presence of inhibitors. In this method a yellow anion derived from the dithiobisnitrobenzoate (Ellman's reagent) when it reacts with TCh is monitored at 412 nm. Chemiluminiscent assays based on coupled enzymatic reactions have also been developed for the evaluation of AChE inhibitors [3, 8, 9].

Dynamic procedures including chromatographic and electrophoretic techniques using AChE immobilized or in dissolution have also been proposed for the evaluation of AChE inhibitors. A chromatographic procedure based on *in situ* AChE derivatized column has been used to determine the inhibition potency (IC_{50}) of known AChE inhibitors [10]. Most recently, the authors developed an immobilized human recombinant AChE-based microenzyme reactor for inhibitor screening [11, 12]. This reactor has been applied for the evaluation of the thermodynamic and kinetic constants, and the mechanism of action of inhibitors [13]. Moreover, an HPLC-MS methodology was used for the screening of AChE inhibitors in natural extracts [14].

A recent trend in the area of enzyme assays is the use of CE. CE has many advantages in this field due to the small dimensions of the capillaries used for reaction and separation, high efficiency separations, fast analysis times, and the ability to employ several detection techniques [15]. Measurement of enzyme activity by CE include enzyme reaction prior CE analysis (*precapillary* assay), enzyme reaction and consecutive on-capillary detection of the product(s) (*on-capillary* assay), and enzyme reaction after CE separation (*post-capillary* assay) [16]. The second alternative, also known as electrophoretically mediated microanalysis (EMMA), is of particular interest since the assay, and all its necessary operations, completely occurs within the capillary. The EMMA method has been successfully used with different enzyme systems for enzyme activity assays, kinetic studies with determination of Michaelis constants and study of inhibitors. Recently some reviews dealing with the basic principle, methodology, variants, and applications of EMMA have been published [15–18].

At present the plug–plug mode of EMMA, which relies on a plug–plug interaction of reactants in the capillary, is probably the most frequently used in the study of enzymatic reactions by CE. In the classical plug–plug mode, after the introduction of enzyme and substrate as distinct plugs, the enzymatic reaction is initiated by the application of an electric field since the zones interpenetrate due to the differences in their electrophoretic mobilities. One of the problems of this methodology, is the high variability in peak areas of reagents and product of enzymatic reaction due to slight variations in the in-capillary contact period of the enzyme and substrate plugs which affect the extent of the reaction [19].

As an alternative to the classical plug–plug mode the at-inlet EMMA method has been proposed [19]. In this

modality, the consecutively injected enzyme and substrate plugs are mixed by simple diffusion and reacted for a given time at the inlet part of the capillary. This variant is especially suitable for enzymes not resistant to an electric field.

For the screening of AChE inhibitors, the classical plug–plug mode [20], as well as the use of an immobilized capillary AChE reactor based on a layer-by-layer assembly [21] has been proposed.

A general problem related with the use of dynamic techniques, such as chromatography and electrophoresis, for the calculation of the inhibition kinetic parameters, inhibition constants, K_i , and IC_{50} values, is the existence of diffusion phenomena during the enzymatic reaction. As consequence, the actual concentrations of substrate, enzyme and inhibitors are lower than the injected concentrations and this affect considerably to the estimated K_i , and IC_{50} values [19].

The purpose of this study was the development of effective and reliable high-throughput screening (HTS) procedure based on the at-inlet EMMA method for the screening and *in vitro* evaluation of the biological activity of AChE inhibitors that overcomes the limitations previously indicated.

2 Materials and methods

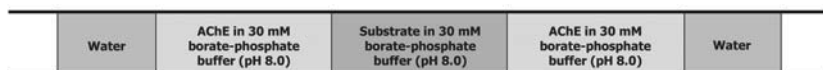
2.1 Instrumentation

An HP^{3D} CE system (Helwlett-Packard, Waldbronn, Germany) equipped with an on-column diode array detector (DAD) and an HP^{3D} CE Chemstation software was used to carry out all CZE separations. A 50 μ m inner diameter (id) and 363 μ m outer diameter (od) fused-silica capillary with total and effective length of 56 and 47.5 cm, respectively was employed (Agilent Technologies, Germany). The capillary temperature was set at 37 °C and a running voltage of 15 kV was used. Detection was performed at 230 nm due to the maximum absorption of the substrate and the reaction product. A Crison Micro-pH 2000 pH meter from Crison Instruments (Alella, Barcelona, Spain) was employed to adjust the pH of the separation buffer.

2.2 Chemicals and samples

All reagents were of analytical grade. AChE from *Electrophorus electricus* (EC.3.1.1.7), tacrine (9-amino-1,2,3,4-tetrahydroacridine hydrochloride), neostigmine bromide, eserine, edrophonium chloride, pyridostigmine bromide, and alprenolol were purchased from Sigma-Aldrich (Steinheim, Germany). AThCh chloride was obtained from Acros Organics (Geel, Belgium), boric acid magnesium sulfate heptahydrate from Scharlau (Barcelona, Spain), and sodium dihydrogen phosphate dehydrate from Fluka (Barcelona, Spain).

A)



B)

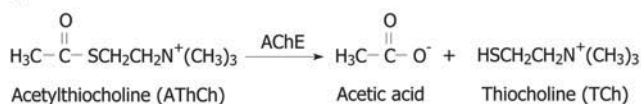


Figure 1. (A) Schematic diagram of the introduction of the different plugs to the inlet of a capillary for AChE activity assay. (B) AChE-catalyzed reaction.

All solutions were prepared by Barnstead E-pure deionized water (Sybron, Boston, MA, USA) and filtered prior to use through 0.45 μm pore size nylon membranes (Micron Separation, Westborough, MA, USA).

2.3 Solution preparation

The running buffer in all EMMA experiments was 30 mM borate-phosphate buffer at pH 8.0 and was prepared by dissolving the appropriate amounts of boric acid and sodium dihydrogen phosphate in water and adjusting the pH with 1 M NaOH. To prepare the working enzyme solution AChE was diluted to 115.2 U/mL with borate-phosphate buffer. Stock solutions of inhibitors (5000 μM), substrate AThCh (100 mM), MgSO_4 (200 mM), and alprenolol used as an internal standard (50 mM) were prepared in borate-phosphate buffer.

The assay solutions for kinetic and inhibitory studies containing increasing inhibitor concentration, a concentration of substrate in the range of 2–20 mM, 20 mM MgSO_4 , and 2 mM alprenolol were obtained by diluting the stock solutions in borate-phosphate buffer.

2.4 Procedures

New capillaries were conditioned for 10 min flush with 1 M NaOH at 60°C. Then, they were rinsed for 5 min with water and 15 min with borate-phosphate buffer at 37°C. In order to obtain good peak shapes and reproducible migration times, the capillary was conditioned at the beginning of each day with the following sequence: (i) 2 min rinse with deionized water, (ii) 2 min rinse with 1 M sodium hydroxide, (iii) 2 min rinse with deionized water, and (iv) 5 min rinse with running buffer at 1000 mbar. Between runs, the capillary was conditioned with deionized water for 1 min, and running buffer for 2 min.

The enzyme solution and the substrate solution, with or without inhibitor, were introduced into the inlet part of the capillary by a sandwich injection mode (Fig. 1), *i.e.*, enzyme solution (50 mbar for 2 s)-substrate solution (50 mbar for 2 s)-enzyme solution (50 mbar for 2 s). Before and after the sandwich injection mode a small plug of water was injected hydrodynamically (20 mbar for 2 s). The consecutively injected plugs were allowed to stand during a predetermined waiting period. Then, a voltage of 15 kV was applied for the separation.

2.5 Software and data processing

AChE activity (initial reaction velocity) was determined by the peak area of the product TCh since the reaction time was constant due to the identical lengths of the enzyme and substrate plugs during all experiments. The percentage of inhibition was calculated according to the following equation:

$$\% \text{inhibition} = 100 - \left(\frac{x}{\text{blank}} 100 \right) \quad (1)$$

where x represents the peak area of the product (TCh) determined at a given concentration of inhibitor, and the blank is the peak area of the product (TCh) determined without inhibitor being present.

The values of peak area of the product TCh determined in this study were averages of triplicate measurements. Microsoft® Excel 2000 and Statgraphics plus version 5.1 were used to perform the statistical analysis of the regressions.

3 Results and discussion

3.1 Method development and optimization of experimental conditions

In order to develop a screening methodology for AChE inhibitors, the use of at-inlet EMMA mode has been eval-

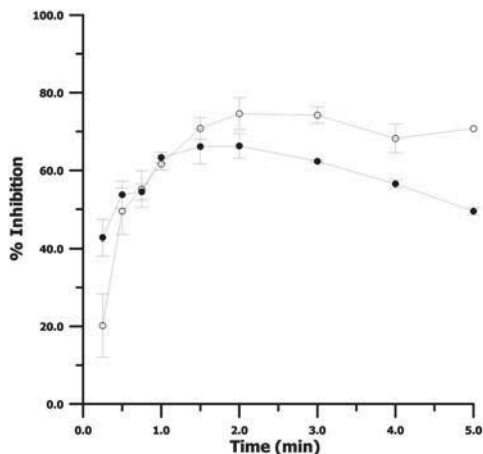


Figure 2. Effect of the incubation time on the percentage of inhibition: (●) tacrine 5 μM ; (○) tacrine 10 μM . Conditions: fused-silica capillary, 50 μm id \times 363 μm od, 47.5 cm of effective length; running buffer, 30 mM borate-phosphate buffer (pH 8.0); concentration of AChE, 0.4 mg/mL; AThCh, 10 mM; MgSO_4 in the substrate solution, 20 mM; capillary temperature, 37 $^\circ\text{C}$; running voltage, 15 kV; detection wavelength, 230 nm.

uated as alternative to the classical plug–plug mode. Tacrine, a well-known AChE inhibitor, was used for optimization. It has been reported in the literature that AChE displayed maximum activity in 30 mM borate-phosphate buffer (pH 8) at 37 $^\circ\text{C}$ and in the presence of 20 mM of MgSO_4 [20]. Therefore these conditions were fixed and used for the enzyme reaction and for electrophoretic separation. The progress of the enzymatic reaction (Fig. 1) was determined by measuring at 230 nm the peak area of the product TCh.

Figure 1 shows a schematic illustration of the disposition used in this work for the at-inlet EMMA analysis. As it was commented previously in the at-inlet EMMA analysis, unlike in the classical mode, the compounds were not electrophoretically mixed prior to reaction. In the method employed the capillary was first filled with 30 mM borate-phosphate buffer (pH 8.0). Subsequently, plugs of (i) water, (ii) AChE solution, (iii) substrate solution with or without inhibitor, (iv) AChE solution, and finally (v) a plug of water were hydrodynamically injected into the capillary, and were allowed to stand (and react) during a waiting period. With the aim to control variations in the sandwich injection, alprenolol was introduced in the substrate solution as an internal standard.

First the waiting time, the time necessary to allow the injected enzyme and substrate plugs be mixed by simple diffusion and react at the inlet part of the capillary was

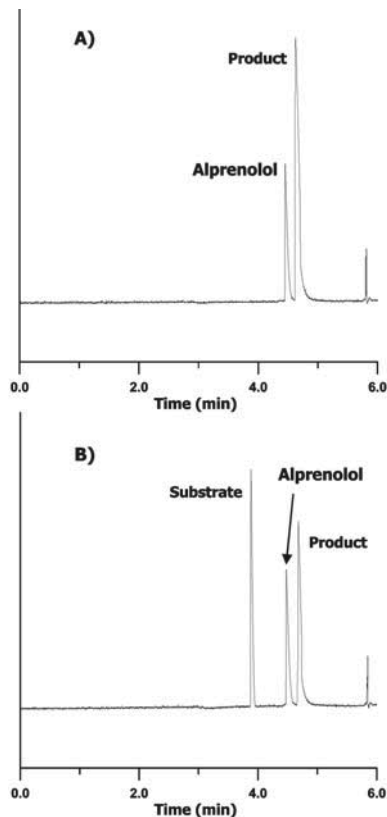


Figure 3. Typical electropherograms obtained after enzymatic reaction at the capillary inlet, in the absence (A) and presence (B) of the inhibitor edrophonium (100 μM) in the substrate solution (AThCh). Alprenolol (50 mM) was used as an internal standard. Conditions: waiting time, 2 min; other conditions as in Fig. 2.

optimized. Figure 2 shows the influence of mixing and reaction time (waiting time) over the percentage of AChE inhibition for two concentrations of the inhibitor tacrine. As can be observed, the maximum inhibition was achieved for a waiting time of 2 min, therefore, this period was selected for further studies. Figure 3 shows typical electropherograms after at-inlet reaction of AChE and substrate AThCh, introduced by sandwich injection mode in the absence of inhibitor (Fig. 3A) and in the presence of edrophonium (Fig. 3B). As can be observed in Fig. 3A, in absence of the inhibitor, the substrate is completely converted into TCh (reaction product). However, in presence of edrophonium (Fig. 3B), the reaction is not complete and the peak corresponding to the unreacted substrate appears, whereas the product peak area dimin-

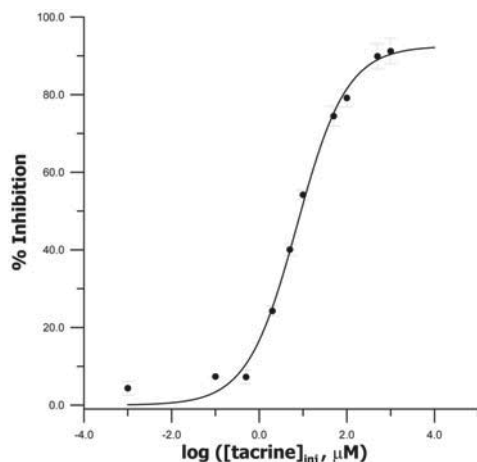


Figure 4. Inhibition plot of AChE in the presence of tacrine. Experimental conditions: fused-silica capillary, 50 μm id \times 363 μm od, 47.5 cm of effective length; running buffer, 30 mM borate-phosphate buffer (pH 8.0); concentration of AChE, 0.4 mg/mL; AThCh, 10 mM; MgSO_4 in the substrate solution, 20 mM; capillary temperature, 37 °C; running voltage, 15 kV; detection wavelength, 230 nm; waiting time 2 min.

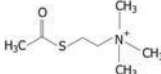
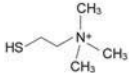
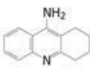
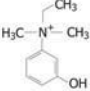
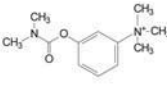
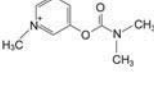
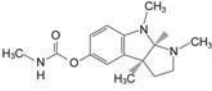
Table 1. Values of inhibitory potency (IC_{50}) for tacrine obtained by different assays reported in the literature

Method	IC_{50} , μM	Ref.
Ellman	0.25 ± 0.02	[22]
Ellman	0.25 ± 0.01	[10]
Chemiluminescent assay	0.20 ± 0.03	[3]
EMMA	0.83	[20]
Immobilized AChE-HPLC	450 ± 30	[10]
Immobilized AChE-capillary	1.97	[21]

ishes. Due to the low concentration of edrophonium used, the peak of the inhibitor does not appear in the electropherogram. As can be seen, no product peak splitting was observed that could be an indication of complete mixing [19].

In order to evaluate the dilution originated during the mixing of the plugs and reaction process, the inhibitory potency of tacrine using the at-inlet EMMA method developed was obtained. For this purpose assay solutions containing increasing inhibitor concentration in the range of 10^{-3} – 10^3 μM in the presence of a fixed AThCh concentration (10 mM), and AChE solution of 0.4 mg/mL were prepared. Figure 4 shows the inhibition curve for tacrine obtained by plotting the %inhibition versus the logarithm of inhibitor concentration in the assay solution injected. As can be seen in Fig. 4, complete inhibition was not reached, even at high inhibitor concentrations. Using

Table 2. Structures and apparent mobilities for the substrate AThCh, the product TCh, and the different inhibitors

Compound	μ ($\text{cm}^2/\text{V/s}$)
AThCh	7.574×10^{-4}
	
TCh	6.382×10^{-4}
	
Tacrine	6.846×10^{-4}
	
Edrophonium	6.605×10^{-4}
	
Neostigmine	6.464×10^{-4}
	
Pyridostigmine	6.329×10^{-4}
	
Eserine	6.411×10^{-4}
	

nonlinear regression the fitted parameters were determined and the IC_{50} value calculated for tacrine was 9.16 μM . Table 1 shows the bibliographic values reported for this compound. As can be observed, the IC_{50} values obtained using inline chromatographic and EMMA methodologies were larger than those obtained with the static Ellman method considered in bibliography as reference method. From the IC_{50} value for tacrine obtained with the Ellman method 0.25 μM [3, 10, 22] and the IC_{50} calculated from the inhibition curves using the at-inlet EMMA method a dilution factor, f , of 0.03 was

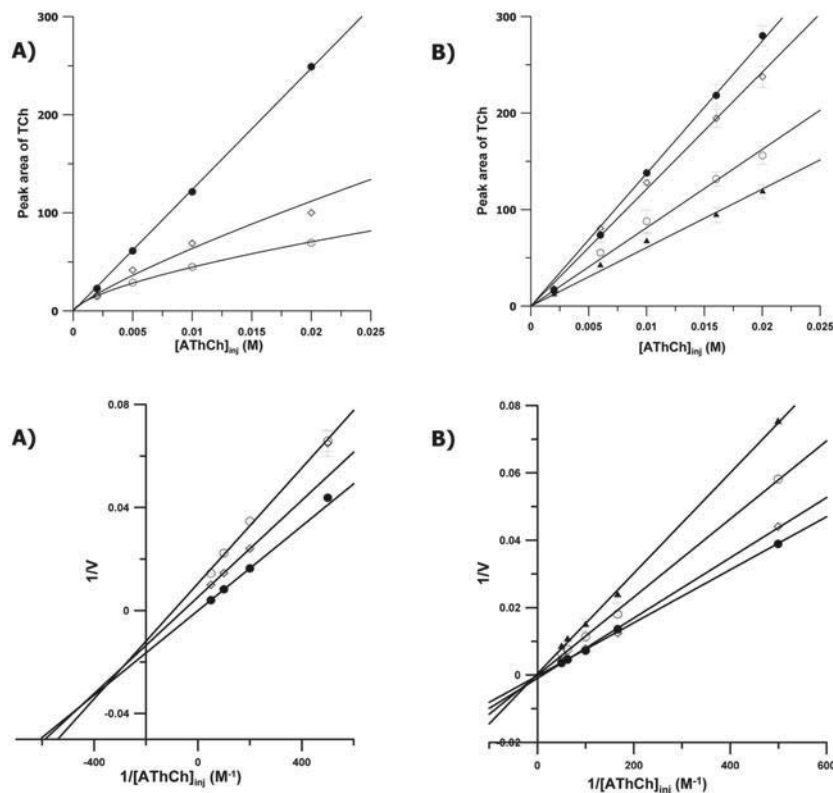


Figure 5. Michaelis–Menten (upper part) and corresponding Lineweaver–Burk plots (lower part) for the enzymatic reaction of AChE inhibited by: (A) tacrine, (●) 0 μM , (○) 5 μM , (◊) 10 μM ; (B) edrophonium (●) 0 μM , (○) 10 μM , (◊) 50 μM , (▲) 100 μM and varying concentrations of substrate AThCh. Experimental conditions as in Fig. 4.

estimated. Obviously the calculated dilution factor correction assumes that the reported literature value is a true value. This dilution factor was applied in all of the subsequent calculations related with the at-inlet EMMA method developed.

3.2 Estimation of kinetic parameters

The applicability of the proposed methodology to estimate different kinetic parameters of interest such as inhibition constants K_i , identification of inhibitory action mechanism and IC_{50} , was evaluated using compounds with known activity, tacrine edrophonium, and neostigmine. Since, the velocity of the enzymatic reaction is measured by the peak area of the formed TCh, it is important to guarantee that no other component co-eluted with the product. Table 2 shows the apparent mobilities of substrate, product and some AChE inhibi-

tors in the 30 mM borate-phosphate buffer (pH 8.0; 37°C). The apparent mobility was calculated from the migration time of the compound, taking into account the capillary length and the applied voltage. As can be seen, all the inhibitors had different apparent mobilities than the product TCh.

Reversible inhibition can be described quantitatively in terms of the inhibitor's binding to the enzyme (dissociation constant K_i) and to the enzyme-substrate complex (dissociation constant K'_i), and its effects on the kinetic constants of the enzyme. In the presence of a reversible inhibitor Michaelis–Menten equation can be described as

$$v_0 = \frac{v_{\max}[S]}{\alpha K_m + \alpha'[S]} \quad (2)$$

where v_{\max} and K_m are the typical parameters for an enzymatic reaction, $[S]$ the substrate concentration, and α and α' are the modifying factors defined by the inhibitor con-

Table 3. Inhibition constants of AChE by tacrine and edrophonium

Compound	Method	K_i (μM)	Mechanism	Ref
Tacrine	At-inlet EMMA	0.138 ± 0.012	Mixed	This work
	Ellman	0.151 ± 0.016	Mixed	[22]
	Ellman	0.23 ± 0.02	Mixed	[23]
	Immobilized AChE HPLC reactor	2.40 ± 0.36	Mixed	[13]
	EMMA	9	Mixed	[20]
Edrophonium	Immobilized AChE-capillary	10	Mixed	[21]
	At-inlet EMMA	3.3 ± 0.2	Competitive	This work
	Ellman	1.9 ± 1.3	Competitive	[24]
	Ellman	1.63 ± 0.23	Competitive	[13]
	Immobilized AChE HPLC reactor	5.38 ± 0.52	Competitive	[13]

Values obtained using the developed at-inlet EMMA methodology and reported in the literature.

centration, $[I]$, and its two dissociation constants K_i and K'_i

$$\alpha = 1 + \frac{[I]}{K_i} \quad (3)$$

$$\alpha' = 1 + \frac{[I]}{K'_i} \quad (4)$$

In order to consider the dilution originated in the mixing process of the plugs during the at-inlet reaction, corrected concentrations for reagents (substrate, inhibitor, enzyme) were introduced. For a compound A the corrected concentration can be calculated as $[A]_{\text{corr}} = f[A]_{\text{injected}}$, where f is the dilution factor and $[A]_{\text{injected}}$ the concentration in the vial. Therefore taking in account the dilution at the capillary inlet, Michaelis–Menten equation can be rewritten as

$$v_o = \frac{v_{\text{max}}[S]_{\text{corr}}}{\alpha K_m + \alpha' f [S]_{\text{corr}}} = \frac{v_{\text{max}} f [S]_{\text{injected}}}{\alpha K_m + \alpha' f [S]_{\text{injected}}} \\ = \frac{(1/\alpha') v_{\text{max}} [S]_{\text{injected}}}{(\alpha/\alpha') 1/f K_m + [S]_{\text{injected}}} \quad (5)$$

and the modifying factors α and α'

$$\alpha = 1 + \frac{[I]_{\text{corr}}}{K_i} = 1 + \frac{f[I]_{\text{injected}}}{K_i} \quad (6)$$

$$\alpha' = 1 + \frac{[I]_{\text{corr}}}{K'_i} = 1 + \frac{f[I]_{\text{injected}}}{K'_i} \quad (7)$$

For kinetic studies, two reversible reference inhibitors with known potency and mechanism of action (tacrine and edrophonium) were selected as model compounds. To obtain estimates of the competitive inhibition constant, K_i , Michaelis–Menten plots (v vs. $[S]_{\text{injected}}$) and reciprocal plots ($1/v$ vs. $1/[S]_{\text{injected}}$) were constructed by injecting in triplicate different substrate solutions, in the range of 2–20 mM, containing increasing reversible inhibitor concentrations, 0–10 and 0–100 μM for tacrine and edrophonium, respectively.

Figure 5 shows the Michaelis–Menten and their corresponding Lineweaver–Burk plots obtained for tacrine and edrophonium. The Michaelis–Menten plots and fitted parameters were assessed by a nonlinear regression analysis according to Eq. 8:

$$v_o = \frac{(1/\alpha') v_{\text{max}} [S]_{\text{injected}}}{(\alpha/\alpha') \frac{1}{f} K_m + [S]_{\text{injected}}} = \frac{a [S]_{\text{injected}}}{b + [S]_{\text{injected}}} \quad (8)$$

The ratio of the fitted parameters b/a , were then plotted against inhibitor injected concentration, and K_i was determined as the ratio of the replot intercept to the replot slope.

$$\frac{b}{a} = \frac{K_m}{v_{\text{max}}} \frac{1}{f} \alpha = \frac{K_m}{v_{\text{max}}} \frac{1}{f} + \frac{K_m}{v_{\text{max}}} \frac{1}{K_i} [I]_{\text{injected}} \quad (9)$$

Table 3 shows the estimated inhibition constants K_i for tacrine and edrophonium calculated from the fitted parameters of the models obtained and bibliographic values. As can be observed, the values obtained were in good agreement with those reported in the literature obtained using static procedures [13, 23, 24]. The use of other dynamic methodologies provided higher and inaccurate results.

Mechanism of action was qualitatively evaluated by comparing Lineweaver–Burk plot trend to the theoretical ones [1]. Reciprocal plots for tacrine inhibition (Fig. 5B) showed increase in slopes (decreased v_{max}) and increase in intercepts (higher K_m) with higher inhibitor concentration, indicating a mixed-type inhibition. In the case of edrophonium inhibition (Fig. 6B) unvaried v_{max} and increasing x -intercepts (higher K_m) at increasing inhibitor concentrations were obtained. This behavior indicates that edrophonium acts as a pure competitive AChE inhibitor.

The results obtained were consistent with data reported in the literature and well reflect the relative potency of the inhibitors, suggesting that this assay could be suitable for the first screening of new potential AChE inhibitors.

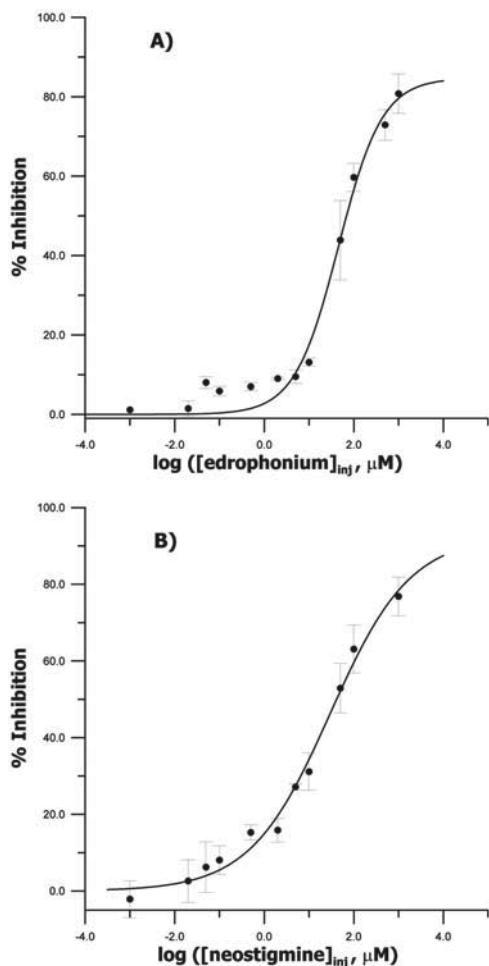


Figure 6. Inhibition curves for (A) edrophonium and (B) neostigmine. Experimental conditions as in Fig. 4.

Table 4. Inhibitor screening results^{a)}

Compound ^{b)}	Percent of inhibition (%)
Tacrine	54.2
Edrophonium	33.7
Neostigmine	31.1
Pyridostigmine	6.1
Eserine	20.1

^{a)} Conditions as in Fig. 4.

^{b)} Concentration of 10 μM .

The inhibitory potency of edrophonium and neostigmine was also determined using the proposed at-inlet EMMA method. For this purpose assay solutions containing increasing inhibitor concentration and a fixed substrate concentration of 10 mM were prepared and the inhibition curves were obtained by plotting the %inhibition versus the logarithm of inhibitor concentration in the assay solution injected in the electrophoretic system (Fig. 6). The IC_{50} values calculated from these curves were 0.68 and 1.06 μM for edrophonium and neostigmine, respectively.

3.3 Method for AChE inhibitor screening

In order to obtain a rapid and efficient method for the screening of new potential AChE inhibitors a new procedure based on at-inlet EMMA analysis was evaluated. The method for screening results used the methodology and electrophoretic conditions previously optimized and fixed concentrations of substrate; 10 mM, inhibitor, 10 μM , and AChE, 0.4 mg/mL. Table 4 shows the screening results, presented in terms of percentage of inhibition, obtained for five known AChE inhibitors. According to the results obtained, the order of inhibitory potency was tacrine > edrophonium > neostigmine > eserine > pyridostigmine. The results obtained agree with the K_i values reported in bibliography for tacrine and edrophonium [13, 22–24]. For neostigmine, pyridostigmine, and eserine no kinetic data have been found in the bibliography. The results obtained can be used as an automated fast screening in the first step of the drug discovery process.

4 Conclusions

The developed procedure based on CE after enzymatic reaction at capillary inlet proved to be useful for the screening and *in vitro* evaluation of the biological activity of AChE inhibitors. The proposed method allows online evaluation of kinetic parameters of interest such as determination the inhibitory constant (K_i), identification of mechanism of action and evaluation of IC_{50} values with increased accuracy and reproducibility and with saving of time and materials. The results obtained were found in agreement with data reported in the literature.

The advantages over the static conventional methods are the system automation which allows a large number of compounds to be processed continuously. Over the dynamic procedures reported in bibliography, the proposed methodology corrects adequately the dilution effects that take place in the columns/capillary providing similar results compared to the reference/static procedures. Due to the reduced analysis time, less than 5 min,

the at-inlet EMMA procedure proposed can be used as an effective screening methodology.

The authors acknowledge the Spanish Ministry of Science and Technology (MCYT), the European Regional Development Fund (ERDF) (project SAF2005-01435) for the financial support.

The authors declared no conflict of interest.

5 References

- [1] Thomas, G., *Medicinal Chemistry*, Wiley, Chichester, England 2000, pp. 231–239.
- [2] Di Giovanni, S., Borloz, A., Urbain, A., Marston, A., Hostettmann, K., Carrupt, P. A., Reist, M., *Eur. J. Pharm. Sci.* 2008, 33, 109–119.
- [3] Guardigli, P., Pasini, P., Mirasoli, M., Leoni, A., Andreani, A., Roda, A., *Anal. Chim. Acta* 2005, 535, 139–144.
- [4] Lee, J. H., Lee, K. T., Yang, J. H., Baek, N. I., Kim, D. K., *Arch. Pharm. Res.* 2004, 27, 53–56.
- [5] Jacobsen, C. F., Leonis, J., Linderstrøm-Lang, K., Otteren, M., *Methods Biochem. Anal.* 1957, 4, 171–210.
- [6] Johnson, C. D., Russel, R. L., *Anal. Biochem.* 1975, 64, 229–238.
- [7] Ellman, G. L., Courtney, K. D., Andres, J. V., Featherstone, R. M., *Biochem. Pharmacol.* 1961, 7, 88–95.
- [8] Sabelle, S., Renard, P.-Y., Pecorella, K., de Suzzoni-Dézard, S., Créminom, C., Grassi, J., Mioskowski, C., *J. Am. Chem. Soc.* 2002, 124, 4874–4880.
- [9] Pasini, P., Musiana, M., Russo, C., Valenti, P., Aicardi, G., Crabtree, J. E., Baraldini, M., Roda, A., *J. Pharm. Biomed. Anal.* 1998, 18, 555–564.
- [10] Andrisano, V., Bartolini, M., Gotti, R., Cavrini, V., Felix, G., *J. Chromatogr. B* 2001, 753, 375–383.
- [11] Bartolini, M., Cavrini, V., Andrisano, V., *J. Chromatogr. A* 2004, 1031, 27–34.
- [12] Bartolini, M., Cavrini, V., Andrisano, V., *J. Chromatogr. A* 2005, 1065, 135–144.
- [13] Bartolini, M., Cavrini, V., Andrisano, V., *J. Chromatogr. A* 2007, 1144, 102–110.
- [14] de Jong, C. F., Derks, R. J. E., Bruyneel, B., Niessen, W., Irth, H., *J. Chromatogr. A* 2006, 1112, 303–310.
- [15] Zhang, J., Hoogmartens, J., Van Schepdael, A., *Electrophoresis* 2008, 29, 56–65.
- [16] Nováková, S., Van Dyck, S., Van Schepdael, A., Hoogmartens, J., Glatz, Z., *J. Chromatogr. A* 2004, 1032, 173–184.
- [17] Van Dyck, S., Kaale, E., Nováková, S., Glatz, Z., Hoogmartens, J., Van Schepdael, A., *Electrophoresis* 2003, 24, 3868–3878.
- [18] Zhang, J., Hoogmartens, J., Van Schepdael, A., *Electrophoresis* 2006, 27, 35–43.
- [19] Van Dyck, S., Vissers, S., Van Schepdael, A., Hoogmartens, J., *J. Chromatogr. A* 2003, 986, 303–331.
- [20] Tang, Z., Wang, T., Kang, J., *Electrophoresis* 2007, 28, 360–365.
- [21] Tang, Z., Wang, T., Kang, J., *Electrophoresis* 2007, 28, 2981–2987.
- [22] Rampa, A., Bisi, A., Belluti, F., Gobbi, S., Valenti, P., Andrisano, V., Cavrini, V., Cavalli, A., Recanatini, M., *Bioorg. Med. Chem.* 2000, 8, 497–506.
- [23] Khalid, A., Zaheer-ul-Haq, Anjum, S., Khan, M. R., Atta-ur-Rahman, Choudhary, M. I., *Bioorg. Med. Chem.* 2004, 12, 1995–2003.
- [24] Yerushalmi, N., Cohen, E., *Pestic. Biochem. Physiol.* 2002, 72, 133–141.

Paper IX

**In-line capillary electrophoretic evaluation of the enantioselective
metabolism of verapamil by cytochrome P3A4**

**L. Asensi-Bernardi, Y. Martín-Biosca, L. Escuder-Gilabert, S. Sagrado
and M.J. Medina-Hernández**

Journal of Chromatography A 2013, 1298, 139-145



In-line capillary electrophoretic evaluation of the enantioselective metabolism of verapamil by cytochrome P3A4



L. Asensi-Bernardi^a, Y. Martín-Biosca^a, L. Escuder-Gilabert^a,
S. Sagrado^{a,b}, M.J. Medina-Hernández^{a,*}

^a Departamento de Química Analítica, Facultad de Farmacia, Universidad de Valencia, Burjassot, Valencia, Spain

^b Centro Interuniversitario de Reconocimiento Molecular y Desarrollo Tecnológico (IDM), Unidad mixta Universidad Politécnica de Valencia-Universidad de Valencia, Spain

ARTICLE INFO

Article history:

Received 12 March 2013

Received in revised form 13 May 2013

Accepted 14 May 2013

Available online 22 May 2013

Keywords:

CYP3A4

EMMA

Enantioselective metabolism

Verapamil

ABSTRACT

In this paper a methodology for the in-line evaluation of enantioselective metabolism by capillary electrophoresis has been developed and applied to the study of verapamil metabolism by cytochrome P3A4. The developed methodology comprises an in-capillary reaction step carried out by electrophoretically mediated microanalysis and a separation step in which highly sulfated β -cyclodextrin with partial filling technique has been employed as chiral selector for verapamil and norverapamil enantiomers resolution, joining the advantages of both methodologies in a unique assay. Kinetic parameters of the enzymatic reaction (K_m and V_{max}) have been evaluated for both verapamil enantiomers by non-linear fitting of experimental data obtained under intermediate precision conditions to Michaelis–Menten equation. K_m and V_{max} estimated values were $51 \pm 9 \mu\text{M}$ and $22 \pm 2 \text{ pmol min}^{-1} (\text{pmol CYP})^{-1}$ for S-VER and $47 \pm 9 \mu\text{M}$ and $21 \pm 2 \text{ pmol min}^{-1} (\text{pmol CYP})^{-1}$ for R-VER. Consequently, slight enantioselectivity was found for the CYP3A4 metabolism of verapamil. However, since confidence intervals of estimates overlap, we cannot assure a significant enantioselectivity. Intrinsic clearance values were also estimated from K_m and V_{max} for both enantiomers.

© 2013 Elsevier B.V. All rights reserved.

1. Introduction

The study of xenobiotics metabolism is a key feature for the pharmaceutical and chemical industries since is a determining factor both in the preclinical development of new drugs and in the toxicity evaluations of chemicals. CYP450 is the main metabolic enzymatic system of the mammals, being responsible for the metabolism of a large number of drugs, steroids, carcinogens and other chemicals. There are different isoforms of CYP450 that catalyze the oxidation of different substrates. Human cytochrome P3A4, one of the four most important CYP isozymes in the human liver, is involved in the metabolism of a large number of compounds and its reactions are categorized as oxidation, mainly hydroxylation, N-demethylation and N-dealkylation of its substrates [1]. The oxidation of xenobiotic substances by CYP450 is a significant focus of scientists in the areas of toxicology, drug metabolism, and pharmacology. The effects of these oxidations can be manifested in poor drug bioavailability and various acute and chronic toxicities,

including adverse drug interactions, cancer susceptibility, and birth defects [2].

Enzymatic metabolism of chiral xenobiotics can show a high degree of stereoselectivity as a consequence of the stereoselective interaction with optically active macromolecules involved in the process [3]. Stereoselectivity in the enzyme–xenobiotic interaction has been extensively reported and is the subject of a number of reviews [3–5]. Some metabolic reactions catalyzed by CYP450 isoforms have shown a certain degree of enantioselectivity for different racemic drugs, such as ketamine [6,7] or amphetamines [8,9], leading to differences in the pharmacokinetic profile of enantiomers, which can affect their concentration in the target organ and their pharmacological activity. To evaluate the enantioselective metabolism of racemic drugs, it is necessary to integrate methodologies that allow, first, the interaction of racemic xenobiotic with the enzymatic system and later the determination of the enantiomers of intact xenobiotic or its metabolites in the reaction mixture.

Metabolism studies can be performed *in vivo*, by administering the drug to the living system and monitoring the free concentration of xenobiotic and its metabolites in body fluids and tissues, or by *in vitro* assays. *In vitro* methods are based on the use of liver subcellular fractions as liver microsomes, isolated hepatocytes, liver slices or individual forms of enzymes, predominantly isoforms of

* Corresponding author at: Departamento de Química Analítica, Facultad de Farmacia, Universitat de Valencia, C/Vicent Andrés Estellés s/n, E-46100 Burjassot, Valencia, Spain. Tel.: +34 963544899.

E-mail address: maria.j.medina@uv.es (M.J. Medina-Hernández).

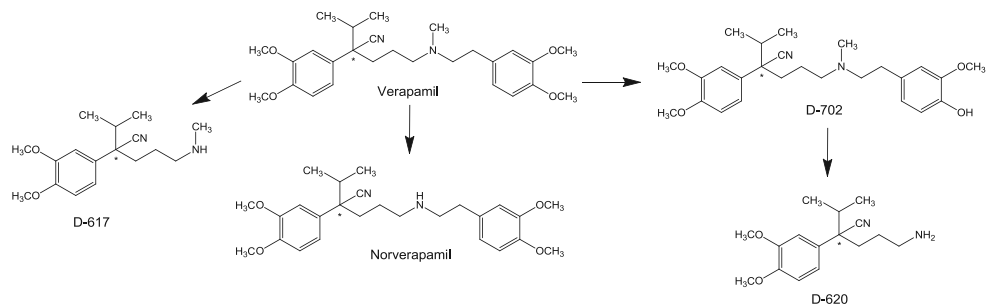


Fig. 1. Major routes of VER metabolism by CYP3A4.

CYP450. In these studies, the components of the enzymatic system are mixed and after an incubation period one or more components of the enzymatic reaction are monitored mainly using liquid chromatography. More recently capillary electrophoresis (CE) has become very useful for enzymatic assays since it is fully automated, requires small sample volumes, provides high peak efficiencies and is environmentally friendly [10,11]. In the electrophoretically mediated microanalysis (EMMA) approach the reaction is carried out in a nanoliter volume of the capillary which serves simultaneously as microreactor, separation system and detection cell, allowing a higher degree of automation and miniaturization [12,13].

Several approaches have been proposed to conduct enzymatic studies in CE [10,12,14] that include off-line assays, microchip methodologies and electrophoretically mediated microanalysis (EMMA) approach. Unless EMMA is the denomination commonly employed, most of these in-capillary reactions are performed in a nanoliter scale. EMMA has been successfully employed for the evaluation of non chiral drugs metabolism by CYP450 and other enzymes: dextromethorphan oxidation by CYP3A4 [15]; phenacetin, dextromethorphan, tramadol and midazolam oxidation by different CYP450 isoforms [16]; testosterone and nifedipine by CYP3A4 [17]; diclofenac by CYP2C9 [18,19] and clozapine metabolism by FMO3 [20]. Inhibition studies with CYP450 [21] have been also investigated by CE-EMMA.

There are only two applications that use the EMMA approach for the characterization of the enantioselective metabolism of compounds, the chiral oxidation of cimetidine by flavin-containing monooxygenases (FMOs) [22] and the enantioselective N-demethylation of ketamine by cytochrome P450 [23]. In these papers, the inclusion of a cyclodextrin in the background electrolyte allows the separation of the substrate and/or metabolite enantiomers after in-line EMMA incubation reactions.

Verapamil (VER) is a Ca^{2+} -channel blocker, used for the treatment of different cardiovascular diseases [1,24]. It has been used as a model substrate of the CYP3A4 metabolism to evaluate *in vitro* reaction systems and study metabolic pathways, and its major metabolic routes, (Fig. 1), including its N-demethylation reaction that forms the active metabolite norverapamil (NOR), are well known. These reactions are catalyzed by CYP3A4 among other isozymes [25]. Different off-line chromatographic and electrophoretic methodologies have been employed for the *in vitro* evaluation of the metabolism of verapamil [1,24–28], in some cases including enantioselective evaluation of these metabolic reactions. However, relatively different results are obtained suggesting influence of the methodology used on the kinetic parameter estimations.

The aim of this work is to develop a methodology for the in-line study of enantioselective metabolism, and apply it to the

study of the verapamil metabolism by CYP3A4. The development of the methodology comprises the study of the EMMA reaction conditions, the separation of verapamil and norverapamil enantiomers employing highly sulfated β -cyclodextrin (HS- β -CD) as chiral selector and the partial filling technique, and the coupling of both parts in a unique step carried out in the CE system. As far as we know, this is the first time in which EMMA (for enzymatic reactions) and partial filling technique (for enantioselective separation) are joined in an enantioselective in-line CYP450 metabolic assay.

The metabolic reaction is evaluated by the estimation of kinetic parameters (K_m and V_{max}) of each enantiomer from non-linear fitting to the Michaelis–Menten equation of data obtained in two different sessions under intermediate precision conditions.

2. Materials and methods

2.1. Instrumentation

A Beckman P/ACE MDQ Capillary Electrophoresis System equipped with a diode array detector (Beckman Coulter, Fullerton, CA, USA), and 32Karat software version 8.0 was used throughout. A 50 μm inner diameter (I.D.) fused-silica capillary with total and effective lengths of 60.2 and 50 cm, respectively, was employed (Beckman Coulter, Fullerton, CA, USA). The CE system is equipped with a temperature controlled garage for sample trays, so samples could be kept cooled during all the experiments. Detection wavelength was fixed at 200 nm for all experiments.

Electrophoretic solutions and samples were filtered through 0.45 μm pore size nylon membranes (Micron Separation, Westboro, MA, USA) and degassed in an ultrasonic bath (JP Selecta, Barcelona, Spain) prior to use. A Crison Micro pH 2000 pH-meter from Crison Instruments (Barcelona, Spain) was employed to adjust the pH of buffer solutions.

2.2. Chemicals and solutions

All reagents were of analytical grade. $\text{NaH}_2\text{PO}_4 \cdot 2\text{H}_2\text{O}$ was from Fluka (Buchs, Switzerland); KH_2PO_4 from Panreac (Barcelona, Spain); HS- β -CD (20%, m/v) aqueous solution was purchased from Beckman Coulter (Fullerton, CA, USA); Ultra Clear TWF UV deionized water (SG Water, Barsbüttel, Germany) was used to prepare solutions. Verapamil hydrochloride, R-verapamil hydrochloride (employed for enantiomers identification) and norverapamil hydrochloride were purchased from Sigma Aldrich (St. Louis, MO, USA). Human CYP3A4 + P450 reductase + cytochrome b5 SUPERSOMES and nicotinamide adenine dinucleotide phosphate (NADPH) regenerating system were from BD Gentest (Erembodegem, Belgium). This regenerating system consists of two independent solutions: solution A (26 mM NADP⁺, 66 mM glucose

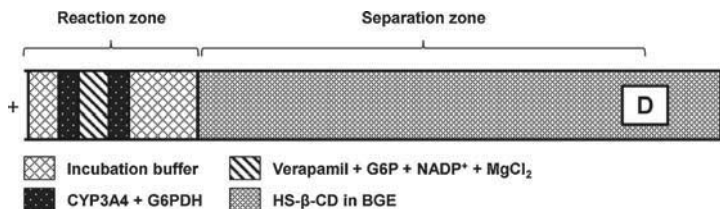


Fig. 2. Scheme of the reaction and separation zones in the proposed enantioselective EMMA assay.

6-phosphate (G6P), 66 mM MgCl₂) and B (40 U/mL glucose 6-phosphate dehydrogenase (G6PDH)). SUPERSOMES and NADPH regenerating system were aliquoted to minimize freeze–thaw cycles and the aliquots were stored at -80°C until their use.

Background electrolyte (BGE) containing 50 mM NaH₂PO₄ was prepared by dissolving the appropriate amount of NaH₂PO₄ in water and adjusting the pH to 8.8 with 1 M NaOH. The same procedure was employed to prepare the incubation buffer: 100 mM KH₂PO₄ at pH 7.4. Verapamil, R-verapamil and norverapamil 1000 μM stock solutions were prepared by dissolving the appropriate amount of each drug in a few drops of methanol (taking into account that the organic solvent concentration should be under 1% (v/v) for CYP450 assays) and bringing to final volume with incubation buffer. For the chiral separation of VER and NOR, 2.5% (m/v) HS- β -CD was prepared by dilution in the BGE.

For EMMA assays, two independent solutions were daily prepared in each case in the incubation buffer. The first one contained 200 nM CYP3A4 and 0.4 U mL⁻¹ G6PDH (NADPH regenerating system solution B). The second one contained verapamil in the adequate concentration for each assay and the reagents of the solution A (1.3 mM NADP⁺, 3.3 mM G6P and 3.3 mM MgCl₂). These solutions were kept at 10°C in the CE system.

2.3. Methodology

2.3.1. Capillary conditioning

New capillaries were conditioned for 15 min flush with 1 M NaOH at 60°C . Then, they were rinsed for 5 min with deionized water and 10 min with separation buffer at 25°C . In order to obtain good peak shapes and repeatable migration data, the capillary was conditioned prior to each injection. In all cases, the conditioning run included the following steps: (i) 1 min rinse with deionized water; (ii) 1 min rinse with 1 M NaOH, to prevent protein adsorption to the capillary wall; (iii) 1 min rinse with deionized water and (iv) 2 min rinse with separation buffer, all of them at 1.38×10^5 Pa (20 psi).

2.3.2. CE separation

For the achiral separation of reagents and products after the incubation step, the experimental conditions were fixed according to the literature [27], as following: 50 mM NaH₂PO₄ at pH 8.8 as BGE; capillary temperature: 25°C ; applied voltage: 20 kV. These conditions allowed the separation of VER and NOR, *a priori* difficult due to the similarity of the molecules.

For the enantioselective kinetic study, the separation of the enantiomers was carried out by partially filling the capillary with a 2.5% (m/v) HS- β -CD solution (by applying pressure of 6.89×10^4 Pa (10 psi) for 2 min) previously to the injection of the reagents and adding a pressure of 1.38×10^3 Pa (0.2 psi) to the separation voltage. No HS- β -CD was included in the BGE vials employed for the separation.

2.3.3. EMMA procedure

After filling the capillary with the 2.5% (m/v) HS- β -CD solution, five plugs of different length were introduced by applying a

pressure of 3.45×10^3 Pa (0.5 psi) for different times (Fig. 2). The order, composition and time of pressure application was as follows: (i) incubation buffer solution (100 mM KH₂PO₄ at pH 7.4), 20 s; (ii) enzyme plug containing 200 nM CYP3A4 and the solution B of the NADPH regenerating system (0.4 U mL⁻¹ G6PDH), 3 s; (iii) substrate plug containing racemic verapamil, and the solution A of the NADPH regenerating system (1.3 mM NADP⁺, 3.3 mM G6P and 3.3 mM MgCl₂), 7 s; (iv) enzyme plug, 3 s; and (v) incubation buffer solution, 10 s. Between injections of plugs, the capillary was shortly dipped into water to avoid carry-over of samples. To determine the kinetic parameters the incubation was performed at 37°C for 5 min.

2.3.4. Estimation of Michaelis–Menten parameters

The estimation of kinetic parameters was carried out by varying the concentration of verapamil in the reaction system. Six VER concentrations between 20 and 200 μM (10–100 μM of each enantiomer) were processed under intermediate precision conditions: two working sessions were carried out, each one with two replicates of each concentration level. All data were combined for the estimations. The use of two short working sessions instead of one long session with more replicates helps to prevent possible degradation or sedimentation of CYP3A4 in the CE vial, which may affect the reaction progress.

The quantification of the reaction turnover was done considering the consumption of VER enantiomers, providing information about the overall VER metabolism by all the major routes described in Fig. 1. With this aim, a calibration curve with six VER concentration levels in the 10–400 μM range (for racemic drug; each point in duplicate) was done in each working session. Corrected peak area of S- and R-VER was employed as response variable to subsequently calculate the reaction rate data. 50 μM racemic NOR was added to all calibration solutions to check that the four peaks were adequately separated.

2.4. Software and calculations

The calculation of the reaction rate includes the number of moles of each reagent involved in the enzymatic reaction. This estimation was done by calculating the injected volume of each plug with the following equation:

$$\text{Vol} = \frac{\Delta P \cdot d^4 \cdot \pi \cdot t}{128 \cdot \eta \cdot L_{\text{TOT}}} \quad (1)$$

where Vol (m³) is the injected volume, ΔP (Pa) is the applied pressure, d (m) is the internal diameter of the capillary, t (s) is the duration of pressure application, η (Pa s) is the viscosity of the injected solution and L_{TOT} (m) is the total length of the capillary.

Velocity rate data (expressed in pmol min⁻¹ (pmol CYP)⁻¹) were obtained from the corrected area of S- and R-VER peaks, and plotted vs. the initial enantiomer substrate concentration following the Michaelis–Menten equation.

Microsoft Office EXCEL[®] (Microsoft, Redmond, WA, USA) and STATGRAPHICS Plus[®] (Statpoint Technologies, Warrenton, VA,

USA) were employed for calculations. Chemical structures of VER and NOR were drawn with ChemBioDraw® (PerkinElmer Informatics, Waltham, MA, USA).

3. Results and discussion

3.1. Optimization of EMMA experimental conditions

The EMMA assays carried out in this paper comprise two steps: the incubation of the reaction mixture in the capillary and the separation of reagents and products by electrophoresis. For the optimization of the EMMA experimental conditions, the corrected area of the metabolite norverapamil, NOR peak, was employed as response variable, since this is the major metabolite formed in this reaction and the only one that could be detected. For the incubation step, some experimental conditions were fixed (temperature 37 °C; the enzyme plug containing 200 nM CYP3A4 and the solution B of the NADPH regenerating system (0.4 U mL^{-1} G6PDH), injected at $3.45 \times 10^3 \text{ Pa}$ (0.5 psi) for 3 s and incubation buffer: 100 mM KH_2PO_4 at pH 7.4) and the incubation time and substrates plug length were optimized in order to achieve a good development of the enzymatic reaction.

Two experimental injection modes were assayed: the at-inlet EMMA and the plug-plug modes. In the at-inlet EMMA mode, the solutions are introduced consecutively into the capillary and are allowed to mix by diffusion during an incubation time. With this configuration, both longitudinal and transverse diffusion are responsible for the mixing of reagents [29]. In the plug-plug mode, little voltages are applied to mix the plugs. The results obtained using both experimental modes did not show significant differences, so for further experiences the reagents were allowed to mix by simple diffusion (at-inlet mode).

The injected order plugs was chosen trying to maximize the contact between the enzyme, cofactor and substrate. A "sandwich" mode was selected. In this modality, a plug of substrate is introduced between two plugs of enzyme, which allows the existence of two contact zones in which the enzymatic reaction can take place. The use of the opposite configuration, that is a plug of enzyme between two substrate plugs, was discarded due to the split of VER and NOR peaks. Fig. 2 shows a scheme of the injected plugs and different zones in the CE capillary for the proposed in-line EMMA enantioselective assay.

The NADPH regenerating system employed in this work comprises two solutions (A and B) that allow the *in situ* NADPH formation. Solution A contains G6P, NADP^+ and MgCl_2 , and solution B contains G6PDH. When these solutions are put into contact, the G6PDH oxidizes G6P and forms NADPH, which can act as cofactor for the CYP3A4 reaction. Two configurations were tested for the inclusion of these solutions in the CYP and substrate vials. In the first one, both solutions A and B were included in the substrate vial, to form NADPH before the injection in the CE system. This strategy allows the immediate starting of the reaction due to the fact that the NADPH formed is present when the CYP and VER plugs contact in the capillary, but it presents the disadvantage of a possible degradation of NADPH. The other configuration studied consisted on the in-line formation of NADPH by the inclusion of solution B in the CYP vial and solution A in the VER vial, which allows always the presence of native NADPH, but can retard the beginning of the enzymatic CYP reaction. The use of both configurations leads to the same metabolite (NOR) formation in short incubation times, so the in-line formation of NADPH was selected in order to preserve NADPH from degradation.

To evaluate the metabolism of drugs in physiological conditions, the enzymatic reaction has to take place at physiological pH and temperature. For this purpose the incubation buffer pH was fixed to 7.4 and the capillary temperature at 37 °C during the reaction progress. The use of high pH values in the background electrolyte can affect the enzymatic activity of CYP3A4. Therefore, in order to avoid the contact of CYP3A4 plug with the background electrolyte, the partial-filling technique was used by injecting two plugs of incubation buffer before and after reagents injection [10,12]. The second plug also assists to mix the plugs and move the reaction zone to the thermostated zone of the capillary.

One of the most difficult aspects of EMMA assays is the selection of the reaction conditions. The adequate mixture of the reagents is critical for the reaction turnover, so the length of the injected plugs and the incubation time are important variables that have to be adjusted carefully. When reagents are mixed by simple diffusion, the incubation time has to be enough to assure their mixture and reaction. However, an excessive incubation time will decrease peak efficiencies (due to the diffusion), that decreases sensitivity and increases the total analysis time. In this paper, five different incubation times were tested: 1, 5, 10, 20 and 30 min. VER concentration was fixed at $200 \mu\text{M}$, and other conditions were kept as described in Section 2.3.2. As can be observed in Fig. 3a, although the amount

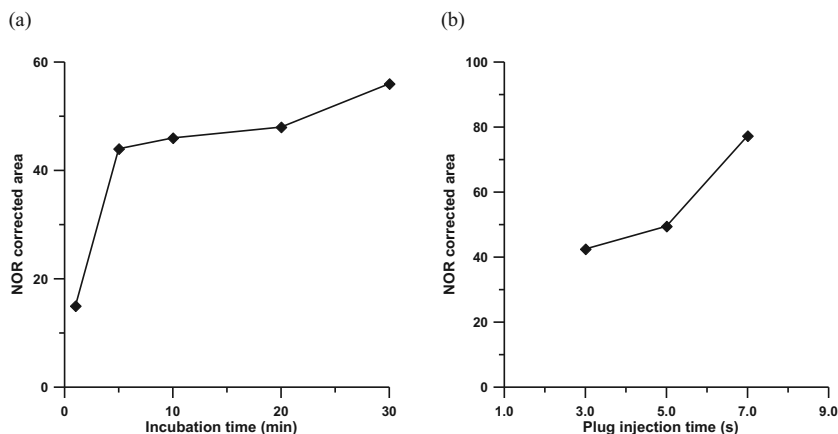


Fig. 3. Effect of (a) incubation time and (b) plug injection time on NOR formation for the in-line EMMA assay. Other experimental conditions are described in Section 2.3.3.

of NOR formed slightly increased as incubation times increased, the broadening of the peak due to diffusion, provoked overlapping with VER peaks and hindered the measurement of NOR formed. So an incubation time of 5 min was selected.

In order to allow a good substrate–enzyme mixture, the injection sequence comprised a substrate plug between two enzyme plugs. The length of the substrate plug may be adjusted to maximize the reaction turnover, considering that an excessive plug length will not provide best results if part of the substrate does not contact with the enzyme. The injection of substrate plug was fixed at a pressure of 3.45×10^3 Pa (0.5 psi), and three injection times: 3, 5 and 7 s were assayed. Other conditions were fixed as previously. As can be observed in Fig. 3b the amount of NOR formed increased with the injection time, so the selected injection of substrate plug was 0.5 psi/7 s. With this injection, the reaction progress was considered enough for the quantitation of the VER consumption in the kinetic study (see Section 2.3.4).

3.2. Electrophoretic separation of VER and NOR enantiomers from the reaction mixture

Initial conditions for the achiral separation of reagents and products after the incubation step were taken from [27] as following: 50 mM NaH_2PO_4 at pH 8.8 as BGE; capillary temperature: 25 °C; applied voltage: 20 kV. Under these conditions, racemic VER and racemic NOR were well separated from NADP^+ and NADPH and baseline separated themselves.

For the chiral separation of $\pm\text{VER}$ and $\pm\text{NOR}$ enantiomers, the same BGE was employed and HS- β -CD was chosen as chiral selector because this cyclodextrin has proved to have good enantio-recognition abilities for basic drugs and it has been employed successfully by our research group [30,31]. As described in those papers the use of the partial filling technique for the enantiomers separation extremely decreases the consumption of chiral selector (comparing with the inclusion of the cyclodextrin in the BGE, which is the conventional methodology). Also, highly sulfated cyclodextrins have proved to be powerful stereoselectors for enantiomers of many other basic and neutral organic compounds [32–35].

Different HS- β -CD concentrations, injected at 6.89×10^4 Pa (10 psi) for 2 min, were tested in the range of 0.25–2.5% (m/v) HS- β -CD. The use of 0.25% (m/v) HS- β -CD did not provide separation of the $\pm\text{VER}$ and $\pm\text{NOR}$ enantiomers. With 2% (m/v) HS- β -CD, each pair of enantiomers was adequately separated but S-NOR and R-VER were overlapped. The increase of the CD concentration to 2.5% (m/v) allowed baseline separation of the four peaks. With 2.5% (m/v) HS- β -CD and an applied voltage of 20 kV, migration times were 18.2, 19.9, 20.6 and 21.5 min for S-VER, S-NOR, R-VER and R-NOR, respectively. To reduce the analysis times and improve peaks shape, a little pressure of 1.38×10^3 Pa (0.2 psi) was added to the separation step, leading to migration times of 9.8, 10.5, 10.8 and 11.2 min, for S-VER, S-NOR, R-VER and R-NOR, respectively. With these conditions, the enantiomers, complexed with the HS- β -CD, migrate anionically to the detector. For enantiomers identification pure R-verapamil enantiomer was used.

Fig. 4 shows the electropherogram corresponding to the separation of VER and NOR enantiomers under selected conditions. NADP^+ and NADPH had longer migration times and did not affect the quantification of VER and NOR enantiomers. As those peaks were not measured, a stoptime of 20 min was chosen for further experiences to shorten the analysis time. In the selected conditions, the total analysis time (including pre-conditioning, injection, incubation and separation) was less than 35 min.

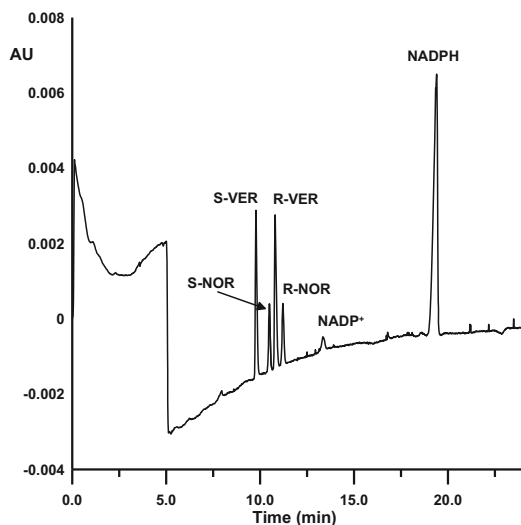


Fig. 4. Electropherogram showing the separation of the components of the enzymatic EMMA assay. The concentrations of racemic VER and NOR are, respectively, 200 and 100 μM . Other experimental conditions are described in Sections 2.3.2 and 2.3.3.

3.3. Estimation of Michaelis–Menten parameters for CYP3A4 metabolism of VER

For many enzyme-catalyzed reactions, the relationship between initial reaction rate (V) and substrate concentration ($[S]$), can be described by Michaelis–Menten equation [5,12]:

$$V = \frac{V_{\max} \cdot [S]}{K_m + [S]} \quad (2)$$

where V_{\max} is the maximum reaction velocity and K_m is the Michaelis constant, *i.e.* the substrate concentration at half the maximum velocity.

The estimation of kinetic parameters was carried out by varying the concentration of racemic verapamil in the range of 20–200 μM (10–100 μM of each enantiomer) in the reaction system. Six VER concentrations were processed under intermediate precision conditions: two working sessions were carried out, each one with two replicates of each concentration level. All data were combined for the estimations.

The quantification of the reaction turnover was done considering the consumption of VER enantiomers, providing information about the overall metabolism of VER by CYP3A4. For this purpose calibration curves for S- and R-VER were done in both working sessions. The experimental procedure for the calibration was the same employed for the reaction study (Section 2.3.2), including the injection of enzymes and incubation times, in order to obtain the VER and NOR peaks in the same conditions of diffusion as in the enzymatic assay. However, the reagents of solution A were not included in the calibration solutions, avoiding the advance of the enzymatic reaction.

Corrected (migration time normalized) peak area of S- and R-VER was used as dependent variable to subsequently calculate the reaction rate data. 50 μM racemic NOR was added to all calibration solutions to check that the four peaks were adequately separated. Table 1 shows the regression statistics for the linear calibration curves of each VER enantiomer together with their corresponding confidence intervals. In both cases the calibration curves showed

Table 1
Calibration model statistics^a for S- and R-VER under the selected separation conditions using corrected peak area as dependent variable.

		$b_0 \pm ts$	$b_1 \pm ts$	R^2
Session 1	S-VER	-50 ± 80	15.9 ± 0.8	0.996
	R-VER	-40 ± 80	13.8 ± 0.8	0.994
Session 2	S-VER	-1 ± 60	20.1 ± 0.6	0.998
	R-VER	-1 ± 60	19.2 ± 0.6	0.997

^a b_0 , intercept; b_1 , slope; ts, confidence interval at the 95% probability level; R^2 , squared correlation coefficient.

adequate regression coefficients. Calculations for each experimental data set were done employing its corresponding calibration curve.

Non-linear fitting of the rate (V) experimental data to the Michaelis–Menten equation was carried out for each VER enantiomer employing a Mardquardt algorithm [36]. It should be mentioned that data obtained by duplicate from two independent sessions (intermediate precision conditions) were combined, so the results become more realistic than those from a single experiment. The use of two short working sessions instead of one long session with more replicates helps to prevent possible degradation or sedimentation of CYP in the CE vial, which may affect the reaction progress.

Michaelis–Menten graphics for both VER enantiomers are shown in Fig. 5. K_m values for the overall metabolism of

VER by CYP3A4 were found to be $51 \pm 9 \mu\text{M}$ for S-VER and $47 \pm 9 \mu\text{M}$ for R-VER. V_{\max} values were 22 ± 2 and 21 ± 2 in $\text{pmol min}^{-1} (\text{pmol CYP})^{-1}$ units, 2800 ± 200 and 2600 ± 200 in $\text{pmol min}^{-1} (\text{mg CYP})^{-1}$ units, respectively. The expressed uncertainty is the asymptotic standard error obtained from the Mardquardt non-linear fitting. Determination coefficients (R^2) of the model were 0.98 for S-VER and 0.97 for R-VER. At all concentrations studied, S-VER showed slightly faster metabolism than R-VER. This conclusion is in agreement with other reported values (Table 2), which shows the capability of the proposed methodology described in this paper.

As can be observed in Table 2 the K_m values obtained with the different *in vitro* estimations [1,24–26] are different. Nevertheless, the Michaelis constant cannot be compared exactly with values from other studies, because it depends on the origin of the CYP3A4 and the exact conditions of the enzymatic assay. Even using the same source of enzyme, different batches can produce different results [27]. Additionally the proposed methodology involves a dilution step as a consequence of the in-capillary reaction which can affect the K_m estimated values. To estimate the dilution factor the peak areas of standards obtained in the reaction conditions were compared with those obtained in zonal CE. A dilution factor of 1.4 ± 0.2 was estimated. By applying this dilution factor the K_m values for S- and R-VER enantiomers were about 73 and 67 μM , respectively, results more closed to the reported values. On the other hand, as can be observed in Table 2, the K_m values for S- and R-VER enantiomers were similar. By comparing the V_{\max} values,

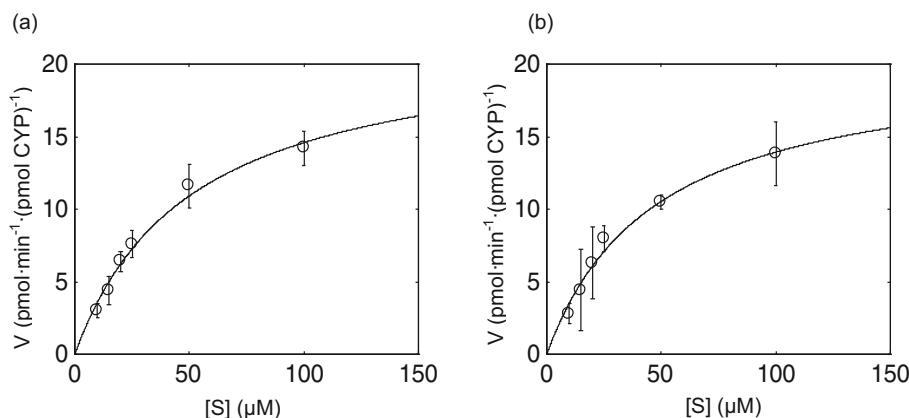


Fig. 5. Michaelis–Menten results for (a) S-VER and (b) R-VER. V represents the mean rate and standard deviation (s) from four replicates in intermediate precision conditions (two replicates in two independent sessions) and $[S]$ represents the enantiomer concentration.

Table 2
Michaelis–Menten parameters for CYP3A4 enantioselective metabolism of verapamil.

Substrate	Enzyme source	Methodology	$K_m \pm \text{SD} (\mu\text{M})$		$V_{\max}^{a,b} \pm \text{SD}$			Ref.		
			S-VER	R-VER	S-VER	R-VER	ES ^c			
Racemic VER	Supersomes (Gentest)	<i>In vitro</i> -EMMA	51 ± 9	47 ± 9	22 ± 2^a	2800 ± 200^b	21 ± 2^a	2600 ± 200^b	1.08	This work
Racemic VER	Supersomes (Gentest)	<i>In vitro</i> + off-line CE	170 ± 20	170 ± 35	$26.7 \pm 1.8^a 3400 \pm 200^b$			$19.5 \pm 2.0^a 2500 \pm 300^b$	1.36	[1]
R-VERS-VER	Supersomes (Gentest)	<i>In vitro</i> + LC	97 ± 13	100 ± 40	2930 ± 190^b			2500 ± 500^b	1.17	[24]
R-VERS-VER	Human HEpG2 cells infected by vaccinia virus	<i>In vitro</i> + LC	120 ± 30	130 ± 30	7.9 ± 0.6^a			6.9 ± 0.7^a	1.14	[25]
R-VERS-VER	Human liver microsomes	<i>In vitro</i> + LC	50 ± 40^d	60 ± 50^d	$800 \pm 600^{b,d}$			$800 \pm 700^{b,d}$	1	[26]

^a V_{\max} expressed in $\text{pmol min}^{-1} (\text{pmol CYP})^{-1}$.

^b V_{\max} expressed in $\text{pmol min}^{-1} (\text{mg CYP})^{-1}$.

^c Enantioselectivity (ES), estimated as the ratio between V_{\max} values.

^d Values obtained for nonverapamil formation.

S-VER is slightly more extensively metabolized than R-VER. However, since confidence intervals of estimates overlap, we cannot assure a significant enantioselectivity. On the other hand, this observation agrees with other previous results obtained for VER (see Table 2). As can be observed in Table 2 the results obtained in this paper agree with others obtained using V_{\max} values previously reported.

Intrinsic clearance is an interesting pharmacokinetic parameter defined as the amount of plasma from which a xenobiotic is removed in a certain time. It reflects the capacity of the body to remove a xenobiotic. The *in vitro* intrinsic clearance Cl_i can be estimated from the K_m and V_{\max} values as V_{\max}/K_m [26]. The enantioselective Cl_i values for verapamil by CYP3A4 have been estimated as 55 ± 10 and $55 \pm 11 \text{ mL min}^{-1} (\text{mg CYP})^{-1}$ for S- and R-VER, respectively. Bibliographic Cl_i values for verapamil enantiomers (expressed as sum of individual metabolites formed) are 53.5 and $40.5 \text{ mL min}^{-1} (\text{mg CYP})^{-1}$ for S- and R-VER, respectively [26].

4. Conclusions

Due to its intrinsic characteristics such as high separation efficiencies, speed of analysis, low reagent consumption and small sample requirements, CE has proved to be a good technique for the evaluation of *in vitro* enantioselective metabolism of drugs. The combination of the EMMA methodology for the in-line development of the enzymatic reaction and the partial filling technique with HS- β -CD for the separation of VER and NOR enantiomers has been employed successfully for the evaluation of enantioselective metabolism of VER by CYP3A4. The methodology developed and applied in this work allows the enantioselective estimation of Michaelis–Menten kinetic parameters in a fast, fully automated and non-expensive way that joins the intrinsic advantages of EMMA and partial filling technique. This methodology can be applied to the estimation of enantioselective kinetic parameters of other CYP450 substrates.

In agreement with previous literature data, in this work we have found that there are slight differences between the CYP3A4 metabolisms of S- and R-verapamil. However, since confidence intervals of estimates overlap, we cannot assure a significant enantioselectivity. Working in intermediate precision conditions provides more realistic conclusions from the experimental results.

Acknowledgments

The authors acknowledge the University of Valencia (UV-INV-AE112-66280) and the Generalitat Valenciana

(GVACOMP2011-002) for the financial support. L. Asensi-Bernardi acknowledges the Spanish Ministry of Education for her FPU pre-doctoral research grant (reference AP2010-1984). The authors declared no conflict of interest.

References

- [1] P.T.T. Ha, I. Sluyts, S.V. Dyck, J. Zhang, R.A.H.J. Gilissen, J. Hoogmartens, A.V. Schepdael, J. Chromatogr. A 1120 (2006) 94.
- [2] D. Li, Y. Wang, K. Han, Coord. Chem. Rev. 256 (2012) 1137.
- [3] J. Caldwell, J. Chromatogr. A 694 (1995) 39.
- [4] D.R. Brocks, Biopharm. Drug Dispos. 27 (2006) 387.
- [5] V.L. Campo, L.S.C. Bernardes, I. Carvalho, Curr. Drug Metab. 10 (2009) 188.
- [6] H.Y. Kwan, W. Thormann, Electrophoresis 32 (2011) 2738.
- [7] S. Portmann, H.Y. Kwan, R. Theurillat, A. Schmitz, M. Mevissen, W. Thormann, J. Chromatogr. A 1217 (2010) 7942.
- [8] M.R. Meyer, F.T. Peters, H.H. Maurer, Biochem. Pharmacol. 77 (2009) 1725.
- [9] M.R. Meyer, F.T. Peters, H.H. Maurer, Drug Metab. Dispos. 37 (2009) 1152.
- [10] H. Nehme, R. Nehme, P. Lafite, S. Routier, P. Morin, Anal. Chim. Acta 722 (2012) 127.
- [11] Z. Glatz, J. Chromatogr. B 841 (2006) 23.
- [12] X. Hai, B. Yang, A.V. Schepdael, Electrophoresis 33 (2012) 211.
- [13] J.M. Bao, F.E. Regnier, J. Chromatogr. 608 (1992) 217.
- [14] T. Křížek, A. Kubičková, Anal. Bioanal. Chem. 403 (2012) 2185.
- [15] M. Zeisbergerova, R. Řemínek, A. Mádr, Z. Glatz, J. Hoogmartens, A.V. Schepdael, Electrophoresis 31 (2010) 3256.
- [16] R. Curcio, R. Nicoli, S. Rudaz, J.L. Veuthey, Anal. Bioanal. Chem. 398 (2010) 2163.
- [17] J. Zhang, J. Hoogmartens, A.V. Schepdael, Electrophoresis 29 (2008) 3694.
- [18] R. Řemínek, Z. Glatz, J. Sep. Sci. 33 (2010) 3201.
- [19] J. Konečný, J. Jurica, J. Tomandl, Z. Glatz, Electrophoresis 28 (2007) 1229.
- [20] X. Hai, J. Konečný, M. Zeisbergerova, E. Adams, J. Hoogmartens, A.V. Schepdael, Electrophoresis 29 (2008) 3817.
- [21] J. Konečný, I. Micikova, R. Řemínek, Z. Glatz, J. Chromatogr. A 1189 (2008) 274.
- [22] X. Hai, E. Adams, J. Hoogmartens, A.V. Schepdael, Electrophoresis 30 (2009) 1248.
- [23] H.Y. Kwan, W. Thormann, Electrophoresis 33 (2012) 3299.
- [24] L. Shen, J.F. Fitzloff, C.S. Cook, Drug Metab. Dispos. 32 (2004) 186.
- [25] T.S. Tracy, K.R. Korzekwa, F.J. González, I.W. Wainer, J. Br. Clin. Pharmacol. 47 (1999) 545.
- [26] H.K. Kroemer, H. Echizen, H. Heidemann, M. Eichelbaum, J. Pharmacol. Exp. Ther. 260 (1992) 1052.
- [27] J. Zhang, P.T.T. Ha, Y. Lou, J. Hoogmartens, A.V. Schepdael, J. Pharm. Biomed. Anal. 39 (2005) 612.
- [28] J. Pauwels, J. Hoogmartens, A.V. Schepdael, Electrophoresis 31 (2010) 3867.
- [29] S.M. Krylova, V. Okhonin, S.N. Krylov, J. Sep. Sci. 32 (2009) 742.
- [30] L. Asensi-Bernardi, Y. Martín-Biosca, R.M. Villanueva-Camañas, M.J. Medina-Hernández, S. Sagrado, Electrophoresis 31 (2010) 3268.
- [31] L. Asensi-Bernardi, Y. Martín-Biosca, E. Fomet-Herrero, S. Sagrado, M.J. Medina-Hernández, Biomed. Chromatogr. 27 (2013) 377.
- [32] C.E. Evans, A.M. Stalcup, Chirality 15 (2003) 709.
- [33] B. Chankvetadze, Electrophoresis 30 (2009) 5211.
- [34] S. Fanali, Electrophoresis 30 (2009) 5203.
- [35] D. Koval, L. Severa, L. Adriaenssens, J. Vavra, F. Teplý, V. Kasicka, Electrophoresis 32 (2011) 2683.
- [36] D.L. Massart, B.G.M. Vandeginste, L.M.C. Buydens, S. De Jong, P.J. Lewi, J. Smeyers-Berbeke, Handbook of Chemometrics and Qualimetrics Part A, Elsevier, Amsterdam, 1997.

Paper X

**Fast evaluation of enantioselective drug metabolism by
electrophoretically mediated microanalysis: application to fluoxetine
metabolism by CYP 2D6**

**L. Asensi-Bernardi, Y. Martín-Biosca, L. Escuder-Gilabert, S. Sagrado
and M.J. Medina-Hernández**

Electrophoresis 2013, 34, 3214-3320

Lucía Asensi-Bernardi¹
Yolanda Martín-Biosca¹
Laura Escuder-Gilabert¹
Salvador Sagrado^{1,2}
María José
Medina-Hernández¹

¹Departamento de Química Analítica, Facultad de Farmacia, Universitat de València, Burjassot, Spain

²Centro Interuniversitario de Reconocimiento Molecular y Desarrollo Tecnológico, Unidad Mixta Universidad Politécnica de Valencia-Universitat de València, Valencia, Spain

Received June 10, 2013

Revised July 23, 2013

Accepted August 12, 2013

Research Article

Fast evaluation of enantioselective drug metabolism by electrophoretically mediated microanalysis: Application to fluoxetine metabolism by CYP2D6

In this work, a capillary electrophoretic methodology for the enantioselective in vitro evaluation of drugs metabolism is applied to the evaluation of fluoxetine (FLX) metabolism by cytochrome 2D6 (CYP2D6). This methodology comprises the in-capillary enzymatic reaction and the chiral separation of FLX and its major metabolite, norfluoxetine enantiomers employing highly sulfated β -CD and the partial filling technique. The methodology employed in this work is a fast way to obtain a first approach of the enantioselective in vitro metabolism of racemic drugs, with the additional advantage of an extremely low consumption of enzymes, CDs and all the reagents involved in the process. Michaelis–Menten kinetic parameters (K_m and V_{max}) for the metabolism of FLX enantiomers by CYP2D6 have been estimated by nonlinear fitting of experimental data to the Michaelis–Menten equation. K_m values have been found to be $30 \pm 3 \mu\text{M}$ for *S*-FLX and $39 \pm 5 \mu\text{M}$ for *R*-FLX. V_{max} estimations were 28.6 ± 1.2 and $34 \pm 2 \text{ pmol}\cdot\text{min}^{-1}\cdot(\text{pmol CYP})^{-1}$ for *S*- and *R*-FLX, respectively. Similar results were obtained using a single enantiomer (*R*-FLX), indicating that the use of the racemate is a good option for obtaining enantioselective estimations. The results obtained show a slight enantioselectivity in favor of *R*-FLX.

Keywords:

CYP2D6 / EMMA / Enantioselective metabolism / Fluoxetine

DOI 10.1002/elps.201300267

1 Introduction

The development of new drugs is a long, complex, and expensive process that involves the evaluation of the pharmacokinetic and pharmacodynamic properties of the new molecule in different stages. In the early stages of drug development, methods for the high-throughput screening of new molecules' properties are commonly employed, in order to have preliminary data about the potential pharmacological activity of a molecule and also its pharmacokinetics. When racemic molecules are employed, both pharmacokinetic and pharmacodynamic properties can show a certain degree of enantioselectivity due to the interaction with optically active biomacromolecules, so the methods applied in these preclinical early stages may allow to evaluate these properties in an enantioselective way [1]. This need comes from the

growing interest of the pharmaceutical industry in the development of single-enantiomer formulations, and also from the regulations concerning racemic drugs, which indicate that enantioselective analysis should be performed also over racemates [2].

One of the most important pharmacokinetic parameters to evaluate is the metabolism by different enzymatic systems. Although a definitive measurement of metabolic rates is performed in vivo, by administering the drug to the living system and monitoring the free concentration of xenobiotic and its metabolites in body fluids and tissues, in preclinical stages in vitro assays are performed in order to obtain a first approach to the drug metabolism and to explore different metabolic routes individually. In vitro methods are based on the use of liver subcellular fractions as liver microsomes, isolated hepatocytes, liver slices or individual forms of enzymes, predominantly isoforms of cytochrome P450 [3]. In these studies, the components of the enzymatic system are mixed and after an incubation period one or more components of the enzymatic reaction are monitored mainly using LC. More recently CE has become very useful for enzymatic assays since it is fully automated, requires small sample volumes, provides high peak efficiencies and is environmentally friendly [4, 5]. CE can be employed just for the separation and detection of substrates or metabolites, after off-line incubation, or also for the enzymatic reaction with the Electrophoretically mediated microanalysis (EMMA)

Correspondence: Dr. María José Medina Hernández, Departamento de Química Analítica, Facultad de Farmacia, Universitat de València C/Vicent Andrés Estellés s/n, E-46100 Burjassot, Valencia, Spain

E-mail: maria.j.medina@uv.es

Abbreviations: CYP2D6, cytochrome P2D6; FLX, fluoxetine; FMO, flavin-containing monooxygenase; HS- β -CD, highly sulfated β -CD; NFLX, norfluoxetine; PFT, partial filling technique

methodology. In the EMMA approach the reaction is carried out in a nanoliter volume of the capillary, which serves simultaneously as microreactor, separation system and detection cell, allowing a higher degree of automation and miniaturization [6, 7]. Several applications of EMMA to the evaluation of nonchiral drug metabolism with different CYP450 isoforms or flavin-containing monooxygenases (FMOs) have been reported in the literature [8–14]: dextromethorphan metabolism by CYP3A4 [8], phenacetin, dextromethorphan, tramadol, and midazolam by different CYP450 isoforms [9], testosterone and nifedipine by CYP3A4 [10], diclofenac by CYP2C9 [11, 12], clozapine metabolism by FMO3 [13], and also inhibition studies with CYP450 [14]. There are only few references about the use of EMMA procedure to study the enantioselective metabolism of drugs. This procedure has been applied to evaluate the chiral oxidation of cimetidine enantiomers by FMOs [15] and to study the enantioselective metabolism of ketamine by CYP450 [16]. In both cases a CD has been added to the BGE to perform the chiral separation. Recently a methodology for the enantioselective evaluation of drugs metabolism by EMMA employing CYP3A4 as model enzyme has been proposed by our research group and applied to the study of enantioselective metabolism of verapamil [17].

Fluoxetine (FLX) is a potent and selective inhibitor of the neuronal serotonin-uptake carrier, used commonly as an antidepressant but also indicated for other psychiatric disorders such as obsessive compulsive disorder or bulimia nervosa [18]. It is used therapeutically as a racemate, although a stereospecificity associated with its interactions with the serotonin-uptake carrier has been demonstrated [19]. FLX is extensively metabolized in the liver, via different metabolic routes. The major active metabolite, norfluoxetine (NFLX) is formed by a *N*-demethylation pathway with the cytochrome P450. Other metabolites, obtained with different phase II enzymatic systems, are inactive conjugates of FLX or NFLX. Different isoforms of CYP450 have been described in vitro as responsible for FLX metabolism, although in vivo is cytochrome P2D6 (CYP2D6), which plays a major role in the *N*-demethylation reaction [18]. Also, FLX and NFLX are potent inhibitors of the CYP2D6, so they are important candidates for causing drug–drug interactions of clinical relevance, since several psychoactive drugs are substrates of CYP2D6 and frequently co-administered with FLX.

To our knowledge, in bibliography there is only one reference about the metabolism of FLX enantiomers by CYP2D6. These kinetic data were obtained in vitro, by incubating at 37°C single enantiomers of FLX with the baculovirus-expressed human CYP2D6. In that procedure, after the incubation step, a liquid–liquid extraction of the enantiomers of NFLX, followed by evaporation of the extract, reconstitution of the residue and analysis by HPLC-MS/MS, was performed [20].

In this work, the EMMA methodology for the enantioselective evaluation of drugs metabolism developed recently by our research group employing CYP3A4 as model enzyme [17], is applied to the enantioselective metabolism of FLX

using other CYP450 isoform, CYP2D6, confirming the adequacy of the methodology for the evaluation of enantioselective drugs metabolism by different isoforms of CYP450. In this methodology the enzymatic reaction and the enantioseparation using highly sulfated β -CD (HS- β -CD) and a partial filling technique (PFT) are joined in a unique step carried out in the CE system, allowing a high degree of automation and an extremely low consumption of all the reagents involved both in the enzymatic reaction and the enantioseparation. Kinetic data are estimated via Michaelis–Menten equation, and also an estimation of the intrinsic clearance of FLX enantiomers by CYP2D6 is provided. The results are compared with those obtained using a single enantiomer.

2 Materials and methods

2.1 Instrumentation

A Beckman P/ACE MDQ Capillary Electrophoresis System equipped with a DAD (Beckman Coulter, Fullerton, CA, USA), and 32Karat software version 8.0 was used throughout. A 50 μ m id fused-silica capillary with total and effective lengths of 60.2 and 50 cm, respectively, was employed (Beckman Coulter, Fullerton, CA, USA). The CE system is equipped with a temperature-controlled garage for sample trays, so samples could be kept cooled at 10°C during all the experiments. Detection wavelength was fixed at 200 nm for all experiments.

Electrophoretic solutions and samples were filtered through 0.45 μ m pore size nylon membranes (Micron Separation, Westboro, MA, USA) and degassed in an ultrasonic bath (JP Selecta, Barcelona, Spain) prior to use. A Crison Micro pH 2000 pH-meter from Crison Instruments (Barcelona, Spain) was employed to adjust the pH of buffer solutions.

2.2 Chemicals and reagents

All reagents were of analytical grade. NaH₂PO₄·2H₂O was from Fluka (Buchs, Switzerland); KH₂PO₄ from Panreac (Barcelona, Spain); HS- β -CD (20% w/v) aqueous solution was purchased from Beckman Coulter (Fullerton, CA, USA); Ultra Clear TWF UV deionized water (SG Water, Barsbüttel, Germany) was used to prepare solutions.

FLX hydrochloride was kindly donated by Alter (Madrid, Spain). R-FLX hydrochloride (employed for enantiomers identification) and NFLX hydrochloride were purchased from Sigma Aldrich (St Louis, MO, USA). Human CYP2D6 + P450 reductase SUPERSOMES and NADPH regenerating system were from BD Gentest (Erembodegem, Belgium). This regenerating system consists of two independent solutions: solution A (26 mM NADP⁺, 66 mM glucose 6-phosphate (G6P), 66 mM MgCl₂) and B (40 U/mL G6PDH). SUPERSOMES, and NADPH regenerating system were aliquoted to minimize freeze-thaw cycles and the aliquots were stored at –80°C until their use.

employed for the calibration was the same as that employed for the reaction samples, in order to obtain FLX peaks in the same conditions. However, the reagents of solution A were not included in the calibration solution, avoiding the advance of the enzymatic reaction. As no significant differences were found between both sessions, all calibration and reaction data were employed together for estimations.

2.4 Software and calculations

For the calculation of the reaction rate, it is necessary to estimate the number of moles of each reagent involved in the enzymatic reaction. This estimation was done by calculating the injected volume of each plug with the following equation:

$$\text{Vol} = \frac{\Delta P \cdot d^4 \cdot \pi \cdot t}{128 \cdot \eta \cdot L_{\text{TOT}}} \quad (1)$$

where Vol (m³) is the injected volume, ΔP (Pa) is the applied pressure, d (m) is the internal diameter of the capillary, t (s) is the duration of pressure application, η (Pa·s) is the viscosity of the injected solution and L_{TOT} (m) is the total length of the capillary.

Velocity rate data (expressed in pmol·min⁻¹·(pmol CYP)⁻¹) were obtained from the corrected area of *S*- and *R*-FLX peaks, and plotted versus the initial enantiomer substrate concentration following the Michaelis–Menten equation. Microsoft Office EXCEL[®] (Microsoft, Redmond, WA, USA) and STATGRAPHICS Plus[®] (Statpoint Technologies, Warrenton, VA, USA) were employed for calculations.

3 Results and discussion

3.1 Electrophoretic separation of the reaction mixture

Initial conditions for the electrophoretic separation (BGE, 50 mM NaH₂PO₄ at pH 8.8; capillary temperature, 25°C, separation voltage, 20 kV + 0.2 psi of pressure; HS- β -CD 2.5% w/v injected at 20 psi/2 min) were taken from [17]. However, based on our previous experience about the chiral separation of FLX with HS- β -CD, the CD concentration used there (2.5% w/v) was considered too high due to the strong interaction between the FLX enantiomers and the HS- β -CD [21]. Therefore, a study was performed in order to select the adequate CD concentration, which allows the separation of all components of the enzymatic reaction. For this purpose variable CD concentrations in the range 0.1–1.25% were assayed, employing also a pressure slightly higher than in [17], 0.4 psi instead of 0.2. The CD concentration range used was selected taking into account that the separation of FLX enantiomers with HS- β -CD implies the formation of an anionic complex with the CD, and the equilibrium between the free and complexed drug fractions provides the enantioseparation and affects the effective electrophoretic mobility of the enantiomers. When the HS- β -CD concentration is increased,

the equilibrium is shifted to the complexed form and the effective mobility of the enantiomers becomes more negative, resulting in longer migration times. Consequently, in order to obtain a better separation of the substrates and products from the other reagents, and assuming that the mobility of bigger molecules such as the cytochrome or the NADP⁺/NADPH system is not (or slightly) affected by the CD concentration, different CD concentrations were tested.

Figure 2 shows some of the results obtained. As can be observed in Fig. 2A, the use of 0.1% CD concentration provided baseline resolution of the four enantiomers peaks of *S*-NFLX, *S*-FLX, *R*-NFLX, and *R*-FLX, but the peaks corresponding to *S*-enantiomers overlapped with the CYP2D6 peaks (see Fig. 3 for all peaks identification).

The use of 0.15% m/v CD concentration (Fig. 2B), produced the overlapping of the *R*-FLX and the NADP⁺ peak. Additionally, when a 0.5% w/v CD concentration was employed (Fig. 2C), the FLX and NFLX peaks migrate after the NADP⁺/NADPH system, but the peak of *S*-NFLX still overlapped with that. Finally, using a HS- β -CD 1.25% w/v concentration, all the reagents and products of the reaction were baseline separated in an analysis time shorter than 30 min. Figure 3 shows the electropherogram corresponding to the separation of all the reaction components under the selected conditions.

3.2 Estimation of Michaelis–Menten parameters

The Michaelis–Menten equation Eq. (2), describes the relationship between the initial reaction rate (V) and the substrate concentration ($[S]$) for many enzyme-catalyzed reactions [6, 22]:

$$V = \frac{V_{\text{max}} \cdot [S]}{K_m + [S]} \quad (2)$$

In this equation, V_{max} is the maximum reaction velocity and K_m is the Michaelis constant, which is defined as the substrate concentration at half the maximum velocity. The estimation of kinetic parameters was carried out by varying the concentration of the racemic FLX in the range of 10–200 μM , employing seven concentration levels. The samples were processed under intermediate precision conditions: two working sessions were carried out, each one with two replicates of each concentration level. All data were combined for estimations, so the results become more realistic than those from a single experiment. The use of two short sessions instead of one longer is also useful to prevent possible sedimentation and/or degradation of the CYP in the CE vial, which can affect the reaction progress. The interday repeatability was evaluated. Averaged intermediate precision coefficients for peak areas of calibration curves and samples, for both enantiomers, were 9 and 16%, respectively. Taking into account the concentration levels and the intrinsic variability of enzymatic reactions, these coefficients can be considered acceptable.

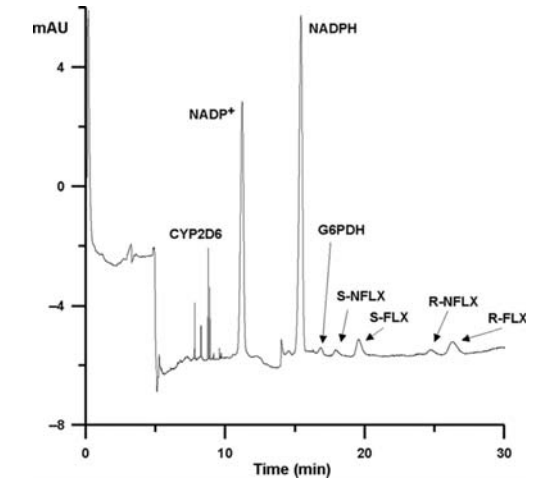
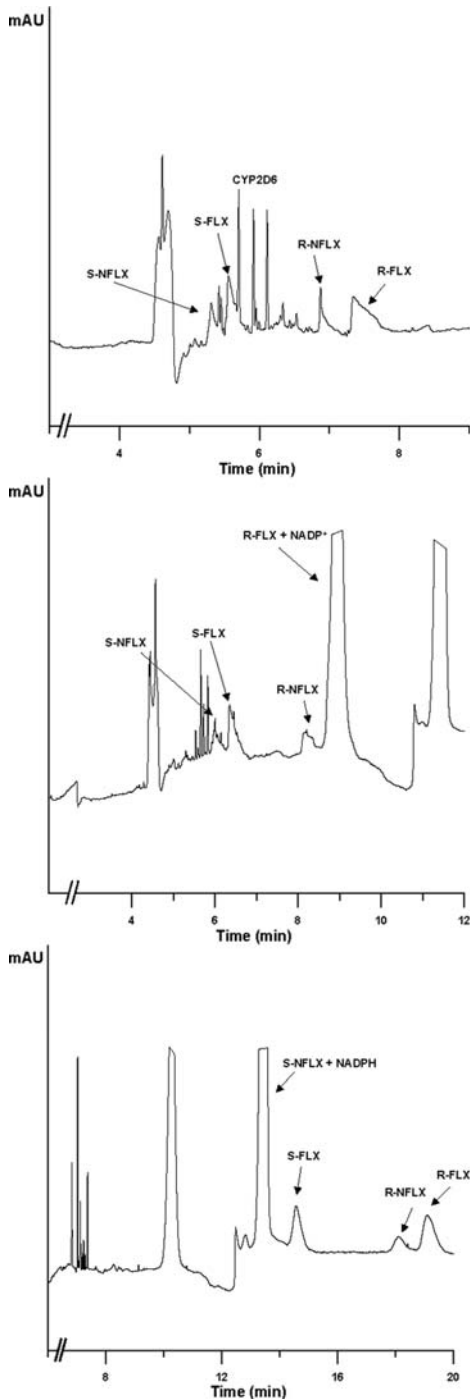


Figure 3. Electropherogram showing the separation of the reaction mixture. Concentrations of racemic FLX and NFLX were, respectively, 100 and 50 μM . Other experimental conditions as described in Section 2.3.2.

Nonlinear fitting of the rate (V) experimental data to the Michaelis–Menten equation was carried out for each FLX enantiomer employing a Marquardt algorithm [23]. Michaelis–Menten plots for *S*- and *R*-FLX are shown in Fig. 4. K_m values (mean \pm SD) have been found to be $30 \pm 3 \mu\text{M}$ for *S*-FLX and $39 \pm 5 \mu\text{M}$ for *R*-FLX. V_{max} estimations were $28.6 \pm 1.2 \text{ pmol}\cdot\text{min}^{-1}\cdot(\text{pmol CYP})^{-1}$ ($3630 \pm 150 \text{ pmol}\cdot\text{min}^{-1}\cdot(\text{mg CYP})^{-1}$) and $34 \pm 2 \text{ pmol}\cdot\text{min}^{-1}\cdot(\text{pmol CYP})^{-1}$ ($4300 \pm 200 \text{ pmol}\cdot\text{min}^{-1}\cdot(\text{mg CYP})^{-1}$) for *S*- and *R*-FLX, respectively. These results show a slight enantioselectivity in favor of *R*-FLX, that we have estimated as the ratio between their V_{max} values ($V_{\text{max-R}}/V_{\text{max-S}}$), giving a value of 1.18.

As indicated in the introduction section, only one estimation of the *in vitro* enantioselective metabolism of FLX by CYP2D6 has been found in the literature [20]. In that paper, the estimated kinetic parameters were: K_m , 3.8 ± 0.4 and $1.4 \pm 0.3 \mu\text{M}$ for *S*- and *R*-FLX, and V_{max} , $8.5 \pm 0.3 \text{ pmol}\cdot\text{min}^{-1}\cdot(\text{pmol CYP})^{-1}$ and $4.1 \pm 0.2 \text{ pmol}\cdot\text{min}^{-1}\cdot(\text{pmol CYP})^{-1}$ for *S*- and *R*-FLX, respectively. The differences with our kinetic data are considerable. However, the Michaelis parameters can only be compared with values obtained using the same enzyme source and identical conditions in the enzymatic assay. Even using the same source of enzyme, different batches can produce different results [24]. In that work, baculovirus-expressed human CYP enzymes, prepared

Figure 2. Effect of the HS- β -CD concentration on the separation of the reaction mixture (FLX and NFLX enantiomers, enzymes, cofactors). HS- β -CD concentrations were: (A) 0.1% w/v; (B) 0.15% w/v and (C) 0.5% w/v. Other experimental conditions as described in Section 2.3.2 and Fig. 3.

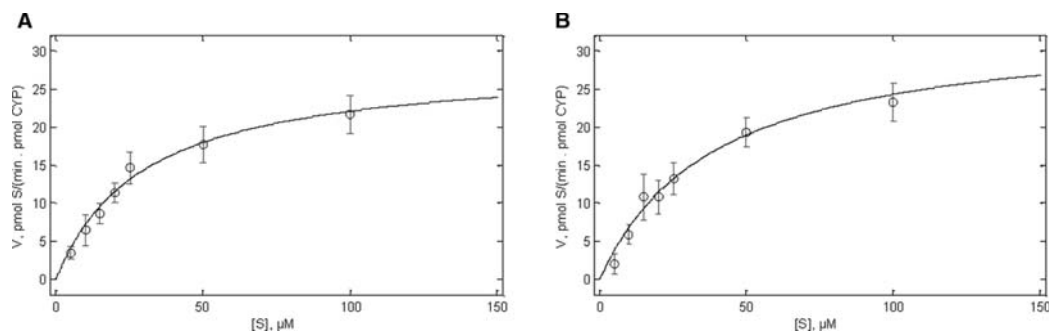


Figure 4. Michaelis–Menten plots for *S*-FLX (A) and *R*-FLX (B). V represents the mean rate and SD (s) from four replicates in intermediate precision conditions and $[S]$ represents the enantiomer concentration.

following a published procedure, were used and the experimental conditions of the assay were very different from ours (see Section 1).

An interesting parameter from a pharmacokinetic point of view is the intrinsic clearance of the drug, defined as the amount of plasma from which a xenobiotic is removed in a certain time. It reflects the capacity of the body (or of a single enzyme, like in this case) to eliminate a xenobiotic. The in vitro intrinsic clearance, Cl_i , can be estimated from the K_m and V_{max} values as V_{max}/K_m [25]. Enantioselective Cl_i values for FLX by CYP2D6 have been estimated as $121 \pm 13 \text{ mL}\cdot\text{min}^{-1}\cdot(\text{mg CYP})^{-1}$ for *S*-FLX and $111 \pm 16 \text{ mL}\cdot\text{min}^{-1}\cdot(\text{mg CYP})^{-1}$ for *R*-FLX.

3.3 Single versus racemic kinetic data estimations

In order to check a possible interaction of the enantiomers in their metabolism, an experiment was carried out by incubating only a single enantiomer, *R*-FLX, instead of the racemic mixture. Kinetic parameters were also estimated for *R*-FLX, obtaining a K_m of $38 \pm 9 \mu\text{M}$ and a V_{max} of $33 \pm 4 \text{ pmol}\cdot\text{min}^{-1}\cdot(\text{pmol CYP})^{-1}$. Comparing these data with those obtaining for *R*-FLX employing the racemates (K_m , $39 \pm 5 \mu\text{M}$, and V_{max} , $34 \pm 2 \text{ pmol}\cdot\text{min}^{-1}\cdot(\text{pmol CYP})^{-1}$), the differences were really small: 1.6% for K_m and 3.9% for V_{max} , so we can conclude that the use of a racemate for the evaluation of enantioselective metabolism of a drug provides the same results as the use of single enantiomers, with the advantage of that no single enantiomers available are needed, which is especially important in the case of new molecules in the early stages of drug development.

4 Concluding remarks

The combination of EMMA for the in-line development of an enzymatic assay and PFT with HS- β -CD for the chiral separation of substrates and/or metabolites has proved to be a powerful tool for a fast evaluation of in vitro enantioselective

metabolism of FLX by CYP2D6, confirming that this methodology, recently developed by our research group, can be extended to other enzymes and substrates. The main advantages of this methodology, comparing with other reported procedures, are its speed of analysis, low consumption of enzymes and other expensive reagents, enantioselective estimations obtained from racemic compounds, and high degree of automation, joining the intrinsic advantages of EMMA and PFT in a unique step carried out in the CE system, and making this method an interesting approach for screening procedures in preliminary phases of drug development. The results obtained in this paper indicate a slight enantioselectivity in favor of the *R*-enantiomer for the metabolism of FLX enantiomers by CYP2D6.

The authors acknowledge the University of Valencia (UV-INV-AE112-66280) for the financial support. L. Asensi-Bernardi acknowledges the Spanish Ministry of Education for her predoctoral FPU scholarship (AP2010-1984).

The authors have declared no conflict of interest.

5 References

- [1] Scriba, G. K. E., *J. Pharm. Biomed. Anal.* 2011, **55**, 688–701.
- [2] Food and Drug Administration, *Development of New Stereoisomeric Drugs*, 1992.
- [3] Brandon, E. F. A., Raap, C. D., Meijerman, I., Beijnen, J. H., Schellens, J. H. M., *Toxicol. Appl. Pharmacol.* 2003, **189**, 233–246.
- [4] Nehme, H., Nehme, R., Lafite, P., Routier, S., Morin, P., *Anal. Chim. Acta* 2012, **722**, 127–135.
- [5] Glatz, Z., *J. Chromatogr. B* 2006, **841**, 23–37.
- [6] Hai, X., Yang, B., Van Schepdael, A., *Electrophoresis* 2012, **33**, 211–227.
- [7] Bao, J. M., Regnier, F. E., *J. Chromatogr. A* 1992, **608**, 217–224.

- [8] Zeisbergerova, M., Řemínek, R., Mádr, A., Glatz, Z., Hoogmartens, J., Van Schepdael, A., *Electrophoresis* 2010, 31, 3256–3262.
- [9] Curcio, R., Nicoli, R., Rudaz, S., Veuthey, J. L., *Anal. Bioanal. Chem.* 2010, 398, 2163–2171.
- [10] Zhang, J., Hoogmartens, J., Van Schepdael, A., *Electrophoresis* 2008, 29, 3694–3700.
- [11] Řemínek, R., Glatz, Z., *J. Sep. Sci.* 2010, 33, 3201–3206.
- [12] Konecny, J., Jurica, J., Tomandl, J., Glatz, Z., *Electrophoresis* 2007, 28, 1229–1234.
- [13] Hai, X., Konečný, J., Zeisbergerova, M., Adams, E., Hoogmartens, J., Van Schepdael, A., *Electrophoresis* 2008, 29, 3817–3824.
- [14] Konecny, J., Micikova, I., Remínek, R., Glatz, Z., *J. Chromatogr. A* 2008, 1189, 274–277.
- [15] Hai, X., Adams, E., Hoogmartens, J., Van Schepdael, A., *Electrophoresis* 2009, 30, 1248–1257.
- [16] Kwan, H. Y., Thormann, W., *Electrophoresis* 2012, 33, 3299–3305.
- [17] Asensi-Bernardi, L., Martín-Biosca, Y., Escuder-Gilabert, L., Sagrado, S., Medina-Hernández, M. J., *J. Chromatogr. A* 2013, 1298, 139–145.
- [18] Agencia Española del Medicamento (Spanish Drug Agency). Available from: <http://www.aemps.gob.es/cima/especialidad.do?metodo=verFichaWordPdf&codigo=57954&formato=pdf&formulario=FICHAS&file=ficha.pdf> [Accessed May 2013]
- [19] Robertson, D. W., Krushinski, J. H., Fuller, R. W., Leander, J. D., *J. Med. Chem.* 1988, 31, 1412–1417.
- [20] Margolis, J. M., O'Donnell, J. P., Mankowski, D. C., Ekins, S., Scott Obach, R., *Drug Metab. Dispos.* 2000, 28, 1187–1191.
- [21] Asensi-Bernardi, L., Escuder-Gilabert, L., Martín-Biosca, Y., Sagrado, S., Medina-Hernández, M. J., *Biomed. Chromatogr.* 2013, DOI 10.1002/bmc.2935.
- [22] Campo, V. L., Bernardes, L. S. C., Carvalho, I., *Curr. Drug Metab.* 2009, 10, 188–205.
- [23] Massart, D. L., Vandeginste, B. G. M., Buydens, L. M. C., De Jong, S., Lewi, P. J., Smeyers-Berbeke, J., *Handbook of Chemometrics and Qualimetrics, Part A*, Elsevier, Amsterdam 1997.
- [24] Zhang, J., Ha, P. T. T., Lou, Y., Hoogmartens, J., Van Schepdael, A., *J. Pharm. Biomed. Anal.* 2005, 39, 612–617.
- [25] Kroemer, H. K., Echizen, H., Heidemann, H., Eichelbaum, M., *J. Pharmacol. Exp. Ther.* 1992, 260, 1052–1057.

